ISSN 0840-8440

ENVIRONMENTAL RESEARCH

TECHNOLOGY TRANSFER CONFERENCE • 1988

Environment
Ontario
Jim Bradley, Minister

PROCEEDINGS

SESSION A
AIR QUALITY RESEARCH

November 28 & 29
Royal York Hotel
Toronto, Ontario
Canada

ISSN 0840-8440

PROCEEDINGS

TECHNOLOGY TRANSFER CONFERENCE 1988

November 28 and 29, 1988
Royal York Hotel
Toronto, Ontario

SESSION A
AIR QUALITY RESEARCH

Sponsored by
Research and Technology Branch
Environment Ontario
Ontario, Canada

Introduction

Environment Ontario holds its annual Technology Transfer Conference to report and publicize the progress made on Ministry-funded projects. These studies are carried out in Ontario Universities and by private research organizations and companies.

The papers presented at Technology Transfer Conference 1988 are published in five volumes of conference Proceedings corresponding to the following sessions:

SESSION A: AIR QUALITY RESEARCH
SESSION B: WATER QUALITY RESEARCH
SESSION C: LIQUID AND SOLID WASTE RESEARCH
SESSION D: ANALYTICAL METHODS
SESSION E: ENVIRONMENTAL ECONOMICS

This volume is comprised of presentations given during Session A of the conference.

For reference purposes, indices for sessions B,C,D and E may be found at the back of this volume, listed in alphanumeric order.

For further information on any of the papers, please contact either the authors or the Research and Technology Branch at (416) 323-4574 or 323-4573.

Acknowledgements

The Conference Committee would like to thank the authors for their valuable contributions to environmental research in Ontario.

Disclaimer

The views and ideas expressed in these papers are those of the authors and do not necessarily reflect the views and policies of Environment Ontario, nor does mention of trade names or commercial products constitute endorsement or recommendation for use.

INDEX

Keynote Papers

Page

Keynote Paper I: Science-based Innovation and Prosperity Within "Sustainable Development"; J. Fraser Mustard, The Canadian Institute for Advance Research, Toronto, Ontario. 1

Keynote Paper II: Deriving Benefits from Environmental Research; Stuart Smith, Rockcliffe Research and Technology Inc., Ottawa Ontario. 7

Environment Ontario Paper

Air Quality Research: Current Status and Future Research Needs; W. Chan, Air Resources Branch, Environment Ontario. 11

Abstract **Page**

SESSION A: AIR QUALITY RESEARCH

Oral Presentations

A1 **Science and Policy: PhotoChemical Oxidants and Acid Bearing Species** K. L. Demerjian, Atmospheric Science Research Center, State University of New York, Albany, New York, U.S.A. 13

A2 **Relationship Between Forest Decline and Root Health in Ontario Sugar Maple** C. Adams, M. Egyed and T. Hutchinson*, Dept. of Botany, University of Toronto, Toronto, Ontario. 15

A3 **A Numerical Decline Index Rating System to Monitor Changes in Tree Condition of Hardwood Forest Species** D. McLaughlin*, W. McIlveen, W. Gizyn, D. Corrigan, R. Pearson and R. Arnup, Air Resources Branch, Environment Ontario 37

A4 **Investigation of Short-term Mutagenicity and Chemical Composition of Organic Solvent Extractable Fraction of Coke Oven Emission** A.J. Horton*, N. Belson, K. Shaw and G.H. Thomas, Ontario Research Foundation, Clarkson, Ontario 53

A5 **Quantitative Measurements of the Genetic Effects of Inhaled Carcinogens in Pulmonary Fibroblasts are Now Possible** J.A. Heddle*, A. Beach and J.D. Gingerich, Dept. of Biology, York University, Downsview, Ontario 61

A6 **Sensitivity of Asthmatic Children to Air Pollution;** D. Pengelly* and C. Goldsmith, McMaster University, Hamilton, Ontario 63

A7 **Hazardous Contaminants in Ontario: Environmental Fate and Human Exposure** D. Mackay* and S. Paterson, Institute for Environmental Studies, University of Toronto, Toronto, Ontario 73

Abstract **Page**

SESSION A: AIR QUALITY RESEARCH

Oral Presentations

A8 **Verification of the Cloud and Wet Deposition Fields of a MesoScale Model of Long-Range Transport of Air Pollutants** H.R. Cho*, S.T. Soong and J.V. Iribarne, Department of Physics, University of Toronto, Toronto, Ontario 101

A9 **Eulerian Model Evaluation** M. Alvo, Department of Mathematics, University of Ottawa, Ottawa, Ontario 103

A10 **Scale Model Studies and Development of Prediction Procedures for Heavy Gas Dispersion in Complex Terrain 1988** P. A. Irwin*, M.C. Murphy and K. C. Heidorn, Rowan Williams Davies and Irwin Inc., Guelph, Ontario 109

A11 **An Investigation of Wind Generated Particle Transport Rates within a Turbulent Boundary-Layer** A.D. Ciccone*, J.G. Kawall and J.F. Keffer, Department of Mechanical Engineering, University of Toronto, Toronto, Ontario 149

A12 **Incineration of Wastes** K. Davies, Environmental Protection Office, City of Toronto, Toronto, Ontario 169

A13 **Detectability of Step Trends in the Rate of Atmospheric Sulphate Deposition** E.A. McBean*, M.G. Kompter and G.J. Farquhar, Department of Civil Engineering, University of Waterloo, Waterloo, Ontario 171

A14 **Incinerator and Steel Plant Contributions to Air Particulates as Determined by Size-Specific Receptor Modelling** A.C. Chan*, Z-J. Kang and R.E. Jervis, Dept. of Chemical Engineering, University of Toronto, Toronto, Ontario 193

Abstract Page

SESSION A: AIR QUALITY RESEARCH

Oral Presentations

A15 **A Study on the Sources of Acid Precipitation in Ontario, Canada** P.K. Hopke* and Y. Zeng, Department of Civil Engineering, University of Illinois, Urbana, Illinois, U.S.A. 201

A16 **Advanced Techniques for Mobile Monitoring of Trace Organics in Air** G.B. De Brou*, E. Singer, M.A. Sage, R.W. Bell, R.E. Chapman and D.J. Ogner, Air Resources Branch, Environment Ontario 221

A17 **Atmospheric Trace Gas Measurements Using a Tunable Diode Laser Absorption Spectrometer** D.R. Hastie* and H.I. Schiff, Department of Chemistry, York University, Downsview, Ontario 251

A18 **Biomedical Waste Incineration Testing Program** V. Ozvacic*, G. Wong, G. Marson, R. Clement, D. Rokosh, S. Suter, G. Horsnell, J.C. Hipfner, S. Burns and H. Corinthios, Environment Ontario 263

A19 **A Study of High Temperature Photochemical Kinetics of Sulphur Dioxide and Nitrogen Oxides For a Flue Gas Treatment Process** J. Hunt*, P. Fellin, K.A. Brice, D. Ernst, D. Glendenning and R. Caton, Concord Scientific, Toronto, and C. Fung and K. Smith, Environment Ontario 277

A20 **Modelling the Photochemical Decomposition of Chlorinated Phenols by Sunlight** N.J. Bunce* and J.S. Nakai, Dept. of Chemistry and Biochemistry, University of Guelph, Guelph, Ontario 279

Abstract **Page**

SESSION A: AIR QUALITY RESEARCH

Poster Presentations

AP1 **Stochastic Modelling of Dispersion from Single Elevated Sources** E. Robertson and P. J. Barry, Atomic Energy of Canada Limited, Chalk River Nuclear Laboratories, Chalk River, Ontario 303

AP2 **Feasibility Study for Assessing and Modelling Microclimatic Conditions on the Fonthill Kame (Phase 1)** T. B. Shaw, Brock University, St. Catharines, Ontario 307

AP3 **Critical Evaluation of Atmospheric Pollutant Parameterization from Satellite Imagery** N. T. O'Neill, A. Royer and L. Hubert, Universite de Sherbrooke, Sherbrooke, Quebec, and J. Miller and J. Freemantle, CRESS, York University, Downsview', ', Ontario, and G. Austin and A. Davis, McGill 309

AP4 **A 3-D Mesoscale Wind Field Model and its Application for Emergency Planning at Nuclear Power Plants in Ontario** H. Sahota, P. K. Misra, R. Bloxam and D. Rhee, Air Resources Branch, Environment Ontario 315

AP5 **The Results from a Meso-scale Model** M. Niewiadomski, University of Toronto, Toronto, Ontario 325

AP6 **Dose Response for Selected Environmental Air Pollutants: Results from a Study on Runners** R. B. Urch, F. Silverman, P. Corey and R. J. Shephard, The Gage Research Institute, University of Toronto, Toronto, Ontario 333

Abstract **Page**

SESSION A: AIR QUALITY RESEARCH

Poster Presentations

AP7 Hamilton Air: Chemical Composition and Genotoxic Activity of Respirable Particulate and Organic Vapours D.W. Bryant, C. Kaiser-Farrell and D.R. McCalla, Department of Biochemistry, McMaster University, Hamilton, Ontario 339

AP8 Mutagenicity Studies and Risk Estimation of Complex Mixtures of Organic Airborne Contaminants A.S. Raj and D.M. Logan, Department of Biology, York University, Downsview, Ontario 345

AP9 In-Situ Monitoring of the Environment for Genotoxicity Levels Using Rodents M. Petras, M. Vrzoc, S. Meddins, K. Hill and T. Sands, Department of Biological Sciences, University of Windsor, Windsor, Ontario 351

AP10 Method Development for the Monitoring and Analysis of Odorous Organics in Ambient Air C.C. Chan, L. Vainer and J.W. Martin, Mann Testing Laboratories Ltd., Mississauga, Ontario, and A. Szakolcai and B. Foster, Environment Ontario 355

AP11 Gas Phase Analysis of Organic Compounds from Structural Domain Modulation within Flourescent Lipid Multilayers U.J. Krull, R.S. Brown and K. Stewart, Department of Chemistry, Erindale Campus, University of Toronto, Mississauga, Ontario 359

AP12 Atmospheric Measurements of Natural Hydrocarbons Using Gas Chromatography/Mass Spectrometry H. Niki and B.H. Khouw, Department of Chemistry and Centre for Atmospheric Chemistry, York University, Downsview, Ontario 363

Abstract Page

SESSION A: AIR QUALITY RESEARCH

Poster Presentations

AP13 **Utilization of Established Air Pollution Monitoring Networks in Ontario Following Nuclear Incidents** J.A. Slade and G. Laszlo, Radiation and Industrial Safety Branch, Atomic Energy of Canada Limited, Chalk River, Ontario 367

AP14 **A Re-Examination of Ontario's 24 Hour Ambient Air Quality Criterion for Hydrogen Fluoride** R.D. Jones and D.S. Harper, Air Resources Branch, Environment Ontario 377

AP15 **Production of Ozone-insensitive White Bean Varieties** T.E. Michaels, Department of Crop Science, University of Guelph, Guelph, Ontario 379

AP16 **Efficacy of Film-forming Chemicals for Protecting Roadside Trees Against Salt Spray** C. Chong, Ministry of Agriculture and Food, Horticultural Research Institute of Ontario, Vineland Station, Ontario 383

AP17 **An Evaluation of the Problems of Particulate Emission from the Wood Products Industry** M.F. Lepage and A.E. Davies, Rowan Williams Davies & Irwin Inc., Guelph, Ontario 387

AP18 **Relationship of Sugar Maple Decline and Corresponding Chemical Changes in Xylem Sap Carbohydrates, Micronutrients and Trace Elements** S.N. Pathak, T. Hutchinson and D.N. Roy, Department of Forestry, University of Toronto, Toronto, Ontario 391

AP19 **Identification of Long Range Aerosol Sources at the Dorset Environment Station** J. Drake, A. Kabir and S. Vermette, Department of Geography, McMaster University, Hamilton, Ontario 395

KEYNOTE PAPER I

Science-Based Innovation

Science-based innovation is critical in today's global economy to sustain and enhance a nation's prosperity. In seeking to sustain and enhance its prosperity by participating in a growing volume of world trade, large and small economies, face critical problems of adapting their institutions, policies and practices to a radically new environment. Key elements of this environment are that world trade now occurs in a global economy in which the interweaving of science, engineering and technology has acquired the power to transform the comparative advantage and prosperity of nations. With the scale, scope and openness of the international enterprise of science, the transferability of technologies and the mobility of capital, science-based innovation has become a driving force for the technological and corporate change that creates new tradeable goods and services. These conditions are radically different from those of the Industrial Revolution.

In a modern economy the sector which produces tradeable goods and services supported by the first service sector of financial, legal, energy, transportation, communication systems, etc., generates the income that enables a country to invest in the second service sector of education, health care and other personal and social benefits. (Figure 1). In some countries financial institutions have been operating in a manner that hampers the developments in the tradeable goods and services sector.

To participate in the global economy driven by science-based innovation it is essential that, on a national or regional basis, the pyramid of research capacity (in terms of knowledge flow) that leads to tradeable products and services has integrity, that is, that there be a reasonable balance of capacity throughout the pyramid. (Figure 2).

Increasingly science-based innovation requires a strong long-term applied research capacity, particularly in relation to emerging generic technologies, that is industry-based and controlled. This capacity has to be linked to a high quality fundamental research base and a strong market focused development capability.

Large and small countries in different stages of development faces problems in;

i) achieving structural integrity necessary for science-based innovation suitable for their limited resources of people and money, and

ii) using their limited resources effectively.

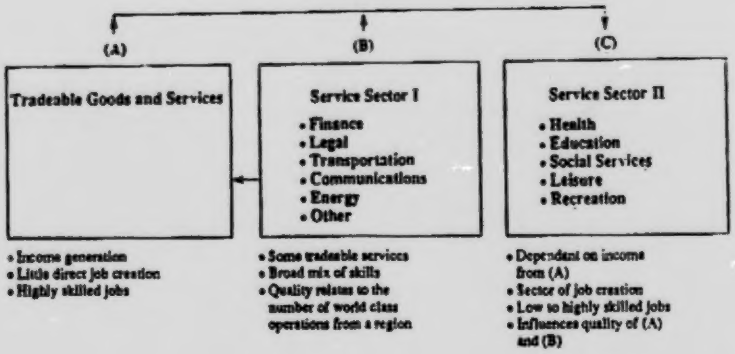
(A)
(B)
(C)
Tradeable Goods and Services
Service Sector I
• Finance
• Legal
• Transportation
• Communications
• Energy
• Other
Service Sector II
• Health
• Education
• Social Services
• Leisure
• Recreation
• Income generation
• Little direct job creation
• Highly skilled jobs
• Some tradeable services
• Broad mix of skills
• Quality relates to the number of world class operations from a region
• Dependant on income from (A)
• Sector of job creation
• Low to highly skilled jobs
• Influences quality of (A) and (B)

Figure 1: A Simple Model of the Economy

In today's global economy it is important to understand the relationship between innovation in the production of tradeable goods and services and the generation of income. A simple model in terms of stating the key issues is given in Figure 1. This model segments the economy into three blocks labeled (A) Tradeable Goods and Services, (B) Service Sector I and (C) Service Sector II. The major source of income which sustains our standard of living comes from sector (A) Tradeable Goods and Services. Canada's current standard of living requires very substantial volumes of trade into world markets. In the globally competitive market of today a nation must be concerned with maintaining and enhancing the environment it creates for business and industry that can innovate in the production of tradeable goods and services. To function effectively, such enterprises require a high quality service sector, namely (B) Service Sector I, comprising such services as finance, legal, energy, construction, communications, transportation, distribution. It is the combination of this business service sector (which produces some tradeable services) and the sector directly producing tradeable goods and services which generate the primary income of a region.

It is the income generated by the foregoing activities which allows the expansion of (C) Service Sector II that is concerned with personal and social services. The social service sector includes health care, education, community services, leisure and recreational activities. Our capacity to sustain and improve the services and opportunities depends on the capacity of sectors (A) and (B) to generate the necessary income.

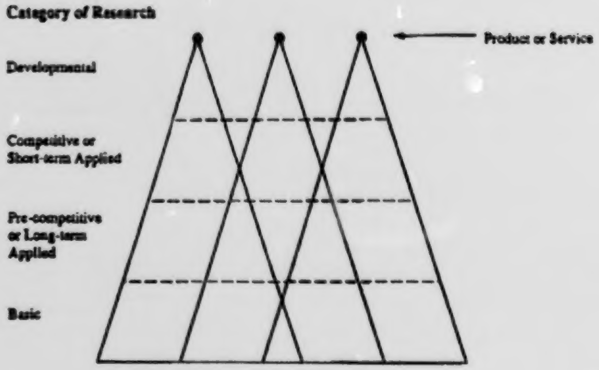

The Science-Based Pyramid of Research

Category of Research
Product or Service
Developmental
Competitive or Short-term Applied
Pre-competitive or Long-term Applied
Basic

Figure 2

Research as an element related to the overall process of innovation, can be broken down into three primary components that must be linked together to be effective:

1. Basic or fundamental research which is usually characterized by the researchers' primary objective being the generation of new knowledge and understanding about man and the world around us. This research is long-term (usually on a time-scale of 10 years or more), and has a high level of uncertainty in terms of what the results will be. In Western culture, basic research is primarily university-based and seldom results in knowledge that is of immediate commercial value. The knowledge gained from such research is rapidly and widely distributed to scientists throughout the world through publication in scientific journals. Because the results from this research are, or have been, considered a public good, this type of research has been financed primarily by the public sector and private benefactors. Increasingly, however, when knowledge contributed by basic research is critical for new product development, industries are becoming involved in basic research (OECD, 1987).

2. Applied research: In most countries, applied research is mainly carried out in industrial or government laboratories, but in some countries, there is substantial university involvement with respect to longer term research, particularly in schools of engineering, medicine and management. Applied research has a strategic target and attempts:

   - to extend the scope of understanding of materials and processes,

   - to determine how the accumulated knowledge from basic research, extend where necessary by focused specialized research, can be used to develop a potential new product or services, or

   - to determine how to modify and improve the performance of existing products or services to sustain their marketability.

   Applied research which is medium to long-term (on a time scale of three to ten years), also has a significant level of uncertainty, but because it is targeted, there is a probability that there will be economic benefit. The means for the financing of this research vary. In some sectors such as the pharmaceutical and chemical fields, the research is largely funded by the private sector primarily through the benefits from patent protection, whereas in fields such as aircraft and electronics, there has been a mixture of public and private financing. In some cases a monopoly position (e.g. AT&T and Bell Laboratories) has encouraged the funding of longer-term applied research, but there are few examples of the private sector being able to finance longer term applied research wholly from its own resources unless there is effective patent protection or the business has a monopoly position.

   It is common in some sectors to associate the processes of engineering design and development of a product or service as discussed above, with the term development or developmental research.

3. Developmental research is research that:

   - makes use of the fruits of applied research specifically to create a new marketable product or service, or

   - improves, through a series of small steps of innovation based on state-of-the-art knowledge, an already existing product or service, or

   - enhances the ease of production of a product or the provision of a service.

   This type of research has the least uncertainty, is carried out on a time scale of less than three years, and has the highest probability of economic benefit. Developmental research is mainly financed by the private sector, although there are exceptions in which there has been substantial public financing.

The foregoing categories of research can be represented by the pyramids shown in Figure 2. At the narrow peak of each pyramid is a product or service, a specific artifact of technology designed to perform a particular function in a market. From its peak each pyramid expands through the three primary categories of research to a broad base in basic research. The category "applied research" has been segmented into two slices labeled competitive (short-term applied) and pre-competitive (long-term applied). Competitive applied research is that which has direct proprietary value to the business. Pre-competitive applied research is that which is generally useful in sectors of industry (This research is often concerned with what can be called generic technology). The relative width of each slice across the pyramid suggests the range of generality of the knowledge associated with it. The overlapping of parts of the pyramids indicates that as one reaches towards the scientific roots pertinent to the development of a particular product, the knowledge base becomes relevant to a range of products. Indeed, the essence of basic science is that it seeks for general principles of understanding within particular circumstances of study, whereas engineering, through the technology it creates, seeks to realize a particular operational function in a market within the domain of possibilities bounded by science.

Science-based innovation then is innovation in which the realization of an effective and competitive product or service utilizes, through the focusing processes of the pyramid of research, the full range of scientific and engineering understanding pertinent to the function of the product or service in the marketplace.

The classification of levels of research in the research pyramid of Figure 2 is based on the diverse literature on innovation. Its pertinence for older, large-scale, science-based industries is clear. However, a key point today is that the research pyramid is relevant to all industry participating in the global economy of science-based innovation.

Copies of "INNOVATION AND CANADA'S PROSPERITY: THE TRANSFORMING POWER OF SCIENCE, ENGINEERING AND TECHNOLOGY" may be obtained by filling out the attached form.

KEYNOTE PAPER II

DERIVING BENEFITS FROM ENVIRONMENTAL RESEARCH

Stuart L. Smith, M.D.
President
RockCliffe Research and Technology Inc.
November 1988

As difficult as research can be, it is still more difficult to apply it swiftly for economic or social benefit. In addition to the usual obstacles to technology transfer, environmental research faces additional ones of a political nature. It behooves us to know a great deal more about how research is transformed into practical benefits and how environmental research in particular can be more rapidly applied. The improvement of the environment is an area where, with appropriate policies, economic and social benefits occur simultaneously.

In supporting research activities, we cannot take for granted that application will naturally follow any improvement in knowledge. More attention needs to be paid to the incentive structures of research organizations, the relationship to our industrial sector, and the interaction with political decision-making. By acting now in some specific areas, we can help guarantee that today's research will produce timely and tangible results.

SESSION A
AIR QUALITY RESEARCH
Oral Presentations

ENVIRONMENT ONTARIO PAPER

AIR QUALITY RESEARCH

Walter Chan
Air Resources Branch
Environment Ontario

The Air Quality Research Needs Document reflects the Ministry's mandate to protect the environment and human health, specifically as it is related to air pollution. The current research requirements are grouped under six categories, thirteen issues, and fifty-three needs. As one might reasonably expect, many of these entries are inter-related.

The six categories fall into two groups: primary and ancillary. The former includes the three basic components in the understanding of air pollution, namely, the environmental impacts/receptor (contaminant effects/toxicology/fates), the source (sources/inventories), and the intermediate processes (atmospheric processes) between the source and receptor. The latter includes regulation (risk management and criteria development), abatement (control and remedial technology) at the source and receptor, and sampling (instrument development and application), which is necessary for source, receptor and process studies.

Each category is broken down into issues which define the area of research more concretely, e.g. contaminant effects into human, ecosystem, and phytotoxicology; and sources into industrial/commercial, stationary/domestic, and mobile sources.

Under each issue, particular research needs are listed. These needs are meant to provide general rather than specific guidance to prospective applicants. Because of the nature of the categories and issues, many of the research needs can be linked to issues other than the one under which they are grouped. Also, atmospheric research is not independent of other environmental disciplines, readers are therefore encouraged to look at other research areas cross-referenced at the bottom of each issue page.

A1

Science and Policy:
Photochemical Oxidants and Acid Bearing Species

Kenneth L. Demerjian
Atmospheric Science Research Center
University at Albany
State University of New York

As scientific findings continue to pour in, pointing to one potential environmental crisis after another, society has become increasingly concerned and confused. It is clear that progress has been made in improving many aspects of the quality of our environment since the initial enactment of environmental legislation in the early 1970's. In spite of these improvements, many environmental problems persist and new and sometimes unanticipated problems have surfaced. Two recent examples being the stratospheric ozone depletion and climate change issues. The focus of this talk will be on the subject of photochemical oxidants and acid bearing species, considering the state of its science, existing environmental policy and regulation, and associate decision making issues.

Air quality management, through the implementation of air quality and emission standards, has been the corner stone of the Clean Air Act legislation within the United States. The air quality management framework is based on the concept that quantitative links between pollutant emission and ambient air quality can be developed which provide viable guidance as to the most effective and efficient pollution abatement strategies to meet existing air quality standards or to consider future policy options for the mitigation of a pending environmental problem.

As our understanding of attendant atmospheric processes governing the transport, transformation and disposition of pollutants evolves, so does our ability to prescribe the predictive accuracy of models which integrate these processes to simulated the fate and transport of pollutants in the atmosphere. But, our understanding is incomplete, as is our ability to precisely monitor the state of the atmosphere at all times and in all space. As a result, models must be viewed as imperfect tools providing imperfect information (predictions). This fact should not be construed as a condemnation of air quality simulation modeling or disincentive for their use in regulatory air quality management. It is meant to convey rather that the limits on our ability to predict the chemical and physical dynamics of atmospheric systems are real and becoming more quantifiable with our expanding knowledge. The development of quantitative measures and the effective utilization and communication of model uncertainty must be at the heart of the development effort so as to better serve the policy and regulatory decision making communities.

Uncertainty in science is generally perceived as relating to those aspects of science which as yet are not completely understood and await only the necessary research to resolve this lack of understanding. But in actuality this is not what uncertainty in science really represents. Though the quest of science is absolute "truth" (complete understanding), the precision of information about processes and the characteristic parameters for generating scientific understanding of observed phenomena is variable and finite.

In many instances the quantification of scientific uncertainty or lack thereof becomes the manipulated factor for contending interests to provide a rationale for decisions they prefer. Scientists, to some extent exacerbate this contention by not maintaining total objectivity in presenting factual data and allowing their value system to affect their scientific judgment. This can occur subtly and unknowingly or it may be done quite blatantly.

In any event the scientist's role is to provide his best objective and factual judgement on the nature and magnitude of the uncertainty associated with the scientific issues that have a direct impact on the public policy choices. The ramifications of the scientific uncertainty with regard to sorting out what public policy choices should be made is not part of the scientist's judgmental process, but the responsibility of the policy analyst/decision maker.

Over and over again science intensive public policy disputes surface where the scientific community is concerned that political contentions distort scientific advice to meet preconceived policy agendas, while political concerns believe that the scientist tend to over-interpret scientific analyses to either distort public policy disputes or attempt to preempt or unduly influence the public policy/political analysis process. In the context of this discussion the non-linearity issue with respect to sulfur control in the acid deposition debate and the current controversy on NO_x control with regard to strategies for meeting the ozone standard in the United States will serve as illustrative examples.

The quantification of the precision and accuracy of mathematical models developed to simulate the distribution and fate of chemical substances emitted into the atmosphere can be achieved if adequate data bases are developed for operational and evaluative purposes. Uncertainty analysis techniques continue to evolve and more efficient and effective techniques are likely to be developed, but present studies are limited more by the lack of evaluation data sets than uncertainty analysis approaches or methodologies.

The utilization of this information and future refined information in the regulatory decision making process as a result of the application of these modeling tools for strategy development and emission control decisions has not been attempted. This talk articulates some of the issues associated with incorporating this knowledge into the decision making process and provides some conceptual ideas as to how this might be approached operationally.

A2

Relationship Between Forest Decline and Root Health in Ontario Sugar Maple Stands.

By: Cindy Adams, Marika Egyed and Tom Hutchinson. Department of Botany and Institute for Environmental Studies, University of Toronto, Toronto, Ontario, Canada. M5S 1A1.

Abstract

In the past decade sugar maple (*Acer saccharum*) has shown a dramatic and decline in Eastern North America, particularly in southern Quebec where 80% of the trees are affected. Similar, more local declines are also occurring in Ontario, New Brunswick, Vermont, Pensylvania and New York. We have initiated a study to examine fine root systems of sugar maple in Ontario to determine whether fine root damage is a factor in their present decline. Specifically, we are assessing the health, biomass, mycorrhizal status, branching patterns and chemical composition of roots of healthy and declining mature sugar maples. Preliminary results show an alteration in the intensity of VA infection of declining sugar maple trees, with significantly higher levels of infection in moderately declining trees compared with the levels in healthy trees. Roots of severely declining trees, however, had very low levels of infection. These results, combined with lower levels of calcium in declining sugar maple roots could be important in their present decline. Soils collected under declining trees were lower in Ca, P, Mg and Mn, and elevated in Al, compared with soils from healthy trees. These "declining" soils resulted in a substantial reduction in root growth into ingrowth cores compared with ingrowth cores containing healthy soil.

INTRODUCTION

In eastern North America, Central Europe and Scandanavia the health of forests has declined dramatically over the past decade. The decline is particularly severe for coniferous species at high elevations where acid fogs and elevated oxidants and SO_2 occur frequently, and for european beech, maple, birch and oak at lower elevations. Hardwood tree species at low altitudes have received little attention but recent surveys in Quebec and Ontario have confirmed general suspicions that almost all hardwoods, including sugar maple, red maple, black cherry, white birch, yellow birch, red oak, basswood, beech, and green ash, are showing varying degrees of dieback. One of the worst affected hardwood species is sugar maple (Acer saccharum Marsh.) which has shown a very severe and rapid decline in southern Quebec, affecting up to 80% of the trees at present (Gagnon, personal communication), and more local declines in Ontario (McLaughlin et al. 1985), New Brunswick, Vermont, Pennsylvania and New York. Tree death may result in 3-5 years after the onset of symptoms.

In Germany, where the first alarms regarding forest decline were sounded, numerous investigations have attempted to determine the cause of specific forest diebacks and the way in which atmospheric pollutants (acid rain, acid fogs, ozone and SO_2) may be involved. In every instance where root systems were studied, damage to fine roots was observed, including mortality of fine rootlets (Ulrich et al. 1980; Murach 1984; Liss et al. 1984; Matzner et al. 1986), a lower ramification index (i.e. outgrowth of long scarcely branched roots) (Meyer 1987), damage of the endodermis (Hüttermann 1982), abnormal branching (Matzner et al. 1986), changes in chemical composition (Bauch and Schröder 1982, Murach 1984), changes in the vertical profile of roots (Murach 1984) and reductions in mycorrhizal infection (Blascke 1986, Vincent 1986).

This paper presents preliminary results of studies conducted to examine fine root systems of sugar maple trees in Ontario in an attempt to determine whether fine root damage is a factor in their decline.

There is already some evidence that the soils in declining sugar maple stands in Ontario and Quebec are inhibiting tree growth. The Ministry of the Environment (MOE) has reported high Al levels associated with fine root mortality in declining trees (McLaughlin 1987). In our laboratory, comparisons between sugar maple seedlings grown on soil collected from beneath healthy or declining mature sugar maples both in Ontario and Quebec, have shown that seedling growth, as well as tissue Ca, Mg, Mn and P is substantially lower on the "declining" soil, while tissue Al may be elevated (Kinch and Hutchinson unpub.; Hutchinson and Adams unpub.). Consistent reductions in the growth of roots of mature sugar maple trees in "declining" soils were shown in a field experiment using mesh bags (ingrowth cores) filled with soil collected from declining or healthy trees (Adams and Hutchinson unpub.).

These results together with the low pH values in these forest soils (3.5 - 4.5) and probable alterations in soil moisture levels due to loss of foliage, suggest a possible alteration in mycorrhizal status of sugar maple in relation to decline, which in fact constitutes a major hypothesis for forest-decline in Europe and North America. Mycorrhiza refers to a symbiotic relationship existing between the roots of vascular plants and a wide range of fungal species, in which the fungal sybiont ameliorates nutrient and water uptake by the plant root system, while assimilates from photosynthesis are transferred from the plant to the fungus(Tyminska et al. 1986; Brownlee et al. 1983). In addition to the reduction reported in the number of active mycorrhizal tips in declining compared with healthy Norway spruce in Bavaria (Blaschke 1986) and in beech exhibiting symptoms of decline in Germany (Vincent 1986), changes in the mycorrhizal fungal community (Kumpfer and Heyser 1986) and declines of mycorrhizal species of macrofungi (Jansen and van Dobben 1987; Termorshuizen and Schaffers 1987) have been associated with increased acidification of forest stands. Field and laboratory studies, manipulating substrate pH values have reaffirmed the sensitivity of tree mycorrhizal infection to reductions in soil pH (Reich et al. 1986; Dighton and Skeffington 1987; Metzler and Oberwinkler 1987; Blaske 1987).

It is known that sugar maple roots should be mycorrhizal at all depths (Kessler 1966). The relationship between the present decline of sugar maple and fine root damage, especially possible alterations in the mycorrhizal associations has not been studied. Accordingly, the specific objectives of this current study are as follows:

1. To make a detailed assessment of levels of mycorrhizal infection of individual sugar maple in Ontario in relation to the decline status of these specific trees.
2. If a relationship exists between the degree of mycorrhizal infection and tree decline, to establish cause-effect relationships by correlating the degree of mycorrhizal infection with soil pH and soil and foliar chemical levels.
3. To determine whether forest soils collected from under declining and healthy sugar maples differentially influence root health, chemical composition, fine structure and levels of mycorrhizal infection of mature sugar maples. Our previous research, using mesh bags (ingrowth cores) filled with healthy and declining soils, buried around maple trees with a range of decline status' at two Ontario sugar maple sites, showed a substantial reduction in root growth into the bags which contained the declining tree soil.

METHODOLOGY

Only a brief summary of our experimental design and methodology will be presented here. Data are preliminary and incomplete as many aspects of the current study were commenced in May of this year. However, we felt that many of the patterns that were emerging in the data were very interesting and provide some insight into the complexity of the forest decline phenomena. In view of the fact that sugar maple stands are dying at an alarming rate we hope that this new evidence of altered mycorrhizal symbiosis and root chemistry may spur new research to be initiated before valuable time is lost. Furthermore, the evidence of decreases in soil nutrients in conjunction with increased soil Al levels, adds to the growing evidence that links air pollution to forest decline and to soil acidification. The project consists of two main studies with the following experimental designs:

1. The relationship of mycorrhizal infection of forest trees with soil and foliar chemistry, and soil pH

In the summer of 1987, four Precambrian Shield study sites were established in the Muskoka and Parry Sound Districts of Ontario. The soils of these sites are podzolic, i.e. they are typically acidic and low in nutrient status. Three of these sites are declining sugar bushes (Miller, Ungard and Alf) and the fourth is a healthy control stand (Griffiths). Twenty trees exhibiting a wide range of decline were sampled in each of the declining sites, and twenty trees were randomly selected in the control site. All trees were accorded an index of decline using a detailed rating method that incorporates percentage of dead branches, chlorosis, premature fall colouration and percentage of undersized leaves (after MOE).

Four fine root samples from each of three main roots (i.e. 12 samples) for each tree (i.e. 20 trees/site) were excavated, washed and fixed in FAA for assessment of mycorrhizal infection. To date, only the declining sites, and for these only two-thirds of the root samples, have been assessed for mycorrhizal infection levels.

For all 80 trees described above, soil samples (5 per horizon) were collected from the A_o, A_e and B horizons and foliage samples from low, medium and high portions of the tree crown were collected in the 1987 field season. Soil samples have all been analyzed for pH but the chemical analyses have not yet been done on either the soils or the foliage.

2. Root ingrowth core study to determine the importance of soil related factors in sugar maple decline

In May, 1986 bulk soil collections were made separately from ten healthy and ten declining trees at two of the declining sugar maple sites used in the first study (Miller and Ungard). These soils were dried and sieved (<2 mm) to remove living and dead roots. Soils were then used to refill corings made around healthy and declining trees at these same sites (a total of 15 trees for the Miller site and 10 trees for the Ungard site). Corings were made to a depth of 10 cm at a distance of 1 m from the tree base, fiberglass screening bags were fitted tightly up against the sides of the hole left by the removed core, and then filled with the test soils. Both healthy and declining soils, as well as steam-sterilized and fertilized treatments of these two soil types were replicated 3 times around each of the sample trees at the two maple sites. The soils for the fertilizer treatment were amended with superphosphate (P_2O_5) and gypsum ($CaSO_4$). The refilled corings were dug out after 8 weeks and the roots which had grown into the bags were recovered by careful washing.

Immediately after the bags were brought back to the laboratory, 2 root samples were taken from each of the 480 root bags and fixed in FAA for future assessment of mycorrhizal infection. Some roots were also fixed in glutaraldehyde and osmium for sectioning and examination of the fine structure using transmission election microscopy.

Soil and tissue (root and foliage) chemistry

Soil samples were analyzed for pH using the distilled water/slurry and $CaCl_2$ methods. Following nitric acid digestion of roots and foliage, and nitric and perchloric acid digestion of soils, chemical analysis (P, Ca, Mg, K, B, Mn, S and Al) of samples was done using either ICP (inductively-coupled plasma emission spectroscopy) or atomic absorption spectroscopy. N was determined using a LECO CHN analyzer. Distilled water-extractable (i.e. an estimate of plant available) levels of these same elements were also determined for soil samples.

Microscopy

Fine root samples were fixed in FAA, cleared and stained for vesicular arbuscular mycorrhiza (VAM, the type of mycorrhiza formed in sugar maple roots) using a modified Trypan Blue staining procedure (Phillips and Hayman 1970). Root samples, mounted on glass slides and gently squashed under glass coverslips, were scored for percent mycorrhizal infection, as well as for the presence of non-mycorrhizal fungi, using a light microscope. Root tissue was fixed in glutaraldehyde and osmium for TEM using a previously published protocol (Scott and Larson 1984), to describe and compare cellular morphology of roots from healthy and declining trees.

Results and Discussion

Preliminary results clearly demonstrate a relationship between the degree of sugar maple crown decline and the amount of VAM infection in the trees' roots. Scatter plots of root mycorrhizal infection as a function of tree health reveal similarly shaped third order polynomial regressions for all 3 declining bushes (Fig. 1a-c). These show that for trees of at least moderate health there is an inverse relationship between tree health and VAM colonization. Declining trees, however, show increased mycorrhizal infection, while infection levels of severely declining trees are very low. These trends are more evident in the Ungard and Miller sites which were in a much more critical state of decline than the Alf site at the time of sampling. The combined data from all 3 declining sites were used for the scatter plot in Fig. 2, which shows a second order correlation between the

Fig. 1. Relation between mycorrhizal infection and tree health. (a=Ungard, b=Miller, c=Alf)

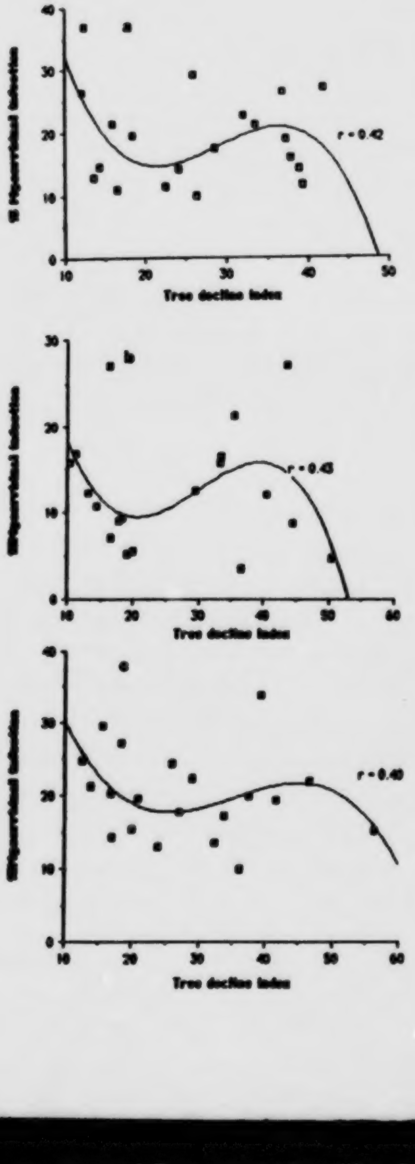

Fig. 2.

Relation between soil pH (A horizon) and mycorrhizal infection of individual trees (3 declining sites)

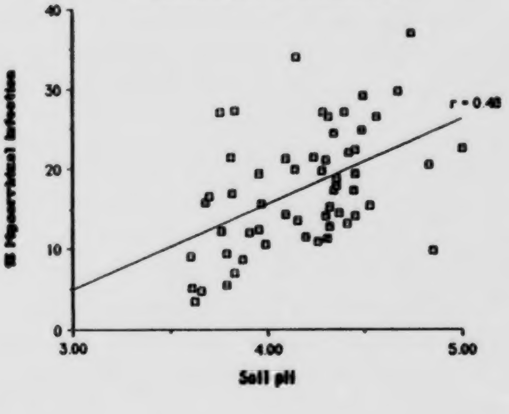

percent of root mycorrhizal infection and soil pH of the A_0 horizon for pH's between 3.00 and 5.00. This may indicate a detrimental effect on the fungal symbiont by soil acidification, either directly or indirectly via a change in the soil microflora resulting in reduced competitive effectiveness of VAM, or via a decreased ability of the trees to support the fungus with assimilates. Mycorrhizal fungal species have been shown to be negatively affected by low pH (Craw 1979; Metzler and Oberwinkler 1987), and field studies have revealed reductions in mycorrhizal communities as a result of acidification (Kumpfer and Heyser 1987; Jansen and van Dobben 1987; Termorshuizen and Schaffers 1987).

Light micrographs of cleared, squashed roots of sugar maple are presented in Plate 1, and show VAM structures similar to those described by Kessler (1966). The darkly stained cells containing VAM structures, as well as clear, uninfected cells are shown in Fig. 3. Figures 4-8 show higher magnifications of VAM structures inside maple roots, including mycorrhizal fungus hyphae, arbuscules and vesicles. Hyphae and arbuscules could usually be observed, while vesicles were abundant in some rootlets and rare in others. Hyphae were frequently seen as coils surrounding cortical cell nuclei (Fig.6).

At the cellular level (Plate 2), Fig. 9 shows bright field microscopy of a cross-section of a typical sugar maple root. The cortical region is heavily infected with VAM and contains abundant tannins. The fine structure of mycorrhizal roots is shown in the TEM micrographs in Figures 10-14. Infected cortical cells contain a highly lobed nucleus (Fig. 11). This altered morphology is thought to be induced by the VAM. A polyphosphate-like substance is seen in some vacuoles in Fig. 11. Hyphae and arbuscules of varying ages and stages of development were observed. In older stages of

Figs.1-6. Light micrographs of cleared, squashed roots of sugar maple (*Acer saccharum*) stained with trypan blue. Roots are, at most, 8 weeks old. Fig.1: A low magnification view showing darkly stained cells containing VAM (arrow), as well as clear, uninfected cells. Figs.2-6: Higher magnifications of VAM, including fungal hyphae (Hy), arbuscules (Ab) and vesicles (Ve).

Figs.7-12. Light and transmission electron micrographs of cross sections of roots of sugar maple. Fig.7: Bright field microscopy of a root cross section stained with TBO, showing a cortical region heavily infected with VAM. Epidermis (Ep); exodermis (Ex); cortex (Co); xylem (Xy). Fig.8: Cortical cells contain hyphae (Hy, black arrows) of varying diameters and age. Older hyphae are filled with lipid. Nuclei (Nu) can be seen in several of the cortical cells. Fig 9. An infected cortical cell containing a highly lobed nucleus (Nu). This altered morphology is thought to be induced by the VAM. Small vacuoles contain a polyphosphate-like substance (Pp). Fig. 10. A cross section through a branched arbuscule (Ab). Fine branches are vacuolated and contain a granular electron-dense deposit. Fig. 11. High magnification TEM of the fungal cytoplasm showing numerous profiles of endoplasmic reticulum (ER) and mitochondria (Mi). The fungal wall (FW) is degraded in appearance. Fig. 12. Cortical cells may contain aging hyphae with large lipid deposits (Li).

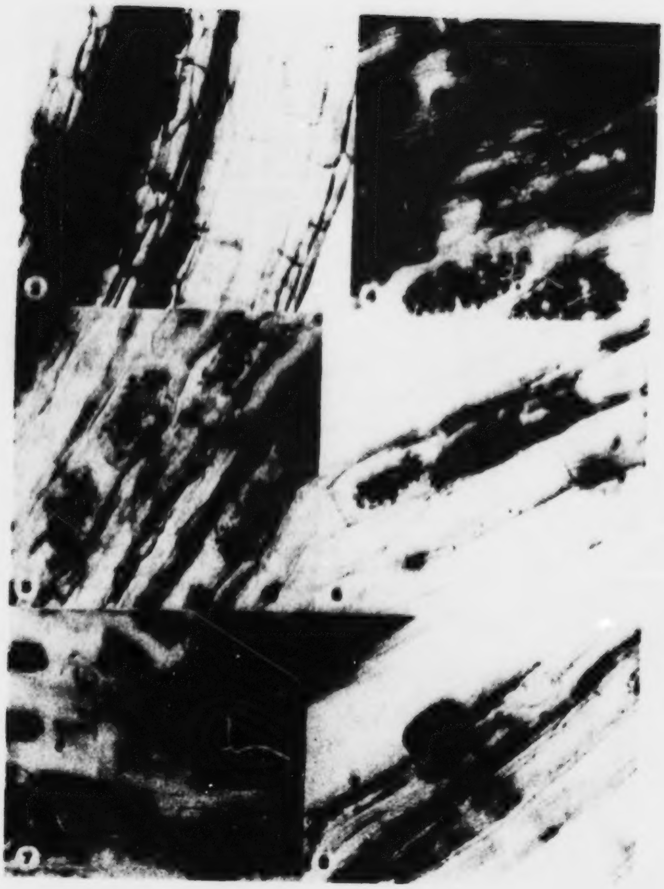

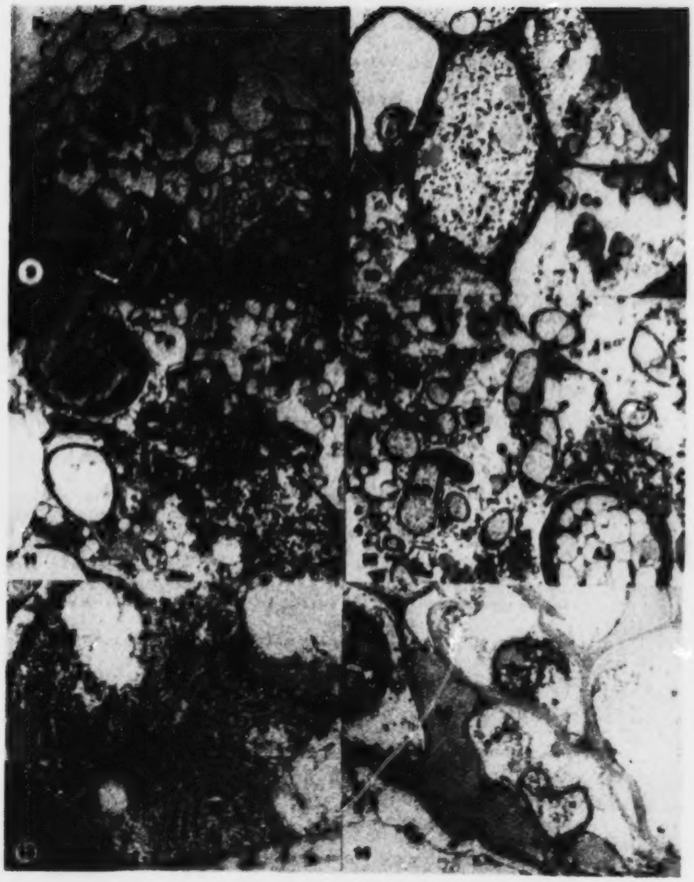

arbuscule formation the numbers of fine branch hyphae increase until much of the cortical cell is filled. Fine branches are vacuolated and contain a granular electron-dense deposit (Fig. 12). Older hyphae are filled with lipid (Fig. 14). Several points of penetration of external hyphae were common along a short length (1 cm) of root and caused overlapping of developmental stages of the fungus. Morphological features of the fungus cytoplasm such as the endoplasmic reticulum and mitochondria seen at the highest magnification in Fig. 13, imply metabolically active fungal tissue.

An important aspect of the TEM study in addition to describing sugar maple roots at the TEM level, which has never been reported, is to compare the fine structure of roots of declining and healthy trees. Early indications show that the root tissue of healthy trees did not preserve as well as root tissues of declining trees (i.e. the fixative penetrated better into declining roots), which may in itself be an indication of breakdown or changes in the cell walls or membranes in declining roots. More root tissue needs to be sectioned and examined to see if this is the case.

In the root ingrowth study we found mycorrhizal infection to be increased in slight to moderately declining sugar maple trees compared with healthy trees, and significantly decreased in the trees with severely declining crowns (Table 1). These results quite closely support the findings for the mycorrhizal infection of roots sampled in the first study; thus, different trees, different ages of roots, different sampling techniques and different years of sampling gave us the same pattern of significantly increased mycorrhizal infection in declining trees, but very low levels of infection in severely declining trees.

In the ingrowth core study preliminary results in Table 1 do not show a relationship between the type of soil (either healthy or declining) in the

Table I. Preliminary data on mycorrhizal infection of sugar fine roots in ingrowth cores containing soils from beneath trees in three categories of decline severity.

Decline index class[*]	Number of trees	Soil in root bag	Percent mycorrhizal infection ($\bar{x}\pm SD$)[†]
DI < 40	9	healthy soil	19±22
		declining soil	17±14
DI 40 - 60	4	healthy soil	53±21
		declining soil	45±16
DI > 60	2	healthy soil	12
		declining soil	15

---

[*] DI < 40 = healthy tree   DI 40-60 = declining tree
DI > 60 = severely declining
Decline indices incorporate loss of crown cover.

[†] Scoring based on number of VAM infected mm of cleared root tissue of the total mm examined for 6 roots/soil treatment per tree. Data are for the Miller site, and the fertilized and steam-sterilized treatments of declining and healthy soil have not as yet been scored.

mesh bags and the degree of mycorrhizal infection. However, the 8 week period in which the roots grew in the different soils may not be long enough to see an effect of soil chemistry on the developing mycorrhizal infection. Furthermore, the fungal inoculum may come primarily from the tree roots as they develop into the bags rather than from the soil itself, particularly since the soils with which the cores were filled were air-dried and sieved in the laboratory to remove any roots.

Strong differences occurred in the concentrations of elements in soils taken under either healthy or declining sugar maple trees (Table 2). The soil from declining trees had significantly lower levels of Ca, Mg and Mn for the Miller site, while for the Ungard site these same three nutrients, as well as P were significantly reduced, and Al was slightly higher in the declining soil. Suprisingly, for the Miller site the declining soil contained significantly higher P than the healthy soil; this finding is in contrast to previous analyses by Kinch and Hutchinson (unpub.) showing much lower P levels in the declining Miller tree soil compared to the healthy tree soil. A possible explanation is that the soil was collected in early May in the current study for the root bags, whereas in the work by Kinch and Hutchinson soil was collected in the summer and in the fall. Soil from the declining trees may release nutrients from the litter from the previous fall at a slower rate, combined with a greater uptake of P by healthy trees in the healthy area of this site when the roots begin to grow actively in April and May. The Ungard site was in a less critical state of decline than the Miller site at the time of this study and these seasonal shifts in P, from being higher in declining soils in early spring to lower in declining soils in the summer and fall were not seen.

The declining soils from both sites caused a dramatic reduction in root

Table II. Differences in the chemical characteristics of surface soils below either healthy or declining sugar maple trees at two Ontario sites. (Concentrations (mg/l) of elements in a 1:10 soil:water extract)

Soil health	pH	P	Ca	Mg	Al	Mn	S
Ungard							
Healthy	4.5	80±2	443±190	62±22	15±1	76±35	78±1
Declining	4.2	46±6	55±4	9±1	23±4	9±1	68±3
Miller							
Healthy	4.0	48+3	229±22	46±4	22±1	115±9	97±6
Declining	4.0	118+9	97±9	26±3	23±2	15±2	104±8

Values are the mean ± 1 standard deviation, n-3.

Table III. Calcium concentration (mg/l) of roots of healthy and declining trees from Miller growing into ingrowth cores containing different soils.

Tree health[†]	Soil health and treatment			
	Healthy	Declining	Healthy fertilized	Declining fertilized
Healthy (DI-10-40)	4972	4019	5793	5105
Declining (DI-50-70)	3752	3385	4634	4602

†: DI - decline index
Decline indices incorporate loss of crown cover.
Values are the mean of roots from 5 trees. For each tree, roots from 3 replicate ingrowth cores were homogenized and pooled.

growth into the mesh bags compared with bags containing the healthy soils (data not shown). These data show that the actual chemical state of the soil, rather than a reduced assimilate supply from stressed trees, is detrimental to sugar maple root growth. The reduction in levels of important soil nutrients in declining soils, combined in some instances with low pH and elevated Al, could account for the present decline in sugar maple.

Although we cannot entirely eliminate the possibility that a root pathogen, present in the declining soil and not in the healthy soil, is involved in the observed root inhibition two lines of evidence suggest this is not the case: (1) steam-sterilization of declining soil gave only a small (non-significant) increase in root biomass in the ingrowth core study (data not shown) and (2) preliminary microscopic examination has shown a number of non-mycorrhizal fungal species, possibly pathogenic, attached to roots, but these are seldom in abundance on the roots and as well they are observed on both healthy and declining tree roots.

Data for the chemistry of roots from Miller showed that Ca is significantly lower in roots of declining trees than healthy trees (Table 3). Furthermore, Ca concentrations were increased when roots grew into healthy tree soil, compared to the declining tree soil. The fertilizer treatment of superphosphate (P_2O_5) and gypsum ($CaSO_4$) increased the calcium levels in every case. Although not all of the elemental analyses are complete other important elements in the roots, including P, Mg and K, showed no response to the different soils. These results clearly show that Ca deficiency is a major factor inhibiting root growth of sugar maples at this site. Other results from various seedling experiments in our laboratory (Hutchinson and Adams unpub.; Kinch and Hutchinson unpub.) have shown that seedlings grown on declining tree soils for various Ontario and Quebec sites have deficiencies of Ca, Mg, Mn or P or any combination of these four. Aluminum was significantly higher in seedlings grown on the declining tree soil for some of the sites we examined.

Calcium plays an important role in cell wall structure and wall integrity in plants. It is interesting to speculate that the very low calcium levels associated with roots of declining trees may account for the significant increase in mycorrhizal infection levels in moderately declining trees, via either easier hyphal penetration or increased leakiness of the membranes to the carbohydrates and sugars the fungus needs to thrive. Rather than the normal symbiotic relationship, the mycorrhizal fungus may actually become parasitic on roots of the declining trees. The severe drop in infection in trees showing advanced stages of decline may show that trees in poor condition can no longer support mycorrhizae, leading to the further demise of the tree.

In conclusion, the findings from this work to date show that an alteration in the mycorrhizal infection of declining sugar maple trees, as well lower levels of calcium in declining tree roots could account for their present decline. Soils collected under declining trees were lower in Ca, P, Mg and Mn, and elevated in Al, compared with soils beneath healthy trees, and substantially reduced maple root growth.

ACKNOWLEDGEMENTS

We wish to thank The Ontario Ministry of the Environment and the Natural Science and Engineering Research Council for funding this study. Dr. Martha Scott collaborated in the TEM work; Steve Bull, Anton Holland and Craig Boljkovac provided field and technical assistance. We are grateful for their help.

REFERENCES

Bauch, J. and W. Schroder. 1982. Forstw. Cbl 101, 285.

Blaschke, H. 1987. In Proceedings of Nijmegen conference, Netherlands.

Blaschke, H. 1986. In Mycorrhizae: Physiology and Genetics, (Ed. V. Gianinazzi-Pearson), Proceedings of the First European Symposium on Mycorrhizae, INRA, Paris.

Brownlee, C., Duddridge, J. A., Malibari, A. and D. J. Read. 1983. Plant and Soil 71, 433.

Dighton, J., Skeffington, R. A. and K. A. Brown. 1986. In Mycorrhizae: Physiology and Genetics, (Ed. V. Gianinazzi-Pearson), Proceedings of the First European Symposium on Mycorrhizae, INRA, Paris.

Hüttermann, A. 1982. Mitt. d. Landesanst. F. Okologie, Sonderheft: Immissionsbelastungen von Waldokosystemen, Recklinghausen.

Jansen, E. and H. F. van Dobben. 1987. Ambio 16, 211.

Kessler, K. J. 1966. Can. J. Bot. 44, 1413.

Kumpfer, W. and W. Heyser. 1986. In Mycorrhizae: Physiology and Genetics, (Ed. V. Gianinazzi-Pearson), Proceedings of the First European Symposium on Mycorrhizae, INRA, Paris.

Liss, B., Blaschke, H. and P. Schütt. 1984. Eur. J. For. Path. 14, 90.

Matzner, E., Murach, D. and H. Fortmann. 1986. Water, Air and Soil Pollut. 31, 273.

McLaughlin, D. 1987.Maplefest, '87, Grand Falls, New Brunswick.

McLaughlin, D. L., Linzon, S. N., Dimma, D. E. and W. D. McIlveen. 1985. MOE Report No. ARB-144-85-Phyto.

Metzler, B. and F. Oberwinkler. 1987. Eur. J. For. Path. 17, 385.

Meyer, F. H. 1987. Allg. Forstzeitschr. 29.

Murach, D. 1984. Gott. Bodenkdl. Ber. 72.

Phillips, J. M. and D. S. Hayman. 1970. Trans. Br. Mycol. Soc. 55, 158.

Reich, P. B., Schoettle, A. W., Stroo, H. B. and R. G. Amundson. 1986. J. Air. Pollut. Cont. Ass. 36, 724.

Scott, M. and D. Larson. 1984. Can. J. Bot. 62, 1947.

Termorshuizen, A. J. and A. P. Schaffers. 1987. Plant and Soil 104, 209.

Tyminska, A., Le Tacon, F. and J. Chadoeuf. 1986. Can. J. Bot. 64, 2753.

Ulrich, B., R. Mayer and P. K. Khanna. Die Deposition von Luftverunreinigungen und ihre Auswirkungen in Waldokosystemen im Solling. Schriften Forstl. Fak. Univ. Gottingen, Bd.58, Sauerlanders Verlag Frankfurt/M., 1-291.

Vincent, J. 1986. In Mycorrhizae: Physiology and Genetics, (Ed. V. Gianinazzi-Pearson and S. Gianinazzi), Proceedings of the First European Symposium on Mycorrhizae, INRA, Paris.

A3

A Numerical Decline Index Rating System to Monitor Changes in Tree Condition of Hardwood Forest Species

D.L. McLaughlin, W.I. Gizyn, D.E. Corrigan, W.D. McIlveen and
R.G. Pearson (Ontario Ministry of the Environment) and R. Arnup
(Ecological Services for Planning Ltd.)

The Problem: Rating the health/decline status of forest trees.

Forest decline has become a serious and contentious issue in many parts of the world. Coniferous forests are affected in Europe, in parts of California and at high elevations in the mountains of the NE US (1,2,4,6,10,11). To date no incidence of coniferous forest decline has been reported in Canada. However, decline in Canadian deciduous forest tree species, particularly sugar maple (Acer saccharum Marsh) is widespread in southern Quebec (3). Recently sugar maple decline has also been reported in Ontario, to a lesser extent in New Brunswick, and sporatically the NE US (9). Decline of deciduous trees in Europe has also been reported, although the extent and severity is marginal relative to the effects observed in the coniferous forests.

There are presently more than 180 theories on the causes of forest decline, which illustrates the complexity and hints at the contentiousness of the phenomenon (5). However, regardless of the causes, all forest decline episodes have a common factor. This factor is the deterioration of the condition of individual trees. Consequently, individual tree condition assessment is required to document the severity of the problems in specific locations or regions. Most tree rating systems are subjective and the assessment parameters are broad. A common approach is to categorize the degree of crown defoliation; e.g. <10%, 11%-25%, 26%-50%, and >50%. Another frequently used rating system assigns a numerical value to the tree which approximates a decline gradient; e.g. 1 to 5 or 1 to 10, usually with the lowest number equivalent to a tree with no symptoms and the highest number representing a dead tree.

The various rating systems are mostly qualitative, nondescriptive and have a relatively poor resolution. Therefore subtle changes in tree condition cannot be measured, thereby severely limiting the value of the data for detecting trends. However, the greatest shortcoming is that the numerous different rating systems in use are not standardized making it impossible to directly compare the forest decline status between regions or countries.

When the decision was made in 1984 to initiate deciduous tree decline studies in Ontario, it was considered imperative that a rating system be developed which was quantitative, reproducable, and had a narrow confidence interval within a large gradient so that subtle differences could be detected. A high resolution, quantitative rating system was necessary so that regional differences in Ontario's deciduous forest could be recognized and to facilitate accurate trend detection analysis. The method developed to rate the health/decline status of Ontario deciduous trees was called the Decline Index.

How the Decline Index Works

In Ontario the symptoms most often observed in declining sugar maple trees are dieback of the fine branch structure, pale green or chlorotic foliage, and leaves which are distinctly undersized. These three descriptive crown parameters are individually assessed and then combined in a weighted formula which yields a numerical Decline Index (DI) value ranging from 0 (a healthy tree with no symptoms) to 100 (a dead tree). The DI formula is:

$$DI = DB + (A * UL) + (A * ST) + (A * SL/2)$$

where DI = decline index
DB = per cent dead branches
UL = per cent undersized leaves
ST = per cent strong chlorosis
SL = per cent slight chlorosis
A = (100 - DB)/400

Laminated field assessment templates were prepared which illustrate a series of deciduous tree crown silouettes in 10% decline gradients (i.e., 0% full crown, 10% defoliation, 20% defoliation ... 100% defoliation or dead tree crown). On the reverse side of the template are three series of colour chips. Each of the the three series contains 6 chips chosen to illustrate the range of foliar colour encountered in sugar maple in Ontario. One series represents normal green foliage, the second represents pale green or slightly chlorotic foliage and the third series illustrates the colour range considered to be strongly chlorotic.

With the assistance of the prepared silouettes on the laminated field template an evaluator who has been trained in the recognition of typical decline symptoms in Ontario, subjectively estimates, to the nearest 10%, the amount of crown branch dieback, slight and strong chlorosis and undersided leaves. This information is recorded on a tally sheet and the data is later transcribed to a spreadsheet file where the DI is automatically calculated.

Table 1 summarizes the DI for ten trees ranging in decline status from healthy to severe. In this example data set healthy trees had a DI ranging from 0 to 4, trees with light decline symptoms had a DI of 11 to 13, moderately declining sugar maple trees ranged from 22 to 25, severely declining trees had a DI between 40 and 45 and the DI of very severely declining trees ranged from 50 to 74. This example data set readily identifies the usefulness of the DI method; whereas the division of trees into ambiguous decline classes based on a subjective assessment is arguable (i.e. is the tree lightly, moderately or severely declining), the difference between the corresponding mean DI for each of these four classifications, (i.e. light = 12, moderate = 24, severe = 43 and very severe = 62), is quantified.

This example data set also illustrates another important component of the DI method, that is, the foliar parameters in the DI formula are weighted proportional to the live crown. Therefore, trees with a relatively low percentage of branch dieback can have an elevated DI if a large percentage of the living crown is chlorotic and the foliage undersized. This is important for two reasons; 1) foliar abnormalities are usually an early warning of crown dieback and 2) foliar characteristics usually change much quicker than branch structure. This adds an additional degree of sensitivity to the DI. Drawing again on the example data set in Table 1, the first three trees all have no crown branch dieback yet the resultant DI's are 0, 4 and 11 respectively. The difference is a progressive increase in the percentage of foliar chlorosis and undersized leaves. Another example is the last two trees in the table, one with 20% crown dieback and the second with 60% crown dieback and resultant DI's of 50 and 75 respectively. The tree with only 20% crown dieback has a high DI because of the foliar characteristics. However, if the subsequent growing season was favourable and the poor foliar conditions were not pathologically induced the foliage would likely recover and the DI the following year would then be much lower. The DI method can identify this rapid annual flucuation whereas such changes could go undetected or unquantified with assessment methods which use only branch characteristics or simply the presence or absence of foliage.

Looks Good, but is it Reproducable?

Although the DI appeared to have the attributes desired for the planned deciduous forest survey in Ontario it was still necessary to conduct a field trial to determine if the rating method was reproducable and to define confidence intervals. Ten trees representing a gradient of decline from perfectly healthly to dead were selected and sequentially numbered in woodlot a in southern Ontario. The ten test trees were scattered throughout the woodlot to such an extent that it was necessary to have a flagging tape trail to get from tree to tree. Ten people were trained for several hours in the identification of deciduous tree decline symptoms as they are used in the DI methodology. They were then provided with the DI field templates and proceeded to rate each of the ten marked trees. When all the trees had been rated by each of the evaluators, the tree identification numbers were changed and the rating sequence was repeated. Each of the ten trees was rated by all evaluators five times, with the tree identification numbers changed between assessments.

The tree numbers were changed and the trees spread throughout the woodlot so that the evaluators would not become familiar with individual trees and therefore bias their rating.

A second set of five assessment runs was conducted on the ten test trees with paired evaluators. Two evaluators discussed the rating parameters for each tree, agreed on one score, and filled in one assessment form per tree. As in the first series of assessment runs, the tree identification numbers were changed between runs. The assessment teams were altered between each of the five paired assessment runs.

The field trial yielded 75 DI values for each test tree. These data are summarized in Table 2. It clearly shows that the DI is reproducable, even with different evaluators trained only for basic symptom identification. It also indicates that the paired assessment provides a slightly better resolution of decline gradient and in most cases a narrower confidence interval. The 99% confidence interval for the single-evaluator assessment ranged from 2.2 to 5.2 whereas the range was 1.4 to 4.5 for the paired assessment. Similarly, the coefficient of variation was lower with the paired assessment for all but the healthiest tree with the lowest DI. The coefficient of variation was inversely rated with DI. This is not surprising because the proportional difference in the DI between individual evaluations is greater with healthier trees relative to trees in a more advanced stage of decline. For example, a healthy tree with a mean DI of 4 may have a range from 2 to 6, whereas a declining tree with a mean DI of 40 may have a range from 35 to 45. Proportionately the variation about the mean is much larger for the healthier tree even though the absolute difference is less.

How the Decline Index has been used in Ontario

1) Site Specific Studies

The DI method for assessing hardwood tree condition has been used at selected sites annually in the Muskoka area since 1984 and in the Peterborough area since 1985. Figure 1 is a histogram illustrating the mean annual DI for these two areas from 1984 to 1988. These data indicate that from 1984 to 1987 the condition of the hardwood forest at these sites was gradually improving. However, in 1988, as a result of high summer temperatures, drought and early season insect defoliation, the forest condition deteriorated significantly. Least significant difference analysis was used to confirm that relative to 1984 the apparent tree recovery and subsequent deterioration were statistically significant.

An examination of the individual rating parameters revealed that the increase in the DI in 1988 was driven by large percentage increases in foliar chlorosis and small leaf size and not an increase in branch dieback. This would suggest the deterioration is temporary and given favourable growing conditions in subsequent years a recovery is likely. Tree rating systems based solely on branch dieback or defoliation status would not have detected the 1988 episode.

2) Province Wide Survey

The DI was the primary assessment method used in a province wide hardwood decline survey conducted in 1986. One hundred and ten permanent observation plots were established across the Deciduous Forest Region of Ontario. Each plot contained 100 trees greater than 10 cm diameter at breast height. The DI was calculated for each tree and the mean DI was determined for each plot. Six DI ranges were selected based on the mean DI frequency distribution. Figure 2 was prepared illustrating each of the 110 plots as one of the six DI classes.

These data suggested a regional pattern of tree condition across the province. Generally, the severity and extent of decline was worse in the south-west and the north-central portion of the range of sugar maple in Ontario. In contrast a band of low decline across south-central Ontario separated these two areas of higher decline. This pattern is better illustrated by calculating the mean DI of plots within nine recognized forest regions in the Province (see Figure 3). These forest regions are based on soil and climatic parameters. Using Least significant difference analysis, the mean DI's in Figure 3 must be different by at least 4.7 to be statistically significant at $p < 0.01$. Therefore the apparent pattern is partially confirmed, that is the deciduous forest in the north-central part of the province is in fact in poorer condition than the south-central area of Ontario. The other area of relatively high decline, the south-west, is not different based on least significant difference analysis. However, using another statistical testing procedure, K-means Cluster analysis, the plots in the south-west, like those in the north, were most frequently grouped as high decline plots.

Advantages of the DI Method

1. Quantitative: - descriptive statistics applicable.
2. Descriptive: - combines both foliar and branch characteristics.
3. High Resolution:- capable of distinguishing subtle changes across a wide gradient.
4. Reproducable: - tests indicate acceptable confidence intervals.
5. Flexible: - individual assessment parameters can be changed to reflect regional symptoms.
6. Fast: - no specialized equipment and an efficiently designed field form yields rapid field assessment.

7. Non-specialized field crews: - field crews can be trained quickly to identify specific decline symptoms, no need to have forestry specialists.

8. Computer compatable: - assessment data lends itself to a spreadsheet-type handling system where only the various decline parameters need to be recorded in the field and the DI can be automatically calculated, thereby reducing data handling time and related error and facilitating descriptive statistics.

9. Standardization: - direct comparison between regions, states, provinces, countries etc. (providing assessment parameters have not been substantially altered).

Conclusions

The DI method of assessing deciduous tree decline has been used successfully in Ontario. Baseline data has been collected from a network of permanent observation plots. Subsequent surveys using the DI method will enable forest managers to identify changes in the condition of the province's hardwood forest and precisely where and to what extent any changes have occurred. The ability to accurately quantify temporal and spacial changes in forest tree condition is a vital component of any study into the effects of regional atmospheric pollutants or other stresses on a forest ecosystem.

Literature Cited

1) Binns, W.O. 1985. Forest decline - the view from Britain. Presented at the NATO Advanced Research Workshop on Effects of Acidic Deposition and Air Pollutants in Forests, Wetlands and Agricultural Ecosystems, Toronto, Canada.

2) Bucher, J.B. 1985. Forest damage in Switzerland, Austria, and adjacent parts of France and Italy in 1984. Presented at the NATO Advanced Research Workshop on Effects on Acidic Deposition and Air Pollutants in Forests, Wetlands and Agricultural Ecosystems, Toronto, Canada.

3) Gagnon, G., Robitaille, L. Roy, G. and C. Gravel, 1985. Dieback in maple stands - the behaviour of some ecological variables. Presented at the NATO Advanced Research Workshop on Effects of Acidic Deposition and Air Pollutants in Forests. Wetlands and Agricultural Ecosystems. Toronto, Canada.

4) Germany, Federal Ministry of Food, Agriculture and Forestry, 1984. 1984 Forest Damage Survey. pp. 1-24.

5) Hinrichsen, D. 1986. Multiple Pollutants and Forest Decline. Ambio, 258-265.

6) Johnson, A.H. and T.G. Siccama, 1983. Acid deposition and forest decline. Environ. Sci. Technol. 17: 249A-304A.

7) McIlveen, W.D., McLaughlin, D.L. and R.W. Arnup, 1988. A survey to Document the Decline Status of the Sugar Maple Forest in Ontario: 1986/87. Ontario Ministry of the Environment, Air Resources Branch, Phytotoxicology Section, Report No. ARB-158-88-Phyto.

Literature Cited (Cont'd)

8) McLaughlin, D.L. Corrigan, D.E. and W.D. McIlveen, 1989. Etiology of Sugar Maple Decline at Selected Sites in Ontario. Ontario Ministry of the Environment, Air Resources Branch, Phytotoxicology Section, Report No. ARB-202-87-Phyto.

9) McLaughlin, D.L. 1987. Maple Decline in Ontario: Situation/Status Report. Presented at Maplefest 87, Grand Falls New Brunswick, June 12-13, 1987.

10) Scott, J.T. Siccama, T.G. Johnson, A.H. and A.R. Breisch, 1984. Decline of red spruce in the Adirondacks, New York. Bulletin of the Torrey Botanical Club, 111: 438-444.

11) Swedish Forestry Association, 1985. Forests in Danger.Cited from J. Air Pollution Control Association, 35: 897.

12) Tomilson, G.H. 1983. Dieback of red spruce, acid deposition and changes in soil nutrient status - a review.in: Effects of Accumulation of Air Pollution in Forest Ecosystems (B. Ulrich and J. Pankrath, eds). D. Reidel Publishing Co., Dordrecht. Holland, pp. 331-342.

13) Vogelmann, H.W. 1982. Castastrophe on Camels Humps. Nat. Hist. 91: 8-13.

Table 1: A sample feild assessment form for 10 example trees ranging in condition from healthy to very severely declining.

Decline Classification	% Crown Dieback	Leaf Colour			Leaf Size		Decline Index
		Normal	Chlorotic		Normal	% Undersized	
			% Slight	% Significant			
healthy	0	X			X		0
healthy	0		10			10	4
light	0		30	10		20	11
light	10		10			10	13
moderate	10		30	20		20	22
moderate	20		10	10		10	25
severe	30		10	20		30	40
severe	40		10	10		20	45
very severe	20		20	60		80	50
very severe	60		20	40		90	74

Table 2: Results of feild trials to test the Decline Index for reproducability and to evaluate single and paired assessment.

Tree No. & Condition	Single Assessment*			Paired Assessment**		
	Mean Decline Index	Coeff. Var.	99% Con. Inter.	Mean Decline Index	Coeff. Var.	99% Con. Inter.
1. healthy	7	92%	2.2	2	165%	1.4
2. healthy	8	84%	2.2	8	49%	1.8
3. light decline	14	70%	3.2	13	35%	2.3
4. light decline	18	59%	3.6	17	54%	4.5
5. moderate decline	18	61%	3.8	21	38%	4.0
6. moderate decline	23	67%	5.2	23	40%	4.5
7. moderate decline	26	48%	4.4	26	21%	2.7
8. severe decline	29	31%	3.1	32	16%	2.6
9. severe decline	41	35%	4.8	45	12%	2.7

* tree assessment conducted by one person (total number of assessments per tree = 50, 5 times by 10 different people).

** tree assessment conducted by 2 people who together filled in one assessment form (total number of assessments per tree = 25, 5 times by 5 different 2-person crews).

Total number of individual tree trial assessments = 750.

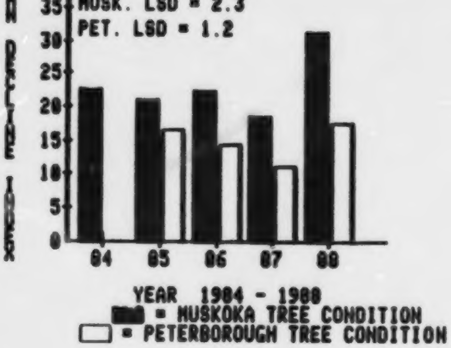

Figure 1: Mean annual Decline Index for test plots in the Muskoka and Peterborough areas of Ontario. LSD = Least Significant Difference.

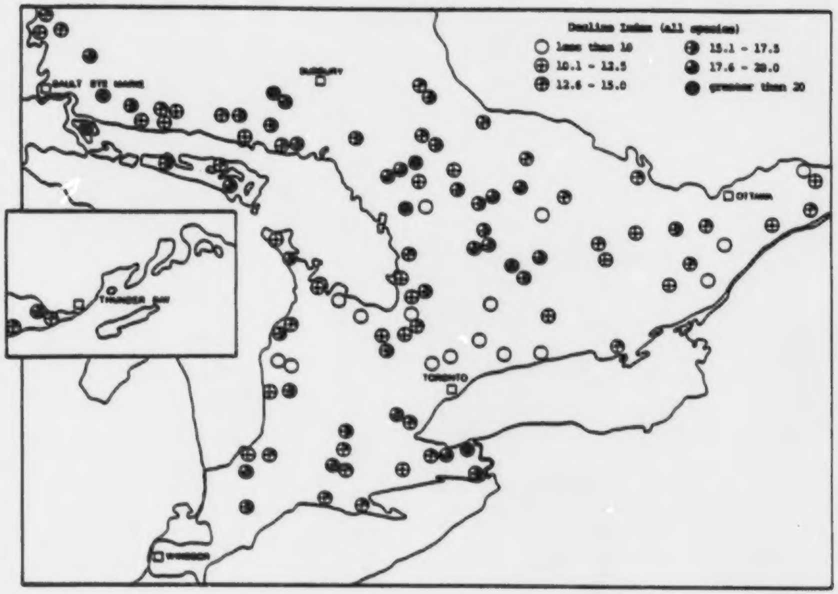
Decline Index (all species)
less than 10
10.1 - 12.5
12.6 - 15.0
15.1 - 17.5
17.6 - 20.0
greater than 20
SAULT STE MARIE
SUDBURY
OTTAWA
TORONTO
THUNDER BAY
WINDSOR

Figure 2: Mean Decline Index of 110 permanent forest observation plots, assessed in 1986.

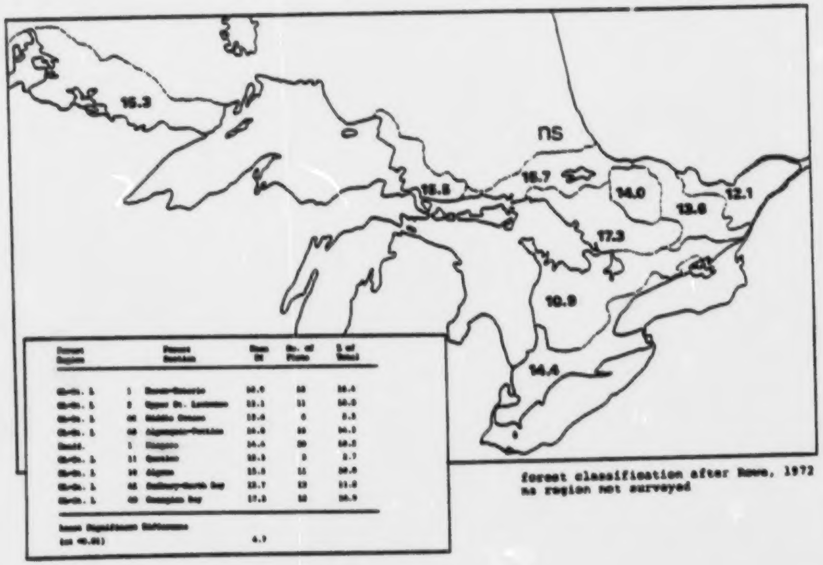
16.3
ns
15.5
15.7
14.0
13.6
12.1
17.3
10.9
14.4
4.7

forest classification after Rowe, 1972
ns region not surveyed

Figure 3: Mean Decline Index of 9 forest sections in Ontario, based on the 1986 assessment of 110 plots illustrated in Figure 2.

A4

Investigation of Short-Term Mutagenicity and Chemical Composition of the Organic Solvent Extractable Fraction of Coke Oven Emissions.

by: A. Horton, N. Belson, K. Shaw & G. Thomas

ORTECH INTERNATIONAL, MISSISSAUGA, ONTARIO

INTRODUCTION

This study represents part of an ongoing investigation, the objective of which was to determine if a practical ambient air standard for PAH is possible based on mutagenic activity. It was not the intent of this investigation to further control coke oven operations. Coke oven locations were selected to obtain large amounts of PAH's for tiered biological tests. Samples were collected at three coke oven sites in Ontario.

BACKGROUND

The Phase I program involved the assessment of sampling protocol and analytical methods. The sampling program included direct sampling of a coke oven throughout the coking cycle by means of a hole drilled through the coke oven lid (LID samples). These samples represent the worst cases and were collected to insure sufficient material was available for all subsequent tests. Concurrently, samples were also collected on top of the coke ovens (Coke Oven Top Side Samples - COTS) during the complete coking cycle. These samples represent the environment on top of the coke ovens that has previously been linked to health effects. LID samples consisted of Hi-Vol filters backed up with polyurethane foam plugs and a Lo-Vol filter. COTS samples consisted of three Hi-Vol filters with foam back up and two Lo-Vol filters. Coefficient of Haze (COH) was also measured on the coke oven top. The use of multiple Hi-Vol samplers was to insure the collection of sufficient material for biological testing. The Lo-Vol coke oven top side samples were collected as the link to health effect studies.

REVIEW

The Phase I study showed that the dichloromethane soluble fraction (DSFTPM) of coke oven emissions was positive and mutagenic for Salmonella tester strain TA-98 in the presence of metabolic activation. The study further showed that the DSF induced Sister Chromatid Exchanges in Chinese Hampster Ovary Cells (SCE-CHO) in the presence and absence of metabolic activation. The highly volatile material collected on PUF's was also positive and mutagenic for Salmonella strains TA-98 and TA-1537 with metabolic activation.

Chemical analysis indicated that most of the compounds present in the DSF, that were gas chromatographable, were polycyclic aromatic hydrocarbons. They consisted of unsubstituted PAH's, alkylated derivatives and nitrogen containing aza-arene type compounds. The study further showed that the concentration of major PAH's was consistent throughout the coking cycle and that the same compounds were present in the top side samples. The PUF samples that collected the pass through gaseous components contained mostly low molecular weight PAH type compounds.

During Phase II, selected samples from Phase I were utilized to further define and quantify the chemical composition of the coke oven emissions and relate these results to the mutagenicity of the unfractionated samples. This was achieved using a fractionation scheme in order to separate the complex mixtures into well defined sub-fractions to better isolate the mutagenicity and chemistry.

RESULTS AND DISCUSSIONS

The collected samples provided information that was used to establish the relationship between Hi- and Lo-Vol samples for specified parameters i.e. TPM, SOF and mutagen density.
This paper discusses the relationships obtained using all available valid data. The plots presented show the data and the results of simple regression analysis performed using the Lotus 123's data regression function. The solid line represents the regression line calculated for the data. The regression was forced through zero since no weight gain by the filters without sample collected was expected. The Coefficient of determination (R-squared) was calculated and reported.

The first relationship to be established was for TPM determined as the weight gained by the sampling filters. For comparative purposes, all solids data were expressed as mg/m^3 of air sampled. Figure 1 shows a plot of the Lo-Vol TPM vs the Hi-Vol TPM at Mill #1. The value of R-Squared was 0.57 indicating a 57% chance of a correlation between Lo-Vol and Hi-Vol TPM at Mill #1.

Figures 2 and 3 show similar plots for Mill #2 and Mill #3 data. The correlation is much better in these cases (R-Squared = 0.95 for Mill #2 and 0.78 for Mill # 3.

Figure 4 shows the result of plotting all Lo-Vol TPM data vs all Hi-Vol TPM data from the three mills. The value for R-Squared was 0.65.

The fact that the LID samples were collected directly from a coke oven and the collection time was very short, usually 30-60 seconds before the filter became plugged, these correlations are considered to be quite acceptable.

A relationship was established for LID SOF. These samples not only represent two different sampling methods (Lo-Vol and Hi-Vol), but the particulate was extracted with different solvents. The Hi-Vol samples were extracted with dichloromethane, and the Lo-Vol samples were extracted with benzene to provide a link with previous health effects studies.

Only a limited number of samples were extracted at each mill. Figure 5 shows the regression analysis for the mill #1 samples where the most data was available. The value for R-Squared was 0.89 considered good for this type of sample, and suggests that the particulate collected by both sampling methods contained similar amounts of extractable material.

Figure 6 shows the regression analysis of plotting all LID SOF data from the three mills together on one graph. The value for R-Squared was 0.88.

The COTS samples were collected for periods of time ranging from 2 to 15 hours in order to collect sufficient material for both chemical and biological testing. Figure 7 shows the regression analysis for averaged TPM in mg/m^3 for the two Lo-Vols and the three Hi-Vols collected at Mill #1. The value of R-Squared was 0.73. The data collected at Mill #2 represents a very narrow concentration range i.e. 3.9 - 4.7 mg/m^3 (Lo-Vol) and 7 - 9.4 mg/m^3 (Hi-Vol). These data are consistent with observations made during the sample collection i.e. poor visibility.

Figure 8 shows the same plot for the Mill #3 data. The value for R-Squared was 0.93.

Figure 9 shows the data obtained at all three mills plotted on the same graph. It is interesting to note that the Mill #2 data appears to represent a single data point. The value of R-Squared was 0.73 and the plot shows how the data all fit the curve.

With respect to the COTS samples, only those selected for biological testing were solvent extracted. Figure 10 shows the correlation obtained for all COTS SOF. The value obtained for R-Squared was 0.88.

The LID and COTS Hi-Vol samples provided sufficient material to enable all required biological and chemical testing to be conducted. The analysis of the data shows that a reasonable correlation exists between the Hi-Vol/Lo-Vol sets of samples for both the LID and COTS. This correlation provides the link for this study with existing health effects studies.

The possibility of a relationship between TPM and Coefficient of haze (COH) was examined. If a relationship exists, then COH measurements might permit a method of real time monitoring of emissions. Figure 11 shows a plot of average COH/1000 ft. vs Hi-Vol TPM mg/M^3. The value of R-Squared was 0.48.

Figure 12 shows the regression analysis of the Lo-Vol and Hi-Vol TPM data for the same samples used for the COH correlation. The value of R-Squared was 0.51, almost identical to that determination for the correlation of COH vs Hi-Vol TPM.

Figure 13 shows the results of regression analysis obtained for the COH vs Lo-Vol TPM. The value for R-Squared was 0.95. This correlation is probably a result of the similarity of the sampling methods used to collect the respective samples.

An important aspect of this study was to determine whether a correlation exists between the SOF of TPM and Ames mutagenicity assays. Mutagenic activity is expressed as the specific activity which is determined as revertants per microgram of sample. The mutagen density which corresponds to the amount of mutagenic material per cubic meter of air at the sampling location was used for the purpose of correlation analysis. The mutagen density is a product of the specific activity for a Salmonella tester strain (revertants/µg) and the weight of SOF/m^3 of air.

Figure 14 shows the plot of all LID sample mutagen densities (TA-98H) versus the corresponding SOF (mg/m^3). The value for R-Squared was 0.91 which indicate a good correlation. Figure 15 shows a similar plot of all COTS sample mutagen densities (TA-98H) versus the corresponding SOF (mg/m^3). The value for R-Squared was 0.82 indicating a good correlation.

Although the data presented is limited, it shows that there is a good relationship between TPM and SOF for both LID and COTS samples. A good relationship is observed between mutagen density (TA-98H) and the concentration of the SOF (mg/m^3) for both LID and COTS samples. Furthermore, the chemical identification evidence, determined on the various fractions collected for selected SOF samples, showed that the mutagenic responses were due mostly to PAH.

The chemical analysis of the various fractions has resulted in the tentative identification of approximately 80 chemical compounds, the majority of which are PAH. The majority of the parent PAH plus alkylated species were present in fraction #2 and the aza-arene type PAH species were present in fraction #3.

A comparison of the fractions collected in terms of percent of the original extract for the different sample types is presented in Figures 16-19. In the case of the LID samples, Fraction #2 represents 54% in Mill #1 and 51.9% in Mill #2. Similarly, in the COTS samples, Fraction #2 represents 41.8% in Mill #1 and 32.6% in Mill #2.

Mutagenicity testing with TA 98 with S-9 activation of the fractions showed that all of the mutagenic activity detected for the unfractionated (FO) samples could be accounted for by the response for the fraction 2 (F2) samples.

Specific Activity (revertants/μg)
TA-98 with S-9 Activation

	Mill #1		Mill #2	
	FO	F2	FO	F2
LID	19.3	23.7	24.9	25.1
COT	14.0	15.9	10.8	Tox

Quantitative data has been produced for the F2 fractions of the various samples. Identification and quantitation was restricted initially to the sixteen PAH on the MOE priority list. That is by using a calibration standard consisting of the sixteen PAH and their respective retention time data, the appropriate compounds were identified in the fractions and quantitated.

Quantitation data was determined for all other peaks present in the GC-TIC profiles using a chrysene standard as the calibration standard. This procedure has permitted the calculation of data for all individual peaks in the GC-TIC profiles to be expressed in terms of µg/mL. Using appropriate base peak data, it was possible to group the major PAH groupings according to molecular weights into actual weights for a given group e.g. all 228 or 252 for the parent PAH or 192, 242 and 266 etc. for PAH alkylated derivatives. Where appropriate, tentatively identified compounds as related to the sixteen PAH standard, could be assessed on an individual weight basis. These µg/mL weights for the individual compounds or for the compound groupings determined in the various fractions have been converted to µg/mg of dry weight. All of the Ames tests were conducted over the same concentration range. Therefore, the actual weights of the various chemicals applied to the plate for each of the fractions tested are related to the amount of each component per µg of material applied to the test plates and can be calculated.

Some examples of the type of data generated are detailed in Figures 20 and 21. These figures show in bar-chart form the actual µg/mg of the various PAH groupings present in the fractions used in the Ames bioassay. Included in the figures are the actual molecular weight groupings and the specific activities calculated for the respective fractions. In these cases B(a)P has been reported on an individual basis since it is known to be a biologically active PAH.

A5

QUANTITATIVE MEASUREMENTS OF THE GENETIC EFFECTS OF INHALED CARCINOGENS IN PULMONARY FIBROBLASTS ARE NOW POSSIBLE.

John A. Heddle*, A. Bouch and John D. Gingerich, Department of Biology, York University, Toronto M3J 1P3

Methods for the routine measurement of chromosomal aberrations and gene mutations have been established for pulmonary fibroblasts after exposure to carcinogens in vivo. After exposure the fibroblasts are isolated by a procedure involving trypsin digestion, plated in vitro, and analysed. For mutations, the frequency of thioguanine-resistant cells is measured at 10 days, when they are most frequent. Plating efficiency is determined by seeding cells on a layer of lethally irradiated feeder cells. The potency of a carcinogen can be expressed as the frequency of mutant cells induced per unit dose applied in vivo.

For chromosome aberrations the frequency of micronuclei is determined after 3 or 4 days of in vitro culture, when they are most frequent, using an in situ assay. Currently experiments are underway to determine if the cytochalasin block method will make these measurements quicker or more sensitive. Again an in vivo mutagenic potency can be calculated.

Validation of these two measurements on carcinogens specific for the lung and for other sites is in progress and will be reported.

A6

EFFECT OF THE ENVIRONMENT ON ASTHMA IN CHILDREN.

L.D. Pengelly* and C.H. Goldsmith;
Departments of Medicine, and
Clinical Epidemiology and Biostatistics
McMaster University
1200 Main St. West, Hamilton, ON, Canada, L8N 3Z5.

INTRODUCTION

"Rates of hospital admission/separation for asthma and rates of death from asthma have increased dramatically among children and young adults during recent years in Canada."(1). In the United States, asthma is the most common chronic disease of childhood, affecting 15 percent of Americans under the age of 15. "It ranks first among the chronic diseases in causing school absenteeism, and it has been linked to lowered academic performance."(2) Asthma is the commonest cause for admission to hospital in North America and twice as common as the next most common cause (6). The rate of hospitalization in the U.S. for children under 15 years old with asthma has increased at least 145% in the period 1970 to 1984 (12). Studies have also shown that asthma often continues into adult life, with only brief improvement in adolescence (3,4). Appropriate diagnosis and treatment reduces morbidity in childhood, and it is possible that good control in childhood may reduce severity in adult life (3,5).

These are disturbing statistics, both from the point of view of public health, and from the point of view of resource costs in the health care system. It is not clear whether the increase in morbidity and mortality is a result of increasing prevalence or severity, or by past underdiagnosis and undertreatment, or by a combination of factors. However, there is some evidence in the literature that the respiratory environment plays a role in the pathogenesis of asthma.

Environmental factors associated with asthma/wheeze.

Becklake et al. were not able to demonstrate any effect of air pollution on the prevalence of asthma in their study in Montreal (10). Weiss et al. found that persistent wheeze was associated with parental smoking, in their study of children in the Boston area. Environmental factors examined included the use of gas heaters in the kitchen, and crowding in the home, neither of which were found to be associated with persistent wheeze (9). Schenker et al. were not able to confirm the observation of Weiss and co-workers that persistent wheeze was associated with parental smoking. In their study, in rural Pennsylvania, they also included socioeconomic status (SES) and the use of gas stoves for cooking. Lower SES was found to be associated both with the use of gas stoves and increased prevalence of persistent wheeze, but when SES was accounted for, no effect of gas stove use on prevalence of persistent wheeze was found (7). Ware and co-workers, in the "Six Cities" study, found strong effects of parental smoking on "wheeze" in their study of over 10,000 children (13). They did not observe an effect of gas stove use on the prevalence of wheeze, and in a later report were not able to observe an effect of air pollution on "wheeze" although significant associations with increased prevalence of lower respiratory illness were observed (8). Fergusson et al. were not able to show an association of asthma with parental smoking, but did observe that parental smoking contributed to increased rates of lower respiratory infection in the first two years of life. A number of other environmental factors (socioeconomic, pets in the home) were examined, and were not reported to be associated with increased asthma prevalence (11). Silverman and co-workers reported acute effects of suspended particulates on asthmatic adult subjects which changed in direction depending on the season, and found difficulty in interpreting these data (17). Thus there is little evidence to date that air pollution has an effect on either the prevalence or the severity of asthma in children.

Background.

We have been examining the effect of environmental factors on the respiratory health of a cohort of over 3200 schoolchildren in Hamilton, Ontario. Design, methods, and some early results have been previously reported (14,15,16). This communication reports on an aspect of the study which has only recently arisen from a specific analysis of asthmatic children found in this cohort.

METHODS

A stratified random sample of over 3200 children was drawn from all children born after 1968 attending Levels (corresponding to 'Grades') 2, 3, and 4 of the schools of the Board of Education of the City of Hamilton in September 1978. The overall design was to use respiratory health as an outcome or dependent variable. Respiratory health was assessed in part from pulmonary function measurements made in the schools, and in part on the basis of parents' responses to questions about the health of the child in the previous year. The major independent variable of concern was air pollution, but important covariables included the child's respiratory history as an infant, as well as other environmental covariables, such as parental smoking and the use of gas for cooking. The objective was to determine the relative importance of the different independent variables in determining the state of respiratory health at the time of measurement.

Parents (usually the mother) were asked questions relative to the child's home environment, in addition to questions on respiratory health. These questions provided information on housing, socioeconomic status, health of family members other than the study child, cooking fuel, and the smoking habits of the household.

Pulmonary function testing was performed in the school. The apparatus used was an Hewlett-Packard pneumotachograph based Pulmonary Calculator System. Computations were performed internally and a graphic output of records was obtained for each child at the time of testing. Measurements were made of indicators derived from the forced vital capacity manoeuvre, as well as the single- and multiple-breath nitrogen washout manoeuvre. For the purposes of this report, two indicators derived from the FVC will be used to describe pulmonary function: FEV_1/FVC (Ratio of volume forcibly exhaled in the first second of a maximum exhalation, to the forced vital capacity); and MET (Mid-Expiratory Time, the period during which the middle half of the forced vital capacity is exhaled).

Exposure to SO_2 was determined using data obtained from a network of 10 continuous SO2 analysers, and exposure to the fine fraction (FF; <3.3 um AMMD) of suspended particles from a network of 7 Andersen cascade impactors. Spatial gradients in SO_2 and FF were found to exist over the city, and 1 year mean exposures were calculated for each child according to the geographical location of their school. The method of calculation of exposure depended on the generation of a 3-dimensional 'surface' based on monthly mean data, which represented the pollutant concentration in the 'z' axis, as a function of the geographical 'easting' and 'northing' coordinates in the 'x' and 'y' axes respectively. From this surface, the exposure of a child to the pollutant was obtained by estimating its concentration from the surface at the location of the school the child attends. A 1-year exposure was obtained by determining the arithmetic mean of 12, monthly mean, school-based values.

For each pollutant, the children were divided into two groups: those with exposure above the median level (for SO_2, 10.6ppb; for FF, 46 ug/m^3), and those below. Each group was further divided into children with a physician diagnosis of asthma, and those without. Comparison of the value of the two pulmonary function variables FEV_1/FVC and MET was made between groups. Data presented here are for what we refer to as "Period 2", corresponding essentially to the calendar year 1980, and the mean age of the cohort at this time was 10 yr.

RESULTS

We analysed the response of the asthmatic children to both SO_2 and FF in Period 2, compared to the rest of the cohort. Results are shown in the Table on the next page. From this Table it may be seen that there were no statistically significant changes in airflow obstruction in asthmatic children associated with a higher level of exposure to fine fraction, but there were statistically significant but clinically unimportant decreases in airflow obstruction in normal children associated with a higher exposure to fine fraction, detected only in MET but not in FEV_1/FVC.

We found statistically and clinically significant increases in airflow obstruction in the asthmatic group demonstrated by two reliable indicators of pulmonary function, associated with increased chronic exposure to SO_2 at the relatively low levels found in Hamilton during this period (median 10.6 ppb, range 8.4-17.5 ppb annual arithmetic mean). This was not observed in the rest of the cohort; in fact statistically but not clinically significant decreases in airflow obstruction were observed in the rest of the group, consistent with the earlier observations with respect to SO_2 we reported in November 1986. The former is a particularly surprising finding, because it demonstrates airflow obstruction in asthmatic children associated with SO_2 exposure levels one to two orders of magnitude less than previously observed for acute exposures in adults.

CROSSECTIONAL ANALYSES OF PULMONARY FUNCTION OF NORMAL AND ASTHMATIC CHILDREN

EXPOSURE TO FINE FRACTION

(Median 46; min 34; max 59 ug/m^3)

PULMONARY FUNCTION	MALES		FEMALES		COMBINED	
	ASTHMA	NORMAL	ASTHMA	NORMAL	ASTHMA	NORMAL
(NUMBER)	(68)	(1564)	(46)	(1493)	(114)	(3057)
FEV1/FVC						
FF ABOVE	0.742	0.796	0.754	0.828	0.746	0.812
FF BELOW	0.764	0.801	0.780	0.829	0.771	0.814
MET				*		*
FF ABOVE	0.791	0.617	0.808	0.538	0.798	0.577
FF BELOW	0.744	0.622	0.721	0.554	0.734	0.590

EXPOSURE TO SULPHUR DIOXIDE

(Median 10.6; min 8.4; max 17.5 ppb)

PULMONARY FUNCTION	MALES		FEMALES		COMBINED	
	ASTHMA	NORMAL	ASTHMA	NORMAL	ASTHMA	NORMAL
(NUMBER)	(68)	(1564)	(46)	(1493)	(114)	(3057)
FEV1/FVC					*	
SO2 ABOVE	0.728	0.797	0.754	0.830	0.737	0.813
SO2 BELOW	0.775	0.800	0.776	0.827	0.776	0.813
MET	*			*	*	*
SO2 ABOVE	0.842	0.618	0.822	0.537	0.835	0.578
SO2 BELOW	0.702	0.622	0.725	0.556	0.712	0.590

Notes:

Decrease in FEV1/FVC reflects increase in airflow obstruction.

Increase in MET reflects increase in airflow obstruction.

Significance: $p < 0.05$ = (*)

DISCUSSION

Increased MET indicates increased airway obstruction, as does a decreased FEV_1/FVC ratio, and children with asthma show both increased MET and decreased FEV_1/FVC compared with normal children. Children with asthma show a further clinically significant increase in MET and decreased FEV_1/FVC associated with increased SO_2 levels, while normal children show a clinically not significant reduction in MET only, with increased SO_2. These observations suggest that 1-year exposure to increased SO_2 in the 10-20 ppb range is associated with an increase in airway obstruction in asthmatic children, not observed in normal children.

We believe that our observations are of major importance, when viewed in the context of the "acid rain" problem. SO_2 is likely to be a component of "acid rain" which has a substantial impact on respiratory health, but the levels associated with "long-range transport" typically are well below the levels where acute effects have been shown on asthmatic subjects in controlled environmental chamber studies. Demonstration of clinically significant effects at low levels in a sensitive population underline the importance of better SO_2 control.

Asthma as a New Public Health Concern.

The recognition of an increase in the prevalence, morbidity, and mortality of asthma has been well documented recently in many industrialized countries, and whether there is a causal link to "acid rain" has not been established. In our own study, asthma prevalence was not found to be associated with higher levels of SO_2; but we have demonstrated that the consequences of chronic SO_2 exposure to asthmatic subjects are to further decrease their already compromised pulmonary function.

Since new estimates of asthma prevalence in children in Canada range from 10 to 20%, and possibly higher, it is clear that a substantial part of the Canadian population may be already suffering the ill effects of low-level exposure to acid gases, particularly SO_2.

(Supported by Ont. Ministry of Envt.; Health & Welfare Canada)

REFERENCES

1. Mao Y; Semenciw R; Morrison H; MacWilliam L; Davies J; Wigle D. Increased rates of illness and death from asthma in Canada. Can Med Ass J. 1987 Oct; 137: P 620-24.

2. Esquibel KP; Foster CR; Garnier VJ; Saunders ML A program to help asthmatic students reach their potential. Public Health Rep 1984 Nov-Dec; 99(6): P 606-9

3. Martin AJ, McLennan LA, Landau LI, Phelan PD. The natural history of childhood asthma to adult life. Br Med J 1980; 280:1397-400.

4. Blair H. Natural history of childhood asthma: 20 year follow-up. Arch Dis Ches 1977; 52:613-9.

5. Speight ANP, Lee DA, Hey EN. Underdiagnosis and undertreatment of asthma in childhood. Br Med J 1983; 286:1253-6.

6. Ellis-EF. Asthma in childhood. J Allergy Clin Immunol 1983 Nov; 72(5 Pt 2): P 526-39

7. Schenker MB; Samet JM; Speizer FE. Risk factors for childhood respiratory disease. The effect of host factors and home environmental exposures. Am Rev Respir Dis 1983 Dec; 128(6): P 1038-43

8. Ware JH; Ferris BG Jr; Dockery DW; Spengler JD; Stram DO; Speizer FE. Effects of ambient Sulfur oxides and suspended particles on respiratory health of preadolescent children. Am Rev Resp Dis 1986; 133: P 834-42

9. Weiss ST; Tager IB; Speizer FE; Rosner B. Persistent Wheeze: Its relation to respiratory illness, cigarette smoking, and level of pulmonary function in a population sample of children. Am Rev Resp Dis 1980; 122: P 697-707

10. Becklake MR; Soucie J; Gibbs GW; Ghezzo H. Respiratory health status of children in three Quebec urban communities: An epidemiologic study. Bull Europ Physiopath Resp 1978; 14: P 205-221

11. Fergusson DM; Horwood LJ. Parental smoking and respiratory illness during early childhood: a six-year longitudinal study. Pediatr Pulmonol 1985 Mar-Apr; 1(2): P 99-106

12. Halfon N; Newacheck PW. Trends in the hospitalization for acute childhood asthma, 1970-84. Am J Public Health 1986 Nov; 76(11): P 1308-11

13. Ware JH; Dockery DW; Spiro A III; Speizer FE; Ferris BG Jr. Passive smoking, gas cooking, and respiratory health of children living in six cities. Am Rev Resp Dis 1984; 129: P 366-76

14. Kerigan AT, Goldsmith CH, Pengelly LD. A three-year cohort study of the role of environmental factors in the respiratory health of children in Hamilton, Ontario. Am Rev Respir Dis 1986; 134:987-93.

15. Pengelly LD, CH Goldsmith, AT Kerigan, W Furlong, and SA Toplack. The Hamilton study: Effect of particle size on respiratory health in children. In: Aerosols; Eds. SD Lee, T Schneider, LD Grant, and PJ Verkerk: Chapter 57, pp. 753-766. Lewis Publishers, Chelsea, Mich.,USA; 1986.

16. Pengelly LD, CH Goldsmith, AT Kerigan, W Furlong, and SA Toplack. The Hamilton Study: Estimating exposure to ambient suspended particles. J.Air.Poll.Contr.Ass. 37: 1421-1428, 1987.

17. Silverman F, P Corey, A Ayiomamitis, and HR Hosein. Health effects on asthmatics of daily variations in exposure to particulate matter. Proc.(Ont.Min.Envt. Tech.Transfer Conf.) A2:1-20; Toronto, ON, November 30 - December 1, 1987.

A7

HAZARDOUS CONTAMINANTS IN ONTARIO: ENVIRONMENTAL FATE AND HUMAN EXPOSURE

by

D. Mackay

S. Paterson

W. Y. Shiu

Institute for Environmental Studies

University of Toronto

Toronto, Ontario, M5S 1A4, Canada

A paper to be presented at the 1988 Annual Technology
Transfer Conference, November 28-29, 1988

ABSTRACT

During recent years our group has been developing and testing various models which describe the environmental fate of hazardous chemicals in Southern Ontario. The current status of these models is reviewed. A capability now exists of estimating the prevailing concentrations of such chemicals in air, water, soil and sediments provided that physical chemical properties and emission rates are available. The models can vary in region of application, in complexity and can be steady and unsteady state in nature. In recent work, these models are being extended to assess the magnitude of exposure of a typical Ontario family by routes of air inhalation and water and food ingestion. The principal challenge in this work is quantifying the air-soil-vegetation-meat and dairy products route. Finally, progress is being made in developing pharmacokinetic models which enable these "external" exposures to be translated into concentrations or "internal" exposures in various human tissues. It is thus becoming possible to quantify the entire journey of a toxic chemical from emission source to human target organ and explore how these target concentrations will respond to various strategies of emission or loading reduction.

INTRODUCTION

During the last decade various environmental models have been developed to describe or predict the multimedia fate and behavior of chemicals (1-5). These models vary in complexity and may be steady- or unsteady-state in nature. The models accept data on the chemical's physical chemical properties, reactivity, transport characteristics, and extent of release to the environment to produce a comprehensive picture of the chemical's pathways between, and ultimate concentrations in, various media such as soil, air, water, and sediment. This modelling capability is a necessary adjunct to toxicity testing when assessing risk from chemical exposure and for determining priorities for research and regulatory action. It can be applied to new and existing chemicals. A major purpose of such models is to produce lists of priority chemicals such as Ontario's "EMPPL" list.

Of most concern are chemicals that are, or may be, in frequent commercial use and therefore will be discharged constantly to the environment over a period of time. Examples are pesticides, PCB's, wood preservatives, and by-products of incineration.

The use of the fugacity approach in some of these models (1,2) simplifies the algebra and clarifies the interpretation. This approach has been used by other groups for example, in the development of the OECD Environmental Exposure Potentials (EEP) model, ECETOC assessments, the U.S. EPA ENPART model (which uses the model as a first level screening method to predict the environmental fate and human exposure potential of new and existing chemicals), the National Institute of Public Health and Environmental Hygiene (RIVM) in the Netherlands and the Mitsubishi-Kasei Institute of Toxicological and Environmental Science in Yokohama (6-12).

In this paper we describe recent studies in our group supported by the Ontario Ministry of Environment which have sought to develop, validate and implement environmental models of the multimedia fate of chemicals. Further, we describe current efforts, hopes for the future, and speculate on how environmental models may evolve as regulatory and scientific tools. First, we describe the development of a novel fugacity model.

THE FOUR MEDIA FUGACITY MODEL

Previous models have described the fate of chemicals in a multitude of media such as air, aerosols, water, fish, particles, sediment, sediment pore water, etc. From an examination of this situation, it has become clear that we can simplify the model with little loss of fidelity by treating only four bulk phases - air, water, soil and sediment, which consist of subcompartments of fluid (air and/or water), solid and biotic matter. Equilibrium partitioning of chemicals is assumed to apply within each of the four bulk phases. As a result only four fugacities are defined, but it is possible to calculate concentrations in subcompartment phases.

Expressions for environmental emissions, advective inflow and outflow, reaction, and diffusive and non-diffusive transfer between these bulk phases are incorporated in a set of mass balance equations as included in previous models. Reducing the number of key environmental media to four permits a simple algebraic solution which can be implemented on a personal computer. Unlike previous models, non-diffusive transfer processes, such as wet and dry atmospheric particulate deposition, rain washout, leaching to groundwater from soil, and sediment resuspension are included.

Fugacity

In this model partitioning of chemical between phases is described by the equilibrium criterion of fugacity as an alternative to chemical potential.

Fugacity can be considered to be the partial pressure of a chemical in a phase and is related to its concentration in that phase by the expression

$$C = fZ$$

where C is concentration (mol/m^3), f is fugacity (Pa) and Z is the fugacity capacity (mol/m^3.Pa) which is specific to the chemical, the medium and temperature. Z values are deduced from physical chemical properties such as molecular mass, solubility, vapour pressure and octanol-water partition coefficient. Methods of calculating Z values for environmental phases have been reviewed by Mackay and Paterson (1). This data set represents an absolute minimum for chemical fate assessment.

Table 1 lists the properties of six priority chemicals which have been the subject of assessment in this project. A significant part of our efforts has been devoted to measuring and correlating these properties which are of fundamental importance in any fate assessment.

Chemicals move between phases by diffusive and non-diffusive processes. The diffusive flux N (mol/h) between two phases, 1 and 2, can be described by

Phase 1 to 2 rate = $D_{12}f_1$

Phase 2 to 1 rate = $D_{21}f_2$

Net rate $N = D_{12}f_1 - D_{21}f2$

where D_{12} and D_{21} are transfer coefficients with units of mol/h.Pa, and f_1 and f_2 are the phase fugacities. The difference between f_1 and f_2

determines the direction of diffusive flux (but not non-diffusive flux) which takes place from high to low fugacity. The coefficients D_{12} and D_{21} are functions of Z values, interfacial areas and diffusion properties, (characterized by diffusivities or mass transfer coefficients) in adjacent phases (2).

Non-diffusive or one-way transfer processes between phases, for example, wet or dry particle deposition from the atmosphere to soil or water, or suspended sediment deposition or resuspension, is described by a one-way transport parameter as

$$N = GC = GZf = Df \text{ mol/h}$$

where G is the volumetric flow rate (m^3/h) of the transported material (eg sediment), and D again has units of mol/Pa.h.

First order reaction processes in a phase can be described by

$$\text{rate of reaction} = k_R VC = k_R VZf = D_R f \quad \text{mol/h}$$

where k_R is a first order rate constant (h^{-1}), V is the phase volume (m^3), and D_R again has units of mol/Pa.h.

In summary all rates of chemical transport and transformation can be expressed as products of fugacities and D values. D values can be summed and compared when the processes apply to the same source phase fugacity.

Environmental Media

Four major bulk compartments are defined - air, water, soil, and sediment consisting of a combination of subcompartments of pure and particulate phases of defined volume fractions. For example, bulk water consists of "pure" water, suspended solids, and fish; soil consists of mineral matter, organic matter, water, and air; air consists of pure air and aerosols; sediment is mineral matter, organic matter, and water.

This environment can be "evaluative" or purely hypothetical in nature as described in previous papers (3,13) or it can represent an actual region. We apply the model here to i) an environment scaled to represent Southern Ontario and ii) an evaluative environment of area 1 sq km with similar phase proportions. The air height has been reduced to 2000 m from 6000 m to reflect conditions of atmospheric accessibility in Southern Ontario.

The assumption that equilibrium exists within each bulk phase, (ie. a common fugacity applies) implies that the times required to reach equilibrium within a bulk phase are short compared to times required to reach equilibrium between bulk phases.

Levels of Model Complexity

Environmental scientists compete within the arena of the refereed scientific literature to produce models which are more reliable, comprehensive and valid. A consequence of this pressure is a tendency to produce increasingly complex models - an understandable direction because the environment is a very complex system.

This produces a problem because individuals in industry and government who use these models have relatively little time to learn the intricacies of the models and acquire the necessary input data. Further, the more conscientious are reluctant to use and trust models which they do not fully understand. We believe that the answer is to offer a series of models, varying in scope, complexity and data needs. Presumably as users become more familiar with the simple models they will become increasingly dissatisfied with their simplifying assumptions and move towards more complex models. Situations of greatest concern which merit most effort will justify the most detailed assessment using the most complex models. Often a simple model will give an adequate answer to a simple question. Accordingly we have developed a series of models, increasing in complexity.

Level I Calculations

Using the phase volumes and Z values (obtained from physical-chemical properties) and an assumed total amount of chemical present, M mols, it is possible to calculate its equilibrium partitioning in this multimedia environmenta. A mass balance gives

$$M = \sum V_i C_i = f\sum V_i Z_i$$

The prevailing fugacity can thus be calculated as $M/\Sigma V_i Z_i$, followed by bulk concentrations, individual subcompartment concentrations (as Zf) and amounts as CV or VZf. This provides a picture of the dominant media into which the chemical partitions and provides a first approximate estimate of relative concentrations. Table 2 gives an example of such calculations.

The primary difficulty is estimating the amount of chemical M. Two approaches can be used. First is to gather concentration data for various media and calculate and sum amounts for the region of interest. Second, if an emission or use rate is available eg. 1000 kg/year and an approximate environmental persistence can be estimated, eg. 0.3 years, then the amount present will be the product of these quantities or 300 kg. If concentration data are available for one or two media (eg. fish and air), it is possible to select M by trial and error to obtain the reported values for fish and/or air. There is usually order-of-magnitude uncertainty about M.

This simple model does not treat reactions, inflow in air and water and other loss processes.

TABLE 1: PHYSICAL CHEMICAL PROPERTIES OF SELECTED PRIORITY CHEMICALS AT 25°C.

Chemical	Mol. Mass g/mol	Vapor Pressure Pa	Solubility g/m^3	logK_{OW}
Hexachlorobiphenyl*	350	5×10^{-4}	3.5×10^{-3}	6.8
benzene	78	12700	1780	2.13
benzo a pyrene	252	7.3×10^{-7}	3.8×10^{-3}	5.98
hexachlorobenzene	285	1.5×10^{-3}	5.0×10^{-3}	5.47
mirex	322	2×10^{-4}	1.93×10^{-5}	6.8
trichloroethylene	131.5	9870	1100	2.29

* average properties of isomers

TABLE 2: LEVEL I CALCULATION OF PCB DISTRIBUTION IN SOUTHERN ONTARIO

Total amount 3×10^6 mol or 1.07×10^6 kg

Fugacity 1.8×10^{-7} Pa

Compartment	Volume m^3	Conc.	Amount mol.	%
Bulk Air	4×10^{14}	3 ng/m^3	36000	1.2
Bulk Water	4×10^{12}	9.5 ng/L	109000	3.5
Bulk Soil	1.2×10^{10}	50 ng/g	2.7×10^6	88
Bulk Sediment	8×10^8	60 ng/g	216000	7.0

Subcompartment example:

Air-gaseous	2.5 ng/m^3	0.95 %
Air-aerosol	0.5 ng/m^3	0.23 %

Level II Calculations

In this model two loss processes are considered, advection ie. loss by outflow mostly in air or water, and degrading reactions. Also included are three "pseudo advection" processes. Transfer from air to higher altitude can be assumed to occur at a specific velocity. Leaching from soil to groundwater can be set at a percentage of the rain rate on soil. Sediment burial rates can be assumed and will equal the difference between sediment desposition and resuspension rates. Values suitable for specific regions can be inserted.

Reaction rates are included as first order rate constants applicable to the bulk or pure phase. These rate constants or half-lives are chemical-specific and usually result from a consideration of the rates of processes such as biodegradation, photolysis, oxidation and hydrolysis, individually and in total.

If emission rate data are available, a steady state, equilibrium calculation can be completed. The emissions rate should include point and nonpoint sources, and to it should be added advective inflow at a suitable "background" concentration or fugacity. From a mass balance, the prevailing fugacity can be calculated, followed by concentrations, amounts and inflow and loss rates. It is illuminating to examine the relative importance of these loss processes. The total amount present M can be calculated and used to estimate the chemical's overall "persistence" or average residence time. This time is a combination of the reaction time or persistence and the advection residence time.

Table 3 gives an illustrative calculation for PCBs in Southern Ontario. This behavior profile contains the assumption that a common fugacity prevails throughout the environment. Clearly this is in error because fugacities tend to be higher in the media which receive direct discharges and lower in those which have relatively rapid loss mechanisms. In particular, it appears that the air often experiences a low fugacity because of the high rate of advective loss. To remedy this assumption it is necessary to allow for fugacity variation between media and include expressions for interphase transport conductivities or resistances and introduce the emissions on a medium-specific basis as in the more complex Level III calculation.

Level III Calculations

Steady state mass balance equations can be set up for each of the four bulk phases which incorporate emissions, transfer rates between adjacent phases, reaction and advection. Four algebraic equations result which can be solved simultaneously. The principal difficulty is to estimate the intermedia transfer rate parameters or D values. These D values depend on the Z values (which are chemical specific) and on other kinetic quantities such as mass transfer coefficients or deposition rates of suspended matter.

It is important to emphasize that in the model single typical values have been assumed for all kinetic terms, ie. they are not chemical specific. There is thus no need to include more chemical-specific data in the Level III calculation. The dependence of transfer rate on chemical properties is

TABLE 3: LEVEL II CALCULATION OF PCB IN SOUTHERN ONTARIO

Fugacity	2.8×10^{-8} Pa		
Input emissions	45 mol/h	Advection	1 mol/h
Residence time	1.2 years		
Amount	4.8×10^{5} mol		

		Loss Rates (mol/h)	
Compartment	Conc.	Reaction	Advection
Bulk Air	0.5 ng/m^3	-	47
Bulk Water	1.5 ng/L	0.03	1.4
Bulk Soil	8 ng/g	6.4	10^{-4} (leaching)
Bulk Sediment	10 ng/g	0.5	0.4 (burial)

TABLE 4: SELECTED REPORTED AND CALCULATED CONCENTRATIONS FOR TEST CHEMICALS USING LEVEL III MODEL. Calculated values in parentheses.

Chemical	
PCB	Air 1-10 (1.4) ng/m^3: Water 1-10 (5) ng/L
	Fish 0-1.7 (0.2) ug/g
Benzene	Air 16 (2.5) ug/m^3
BaP	Air 1.3-7.1 (3.0) ng/m^3: Soil 0.1-0.5 (0.04) ug/g
	Sediment 80-300 (190) ng/g
HCB	Air 0.2 (0.2)* ng/m^3: Water 0.05-1 (2.7) ng/L
	Fish 0.003-0.05 (0.1) ug/g
TCE	Air 6.4 (11) ug/m^3
Mirex	Water 0.002-30 (0.002) ng/L
	Fish 0-0.04 (0.0001) ug/g

* Emissions adjusted to give reported air concentrations

contained entirely in the Z values which comprise part of the D values. No claim is made that the assumed coefficients are applicable to other environments, indeed there is considerable doubt about some of the values in Southern Ontario. The user is encouraged to modify these values in the light of experience. The values given should be regarded as only reasonable first estimates.

This model contains approximately 40 environment-specific parameters (volumes, velocities, diffusivities etc.) which are assumed to apply to all chemicals. In many cases the values are not well established (eg sediment deposition rate), thus the user should regard these parameters as initial order-of-magnitude estimates which will be subject to change in the light of experience. Reaction rate constants are both chemical and environment specific. Finally emission rates are region-specific and are often the most poorly quantified of all variables.

Reasonable parameter values have been assembled for the Southern Ontario - lower Great Lakes Basin Region. They can be modified for other regions. The differences between the regional and evaluative models are the volumes, areas and advective flow rates. All other rates are expressed on a unit area or volume basis and thus apply to both models.

The level III output can include all fugacities, concentrations (in mol/m^3 and conventional units) and transfer rates for individual and combined processes. A total mass balance can be assembled, as illustrated for PCBs in Figure 1, and the overall chemical persistence can be calculated.

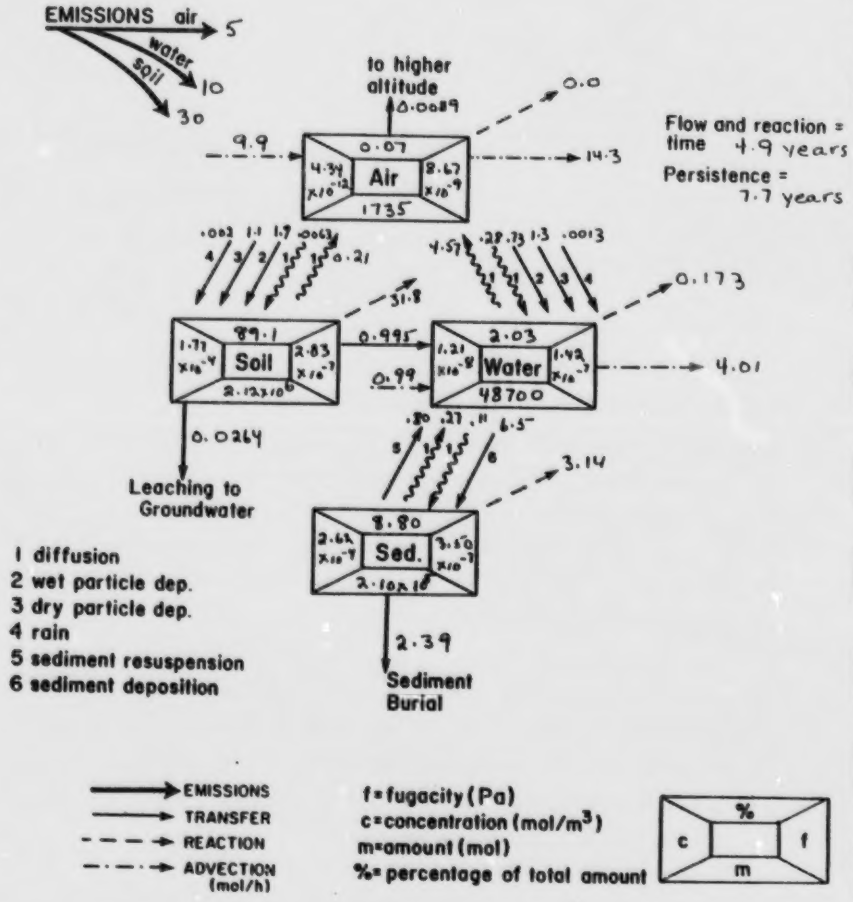
EMISSIONS air 5
water 10
soil 30
to higher altitude
0.0089
0.0
9.9
0.07
4.34 x10^-12
Air
8.67 x10^-9
1735
14.3
Flow and reaction = time 4.9 years
Persistence = 7.7 years
.002 1.1 1.7 .0063
4 3 2 1 1
0.21
4.57 .28 .73 1.3 .0013
1 1 2 3 4
0.173
31.8
89.1
1.77 x10^-4
Soil
2.83 x10^-7
2.12x10^6
0.995
0.99
2.03
1.21 x10^-8
Water
1.42 x10^-7
48700
4.01
0.0264
Leaching to Groundwater
.80 .27 .11 6.5
5 1 1 6
3.14
8.80
2.62 x10^-9
Sed.
3.50 x10^-7
2.10x10^6
2.39
Sediment Burial
1 diffusion
2 wet particle dep.
3 dry particle dep.
4 rain
5 sediment resuspension
6 sediment deposition
EMISSIONS
TRANSFER
REACTION
ADVECTION (mol/h)
f=fugacity (Pa)
c=concentration (mol/m³)
m=amount (mol)
%= percentage of total amount
%
c
f
m

FIGURE 1: Level III mass balance for PCBs in Southern Ontario

"VALIDATION" USING TEST CHEMICALS

Models such as this cannot be "validated" in the same sense that a simpler physical or chemical model can be validated. Environmental concentrations vary in time and space, and few reliable data are usually available. Reaction rate constants vary diurnally and seasonally. Emissions are rarely known accurately. There are variations and uncertainties in transport rate parameters, such as deposititon and resuspension rates. Few environments are at steady state. The best that can be hoped for is that the model corresponds with order of magnitude fidelity to fragmented observations for a variety of chemicals of quite different properties and pathways. The chemical-to-chemical variation should be described entirely by the chemicals' properties and emission rates and not by chemical-specific adjustable parameters. But even this modest model capability is invaluable for predicting the behavior of new chemicals and for estimating order of magnitude concentrations.

The model was run for selected chemicals (Table 1) of varying properties, and environmental concentrations were calculated, and compared with observations. A common problem is estimation of emission rates. In some cases, it is necessary to back-calculate what the emissions may be, or must be, to create prevailing concentrations, then check if these emission rates are in reasonable accord with rates of production or use.

Table 4 lists some illustrative calculated bulk compartment concentrations and fugacities and gives reported values for comparison. There is generally order-of-magnitude agreement.

DISCUSSION

The set of models provides a relatively simple, rapid method of establishing the relative importance of environmental fate processes for specific chemicals using minimal data. It is believed to give an adequate characterization of the dominant phases of accumulation. For example, mirex is 62% in soil and 35% in sediments, while benzene is 46% in air and 54% in water. These percentages are controlled by the nature of the emission sources and the chemicals' properties. An overall persistence or residence time can also be estimated which ranges from 6 days for benzene to 12 years for mirex. This persistence is a function of partitioning, and rates of reaction and advection. The relative importance of advective inflow and local emissions can be estimated.

The evaluative version can be used to determine the dominant environmental partitioning pathways and the persistence of a chemical, using illustrative rather than real emissions. The computed absolute concentrations then have no significance. Since many jurisdictions have a common interest in estimating the environmental fate of chemicals, but the regions corresponding to these jurisdictions have differing ratios and natures of air, water, soil, and sediments, it is useful to have a common evaluative test system which can be used to inter-calibrate environmental assessments. The combination of evaluative and region-specific environments thus provides a convenient system for international assessment of chemicals.

A useful feature of both models is that a sensitivity analysis is possible by which the effects of varying properties of the chemicals and the environment can be explored. This establishes which properties should be estimated most accurately and can provide an estimate of likely error in concentration as a function of error in property.

If emission estimates are available, the model can be used to estimate concentrations with, it is believed, order of magnitude (factor of 10) accuracy. It is most reliable for substances, such as PCBs, which are persistent and widely dispersed in the environment. The model can be used as an interpretive tool to explore temporal and spatial variations in concentrations. For example, it appears that mirex has been discharged over two time periods at emission rates which have differed by a factor of approximately 500. Since the model is linear, concentrations are linearly related to total emissions, thus there is no need to run the model repeatedly to explore such changes. Because certain contaminants, such as benzene and BAP are emitted with considerable spatial variation, it can be misleading to use average emissions and concentrations. It may be possible to develop "rules", which may be region-specific, that one would expect to encounter local concentrations which are perhaps a factor of 10 or 20 higher than average.

The model has been described in steady state form, but with little additional effort it can be written in differential equation form and solved numerically to give the response in the region to time-varying emissions. This is a Level IV calculation.

These estimated concentrations are of potential value in three respects.

First, they provide guidance about likely prevailing environmental concentrations in the various media which result from present or possible future emissions. This is useful when designing analytical monitoring and identification programs. Second, they provide information about the proximity of the concentrations to those which are judged to be of toxicological or aesthetic significance.
Third, the concentrations provide a starting point for estimation of human exposure. These issues are discussed more fully in the next section.

FROM CONCENTRATIONS TO EXPOSURE AND EFFECTS

Exposure assessment calculations can take one or both of two directions; comparison with targets, and dosage assessment.

"Target" concentrations may be defined for each medium. For example, from considerations of toxicity or aesthetics it may be possible to suggest that water concentrations of a specific chemical should be maintained below 1 ug/litre, air below 1 ug/m^3, and fish below 1 mg/kg. These target concentrations can then be compared as a ratio or quotient to the estimated environmental concentrations. A hypothetical example is given in Table 5 showing the application of this "quotient" method. In this case it is apparent that the primary concern is with air and fish. The proximities of the estimated prevailing concentrations to the targets are quantified by these quotients, a large value implying a large safety factor. The high-risk situations correspond to low quotients. The concentration level in fish is not directly toxic to the fish but poses a possible threat to humans if consumed on a regular basis.

There are often problems associated with suggesting target concentrations in soil and sediment because these media are not normally consumed directly by organisms. Whereas simple lethality experiments can be designed using air, water, or food as vehicles for toxicant administration, it is not always clear how concentrations in the solid matrices of soils and sediments relate to exposure or intake of a chemical by organisms. It is difficult to design meaningful bioassays involving interactions between organisms, soils, and sediments.

The second approach is to use these media concentrations to calculate dosages to human and other organisms, as illustrated in Table 5 and Fig. 2 which are reproduced from reference 5.

An average human inhales some 20 m^3 of air per day, thus the associated amount of chemical can be easily calculated. Not all this chemical may be absorbed, but at least a maximum dosage can be evaluated. The same human may consume 2 litres/day of water with its contained chemical, enabling this dosage to be estimated. Food, the other vehicle, is more difficult to treat. An average diet may consist of 1 kg/day broken down as shown in Table 5. Fish concentrations can be estimated directly from the model, but meat, vegetable, and dairy product concentrations are still poorly understood functions of the concentrations of chemical in air, water, soil, animal feeds, and of agrochemical usage. It is likely that techniques will emerge for calculating food - environment concentration ratios, but at

TABLE 5: COMPARISON OF ENVIRONMENTAL CONCENTRATIONS AND HUMAN INTAKE RATES WITH EFFECT LEVELS

Comparison of environmental effect concentrations with predicted concentrations

	Effect level	Actual level	Quotient or ratio
Air pollution (µg/m³)	15	2.82	5.3
Fish toxicity (g/m³)	5	2.91×10^{-4}	17,160
Soil contamination (µg/g)	5	3.58×10^{-2}	140

Comparison of allowable human intake with predicted intakes[a]

	Concentration (g/m³)	Volume of intake (m³)	Actual intake (µg/day)	Percent of permissible intake	Percent of actual intake
Ingestion of food and water					
Fish	0.140	0.00025	35	0.7	34
Meat products	0.140	0.00005	7	0.14	6.8
Dairy products	2.9×10^{-4}	0.00025	0.073	0.001	0.07
Vegetable products	2.9×10^{-4}	0.00045	0.13	0.003	0.13
Water	2.9×10^{-4}	0.002	0.58	0.012	0.56
Air inhalation	2.82×10^{-6}	20	56	1.1	54.4
Domestic exposure			1	0.02	1
Occupational exposure			3	0.06	3
Total			103[b]	2.04	100

[a] Average daily intake (ADI) = 5000 µg/day

[b] Ratio of ADI intake = 5000/103 = 48.5

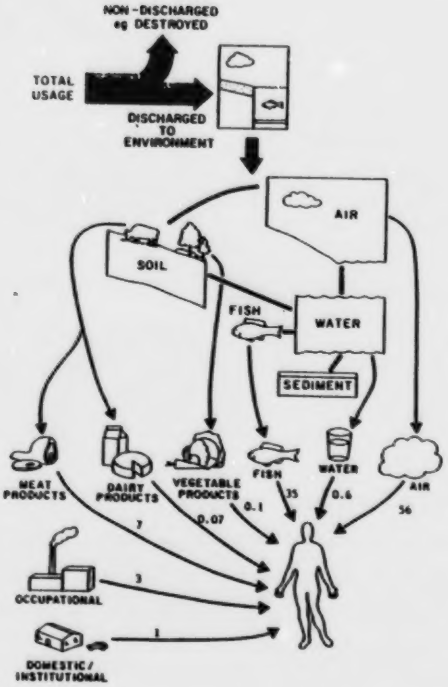
NON-DISCHARGED
eg DESTROYED
TOTAL USAGE
DISCHARGED TO ENVIRONMENT
AIR
SOIL
FISH
WATER
SEDIMENT
MEAT PRODUCTS
DAIRY PRODUCTS
VEGETABLE PRODUCTS
FISH
WATER
AIR
7
0.07
0.1
35
0.6
56
3
OCCUPATIONAL
1
DOMESTIC/ INSTITUTIONAL

FIGURE 2: Predicted routes of human exposure to a hypothetical compound (ug/day).

present the best approach is to analyze a typical "food basket". The food concentrations used here are illustrative and were obtained by assuming that the meat consumed had partitioning properties similar to fish, and that dairy and vegetable products consisted largely of water. This issue is complicated by the fact that much food is grown at distant locations and imported. Beverages, food, and water may also be treated (deliberately or accidentally) for chemical removal commercially or domestically during food preparation.

It is becoming clear that food ingestion is often the dominant route by which humans are exposed to chemicals, especially agricultural chemicals and those which are emitted into the atmosphere and are subject to wet and dry deposition and absorption on leaf surfaces. This area is the subject of our current efforts in which we are attempting to develop correlations between environmental concentrations (especially air and soil) and those in vegetation, meat and dairy products. Further, we are assembling various models of human intake corresponding to defined population groups with specified diets. One group is young children who may ingest quantities of soil. We hope that it will be possible to identify the more susceptible, more highly exposed groups in a systematic manner and validate these findings by actual market basket and diet measurements.

It is worth emphasising at this point that we do not expect to find that human intake levels will be close to lethal levels, or even to levels of possible concern. But we believe that it is essential for a responsible government to know the principal routes by which the population is exposed to individual priority chemicals. It should also ascertain the proximity of intake rates to "allowable" levels. When such information is lacking there may be distortion of regulatory actions and scientific efforts into areas which are of high profile in the news media, but in reality are of little concern relative to other more "mundane" issues.

Much chemical exposure may also occur in occupational (e.g., factory) and institutional or commercial (e.g., schools, stores, cinemas) settings, and at home, but these exposures vary greatly from individual to individual and depend on lifestyle. For illustrative purposes and to give a complete picture, exposures from these sources are included in Table 5.

The picture that emerges from this model is a profile of relative exposures by various routes from which the dominant route(s) can be elucidated. If desired, appropriate measures can be taken to reduce certain critical exposures. For example, fish consumption could be reduced. An advantage of this approach is that it places the entire spectrum of exposure routes in perspective. There is little merit in reducing an already small exposure.

CONCLUSIONS

In this project a series of regional fugacity models has been developed, tested with selected priority chemicals, and found to give a reasonable picture of environmental partitioning, reaction, advection, and transport characteristics. Estimated concentrations are in order-of-magnitude accord with reported values, but there are considerable uncertainties in the emission rates on which these concentrations depend. The estimated concentrations may be of value for designing analysis programs, for setting priorities, and for asssessing human exposure to present and new chemicals.

Our current work is focussing on further validation, developing air-soil-vegetation-meat-dairy product contamination relationships, and in assembling models for human exposure applicable to various groups in Ontario.

We believe that the model can be, and should be, improved by obtaining better estimates of certain transport and partitioning parameters. For example, the mass transfer coefficients and diffusivities are average values applied to all chemicals. Chemical specific and region specific values could be used instead to increase accuracy. Most important, the model should be tested more thoroughly against a variety of chemicals of widely differing properties. The principal difficulties in accomplishing this are the lack of emission data, environmental concentration data, reaction rate constants and physical chemical properties.

The exposure assessment process can be, and should be, extended further to include a physiologically based pharmacokinetic model (15) to predict partitioning, accumulation, and persistence in various animal or human tissues after prolonged, continuous exposure.

Ultimately, a capability is likely to emerge to combine environmental, human exposure, and pharmacokinetic models in an overall process of tracking the pathways of a chemical from its sources, to its distribution in various environmental media, such as air, water, soil, sediment, and food, to its availability or exposure to animals and humans, and finally to target tissues. The model presented here contributes one small step to this process.

REFERENCES

1. Mackay, D., Paterson, S., Environ. Sci. Technol., 1981, 15, 1006-1014.

2. Mackay, D., Paterson, S., Environ. Sci. Technol., 1982, 16, 654-660.

3. Mackay, D., Paterson, S., Cheung, B., Neeley, E.B., Chemosphere, 1985, 14, 335-374.

4. Mackay, D., Paterson, S., in "Pollutants in a Multimedia Environment", Cohen, Y., ed. Plenum: New York, 1986, 117-131.

5. Mackay, D. and Paterson, S., Partitioning Models, pp. 77-86 in Carcinogen Risk Assessment, C.C. Travis (ed)., Plenum Publ. Corp. 1988.

6. ECETOC 1988 Technical Report of the European Chemical Industry Ecology and Toxicology Centre, No. 29 Concentrations of Industrial Organic Chemicals measured in the Environment: The Influence of Physico-Chemical Properties, Tonnage and Use Pattern. Brussels.

7. Klein, A.W., Environmental Exposure Potential (EEP) in Compendium of Environmental Exposure Assessment Methods for Chemicals. OECD Hazard Assessment Panel, Paris, 1988.

8. Wood, W.P., Nold, I.A., Lefler, J., Environmental Partitioning Model (Draft Documentation), Office of Toxic Substances, U.S. EPA, 1982.

9. Calamari, D., Vighi, M., Bacci, E., Chemosphere, 1987, 16, 2359-2364.

10. Zitko, V., McLeese, D.W., Evaluation of Hazards of Pesticides used in Forest Spraying to the Aquatic Environment. Can. Tech. Rept. Fish Aquat. Sci. No. 985, 21pp. 1980.

11. Sloof, W., Cleven, R.G.M.J., Janus, J.A. and Ros, J.P.M. (eds) 1987. Draft Basis Document Copper. RIVM Report No. 758474003, pp. 78-84, RIVM, The Netherlands.

12. Yoshido, K., et al., Toxicol. Environ. Chem., 1987, 15, 159-183.

13. Neely, W.B., Mackay, D., in "Modelling the Fate of Chemicals in the Aquatic Environment", Dickson, K.L., Maki, A.W., Cairns, J. Jr., eds. Ann Arbor Science: Ann Arbor, 1982, 127-143.

14. Mackay, D., Paterson, S., Schroeder, W.H., Environ. Sci. Technol., 1986, 20, 810-816.

15. Paterson, S. and Mackay, D., Environ. Toxic. Chem., 1987, 6, 395-408.

A8

VERIFICATION OF THE CLOUD AND WET DEPOSITION FIELDS OF A MESO-α SCALE MODEL OF LONG-RANGE TRANSPORT OF AIR POLLUTANTS. Han-Ru Cho*, S.T. Soong and J.V. Iribarne, Department of Physics, University of Toronto, Toronto, Ontario, Canada M5S 1A7

MANUSCRIPT NOT AVAILABLE

A9

Eulerian Model Evaluation

M.Alvo
Department of Mathematics
University of Ottawa

1.Introduction

Eulerian models for acid deposition represent a powerful tool for examining the relationship between the source of a pollutant and the receptor at which it is deposited. Such models take into account the complex interactions among the variables which play a key role in the acid deposition system. Sulphur dioxide and the oxides of nitrogen are emitted into the atmosphere mostly from anthropogenic sources. These species undergo photochemical reactions in the gas phase and are also oxidized in the cloud system through complex homogeneous and heterogeneous reactions.

In addition to the complex photochemistry, Eulerian models also take into account both the role of transport, itself governed by three-dimensional wind patterns, as well as the part played by cloud physics. The pollutants come to earth through deposition of gases and particulates and in the form of precipitation.

It is of interest to ask why the use of complex models should be favoured over simpler existing models which do not assume complex chemistry and are cheaper to run. Simpler, so-called Lagrangian models, fail to take into account the non-linear terms which may be important for emission control scenarios. Such models assume that processes as scavenging and chemistry occur at a constant rate independent of the concentration of the associated pollutant. In turn, that assumption serves to establish a proportional relationship between changes in emission and changes in deposition. On the other hand, a non-constant scavenging rate and non-linear chemistry would imply that decreases in the emission rate at a source may have a non-proportional effect on the deposition rate at a receptor. On which of these two types of models should control scenarios be evaluated is now the subject of an important study involving several U.S. and Canadian government agencies and industries. More specifically, how adequate are the Eulerian models in predicting acid deposition under various emission conditions and in ellucidating source-receptor relationships?

There are at present at least two Eulerian models which incorporate non-linear chemistry and cloud physics; they are:1) the Acid Deposition and Oxidant Model (ADOM) being developed at ERT under the sponsorship of the Ontario Ministry of the Environment (OME), the German Umweltbundesamt (UBA), the Electric Power Research Institute (EPRI) and Environment Canada and 2) the Regional Acid Deposition Model (RADM) being developed under the Environmental Protection Agency (EPA) in the United States. Before these models can be adopted, it is necessary to evaluate them against observational data and to ascertain their scientific credibility; that is to say, do these models predict deposition for the right reasons ? An extensive field program has been established to collect 2 years of surface data interspersed with at least 2 periods of intensive data collection. A key issue in the evaluation is that model predictions and observational data are intrinsically incompatible : models predict ensemble quantities over a grid scale whereas observational data are point measurements. As well, models produce grid average hourly data while the monitoring networks produce point measurements on variable time scales. It is the objective of the present research to address this issue and to suggest ways of resolving this discrepancy.

2.Evaluation Data

Past data which have been used for the preliminary evaluations of ADOM and RADM corresponded to events I,II,and IV in the Oxidation and Scavenging Characteristics of April Rains (OSCAR) experiment conducted during April 1981 to investigate wet removal by cyclonic storms. A network of 37 stations located in the eastern

United States and Canada collected simultaneaous measurements of precipitation and ion chemistry at successive half-hourly and hourly intervals consistent with the model integration cycle. Both models have been used to simulate periods during OSCAR and examples of their evaluations are found in Middleton et al (1987), Venkatram et al (1988), and Misra et al (1988).

A field study spanning a period of two years began in July 1988. The main objective is to provide further data to be used for operational and diagnostic evaluations. A planning document describes the details of the collection effort which includes provision for aircraft measurements (Hansen, 1988). It is anticipated that daily precipitation and air quality data will be available for various species at representative sites in North America.

3.Progress Report

Site data can be variable for several reasons. There may be local variability resulting from micro-climatic conditions or from local emission sources. In addition, there may be differences in network protocols including the use of different instrumentation or the length of the measurement period. For longer sampling periods, the concentration in precipitation tends to be greater owing to evaporative losses.

In order to quantify the annual within site variability, the standard deviation relative to the mean was computed at co-located and closely located sites for both sulphate and nitrate for the period 1980-1984 using eastern North American data. It was observed that the variability for both species was comparable. As well, there did not appear to be a strong dependence of the variability on distances of less than 50 km between sites within the cluster of closely located sites. For nitrate, the variability did not exhibit any obvious temporal trends although for sulphate, there appeared to be a significant drop in 1984. The within site variability appears to be a function of space and time (it is lowest in spring and largest in summer); in some cases, it could be as large as 40% of the estimate itself. In view of these results, it seems appropriate to study the variability of precipitation and of concentration separately instead of just deposition.

4.Proposed research

The main thrust of our future research consists of an in-depth analysis of the discrepancy between what a model predicts and what the observed site data represents. This entails looking at the sub-grid variability of the observed data at various time scales. A model generally predicts the average precipitation and average concentration of a pollutant on a grid scale of approximately 127x127 km square. The product of these then yields the estimated deposition for that grid. On the other hand, an observation represents a point measurement which is not necessarily a good estimate of the grid average. Consequently, it is important to verify to ascertain the representativeness of a single site measurement. If the site data is grossly incompatible with the model predictions, are there ways of enhancing the former ?

Since Eulerian models will be evaluated on various time scales, it is necessary to determine the sub-grid variability on those time scales for both concentration of a pollutant and for precipitation. Is the sub-variability in precipitation greater than the corresponding variability in concentration? In order to try to answer this question, it is proposed to consider a number of data sources. In particular, the OSCAR data can be used for the analysis of variability at both the episoidal as well as at the daily time scale. The APIOS, APN and CAPMoN data can be used for both daily and monthly analysis. Finally, the Quebec provincial data can be used for the analysis of weekly variability. In addition, it is proposed to examine the precipitation data available from the Canadian Climate Centre which is far more dense than the site precipitation data. If the differences between these two sets is substantial, can use be made of the former to enhance the site data and render it more compatible with what the model predicts?

5.Conclusion

In this article, we have reviewed work done to date and have established a direction for future research. It is apparent that any Eulerian model evaluation must be made on the basis of compatible predictions and observations. The object of the present research is to quantify the degree of uncertainty which exists in the observed data on various time scales and to propose ways of enhancing its suitability for model evaluation.

6.References

a. W.Richard Barchet (1988). An Overview of Previous Evaluations of RADM and ADOM. EPRI Research Project 1630-40

b.D.Alan Hansen (1988). Project Plan for the ACID DEPOSITION EULERIAN MODEL EVALUATION AND FIELD STUDY. Project Management Group report

c.Paulette Middleton, Julius S. Chang, John C.del Corral (1988). Comparison of RADM and OSCAR Precipitation Chemistry Data. Accepted for publication in Atmospheric Environment.

d.P.K.Misra, R.Bloxam, C.Fung, S.Wong (1988). Non-Linear Response of Wet Deposition To Emissions Reduction: A Model Study. Accepted for publication in Atmospheric Environment.

e.A.Venkatram, P.K.Karamchandani, P.K.Misra (1988). Testing A Comprehensive Acid Deposition Model. Atmospheric Environment, 22,pp.737-747.

A10

SCALE MODEL STUDIES AND DEVELOPMENT OF PREDICTION PROCEDURES FOR HEAVY GAS DISPERSION IN COMPLEX TERRAIN 1988

by

M.C. Murphy, K.C. Heidorn and P.A. Irwin
Rowan, Williams, Davies and Irwin Inc.
Guelph, Ontario

Presented at TECHNOLOGY TRANSFER CONFERENCE 1988, Toronto, Ontario

ABSTRACT

The overall goal of the "Heavy Gas Project" is to develop an improved computer model for the prediction of heavier-than-air gas dispersion in complex terrain.

Three basic areas of investigation comprise the Project: 1) experimental - zero wind releases; 2) experimental - releases into wind; and 3) mathematical modelling. In this paper we present our work on Part 1. More specifically, the spreading rate of a heavier-than-air gas cloud into a zero-wind environment is studied using flow visualization techniques. Smoke was used to follow the instantaneous release of a heavy gas onto firstly, a smooth level surface, and subsequently onto surfaces with obstacles arranged in different configurations. Overhead and side-view cameras were used tp photograph the spill events. Still photos were obtained from freeze-frame analysis of the video, and were then used to produce data on cloud front distance versus elapsed time.

Photos of the release showed a very uniform circular cloud spread onto a smooth surface. A release into obstacles appeared to start out initially as a uniform circular cloud, but at later times the cloud developed into a diamond or hexagonal shape, depending on the obstacle arrangement. Surprisingly, the cloud spreading rate was higher with obstacles present than for spreading on a smooth surface. This, however, was true only for cloud spreading through an open corridor in a uniform array of obstacles. A modified MOE model predicted the cloud spreading history with reasonable results.

Keywords: heavy gas, still-air, flow visualization, smooth, obstacles, model

1. INTRODUCTION

The widespread transport and storage of toxic and/or inflammable gases has increased interest in recent years in the behaviour of heavier-than-air gases released into the ambient atmosphere. In the event of a spill of a toxic or flammable heavy gas, an emergency response team must be able to respond quickly and efficiently to ensure that danger to the local community is minimized. This requires a real-time ability to predict the flow path and concentration pattern of the gas cloud for the duration of the spill event. In many cases, the gas is heavier than air, especially during the early stages of the release. The behaviour of the heavier-than air gas cloud depends on several variables such as local terrain roughness and slope, gas density, physical nature of the gas release (instantaneous, semi-continuous or continuous), spill rate and/or spill volume as well as weather conditions including wind speed and direction, atmospheric stability, precipitation, and humidity.

Perhaps the most important parameters in determining the behaviour of the gas cloud are gas volume and density, wind speed and direction and local terrain characteristics. The fact that weather conditions play a large role in heavy gas behaviour emphasizes the complex nature of the problem. Nevertheless, a large body of research has been, and is being, completed in an effort to help provide a quick and efficient response to a spill of toxic or inflammable heavy gases. Much of this work has been sponsored by industry and government in a approach similar to the joint venture at Thorney Island (McQuaid, 1985).

Research into heavier-than-air gas dispersion has proceeded on three fronts: 1) full-scale field trials, 2) wind tunnel simulations, and 3) theoretical prediction or computer simulation. Full-scale tests represent an enormous effort in manpower and funding. Wind tunnel and computer simulations are considerably less expensive and are very useful for validation purposes. In this study, the instantaneous release of a volume of heavy gas is simulated under zero-wind conditions and several different obstacle configurations. Similar tests are currently being carried out with non-zero wind, and these will be the subject of a later paper. Ultimately, the results of flow visualization and concentration monitoring from these tests will be used to improve mathematical models of heavy gas dispersion.

In the first series of heavy gas dispersion experiments, a known volume of gas was released into a calm environment under a variety of obstacle arrays. For each of these releases, the flow of the gas cloud was observed and recorded on video tape. By varying the size and density of the obstacles as well as the initial cloud dimensions, the effects of these obstacles could be studied and then compared to simple box model predictions of the horizontal cloud dimensions. Improved mathematical expressions are proposed to describe the horizontal motion of the gas cloud in its early stages of dispersion.

2. EXPERIMENTAL PROCEDURES

The scale modelling of a heavy gas release consists of holding certain physical parameters constant for both the full scale and laboratory tests. Similarity criteria include the Reynolds (Re) and Froude (Fr) numbers based on wind velocity, Richardson number (Ri) based on wind velocity and density difference between gas spill and air, initial density ratio, volume and rate of release, wind velocity profile, surface roughness, turbulence (length scale and intensity) and weather stability class. The Reynolds number is given by:

$$Re = L\,U\,\delta_a / \mu \qquad (1)$$

where L is a length scale (arbitrarily defined), U is local wind velocity, δ_a is the air density, and μ is the viscosity. The Richardson number is:

$$Ri = g\,\Delta\delta / \delta_a\,L/U^2 \qquad (2)$$

where g is the gravitational constant, $\Delta\delta = \delta_g - \delta_a$, and δ_g is the gas density.

Not all criteria can be satisfied in practice. The Reynolds criteria cannot be satisfied for models at 1:500 scale because the velocity over the model becomes very low, and it is difficult to obtain a good simulation of the boundary layer at low speeds in the wind tunnel. Fortunately, a reasonably complete simulation can be obtained, even in violation of Reynolds similitude (Meroney, 1982), (Meroney and Neff, 1986). This "non-exact" simulation can be established by ensuring that the Richardson number, Ri, is equal at both model and full scale. The density ratio may be increased in the model case so that the velocity on the model may be increased. This is done because a higher velocity simulation is much easier to perform.

The velocity profile over the model should be similar to the full scale wind profile. The absolute values of the velocities are obtained from Ri similitude. The surface roughness is scaled simply by geometric scaling. The turbulence intensity of the wind in the along-wind direction should be similar at model and full scale. In partial boundary layer simulation, some of these criteria may not be satisfied exactly. The velocity profile and surface roughness criteria are relatively easy to satisfy, but the length scale and turbulence intensity are more difficult. However, because the turbulence generated during the instantaneous release of a heavy gas spill is generally higher than atmospheric turbulence, exact similitude is not required. Thus, although the simulated boundary layer lacks some turbulent elements, the model spill will remain a reasonable representation of the full scale event.

The release mechanism developed for this study is illustrated in Figure 1. Design criteria included the following:

i) scale release volume;
ii) geometric shape;
iii) minimum interference from release;
iv) leak proof; and
v) flexible pull down mechanism.

Two release canisters were constructed to represent significantly different volumes of gas release. At 1:100 scale, the small canister (2000 cm^3) represented a Thorney Island release of 2000 m^3. The large canister (14000

cm^3) represented a 1:50 scale release. Figure 2 shows the release from the small canister into a zero-wind environment with no blocks. A small puff of smoke from the top of the release canister signals the beginning of the release, as shown in Figure 2-A. Less than 100 msec after the release, the cylinder disappears through the floor. The cloud remains cylindrical, is sheared uniformly along the sides, and begins to collapse before 100 msec. Figure 4-C and D show the overhead view of the spill. It can be seen that the spread of the cloud is uniform in all directions, indicating that the release mechanism was performing satisfactorily.

The gas used in the flow visualization study was Freon-12 mixed with carbon dioxide and smoke generated from mineral oil. By a careful weighing of a known volume of the Freon-CO_2-smoke mixture, the density of the heavy gas used in this study was found to be 3.89 kg/m^3.

The test arrays used in the initial flow visualization experiments resulted in 18 different test configurations which are defined in Table 1. Two block sizes were used: a small cube with 3.5 cm sides and a medium cube of 7 cm sides. Block coverage was either none, half or full. A schematic of full coverage is given in Figure 3. Half coverage has blocks only in the semicircle to the south of the canister location; and north of the canister there were no blocks (see North arrow on photos).

In most of the experiments using the cubes, the spacing of the blocks on the platform was 1:1 as shown in Figure 3. The 1:1 spacing indicates that the distances between the blocks (as indicated by E and D on Figure 3) is equal to the block width (as indicated by A and B on Figure 3). In two release series, a staggered spacing of 1:1 was used in which alternate rows are shifted one spacing to the left of the row below and above it. This spacing results in a 1:1 spacing within all rows and between the rows and a 1:3 spacing in each column. A 1:3 spacing indicates 3 block widths between adjacent blocks. In the regular 1:3 spacing, the blocks are so spaced in both the row and column directions.

Two canister sizes were also used in the release experiments. The small canister has a volume of 1995 cm^3, a height (indicated by G on Figure 3) of 12.5 cm and a diameter (F on Figure 3) of 14.1 cm. The large canister was 25.1 cm in diameter and 27.6 cm in height giving a volume of 13 615 cm^3.

In order to better scale the flow visualization records, two white tapes were located on model platform: one "above" and the other "below" the canister (e.g. see Figure 4). These tapes were located equidistant from the canister centre and were spaced 120.9 cm apart for the small canister and 192.7 cm apart for the large canister. In the later releases, the tapes were consistently placed 193 cm apart; white blocks were placed at the edge of the disk on the horizontal and vertical axes to facilitate the location of the canister centre (e.g. Figure 4).

For each obstacle array, the instantaneous release event was recorded on video tape by a camera mounted overhead. In several tests, a camera was also positioned to give a side view of the event. A digital time display added to the video tapes is seen in the upper corner of each of the photographs presented in this paper (e.g. Figure 4) and gives the time in hours, minutes, seconds and 1/30 second increments. In order to analyze the history of the cloud spread, the video tape was stopped at intervals and a photographic record made of the freeze-frame. These photographs were then used to determine the horizontal dimensions of the cloud at several instances after release.

3. FLOW VISUALIZATION OF STILL AIR RELEASES

In this first series of experiments, the horizontal spread of an instantaneous release of heavy gas under calm-wind conditions was simulated. Both the large and the small gas canisters were used in the flow visualization. Each canister offered desirable features in addition to the simulation of a number of different source/obstacle ratios. The large canister produced a more visible cloud than the small cylinder which facilitated tracking of the cloud front. The disadvantage of the large canister, however, is that its cloud reached the outer limits of the table much more quickly than the smaller canister. The small canister thus allowed longer event observations; in many cases reaching the final passive stage of the heavy gas event for which the cloud no longer spreads primarily as a result of gravity forces.

The obstacle array and canister size variations for the 18-test series are presented in matrix form in Table 1. Brief discussions of those tests are given below. For ease in the discussion, the cloud will be described as a flat, two-dimensional figure with the "vertical" axis and direction indicated by the line running through the canister centre "up and down" on the photograph and the "horizontal" axis and direction taken as running "left and right" through the canister centre. Start times for the releases shown in these figures are given in Table 2 in hours, minutes, seconds and 1/30 second increments corresponding to the time signature shown in the individual photographs.

Test Series 8 and 9 were run with no obstacles and with the small and large canisters respectively. In both cases, the heavy gas cloud spread in a circular manner as expected with the radius of the cloud increasing with time. The comparison of these clouds at an equal time after release is shown in Figure 4. It should be noted that the clouds are nearly perfect circles indicating that the experimental surface is very level and that there is no major influence by the release mechanism on the cloud dispersion. The upper photographs in Figure 4 are of the cloud at 0.33 seconds after release and the lower photographs are from 1.00 seconds after release. As expected, the cloud from the large canister has a larger radius than the cloud from the small canister after an equal time interval. It is also interesting to note the very visible outer "halo" at the cloud front and the thinner cloud density within the ring. (The bright inner circle is due to reflection from the release mechanism pad.)

Series 1, 2, 5, 6 and 10 were run with full coverage (sheets of blocks both to the north and to the south of the canister) using both the small blocks and the medium blocks with the small and large canister releases. (See Table 1 for each setup for these series.) All of these runs are characterized by a cloud pattern which initially begins as a circular shape but soon transforms into a diamond pattern with apices at the "north-south" and "east-west" axes through the cylinder centre. An example of this flow pattern is given in Figure 5 for the large canister and medium blocks. The start time for this series was at 03:40:00. As with the "no blocks" cases, the large canister cloud moves more quickly than that from the small canister (photos of small canister release not shown).

Series 3, 4 and 7 were trials with "half coverage", i.e. blocks only on the southern half of the study platform. (See Table 1 for configuration details.) We see that the cloud patterns (Figure 6) generated by this configuration are half like the "no blocks" case and half like the "full coverage" case: a semicircle to the north and a half-diamond to the south. In the early life of the cloud, the spread is in a nearly perfect circular pattern with cloud front movement through the blocks as rapid as that in the block-free half. The most surprising result of these trials is that the rate of spread of the cloud front is the same along the circle radii as it is along the apex of the diamond in the southern half. This similar rate of spread is found to occur regardless of the canister or block size. The indication is that, for this half-coverage configuration, a heavy gas cloud will flow along an unobstructed corridor between obstacles at the same rate as it would if no obstacles were present. Further discussion of this phenomenon will be given in the next section.

Series 11 and 12 were trials using half and full coverage of medium-size blocks with 1:1 spacing and the large canister release. The difference between these two series and Series 4, 5 and 10 is that the alternate rows of blocks are staggered by one block width. With this arrangement for the full coverage case, the open corridors along the north-south axis no longer exists. The arrangement does, however, still have an open east-west axis. The initial cloud spreads as a circle (Figure 7) and then transforms into a hexagon pattern. The half-coverage configuration results in an arrangement with a half-hexagonal pattern to the south and semi-circle to the north (Figure 8). The point of interest in these series is that the apices of the hexagon in the southern half (and in the northern half, in the case of full coverage) can be seen to occur in a diagonal direction from the release area, a path which is free of intersections with any blocks. The movement along the north-south axis, however, is now impeded by the blocks and thus is slowed. The distance travelled from the canister centre to the centre points of the hexagon faces is essentially equidistant in all directions once the figure is established. The hexagon is elongated along the east-west axis as the cloud moves along the corridor free of impediment as it did in the regular array case.

Series 15 and 16 consist of a heavy gas spill with the large and small canisters for full coverage of medium blocks at a 1:3 spacing. Again, the spread begins as a circle (Figure 9) and remains nearly circular although there is the hint of a diamond shape in the later times with the large canister. The edges of the cloud front are seen to be "scalloped" around the obstacles indicating the flow pattern around the blocks.

Series 17 and 18 were run with the large canister and medium blocks with 2 cm-spacing (3.5:1 spacing) for full and half coverage respectively. Because of the narrowness of the corridors between blocks, some of the gas "sloshes" over the blocks upon release and forms a secondary cloud above the blocks. The pattern is further complicated by a rebound of the gas from the blocks. This process is dramatically seen in a series of scenes taken of the release region with a hand-held video camera (Figure 10). The cloud is seen to break over the blocks, initially clearing the floor of the canister. The gas then returns to fill the release area and a second wave is formed. This process is repeated with ever-diminishing strength. A side view of the process from a wider angle is shown in Figures 11 and 12. Very evident from this series is the secondary cloud spreading over the top of the blocks. This upper level cloud is evident from the overhead photographs (Figure 13) as a brightening and obscuration of the block tops. The horizontal pattern initially spreads as a diamond and likely continues to spread in that pattern although the gas becomes difficult to see in the corridors after some time. The cloud moving over the blocks hints at a four-pointed star pattern which evolves toward a hexagon.

For the half-coverage case (Figure 14), the clear-area semi-circle is present with a diamond shape evolving in the corridors between the blocks. The initial overflow of the blocks is evident as a rectangular bright area which quickly dissipates. Since the rebounding material has open terrain ahead of it, there is no back-and-forth slosh as there was with the complete coverage.

Series 13 and 14 were trials using simple solid barriers. In one, a pair of barriers were angled at 45 degrees and spaced so that a gap existed between them. In the other, a single barrier was placed horizontally. The cloud front was unaffected in all directions except where it touched the barrier which stopped the cloud front. The cloud wrapped around the barriers and would eventually fill in the space behind. Figure 15 shows these releases about a second after release.

4. ANALYSIS OF FLOW VISUALIZATION RESULTS

The flow visualization experiments provided a good record for analyzing the movement of the heavy gas cloud after its release. By reducing the videotape record to a series of photographs, the horizontal dimensions of the cloud could be determined and a time/distance history of the cloud front under a variety of release conditions ascertained. This was accomplished by measuring the distance on an enlargement of the photograph of various points along the cloud front from the canister centre and scaling the result by the known distance between the horizontal tapes above and below the canister.

The error in the measurement of points on the cloud front was ±0.5 mm from the photographs. The scale factor, between the photograph and the model, ranged from 22 to 25. Thus, the actual error in the placement of the cloud front is 1.1 cm to 1.3 cm. The clock used resolved time into increments of 1/30 of a second.

The distance of the cloud front from the canister centre as a function of elapsed time is shown in Figure 16 for both the large and small canisters under "no blocks" configurations. As expected, flow from the large canister spread at a faster rate than from the small canister. The solid lines represent the current MOE model with coefficient equal to unity. Modelling, including the definition of the coefficient, is discussed in detail in the next section.

In this paper, only the 1:1 regular block spacing has been analyzed for cloud spread. For the large canister, the cloud front distance as a function of elapsed time is shown in Figures 17 and 18 for a variety of block size and coverage configurations. Figure 17 shows the distance measured along the axes (90 degrees) and Figure 18 shows the distance as measured at a 45 degree angle through the blocks. Similarly, Figure 19 (90 degrees) and Figure 20 (45 degrees) show measured distances for the small canister under several block configurations.

When compared with the configurations with blocks, the frontal distances for large canister releases along the axes for the "no blocks" configuration are less than distances measured with blocks present as full coverage (Figure 17). In other words, the cloud front moves faster with blocks present than without, at least along the corridors, and this holds for full coverage and no-blocks configurations only. Despite some scatter in the data, there is a distinct pattern of the distances aligning in relation to the block configuration. The distance travelled after a given time, i.e. the cloud spread, is seen to increase in the following sequence of block patterns: no blocks, medium blocks-half coverage, medium blocks-full coverage, small blocks-full coverage. The spread of the cloud from the small canister, however, shows only a slight differentiation between configurations with the "no blocks" spread being marginally faster (Figure 19). The velocity difference between configurations may be due to the different combinations in the source size, obstacle size and obstacle spacing but how the process evolves has not yet been fully determined. It is interesting to note that, in the half-coverage cases, the rate of spread along the north-south axes, through blocks on southern half and open in northern half, is virtually identical. For full block and no block coverage, the reason is obvious, the symmetry of obstacle placement. However, why this holds also for the half coverage cases is also not yet understood.

The distances travelled along the 45 degree paths (Figures 18 and 20) do not show a distinct pattern among block configurations, during the initial stages of the spill. In later stages, however, the rate of spread was higher for the "no-blocks" configuration. This difference in spreading rate seems to distinguish a transition from a circular spreading pattern (initial stage) to a diamond spreading pattern (next stage). The transition occurs earlier for a large canister release (0.6 - 1.0 seconds) than for the small canister release (1.0 - 1.5 seconds). This was expected because of the higher pressure head afforded by the large canister.

5. MODELLING OF HORIZONTAL CLOUD SPREAD

The atmospheric dispersion of heavy gases cannot be described fully by general gas dispersion methods. Mathematical models which treat the gravity spreading of a heavy gas cloud and the entrainment of ambient air into the cloud have been developed by a number of investigators over the past two decades. An excellent review was presented by Havens (1982). The modelling of an instantaneous heavy gas release is generally considered to be comprised of three phases. The first phase is the "blow-up" phase where the gas is initially released into the environment. The second phase is the "initial spreading" phase where the cloud moves as a slumping column of nearly uniform gas which mixes via turbulent entrainment of ambient air. The second phase ends and the third phase begins when the density difference between the cloud and ambient becomes sufficiently small. In this third phase, the gas cloud is sufficiently dilute that its dispersion may be treated by the traditional puff dispersion theories.

We consider here the initial stages of the second phase. It is assumed that the result of the gas release is a cylindrical cloud of known dimensions. Using a simple box model approach to heavy gas dispersion (MOE, 1983), the gas slumping phase is assumed to be controlled by gravitational effects. Assuming a constant cloud volume during this phase gives the following relationship for the rate of spread of the cloud under still air conditions:

$$r^2 = r_0^2 + 2\,C\,t\,[\,\Delta\delta/\delta_a\, g V_0/\pi\,]^{1/2} \qquad (3)$$

where r is the cloud radius at time t, r_0 is the initial cloud radius at t=0, C is a constant, $\Delta\delta = \delta_g - \delta_a$, δ_g and δ_a are the gas and air densities respectively, V_0 is the initial gas volume, and g is the gravitational constant.

In theory, the constant C could be either 1 or 1.414 (Hoult, 1972), but experimental results have shown C=1 to be the better choice (van Ulden, 1974; de Nevers, 1984). We next consider the value of C in light of our data.

Applying equation (3), with C=1, to the experimental data from the "no blocks" case (presented in Figure 16) results in a slight under prediction of the distance to the cloud front. (Note the lines in Figure 16 refer to the model values). The model consistently underpredicts the cloud radius for both canisters. In order to improve the model fit, the constant C was determined empirically through (3) for each time segment and the resulting values averaged. Under the "no block" configuration for the large canister, the average value of C was found to be 1.19. When this value for C is used in (3), the lower curve on Figures 17 results. The upper set of points in Figure 17 are the results of the "small block-full coverage" scenario. The value for C calculated for this configuration is 1.75, and a plot of (3) using this value of C is shown as the upper solid curve in Figure 17. A value of C=1.54 which is an average of all values of C from all large canister releases with blocks gives a line (not shown) midway between the two extremes.

For the small canister releases, the value of C determined from several different configurations ranges between 1.24 and 1.27. Only the plot of (3) with C=1.27 is shown on Figure 19.

From these physical model experiments, the "constant" C in equation (3) is found to vary with release size and, for the large release, with the obstacle configuration. We next consider whether this constant can be related to block size or spacing.

In those releases with a regular 1:1 block array, the heavy gas cloud was observed to begin as a circular cloud and then take on a diamond shape as it moved through the blocks. This flow regime shows the portion of the cloud moving down the unobstructed corridors between the blocks along the two horizontal axes to be spreading the quickest while the flow on the 45° pathway moves slowest after an initial period of equal speed. From the geometry of the final configuration, a simple model of the flow regime is proposed to be:

$$r_d = r\ f(t) \qquad (4)$$

where r_d is the distance of spread from the canister centre, r is the distance calculated by (3) down the axes, f(t) is the shape factor as a function of time t. Note f(t) is defined as:

$$f(t) = [\sin 45/\sin(135-\alpha)][e^{-\beta t}[\sin(135-\alpha)/\sin 45] + (1-e^{-\beta t})] \quad (5)$$

where α is the angle (in degrees) of the radius from the horizontal axis and β is a factor which is equal to 1 for blocks and 0 for no blocks. Note that for $\beta = 0$, $f(t) \rightarrow 1$, and equation (4) becomes $r_d = r$, i.e. the equation of a circular cloud front. With $\beta = 1$, as $t \rightarrow \infty$, equation (5) reduces to $\sin(45)/\sin(135-\alpha)$. Equation (4) then describes a linear cloud front connecting the two maximum radii at $\alpha=0^{\circ}$ and 90°. Figures 18 and 20 show the results of this model for the 45° radius for the large and small canisters respectively. In Figure 18, the distance was calculated using $C=1.54$, the value which gave the best fit for all the block data.

The mathematical model for heavy gas cloud radius (gas cloud spread) as a function of time given by (4) provides a good fit to the measured cloud dimensions under calm winds for dispersion though a regular array of blocks as well as the "no blocks" situation. This model is similar in form to the gravitational spread models proposed by many authors (e.g. van Ulden, 1974; MOE, 1983; de Nevers, 1984) with the "constant" term, generally taken as 1, increased to between 1.19 and 1.75 depending upon the obstacle configuration.

This very specific approach of fitting data must be generalized to incorporate other types of complex terrain. As more data become available, two approaches may be considered. Firstly, data from several different terrain types may be fitted to a specific model, where for each terrain type a different set of empirical constants are recommended. This leaves the end user to make a judgement on the terrain type. A second approach is to determine a set of empirical constants averaged over all terrains tested, and including the error band. The end user can than use the error bands in making judgements on the cloud path. In subsequent work we shall look at both approaches in light of wind tunnel data on heavy gas concentration measurements.

6. CONCLUSIONS AND FUTURE WORK

The flow visualization experiments for an instantaneous heavy gas released in an array of regularly spaced obstacles have resulted in a number of interesting spread patterns. The analysis of the visual record of these releases has given a cloud spread history for each of the various configurations which has been used to test a basic mathematical model of cloud radius under gravitational spreading. The results of that comparison indicate that the models fit the observations well when an empirical constant is introduced.

The next step in this study is to measure the gaseous concentration at a number of locations and to expand the gas spread model to predict concentrations. In addition, other release conditions will be studied including the non-zero wind case..

REFERENCES

de Nevers, N. (1984) 'Spread and Down-Slope Flow of Negatively Buoyant Clouds', Atmos. Environ., 18:2023-2027.

Havens, J.A. (1982) 'A Review of Mathematical Models for Prediction of Heavy Gas Atmospheric Dispersion', I.Chem.E. Symp. Series NO. 71:1-24.

Hoult, D.P. (1972) 'Oil Spreading on the Sea', Ann. Rev. Fluid Mech. 4:341-368.

McQuaid, J., ed. (1985) 'Heavy Gas Dispersion Trials at Thorney Island', Chem. Eng. Monograph, Vol. 22, Elsvier, 435pp.

Meroney, R.N. (1982) 'Wind tunnel experiments on dense gas dispersion', in 'Dense Gas Dispersion', Britter, R.E. and R.F. Griffiths, Chem. Eng. Monograph v16, pp. 85-106.

Meroney, R.N. and D.E. Neff (1986) 'Heat transfer effects during cold dense gas dispersion: wind tunnel simulation of cold gas spills', J. Heat Transfer, v108, p9-15.

MOE (1983) 'Portable Computing System for Use in Toxic Gas Emergencies', Ontario Ministry of the Environment Report ARB-162-83-ARSP, Toronto.

van Ulden, A.P. (1974) 'On the Spreading of a Heavy Gas Released Near the Ground', 1st Int'l Loss Prevention Symp., The Hague/Delft. Elsevier, Amsterdam, p221-226.

TABLE 1
TEST SERIES CONFIGURATIONS

Test Series Number	Canister Size	Block Size	Block Spacing	Block Coverage
1	L	S	1:1	Full
2	S	S	1:1	Full
3	S	S	1:1	Half
4	L	M	1:1	Half
5	L	M	1:1	Full
6	S	M	1:1	Full
7	S	M	1:1	Half
8	S	-	-	None
9	L	-	-	None
10	L	M	1:1	Full
11	L	M	1:1	Full Staggered
12	L	M	1:1	Half Staggered
13	L	-	-	2 Barriers, 45°
14	L	-	-	1 Barrier
15	L	M	1:3	Full
16	S	M	1:3	Full
17	L	M	3.75:1	Full
18	L	M	3.75:1	Full

Legend: Canister Size: S - small; L - large
Block Size: S - small; M - medium

TABLE 2

START TIME FOR EXAMPLE RELEASES IN PHOTO SEQUENCES

Figure Number	Start Time
2	01:23:36:05
4a	00:03:24:05
4b	00:02:42:20
5	00:03:40:00
6	00:03:57:15
7	00:08:37:20
8	00:09:17:05
9	00:08:18:00
10	
11	00:04:51:11
12	00:04:51:11
13	00:04:14:20
14	00:05:44:15
15a	
15b	

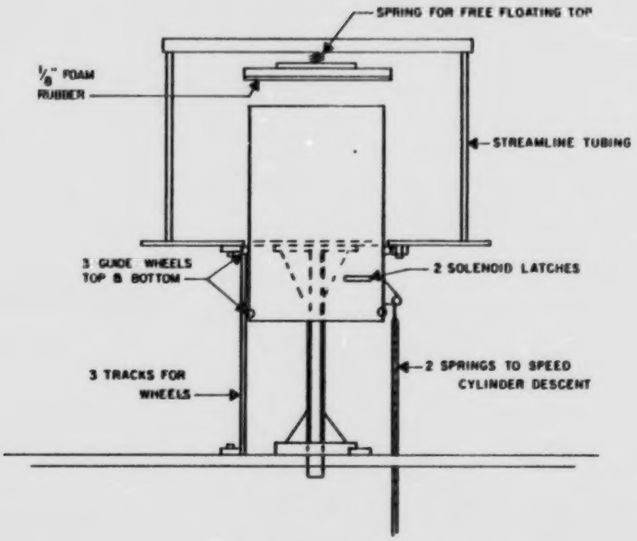
SPRING FOR FREE FLOATING TOP
$^1/_8$" FOAM RUBBER
STREAMLINE TUBING
3 GUIDE WHEELS TOP & BOTTOM
2 SOLENOID LATCHES
3 TRACKS FOR WHEELS
2 SPRINGS TO SPEED CYLINDER DESCENT

FIGURE 1
RELEASE MECHANISM SCHEMATIC

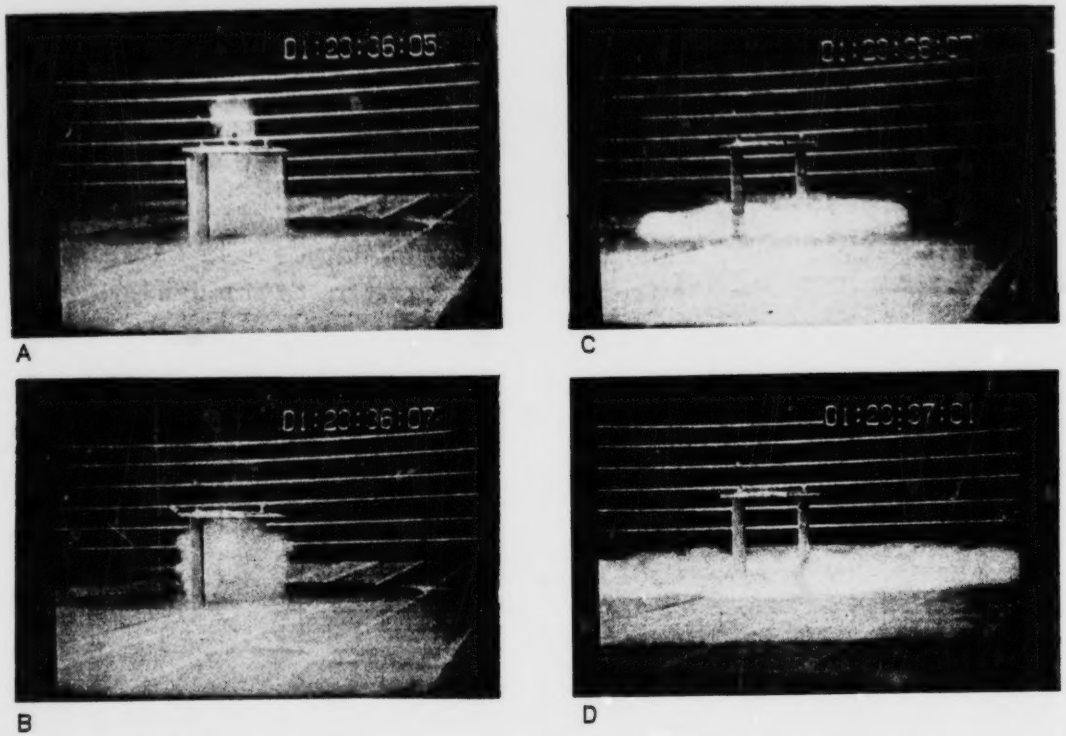
01:23:36:05
A
01:23:36:07
B
C
01:23:37:01
D

FIGURE 2
HEAVY GAS RELEASE MECHANISM

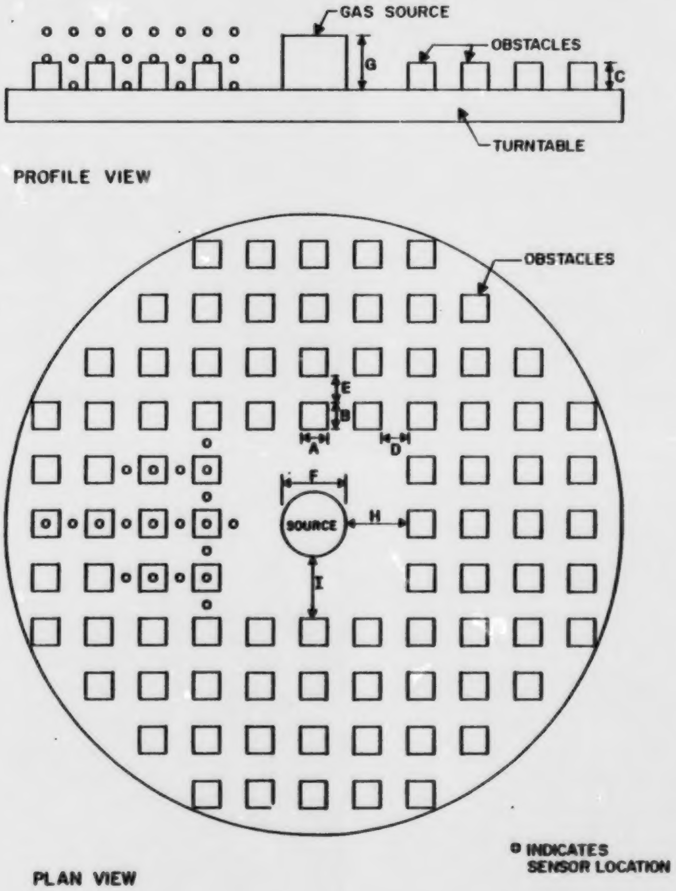
GAS SOURCE
OBSTACLES
G
C
TURNTABLE
PROFILE VIEW
OBSTACLES
E
B
A
D
F
SOURCE
H
I
o INDICATES SENSOR LOCATION
PLAN VIEW

FIGURE 3
UNIFORM TERRAIN IN THE WIND TUNNEL

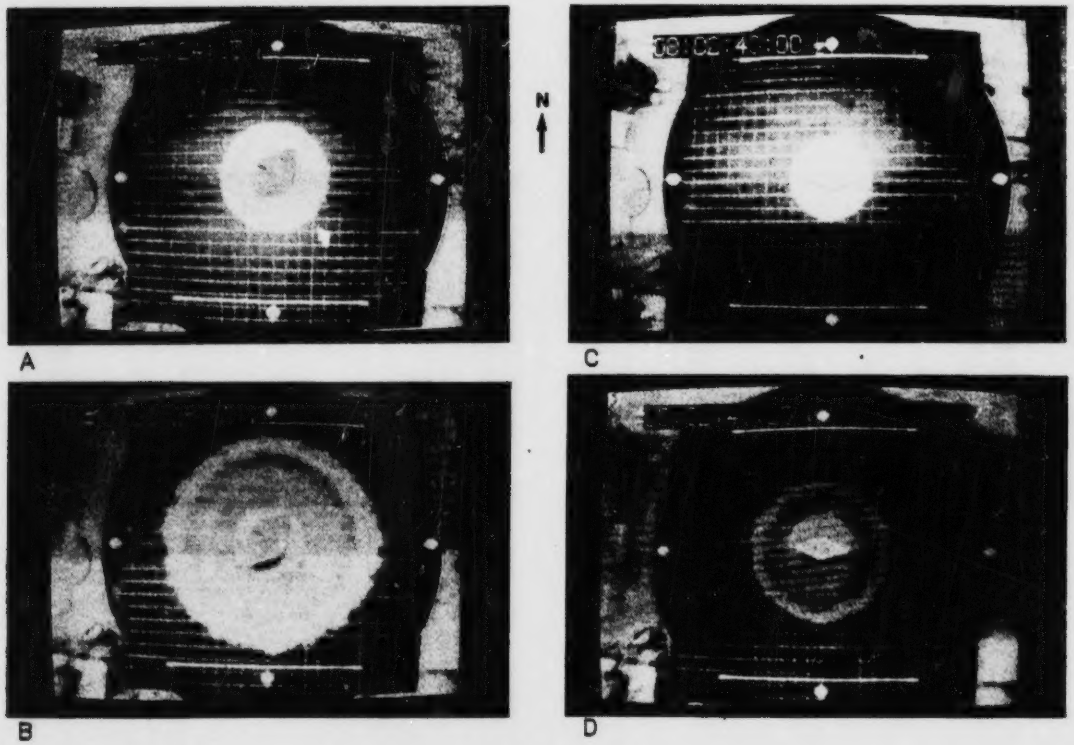

FIGURE 4

OVERHEAD VIEW OF HEAVY GAS RELEASE: NO OBSTACLES
A & B LARGE CANISTER C & D SMALL CANISTER

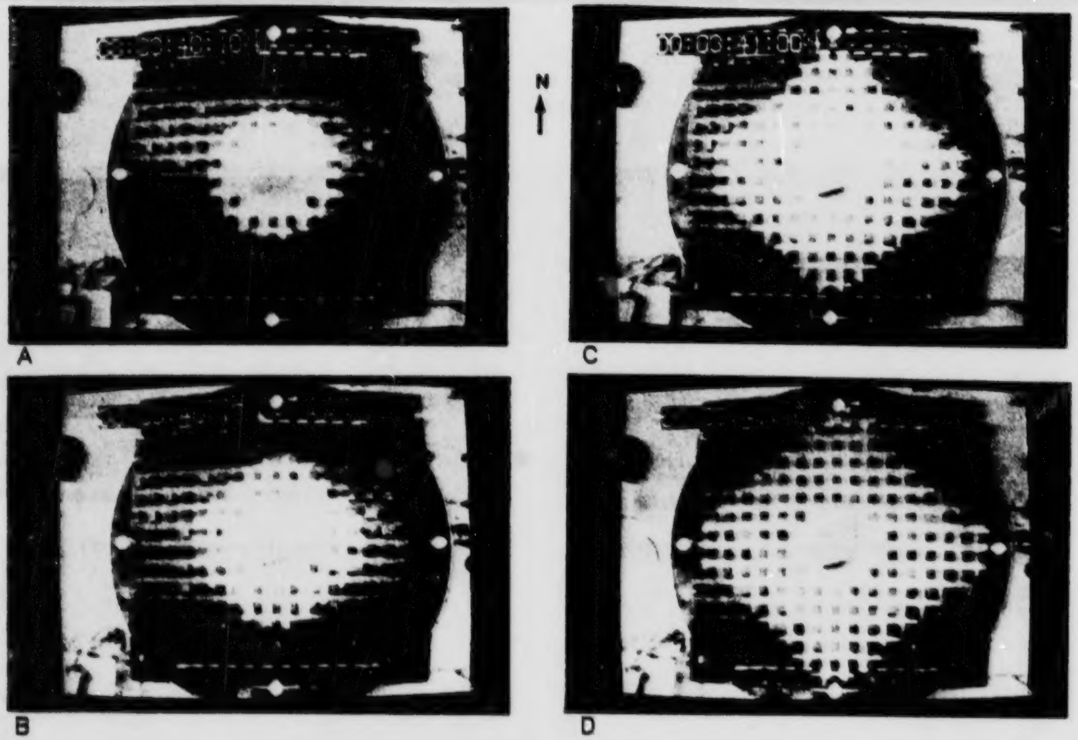

FIGURE 5
OVERHEAD VIEW OF HEAVY GAS RELEASE: LARGE CANISTER, MEDIUM BLOCKS, 1:1 SPACING, FULL COVERAGE

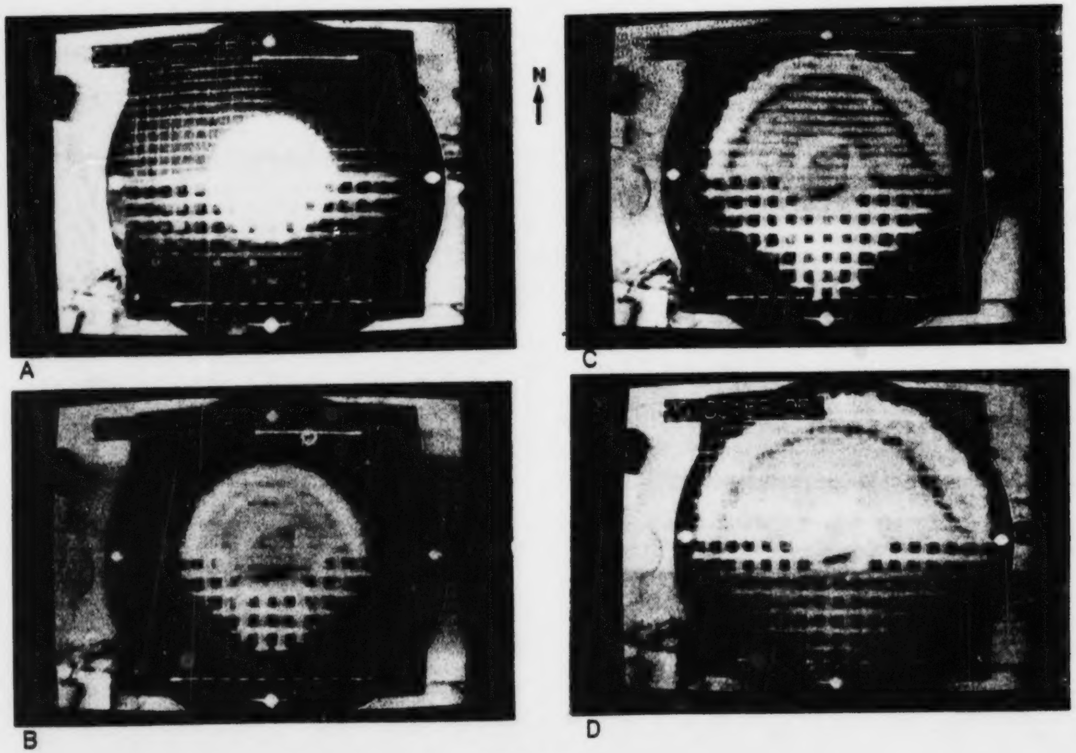

FIGURE 6

OVERHEAD VIEW OF HEAVY GAS RELEASE: LARGE CANISTER, MEDIUM BLOCKS, 1:1 SPACING, HALF COVERAGE

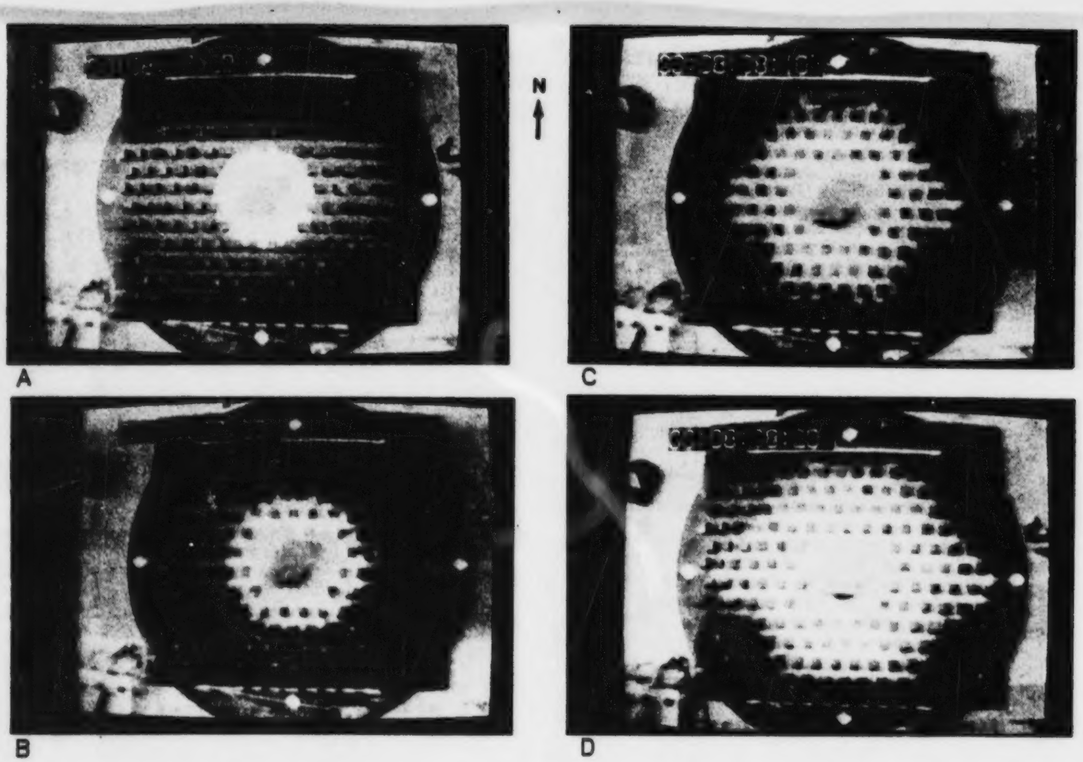

FIGURE 7

OVERHEAD VIEW OF HEAVY GAS RELEASE: LARGE CANISTER, MEDIUM BLOCKS, 1:1 STAGGERED SPACING, FULL COVERAGE

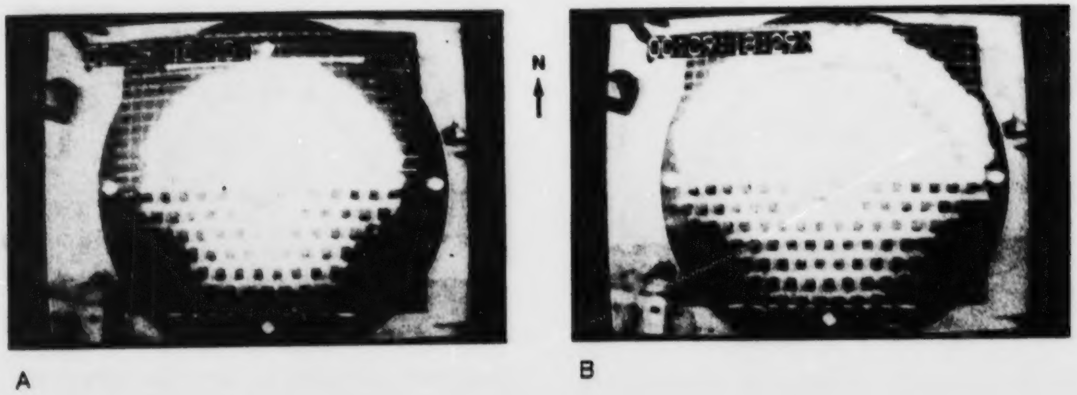

FIGURE 8
OVERHEAD VIEW OF HEAVY GAS RELEASE: LARGE CANISTER, MEDIUM BLOCKS, 1:1 STAGGERED SPACING, HALF COVERAGE

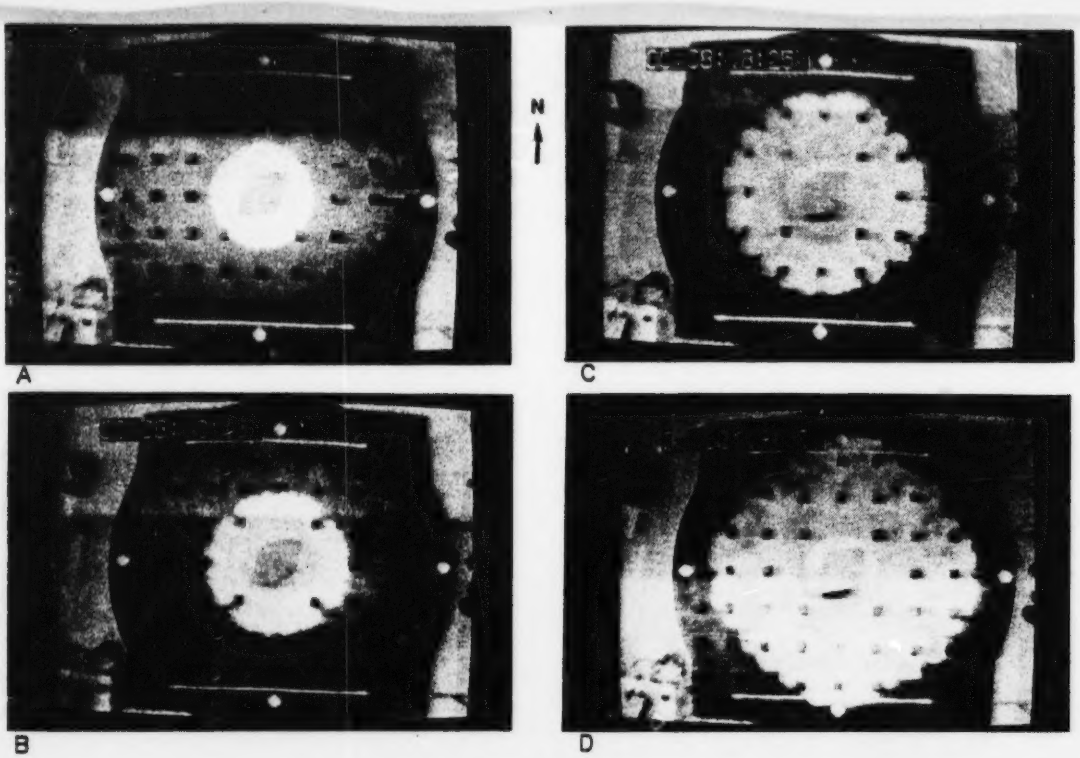

FIGURE 9
OVERHEAD VIEW OF HEAVY GAS RELEASE: LARGE CANISTER, MEDIUM BLOCKS, 1:3 SPACING, FULL COVERAGE

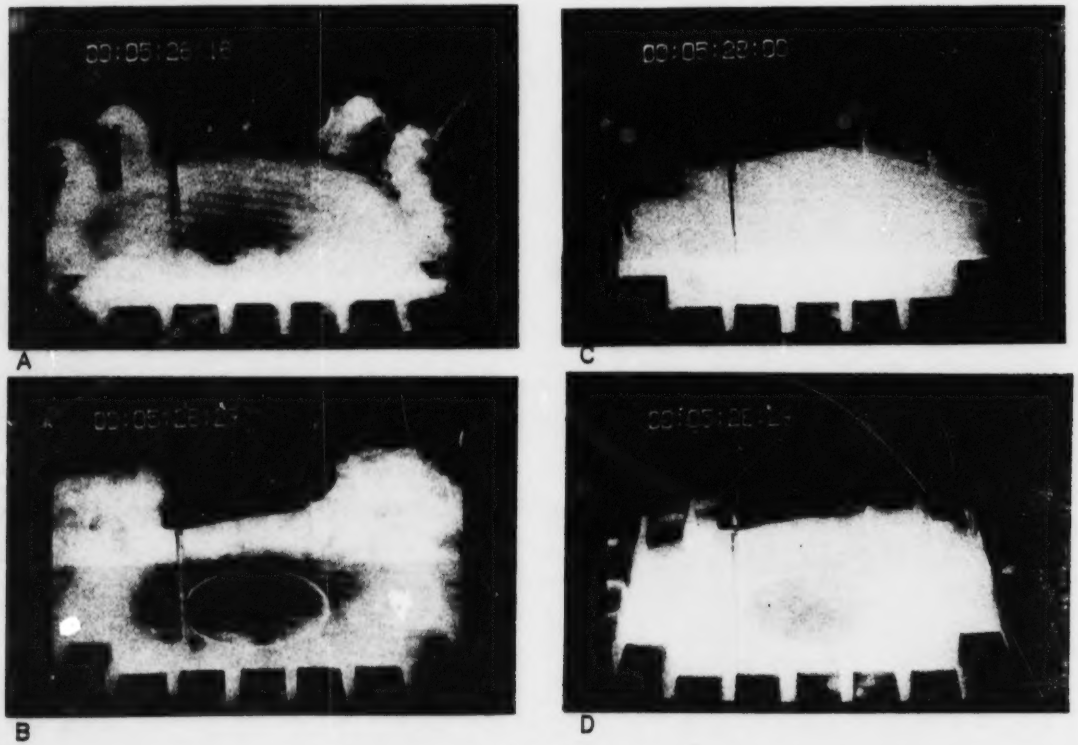

FIGURE 10
RELEASE AREA FOR HEAVY GAS RELEASE: LARGE CANISTER,
MEDIUM BLOCKS, 3.5:1 SPACING, FULL COVERAGE

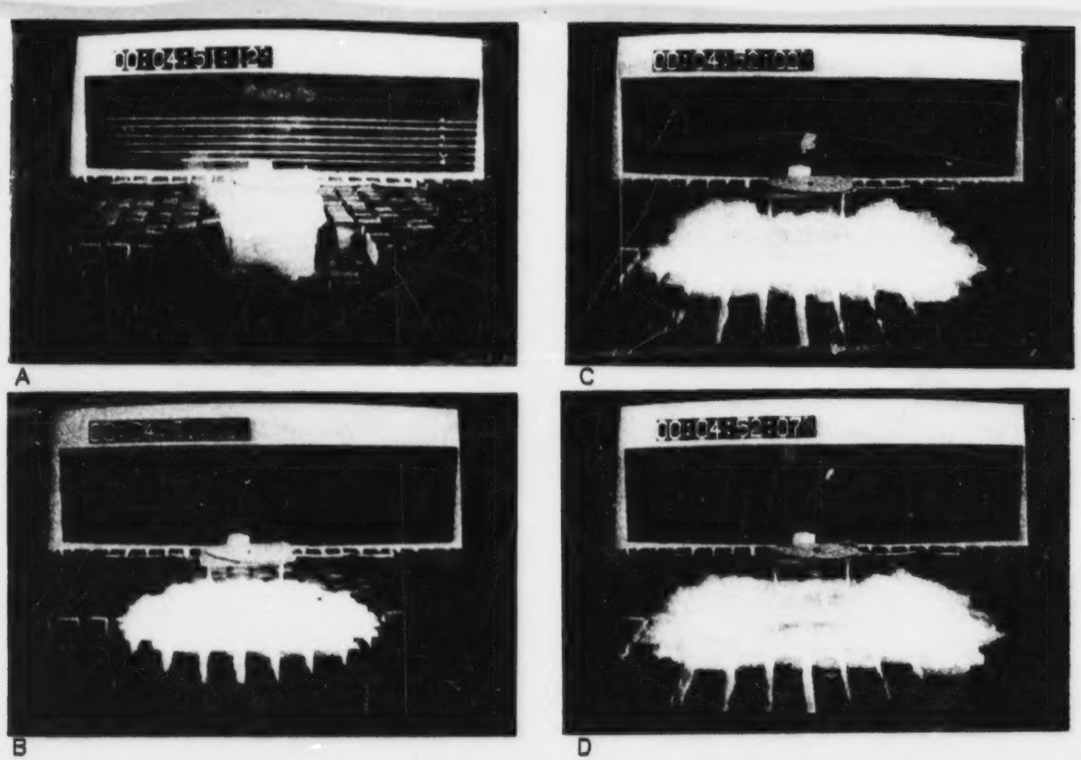

FIGURE 11
SIDE VIEW OF HEAVY GAS RELEASE – EARLY STAGES: LARGE CANISTER, MEDIUM BLOCKS, 3.5:1 SPACING, FULL COVERAGE

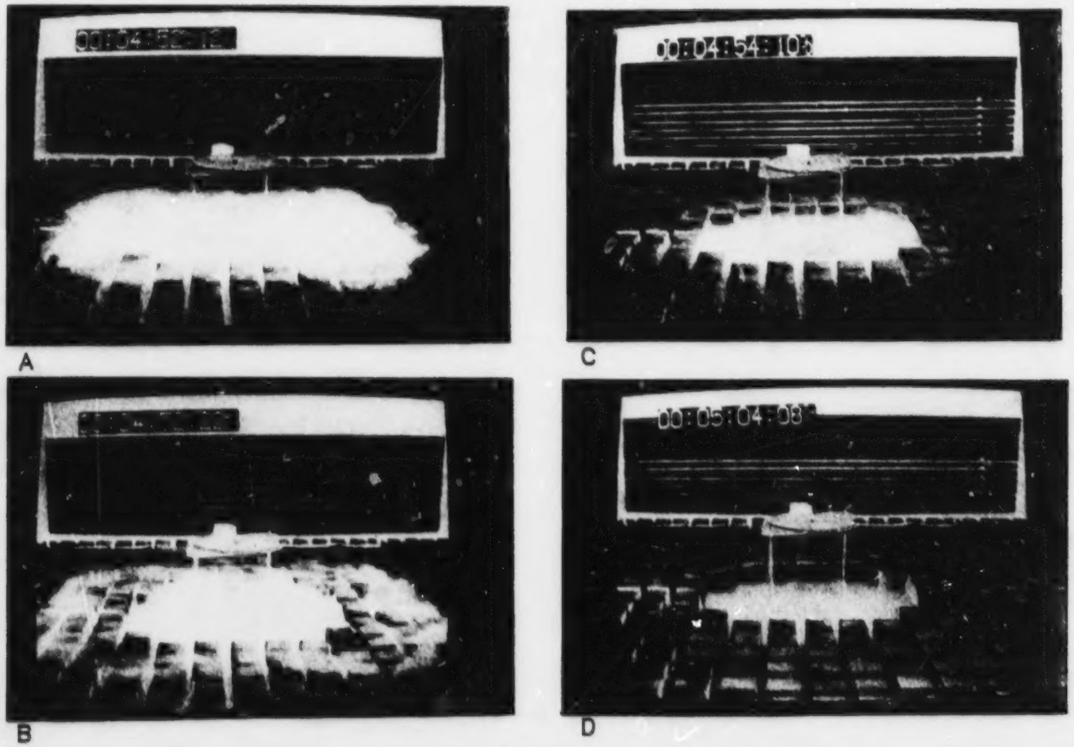

FIGURE 12
SIDE VIEW OF HEAVY GAS RELEASE – LATE STAGES: LARGE CANISTER, MEDIUM BLOCKS, 3.5:1 SPACING, FULL COVERAGE

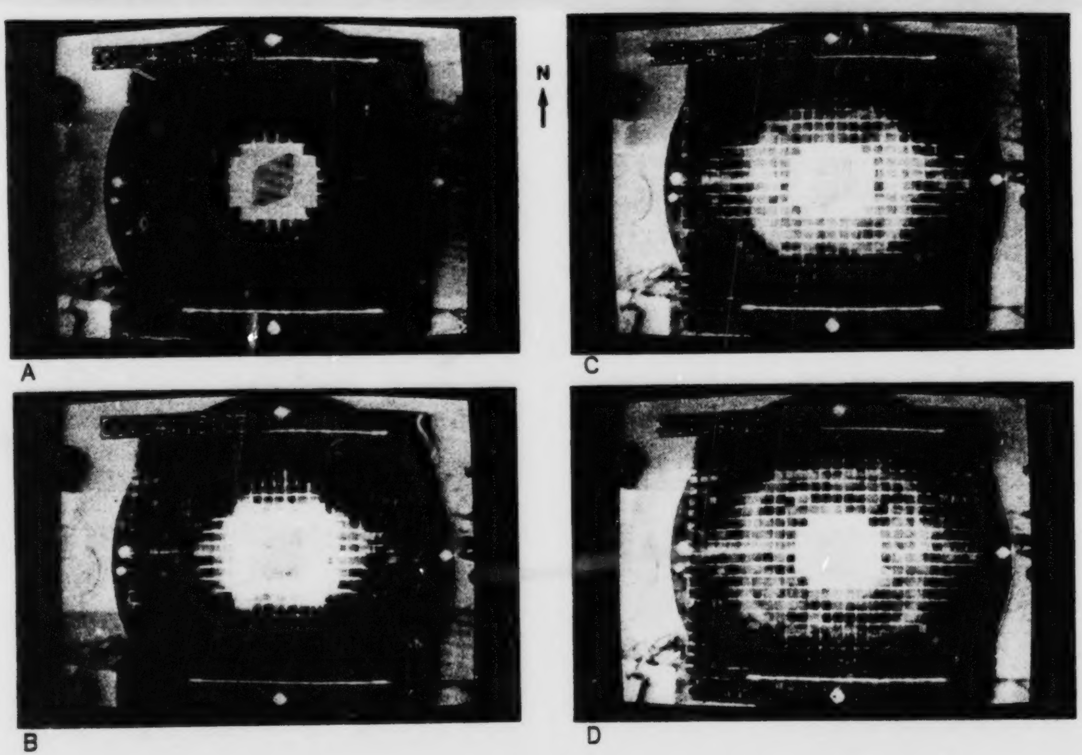

FIGURE 13
OVERHEAD VIEW OF HEAVY GAS RELEASE: LARGE CANISTER,
MEDIUM BLOCKS, 3.5:1 SPACING, FULL COVERAGE

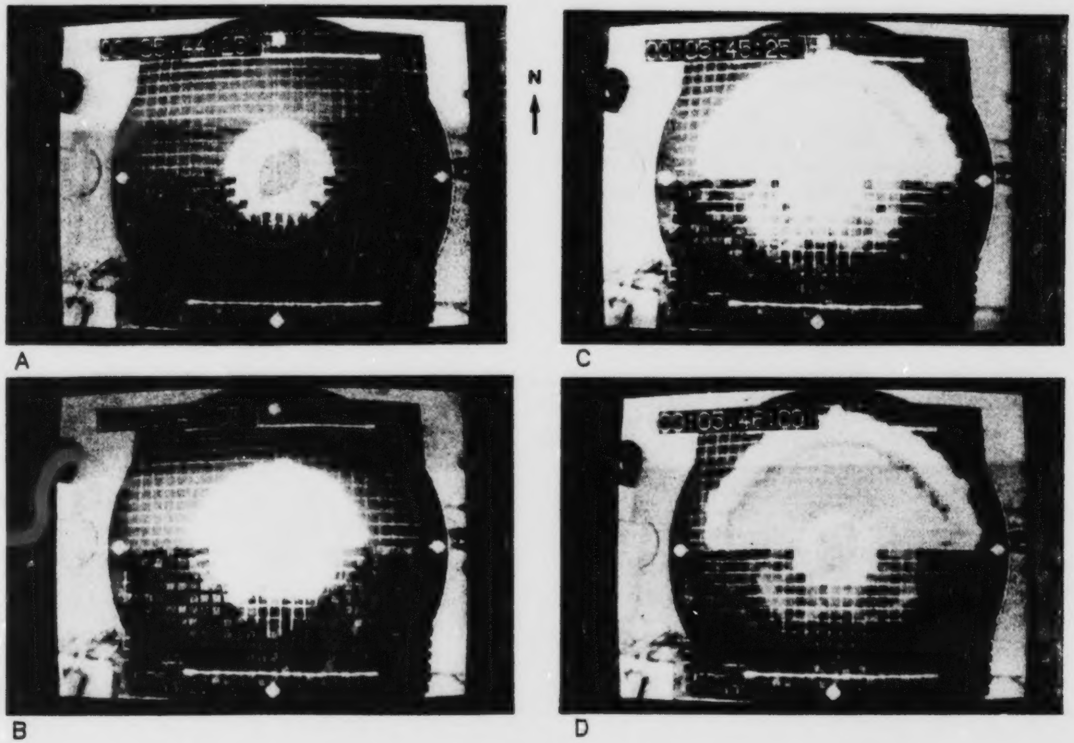
A
C
N
B
D
00:05:45:25
00:05:46:00

FIGURE 14
OVERHEAD VIEW OF HEAVY GAS RELEASE: LARGE CANISTER,
MEDIUM BLOCKS, 3.5:1 SPACING, HALF COVERAGE

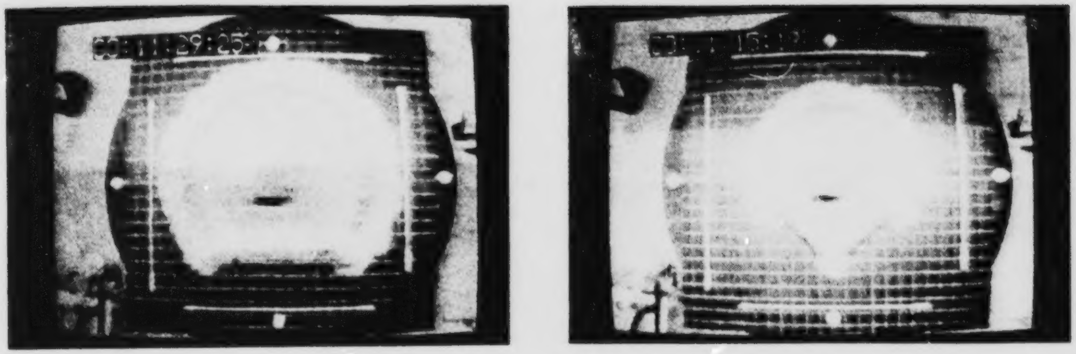

A

B

FIGURE 15

OVERHEAD VIEW OF HEAVY GAS RELEASE: LARGE CANISTER
A SOLID BARRIER, B TWO BARRIERS WITH GAP

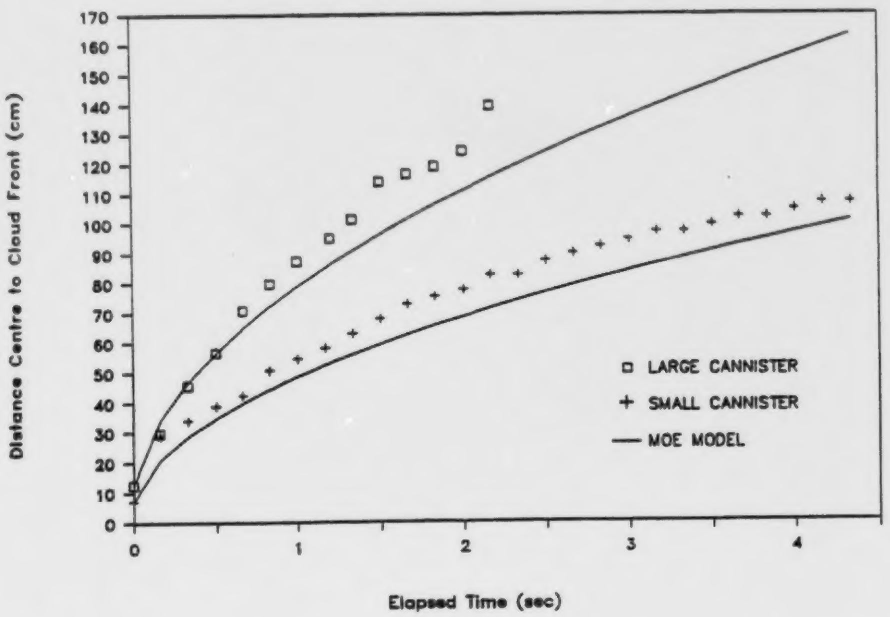

FIGURE 16
DISTANCE vs TIME: NO BLOCKS

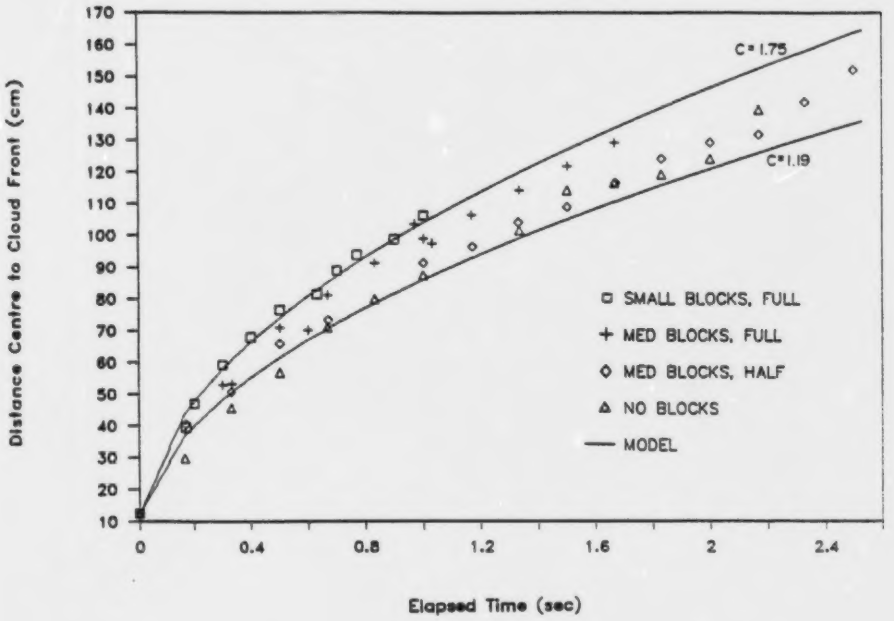

FIGURE 17
DISTANCE vs TIME: LARGE CANNISTER 90deg

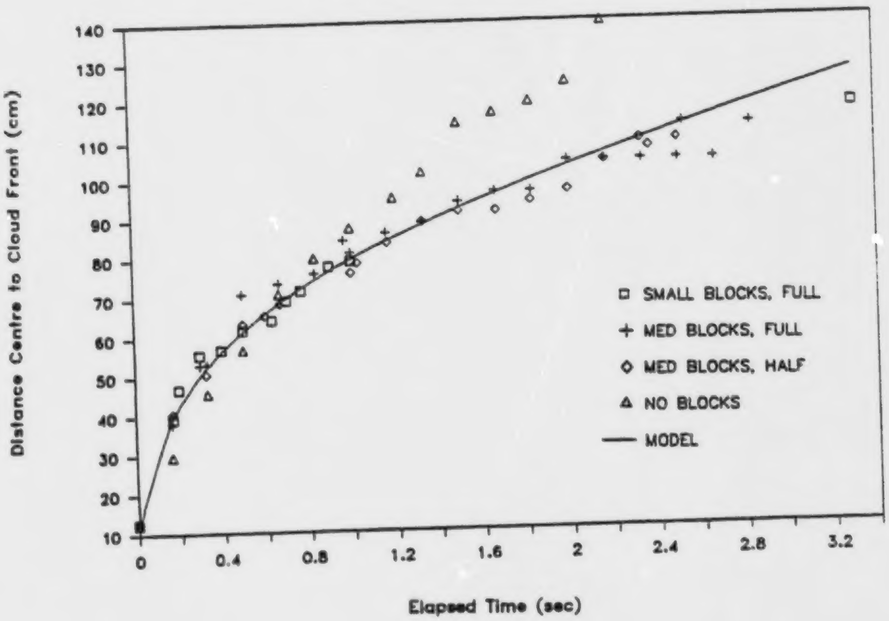

FIGURE 18
DISTANCE vs TIME: LARGE CANNISTER 45deg

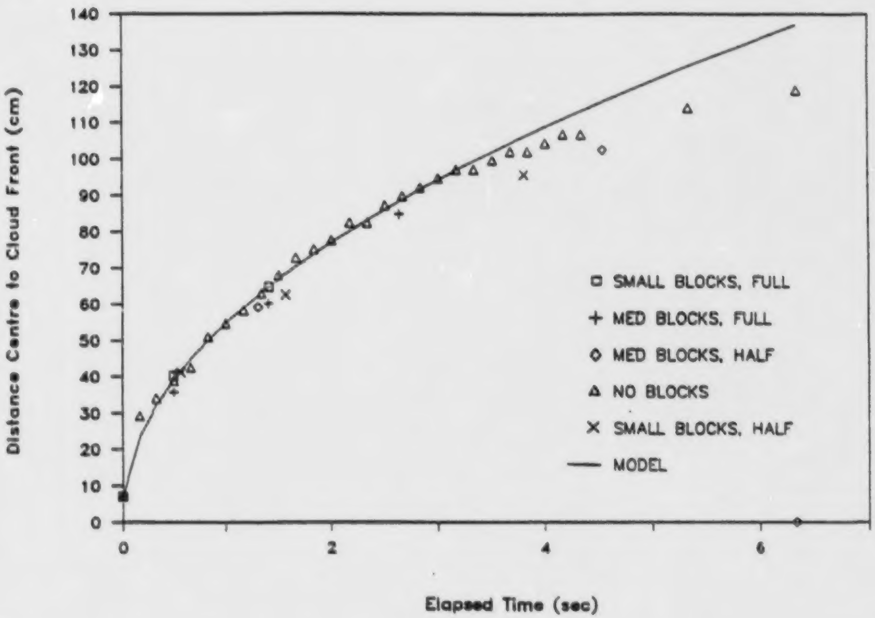

FIGURE 19
DISTANCE vs TIME: SMALL CANNISTER 90deg

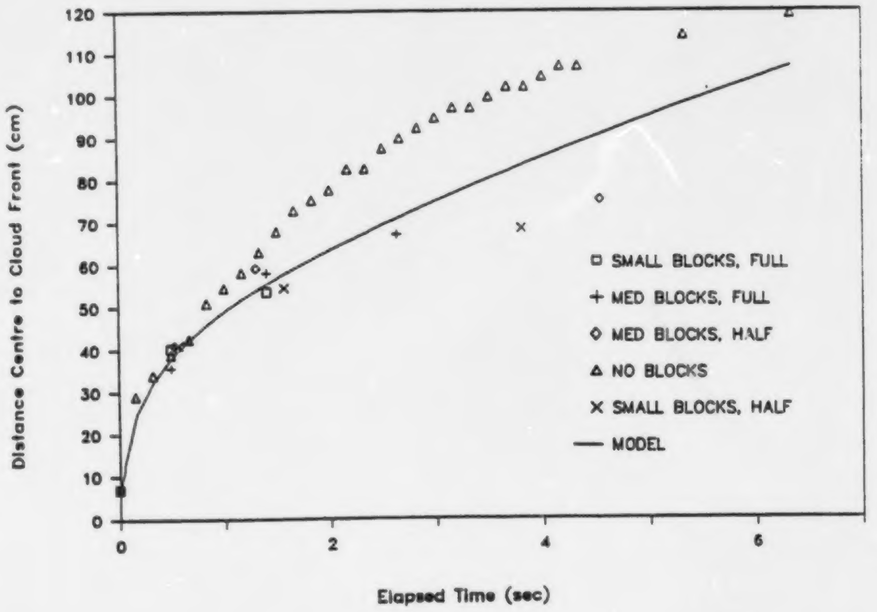

FIGURE 20
DISTANCE vs TIME: SMALL CANNISTER 45deg

A11

AN INVESTIGATION OF WIND GENERATED PARTICLE TRANSPORT RATES WITHIN A TURBULENT BOUNDARY-LAYER

A. D. Ciccone, J. G. Kawall and J. F. Keffer
Department of Mechanical Engineering
University of Toronto
Toronto, Ontario, M5S 1A4

Abstract

Most research and experiments carried out on the movement of particles in air have been concerned with the total mass transport or flux of material from a surface. It has been established that the total rate of transport can be attributed to three modes of motion which are not mutually exclusive: saltation, surface creep and suspension. Here, saltation is the most important since it is a prerequisite for the other two. The empirically determined saltation rates for wind generated particle movement are, in many cases, not in accord. Investigators have either modified the constants in Bagnold's saltation formula or developed complicated empirical equations to determine the transport rates. These equations are not likely to give further insight into the physics involved in the transport mechanisms. An alternative procedure is to examine the various components of the transport rate and determine the parameters on which it depends. A novel flow-visualization/digital image analysis technique has been developed to determine individual particle trajectories, from which saltation rates can be computed. This technique involves recording individual particle motions, which have been illuminated with a strobed light source, on 35 mm high-speed film, digitizing the film and using a high-speed computer to track the particle trajectories. The transport rates are determined subsequently from the particle-trajectory data.

Introduction

In recent years, wind generated particle transport or wind erosion has been receiving increasing attention (Barndoroff-Nielsen, 1985) from scientists and engineers interested in the effects of soil erosion, snow drift, sand movement and other related natural phenomena on local environmental, agricultural and economic conditions. For example, fugitive emissions are generated from open-area sources such as coal or iron ore stockpiles by the wind. These emissions are either transported downwind, affecting the air quality of near-by air-sheds or fall out locally, acting as a hindrance to a clean work place. Wind induced erosion can also seriously affect the agricultural yield of a region, as was the case this year in the prairie provinces. In both of the above situations, valuable resources can be lost if appropriate control strategies are not adopted. In order to develop such control strategies, an understanding of the physics associated with wind erosion is required.

Previous studies (Bagnold, 1941, Chepil, 1945, Gillette, 1978) have identified three primary modes of particle transport: surface creep, suspension and saltation. Surface creep pertains to particles greater than 1000 μm in diameter, which are too heavy to become airborne but which can roll or slide along the surface. This transport mechanism accounts for about 10% of the total mass movement. Suspension pertains to particles that generally have diameters less than 100 µm. These particles remain airborne for long periods of time and are carried along at roughly the fluid stream velocity. The dominant mass movement (about 50% to 75% of the total) occurs by saltation, which pertains to particles having diameters between 100 to 1000 µm. In this mode of transport, particles never go into complete suspension; rather, they remain close to the surface (usually within about 5 cm) forming a relatively thin "saltation layer". Within this layer the particles travel in a series of jumps or hops of about 10 cm in length. A fundamental finding of the aforementioned studies is that suspension of particles cannot occur without saltation as a prerequisite.

Investigators have basically used a mass-flux technique in which the mass uplifted from a surface is collected by a vertical array of traps and subsequently analyzed in order to develop empirical relationships for the vertical and horizontal fluxes as a function of the surface shear velocity (u_*) and other parameters. The first empirical relationship for the saltation rate (Q) was proposed by Bagnold (1941) as

$$Q \propto u_*^3 \tag{1}$$

This has been modified and extended (White, 1979; Gillette, 1978) to include various parameters and is the basis for most calculations to determining the erosion rate associated with a surface. Agricultural engineers have developed an empirical soil-erosion model, which involves a set of parameters, to predict the potential annual soil loss,

$$E = f(I', C', K', L', V), \tag{2}$$

where I' is the soil erodibility, C' is the local climatic factor, K' is the soil ridge roughness factor, L' is the field length and V is the vegetation factor (Chepil and Woodruff, 1963). The above equation serves to illustrates the empiricism involved in determining the erosion rate.

The mass-flux approach generally yields good engineering results for the quantity of material transported by the wind but does not provide any understanding of the physics of the wind erosion process. An approach which does so is to consider the saltation process in terms of the motion of individual saltating particles within a turbulent boundary-layer in a Lagrangian frame of reference. Such an approach has been adopted by the Turbulence Research Group (TRG) in the University of Toronto's Mechanical Engineering (UTME) Department. This involves the use of a novel flow-visualization/digital-image-analysis technique for obtaining the characteristics of individual particle trajectories. In the present work, the technique used to obtain the trajectories is described, the governing equations of motion for the particles are discussed, and results for the particle flux profiles within the saltation layer, the saltation rate and the vertical mass flux of material are presented.

Experimental Details

The acquisition of good quality images or pictures is of crucial importance in the implementation of the aforementioned technique. The elements required for this include a wind tunnel facility, a lighting system, photographic equipment and film, and a digital image data acquisition system.

Experiments were carried out in a blow-through open circuit wind tunnel located in UTME. This tunnel has a rectangular test-section (180 cm long, 31 cm wide and 61 cm high) with a plexiglass top for transmitting light and a plexiglass side for viewing. Mono-dispersed (195 μm) silica sand particle beds, 100 cm long, 10 cm wide and 0.5 cm thick, were placed along the test-section centerline. The entire test section was shrouded in black, except for a 25 cm by 25 cm viewing port located 40 cm from the leading edge of the particle bed and a 10 cm slit directly above the viewing port located along the centerline of the test section. A 35 mw He-Ne laser was used as a continuous collimated light source. The laser beam was aligned above and along the centerline of the test-section and the beam deflected 90° by a prism and passed through a cylindrical lens (4.4 cm focal length) to generate a 12 cm by 0.2 cm plane of very intense light.

Still photography was chosen in preference to high-speed cinematography, since with the former it was possible to capture most of the trajectory of an individual particle in a single frame. As a consequence, it was easier to observe the particle's path, and the amount of digitization required was reduced. In order to resolve rapid changes in particle position and velocity, the light source was "strobed" at 300 Hz by means of a rotating disk with an equal number of open and closed sectors.

A 35 mm Contax 139 SLR camera fitted with a 105 mm telephoto lens was positioned perpendicular to the flow, outside of the test-section on a tripod. The distance from the plane of the film to the plane of light was approximately 41 cm, giving a field of view of 7.5 cm by 5 cm and a depth of view of 1 mm at an aperture opening of f2.8. Kodak Recording 1000 ASA film was used as the recording medium. The camera shutter was held open for 0.5 s and, with the particles illuminated by the stroboscopic light, "dashed" particle trajectories were recorded. These enabled measurements of velocity and position to be made in a Lagrangian frame of reference.

A pitot tube was situated above the field of view to monitor the wind speed (5.5 m/s) during each experiment. Once particle motion was initiated, a roll of 36 frames, each containing a 0.5 s exposure, was shot every 2 seconds with the aid of a remote shutter cord and winder. Instantaneous wind velocity data were acquired without the particle beds present using constant temperature cross-wire hot-wire anemometers. These data were recorded and subsequently computer-analyzed to obtain the mean longitudinal and vertical velocity components, turbulent intensities, velocity spectra and Reynolds stresses.

After all the film was developed, the negatives were digitized on the UTME Digital Image Analysis System. This system has a Cohen CCD scanner with a Panasonic 25 mm T.V. lens, attached to a Quantex video processor, which is in turn connected to a microVax computer. The scanner converts the image into 512 analogue scan lines which are digitized at a rate of 512 points per line by the Quantex, and the digital data are retrieved by the computer. Thus, each image is represented as a 512 by 512 matrix with each picture element or "pixel" containing 8 bits of light intensity values, giving grey-levels between 0 and 255. The digital data are subsequently stored on magnetic tape.

Image Processing and Analysis

A typical digitized image is presented in Figure 1, where the dark dashed lines on the light background represent the particle trajectories. Prior to the extraction of the dashed-line data, the images had to be enhanced to remove the noise (i.e., the uneven shades of background light and thin vertical lines due to the plexiglass) while still maintaining the integrity of the image. Due to the large number of particles present and their various orientations, an "artificial intelligence/computer-vision" approach was needed to objectively analyse the pictorial data. Conventional approaches, such as thresholding the grey levels or their gradients (Rosenfeld and Kak, 1982), did not provide adequate image enhancement, as is evident from Figure 2. Here, a modified gradient operator was used to enhance and detect the particle lines (Ciccone et al., 1987).

A sophisticated scheme to further enhance the data was developed by considering the image as a two-dimensional signal and applying the Fourier transform to this signal. The dashed lines were found to have a particular "frequency" range which was different from that associated with the uneven background grey-level and spurious noise. A description of this scheme follows.

The two-dimensional Fourier transform of an image, a complex function with real and imaginary components, is given by:

$$F(u,v) = \iint_{-\infty}^{\infty} f(x,y)e^{-j2\pi(ux+vy)}dxdy, \tag{3}$$

where F is the Fourier transform of the image f, and u and v are the image frequencies associated with the x and y directions. Since the kernel function can be separated into two parts, (3) can be carried out via two one-dimensional Fast Fourier Transforms (FFT) by first transforming the rows and then the columns of the image matrix or vice versa. Once the image has been transferred into frequency space, it can be readily filtered by means of a variety of digital filters. The "digital" representation of a band-pass filter is,

$$H(u,v) = H_h(u,v)\,H_l(u,v), \tag{4}$$

where $H_h(u, v)$ and $H_l(u, v)$ are the high and low pass components of the filter. The frequency-domain form of the filtered image is given by,

$$G(u,v) = F(u,v)\,H(u,v), \tag{5}$$

This is transformed back into the real domain via an inverse Fourier transform, i.e.,

$$g(x,y) = \iint_{-\infty}^{\infty} G(u,v)e^{-j2\pi(ux+vy)}dudv. \tag{6}$$

In selecting the appropriate high and low filtering frequencies, an understanding of what contributes to each domain is required. Edges and other sharp transitions in grey levels are associated with the high-frequency components while the uneven background levels contribute to the low frequency components. Thus, an image is sharpened by attenuating the low frequencies (high-pass filtering) and smoothed by attenuating the high frequencies (low-pass filtering). In the present study, a symmetrical Butterworth band-pass filter was applied to the image using 25 and 250 as the appropriate high and low cut-off frequencies. The result of applying the "Fourier" enhancement scheme is illustrated in Figure 3. As can be seen the integrity of the image is maintained, but the spurious noise has been removed and an even background of grey provided. It should be noted that this procedure is a robust and efficient means of enhancing an image.

In order to locate the particle trajectories, which are thick lines, one could use a pattern-recognition technique to compare lines of various lengths and angles with the enhanced image. This approach, however, would be extremely cumbersome and time consuming. A more efficacious approach has been developed based on the fact that a line can be considered as a series of overlapping points, vis-à-vis the present situation . Thus, correlating the template representation of a solid circle with the image and subsequently normalizing the resulting cross-correlation function produces a series of adjacent points which represent the centers of the dashed lines. The normalized cross-correlation function (Gonzalez and Wintz, 1977) is given by:

$$C_{tg}(x,y) = \frac{\iint t(\alpha,\beta)\, g(x+\alpha,y+\beta)d\alpha d\beta}{[\iint t^2(\alpha,\beta)d\alpha d\beta]^{1/2}[\iint g^2(x+\alpha,y+\beta)d\alpha d\beta]^{1/2}}, \tag{7}$$

where t represents the template and g represents an image. The template used is shown in Table 1.a. Since this template also responds to vertical lines, a second template of a vertical line (Table 1.b) was cross-correlated with the image and high responses to it were ignored. Figure 4 shows the local maxima of the above cross-correlation function and, as can be seen, the dashed lines have been extracted. The computer now knows the location of each pixel but does not know the pixel-to-pixel relationship. These pixels form a set of candidate points to be arranged into subsets which make up lines of finite length. Similarly, these subsets form the particle trajectories which must be linked together. This line tracking analysis can be considered a type of artificial intelligence/computer-vision analysis.

Initially, the candidate pixels are extracted from the digitized image column by column, i.e., all candidates in column 1 followed by all candidates in column 2, etc. The following three tracking criteria are used: (i) the nearest neighbour (i.e., Euclidean) distance $\leq \sqrt{2}$; (ii) a minimum number of pixels is required to form a line; (iii) the pixels form a line which has no curvature. Criterion (i) is used to either initiate a line or to extend a line which is being tracked; (ii) is used to rid the image of residual noise; (iii) is used to break up lines which either cross or make sudden deviations, as is the case when a particle rises from or impacts upon a surface. This process is a combined parallel and serial approach where more than one line is followed at any one time. Note that when lines cross, they are flagged and any pixel which is accepted for one line is cross-checked with other line to see if it may belong to both lines. The line subsets are then used to link the line segments together and reconstruct the trajectories. Figure 5 shows a typical result of applying the procedure.

Since the light source was strobed at a 300 Hz, each particle trajectory was divided into small straight line segments, with adjacent segments having similar characteristics, i.e., direction of flight and length. Thus, the difference in characteristics between dashed lines which belong to the same trajectory should be small. The line segments are linked together by first extending a given line by its own length in its direction of flight from left to right, i.e., the "end" coordinates of the extended line are given by:

$$x_{end} = x_2 + \Delta x \tag{8.a}$$

$$\text{and} \quad y_{end} = y_2 + \Delta y, \tag{8.b}$$

where x_2 and y_2 are the end coordinates of the original line of length $\Delta l=(\Delta x^2+\Delta y^2)^{1/2}$. Lines are linked together using the following three criteria: (i) the product of the slopes of any two lines must be positive or zero; (ii) the difference between the start of a candidate line and the end of the extended line must be less than a specified threshold; (iii) the size of the lines must be similar. The first criterion is used to ensure that the lines are collinear and the second and third are used to ensure that they belong to the same particle path. The result of using these criteria is presented in Figure 6. Note that the particle velocities are obtained by multiplying the length of the line segments by the strobing frequency. As illustrated, the particle trajectories are incomplete. In order to complete the trajectories, a Lagrangian random-flight model, based on the particles' equations of motion is used.

Lagrangian Random-Flight Model

In the present case, the particles can be considered spherical, and the requisite equation of motion can be derived from a force balance on an individual particle as follows. Newton's second law yields:

$$m_p \frac{d\bar{V}_p}{dt} = \sum \bar{F}_i, \tag{9}$$

where m_p is the particle mass, V_p is the particle velocity and ΣF_i is the sum of the relevant forces comprising drag, lift, pressure, gravity and virtual mass as given below.

$$\bar{F}_{drag} = -C_d \frac{\pi}{4} D^2 \rho_f \frac{\bar{V}_R |\bar{V}_R|}{2} \tag{9.a}$$

$$\bar{F}_{lift} = -C_l \frac{\pi}{6} D^3 \rho_f (\bar{V}_R \times \bar{\Omega}) \tag{9.b}$$

$$\bar{F}_{pressure} = \frac{\pi}{6} D^3 \rho_f \frac{d\bar{V}_f}{dt} \tag{9.c}$$

$$\bar{F}_{gravity} = -(\rho_p - \rho_f)\bar{g} \tag{9.d}$$

$$\bar{F}_{virtual\ mass} = C_{vm} \frac{\pi}{6} D^3 \rho_f \left(\frac{d\bar{V}_f}{dt} - \frac{d\bar{V}_p}{dt} \right) \tag{9.e}$$

In equations (9.a) to (9.e), C_d, C_l and C_{vm} are the coefficients of drag, lift and virtual mass, respectively, g is gravity, D is the particle diameter, ρ_p and ρ_f are the particle and fluid densities and V_R is the particle relative velocity given by:

$$V_R = (V_{xR}{}^2 + V_{yR}{}^2)^{1/2}, \tag{10}$$

with

$$V_{xR} = V_{xp} - U, \tag{10.a}$$

$$V_{yR} = V_{yp} - V, \tag{10.b}$$

where U and V are the components of the fluid velocity (V_f) in the x and y directions, respectively.

After substitution and rearrangement, the resulting equation is

$$\left(\frac{\rho_p}{\rho_f}+C_{vm}\right)\frac{d\bar{V}_p}{dt}=-\frac{3}{4}C_d\frac{\bar{V}_R|\bar{V}_R|}{D}+\left(1+C_{vm}\right)\frac{d\bar{V}_f}{dt}+-\left(\frac{\rho_p}{\rho_f}-1\right)\bar{g}-C_l(\bar{V}_R\times\bar{\Omega}). \quad (11)$$

Since $\rho_p >> \rho_f$, the above equation can be reduced to the following, with only the drag, lift and gravity forces being retained:

$$\frac{d\bar{V}_p}{dt}=-\frac{3}{4}C_d\frac{\rho_f}{\rho_p}\frac{\bar{V}_R|\bar{V}_R|}{D}-C_l\frac{\rho_f}{\rho_p}(\bar{V}_R\times\bar{\Omega})-\bar{g}. \quad (12)$$

This equation provides a Lagrangian description of the particle path. The drag coefficient C_d, varies with the particle Reynolds number

$$Re_p=\frac{|\bar{V}_R|\,D}{\nu}, \quad (13)$$

and is calculated from empirical relationships (Morsi and Alexander, 1972). The lift force is given in terms of the vector product of the relative particle velocity and the fluid vorticity,

$$\bar{\Omega}=\nabla\times\bar{V}_f, \quad (14)$$

and was considered by Hunt et al. (1984). This force is similar to the lift force which acts on an airfoil in an inviscid flow with circulation.

Given an initial particle velocity and position and the wind field, (12) can be integrated numerically, both forward and backward in time, to determine the particle impact and ejection points and velocities. By *randomly* varying the wind field components and ensemble averaging the trajectories, a stochastic description of the particle's trajectory can be realised. Using the wind field measured by the hot-wire anemometers, the trajectories are completed as shown in Figure 7. It should be noted, that the fluid has been assumed to be unaffected by the presences of the particles.

Approximately 100 trajectories were recorded and analyzed to determine various physical characteristics such as the particle ejection velocity vector, maximum height and jump length. These trajectories are consistent with those described by Owen (1964), White and Schulz (1977) and Hunt and Nalpanis (1985). A synopsis of the 195 µm particle results for a 5.5 m/s wind are presented in Table 2. From the latter, it is apparent that the mean ejection velocities are greater than both u_* and the fluid threshold velocity (u_{*t}). This would indicate a mechanism other than mean shear stress acts to eject particles in to the boundary-layer. The most likely mechanism is impaction from other particles rather than the lift force generated by the wind shear, since this force corresponds to less than 6% of gravity.

Estimation of the Mass Movement

With the aid of the actual trajectories, estimates of the particle fluxes, concentrations and saltation rates can be made, i.e, Lagrangian data can be used to obtain Eulerian point data. On the assumption that saltation is uniform and stationary, the mass flux of particles across unit width of a plane perpendicular to the fluid stream is

$$G(D) = \int_0^{y^*} m \chi V_{sp} \, dy, \tag{15}$$

where G is the saltation rate, χ is the particle concentration, m is the mass of a particle of diameter D, V_{sp} is the particle horizontal velocity and y^* is the height of the trajectory traced out by the particle (Owen, 1964). The integrand represents the horizontal flux of material. Now, (15) can be rewritten as,

$$G(D) = m \phi(D) \int_0^{t^*} \dot{x}(t;D) \, dt \tag{16}$$

where $\phi(D)$ is the vertical flux of particles, $\dot{x}(t;D)$ is the particle horizontal velocity as a function of time and t^* is the time of travel. This results in:

$$G(D) = m \phi(D) \bar{x}(D), \tag{17}$$

where $\bar{x}(D)$ is the particle jump length (Jensen and Sorensen, 1982).

Evaluation of (15) and (17) using the calculated particle trajectories is carried out by recording the number of particles caught in an ideal "numerical trap" and their horizontal velocities. This trap is unit width, Δy units high and is located at the maximum height of a particle trajectory. The horizontal flux of particles is determined at each trap height, and from this, the saltation rate is calculated using (15). Also, since the mean particle jump length is known, the vertical flux is calculated from (17).

In order to obtain stable concentration and flux profiles, the ejection velocity components of each particle are varied several times, using a Gaussian random number generator, particle jump lengths are determined and particle data are ensemble-averaged until convergence is attained. It was found that repeating the procedure (i.e., varying the velocity components) 500 times provided adequate convergence. Figure 8 presents the normalized horizontal fluxes as a function of height obtained for the 195 μm particles. The saltation rate was calculated to be 0.124 g/cm/s using (15) and the vertical suspension rate was calculated to be 0.017 g/cm^2/s using (17). It is noted that the trend of the present results is similar to that of the data presented by Hunt and Nalpanis (1985).

Conclusions

Flow-Visualization of saltating silica-sand particles in a wind-generated boundary-layer has been achieved. The resulting particle-trajectory data have been objectively analyzed using an artificial intelligence/computer-vision approach. A two-dimensional Lagrangian model has been developed and implemented to complete the particle trajectories and from this, the mass flux of material has been estimated.

The particle statistics, indicate that impacting particles have a substantial effect on the ejection of other particles since the particle ejection velocities are greater than the surface friction velocity. But, as suggested by Owen (1964), the introduction of particles into the fluid boundary-layer results in a slowing down of the fluid velocity, since the particles act as momentum sinks; thus, particles that are subsequently ejected do not gain as much momentum. It is suggested that the fluid boundary-layer acts as a feed back mechanism.

A hypothetical scenario for the saltation process would be as follows.

(i) Initial particles begin to saltate when the wind exceeds the particles fluid threshold velocity.

(ii) Particles gain momentum from the boundary layer and impact onto the surface; the boundary-layer adjusts itself due to this exchange of momentum.

(iii) Impacting particles transfer momentum to the surface, in addition to that transferred via the boundary-layer.

(iv) The momentum transmitted to the surface is partitioned between the impacting particles which continue to saltate and other particles causing them to eject.

(v) Steps (ii) to (iv) are repeated until a steady-state condition is reached.

Acknowledgements

This research was supported by the Ontario Ministry of the Environment, Grant 372G.

References

[1] Bagnold, R.A., 1941: *The Physics of Blown Sand and Desert Dunes*, Metheun and Co. Ltd., London.

[2] Barndoroff-Nielsen, O.E., Muller, J.T., Remer Rasmussen, K. and Willetts, B.B., 1985: eds., *Int. Workshop on Physics of Blown Sand*, Univ. of Aarhus, May.

[3] Chepil, W.S., 1945: Dynamics of Wind Erosion: I, Nature of Movement of Soil by Wind, *Soil Science*, 60, 305-320.

[4] Chepil, W.S. and Woodruff, N.P., 1963: The Physics of Wind Erosion and its Control, *Advances in Agronomy*, Academic Press, Toronto, 15, 1-301.

[5] Ciccone, A.D., Kawall, J.G. and Keffer, J.F., 1987: Digital Image Analysis of Macroscopic Particle Motions Generated by a Turbulent Wind, *Sixth Symposium on Turbulent Shear Flows*, Toulouse.

[6] Gillette, D., 1977: Fine Particulate Emissions Due to Wind Erosion, *Trans. ASAE*, 890-897.

[7] Gonzalez, R.C. and Wintz, P., 1977: *Digital Image Processing*, Addison-Wesley, Massachusetts.

[8] Hunt, J.C.R. and Nalpanis, P., 1985: Saltation and Suspended Particles over flat and Sloping Surfaces, *Proc. Int. Workshop on Phys. of Blown Sand*, Aarhus.

[9] Hunt, J.C.R., Thomas, N.H., Auton T.R. and Sene, K., 1984: Entrapment and Transport of Bubbles by Plunging Water, *Gas Transfer at Water Surfaces*, eds. Wilfried Brutsaert and Gerhard H. Jirka, D. Reidel Publishing, Boston, 255-268.

[10] Jensen, J.L. and Sorensen, M., 1982: On Mathematical Modeling of Aeolian Saltation, *Euromech 156*, Istanbul.

[11] Morsi, S.A. and Alexander, A.J., 1972: An Investigation of Particle Trajectories in Two-Phase Flow Systems, *J. Fluid Mechanics*, 55, 193-208.

[12] Owen, P.R., 1964: Saltation of Uniform Grains in Air, *J. Fluid Mechanics*, 20, 225-242.

[13] Phillips, C.J. and Willetts B.B., 1978: A Review of Selected Literature on Sand Stabilization, *Coastal Engineering*, 2, 133-147.

[14] Rosenfeld, A. and Kak, A.C., 1982: *Digital Image Processing, Vol 2*, Academic Press, Toronto.

[15] Rubinow, S.I. and Keller, J.B., 1961: The Transverse Force on a Spinning Sphere Moving in a Viscous Fluid, *J. Fluid Mechanics*, 11, 447-459.

[16] White, B. R., 1982: Two-Phase Measurements of Saltating Turbulent Boundary-Layer Flow, *Int. J. Multiphase Flow*, 8, 459-473.

[17] White, B.R. and Schulz, J.C., 1977: Magnus Effect in Saltation, *J. Fluid Mechanics*, 83, 497-512.

Table 1.a Template representation of a solid circle used in template matching with image.

$$t(\alpha,\beta)= \begin{array}{ccccccc} -1 & -1 & -1 & -1 & -1 & -1 & -1 \\ -1 & -1 & 0.7 & 1 & 0.7 & -1 & -1 \\ -1 & 0.7 & 1 & 1 & 1 & 0.7 & -1 \\ -1 & 1 & 1 & 1 & 1 & 1 & -1 \\ -1 & 0.7 & 1 & 1 & 1 & 0.7 & -1 \\ -1 & -1 & 0.7 & 1 & 0.7 & -1 & -1 \\ -1 & -1 & -1 & -1 & -1 & -1 & -1 \end{array}$$

Table 1.b Template representation of a vertical line used in template matching with image.

$$t(\alpha,\beta)= \begin{array}{ccccccc} -1 & -1 & 1 & 1 & 1 & -1 & -1 \\ -1 & -1 & 1 & 1 & 1 & -1 & -1 \\ -1 & -1 & 1 & 1 & 1 & -1 & -1 \\ -1 & -1 & 1 & 1 & 1 & -1 & -1 \\ -1 & -1 & 1 & 1 & 1 & -1 & -1 \\ -1 & -1 & 1 & 1 & 1 & -1 & -1 \\ -1 & -1 & 1 & 1 & 1 & -1 & -1 \end{array}$$

Table 2. Mean trajectroy characteristics for 195 μm particles

Mean wind velocity	(U)	5.5 m/s
Surface friction velocity	(u_*)	25 cm/s
Threshold friction velocity	(u_{*t})	29 cm/s

		Ejection		Impact	
		Mean	Std Dev	Mean	Std Dev
V_{xp}	(cm/s)	5.4	6.8	134.	6.2
V_{yp}	(cm/s)	38.	1.8	-32.	1.6
V_p	(cm/s)	49.0	7.2	138.	6.4
Angle	(deg)	74.	36.	-13.0	3.0
V_p/u_*		1.9		5.5	
Height_{max}	(cm)	0.86	0.7		
Length	(cm)	7.2	5.5		
Height/Length		0.12			
No. of trajectories		123			

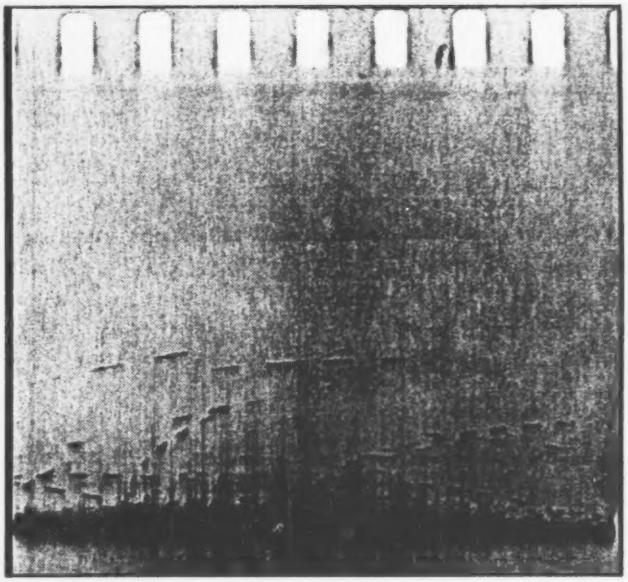

Figure 1 Digitized negative of 195 um particles moving left to right.

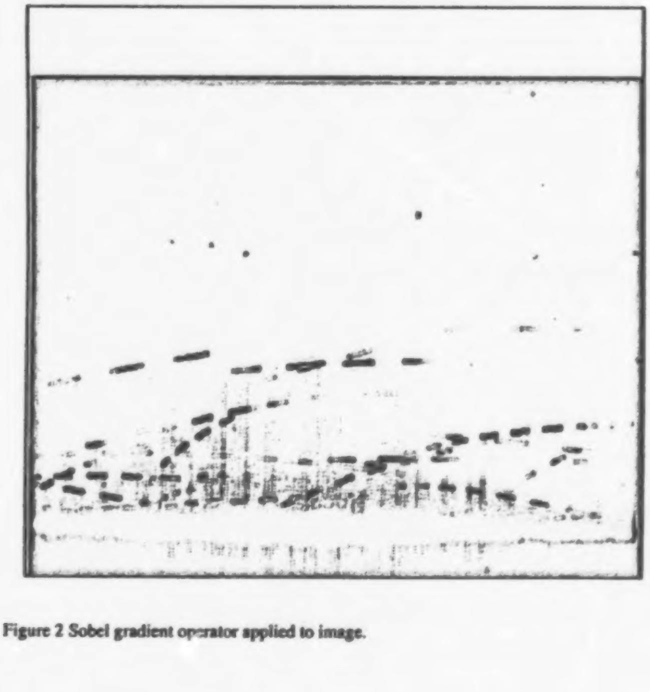

Figure 2 Sobel gradient operator applied to image.

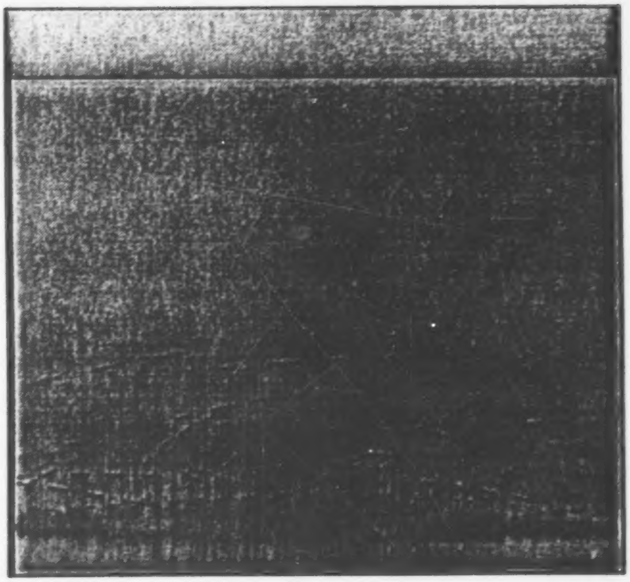

Figure 3 Fourier enhancement of raw image using a Butterworth band pass filter (25 to 250).

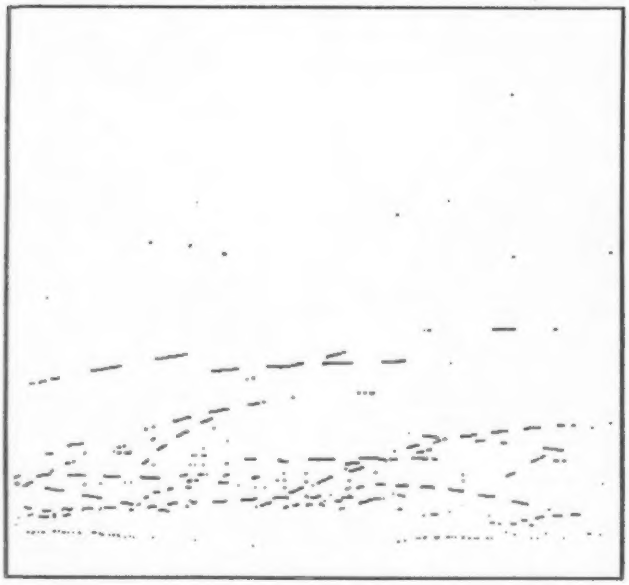

Figure 4 Image after applying template matching to enhanced image.

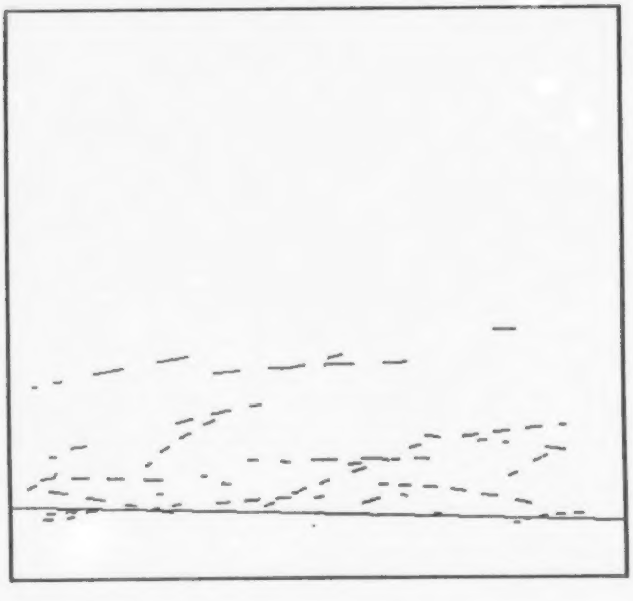

Figure 5 Results after applying line tracking procedure.

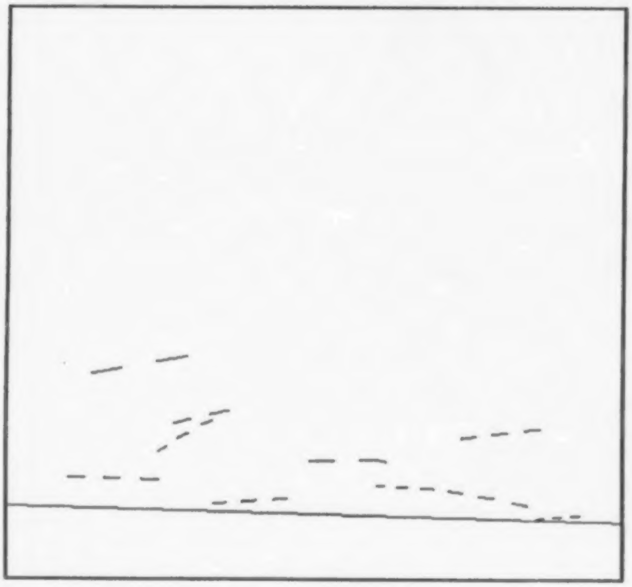

Figure 6 Results after applying line tracing routine.

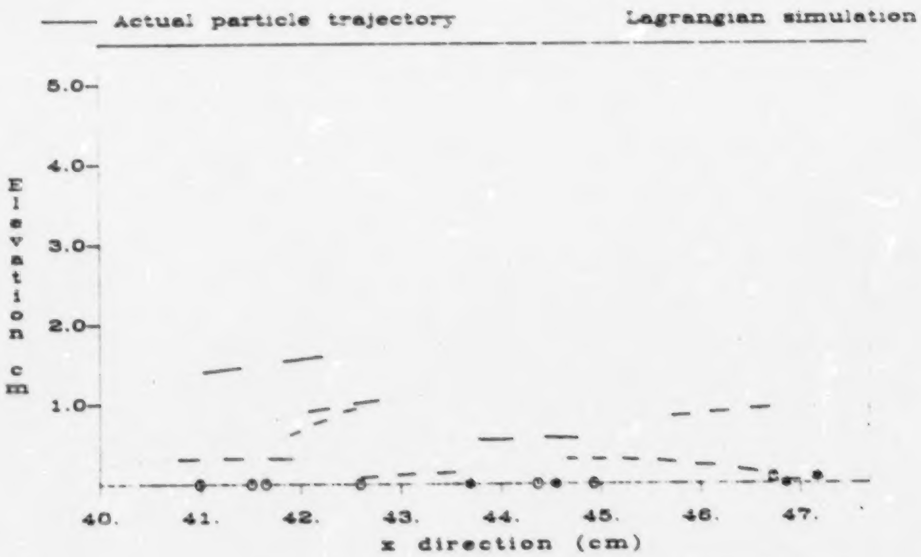

Figure 7 Reconstruction of 195 μm particle trajectories in a 5.5 m/s wind and a 25 cm/s friction velocity.

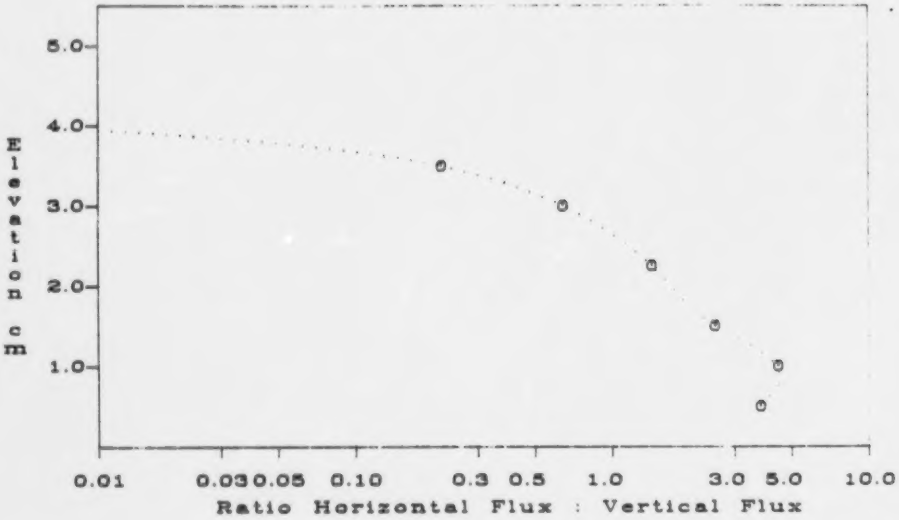

Figure 8 Ratio of Horizontal to Vertical flux for 195 μm particles under a 25 cm/s friction velocity.

A12

INCINERATION OF WASTES; K. Davies, Environmental
Protection Office, City of Toronto, Toronto, Ontario.

MANUSCRIPT NOT AVAILABLE

A13

DETECTABILITY OF STEP TRENDS IN THE RATE OF ATMOSPHERIC SULPHATE DEPOSITION

by

Edward A. McBean, Michel G. Kompter and Grahame J. Farquhar
Department of Civil Engineering
University of Waterloo
Waterloo, Ontario, N2L 3G1, Canada

ABSTRACT

Step trend analyses are performed on acid deposition rates using a combination of monitored sulphate deposition data and a long-range transport of acid precipitation (LRTAP) model. The step trend analyses considers Sudbury's emissions and eastern North America's emissions to explore strategies for reducing sulphur dioxide emissions such that a decrease in sulphate deposition is detected in a specified time period. Results indicate Sudbury's emissions could be reduced with significant detectable reductions in sulphate deposition occurring at the Muskoka region. Significant detectable reductions do not occur elsewhere due to the variability of monitoring data "masking" the small change in sulphate depositions associated with abatement. Reductions in eastern North America's emissions would result in widespread evidence of significant detectable reductions.

DETECTABILITY OF STEP TRENDS IN THE RATE OF ATMOSPHERIC SULPHATE DEPOSITION

Edward A. McBean, Michel G. Kompter and Grahame J. Farquhar

INTRODUCTION

Acid rain is an important Canadian/American transboundary air pollution problem with detrimental effects observable over eastern North America. The problem has been acknowledged by both the Canadian and American governments as requiring remedial action and clean-up (e.g. Schiermeier and Misra, 1982). Mandates have been set to control emission levels, such as at Sudbury's smelting industries (INCO and Falconbridge Ltd.). However, there are still considerable needs for reduction in emissions before attainment of suggested depositon rates of 20 kg/ha are achieved at selected sensitive locations in eastern North America (Ontario Ministry of the Environment, 1980).

Decision-makers require information relating emission controls (or reductions) to the number of years of monitoring required to detect a significant change in sulphate deposition. A reduction of emissions does not simply imply reductions in sulphate deposition will be detected due to the introduction of wind and precipitation variability. If reductions occur, reductions in sulphate deposition may occur if wind and precipitation effects are minimal, i.e. average meteorological effects occur. However, if it should rain more in a specific year or wind effects occur such that a larger portion of sulphates are transported to a specific location, then sulphate depositions may be higher than in previous years, even with an emission reduction. As a result, a detectability of step trends analysis is required such that decision-makers may be able to report changes. Detectability of step trends in the rate of atmospheric sulphate deposition represents the evaluation of the number of years of monitoring required to detect a significant change in sulphate deposition, given a specified reduction in sulphur dioxide (SO_2) emissions at various emission sources.

The major sources of SO_2 emissions in eastern North America are (i) coal-powered electricity generating stations, and (ii) industrial processes with the majority of SO_2 emissions coming from the smelting industry (Ontario Ministry of the Environment, 1980). The intensity of the emissions for 1980 are illustrated in Figure 1, from Barrie and Hales (1984) and have remained essentially constant throughout the early eighties. Canada has the largest point source of sulphur dioxide emission, consisting of INCO and Falconbridge Smelting Ltd., producing 944,000 tonnes of SO_2 per annum or 2.8% of the total North American sulphur dioxide emissions. Studies have been completed to characterise the effects of Sudbury's emissions on the wet and dry acid deposition on surrounding areas (Tang et al, 1984), but little work has been attempted in step trend analysis. Hirsch and Gilroy (1985) attempted a step trend analysis; however, they used an over-simplified model using precipitation as the only variable source of input into their model. They fit a relationship of precipitation data to wet sulphate deposition. However, wet sulphate deposition is calculated by multiplying concentration by precipitation. Therefore, their findings are debatable since precipitation and deposition are not independent.

Sulphur dioxide emissions result in the deposition of sulphur dioxides throughout eastern North America. Figure 2 from Barrie and Hales (1984) gives a spatial distribution of the sulphate deposition in eastern North America for 1980.

OBJECTIVES

Of concern, is the development of a methodology for detecting a step trend in the rate of atmospheric sulphate deposition. Existing sulphate deposition data are used to develop a relationship between changes in deposition levels and the number of years required to detect a significant change in the deposition level. The t-test is used to identify a significant change at the one-tailed 95% level of significance (LOS). This analysis is not to be confused with reducing deposition levels to suggested levels of 20 kg/ha/yr, but describe the ability to detect significantly reduced deposition levels (i.e. the step trend) after a reduction in emissions has occurred.

The above analyses require monitored sulphate deposition data for various selected locations or receptors to quantify statistics. Receptors must be selected based on the locations' sensitivity to acid rain. Data are accumulated for these locations and statistically analyzed for their validity in being able to spatially represent the location.

A model capable of simulating sulphate deposition data is required to relate percent emission reductions and the corresponding change in deposition levels. The annual UW-LRT model (Shipley et al, 1987) is used for this purpose. It has been revised into a seasonal model with the addition of precipitation variability, and calibrated and validated to existing monitored data (see Kompter and McBean, 1988 for details).

The final stage requires the combination of the above two analyses such that the resultant step trend is quantified as the percent emission levels to the number of years of monitoring required to detect a signficant reduction in sulphate deposition.

The foci of the step trend analysis is on:

1) the emissions from Sudbury's smelting companies, INCO and Falconbridge Ltd., and,
2) the entire eastern North American emissions network.

MONITORING DATA ANALYSES

The monitored data are obtained from sulphate deposition monitoring stations (Unified Deposition Data Base Committee, 1980 and 1984, Olsen and Slavich, 1986, and Barrie and Hales, 1984). Seven receptor locations are chosen based on their regional sensitivity to acid precipitation. Examining the monitored data for these locations, it is found that a large degree of variability exists between monitoring stations at any receptor location. Monitoring sulphate deposition data were aggregated for each receptor location, indicating the mean and variance of the sulphate deposition (listed in Table 1). This aggregation of the monitored data for each receptor location is denoted as an "airshed". Delineations of the airsheds are given in Figure 3. These airsheds and the basis for their delineation are discussed in Kompter, (1987).

The estimates of the statistics in the step trend analysis were calculated excluding the monitored data for the seasons of summer and fall of 1982 and winter 1983, since the emissions at Sudbury, during this time period were non-existent, and it is assumed that Sudbury is a major contributor to sulphate deposition. The resulting mean and standard deviations, are given as the first two columns in Table 2, along with n_i, the number of monitoring stations of data.

STEP TREND ANALYSIS

The monitored data were analyzed to relate the magnitude of sulphate deposition change, to the number of years of monitoring required to detect the change. The analysis was performed using the t-statistic (Iman and Conover, 1983), given as:

$$t_{0.95(1),n_1+n_2-2} = \frac{\overline{X}_1 - \overline{X}_2}{S_p\sqrt{\frac{1}{n_1} + \frac{1}{n_2}}} \tag{1}$$

where:

$t_{0.95(1),n_1+n_2-2}$ is the t-statistic at the one-tailed 95% level of significance (LOS) with n_1+n_2-2 degrees of freedom;

n_1 is the number of years of data (or data points before the change);

n_2 is the number of years to detect a change of magnitude $\overline{X}_1-\overline{X}_2$;

$\overline{X}_1-\overline{X}_2$ is the magnitude of change;

$S_p{}^2$ is the pooled variance given as:

$$S_p{}^2 = \frac{(n_1-1)^2 S_1 + (n_2-1)S_2{}^2}{n_1 + n_2-2} \tag{2}$$

where:

S_1 is the standard deviation in the observed (monitored) data of n_1, and

S_2 is the standard deviation in the abatement data of n_2.

The standard deviation is assumed to be the same for S_1 and S_2, i.e. the variance is assumed to be the same before and after remediation. As a result, $S_1 = S_2 = S$ and rearranging the t-statistic, the magnitude of change, $(\overline{X}_1-\overline{X}_2)$ may be written as the following:

$$\overline{X}_1-\overline{X}_2 = t_{0.95(1)n_1+n_2-2} \quad S\sqrt{\frac{1}{n_1} + \frac{1}{n_2}} \tag{3}$$

The magnitude of change $(\overline{X}_1-\overline{X}_2)$ from a reduced emission level to cause a significant reduction in deposition levels can be calculated given S, n_1, n_2 and using the corresponding t-statistic.

The calculations were performed using n_2 values of 1,2,3,4,5,10,25 and infinity (∞). Using the value of infinity for n_2 results in Equation 3 being reduced to:

$$X_1-X_2 = t_{0.95(1),\infty} \; S\sqrt{\frac{1}{n_1}} \qquad (4)$$

The resultant calculations of $\overline{X}_1-\overline{X}_2$ are given in Table 2. Muskoka will be used as an example to demonstrate how to read Table 2. From Table 2, to detect a significant change in deposition on an annual basis in one year of monitoring at Muskoka would require a change in deposition of 5.59 kg/ha. Monitoring over a two year period would require a reduction of 4.09 kg/ha on average to produce a significant reduction in sulphate deposition (at the one-tailed 95% L.O.S.). It may be noted that the required changes in deposition are large and arise because of the large variability from year to year and between monitoring stations.

LONG RANGE TRANSPORT OF ACID PRECIPITATION MODEL

The Long Range Transport of Acid Precipitation (LRTAP), Ontario Ministry of the Environment statistical model given in Shipley et al (1987) has been revised to simulate seasonal sulphate deposition data. Parameters used to revise the model are obtained from Venkatram et al, (1982), Ellenton et al (1985) and are used in the model described in Kompter and McBean (1988), which incorporates precipitation variability. Calibration and verification of this model (UW-LRT) is provided in Kompter and McBean (1988). Also, the revised model is capable of simulating at reduced emission levels. Sudbury's emissions are a significant contributor to sulphate deposition and during the seasons of summer and fall of 1982 and winter 1983, Sudbury's emissions were non-existent due to a shut-down. With these reduced emissions in the model, the model was capable of simulating the resultant sulphate deposition levels.

Model runs, for the step trend analysis were undertaken by setting the emission levels at percentages of 0% (i.e., no change), 25%, 50%, 75% and 100% (or reductions of 100%, 75%, 50%, 25%, and 0%, respectively). The changes in deposition $(\bar{X}_1-\bar{X}_2)$ are given in Table 3 for emission controls at Sudbury's smelters and Table 4 for emission controls across eastern North America.

COMBINING MONITORED DATA ANALYSES AND MODEL ANALYSES

Combining the relationships of Table 2 with Table 3 and Table 2 with Table 4, and eliminating $\bar{X}_1-\bar{X}_2$, results in percentage emissions as a function of n_2, as is indicated in Table 5 for Sudbury's emissions and Table 6 for eastern North America's emissions. As an example, consider Muskoka for a 75% emission level across eastern North America. A change of 5.0 kg/ha (from Table 4) will have occurred. Interpolating from Table 2, a change in deposition of 5.0 kg/ha would require more than one year but less than two years of monitoring to identify a statistcal reduction from the pre-abatement levels.

ANALYSIS OF SUDBURY AS AN EMISSION SOURCE

The results given in Table 5, indicate that the Muskoka airshed is the only airshed which would detect a significant reduction in sulphate deposition given the reduced emission levels at Sudbury. The remaining airsheds would take an indefinite number of years to detect a change in deposition, i.e. Sudbury's emissions would not cause a significant reduction in sulphate deposition at the other airsheds. This indicates that statistically-significant detectable reductions in sulphate deposition would only occur near Sudbury, i.e. the Muskoka region. This becomes apparent when you consider the magnitudes due to the variance in the monitored data and compare them to the relatively small changes in deposition which occur due to the reduction of only Sudbury's emissions. The variability "masks" any reduction in sulphate deposition which may have occurred due to Sudbury's emissions.

ANALYSIS OF EASTERN NORTH AMERICA

A similar analysis to that performed on Sudbury's emission is performed using eastern North America's emissions. In other words, all of the emission sources in the model were computed at 0%, 25%, 50%, 65%, 75% and 100% emission levels. The results are given in Table 6, relating the percent emissions with the number of years to detect a significant difference (n_2).

As Table 6 indicates, if all of the sulphate emission sources in eastern North America were to reduce their emissions by 50%, it would take five years of monitoring (or less) to detect a significant change in acid deposition (at the 95% LOS), at all of the airsheds. At 65% sulphate emissions (or a reduction of 35%), it would take 12 years or less to detect a significant change in acid deposition at all of the airsheds. It should be noted that a 50% or 35% reduction of emissions does not indicate a 50% or 35% reduction at the airsheds because of the non-anthropogenic sources (quantified as background deposition). As an example demonstration, 2/3 of Boundary Waters deposition and 1/2 of Algoma's deposition is due to background sulphate deposition; they require large reductions in emissions before detectable changes occur. In addition, the deposition at these two locations is below the suggested maximum deposition level of 20 kg/ha/yr. As a result, the major focus should be on the remaining five receptors.

CONCLUSIONS

The conclusions arising from this study include:

1) step trend analyses for acid precipitation require the combination of monitored statistical data and a model to relate the emission levels to the number of years of detection required to detect a significant reduction in sulphate deposition;
2) the step trend analysis of Sudbury's emissions abatement indicate that the Muskoka region would result in significant detectable reductions in sulphate deposition; however, decision-makers would not be able to detect significant reductions of sulphate deposition at the other selected airsheds;
3) the control of eastern North America's emissions indicate that a 50% reduction in emissions would require 5 years of monitoring or less to detect a significant reduction. For a 35% reduction, 12 years of monitoring or less would be required to detect a significant reduction in sulphate deposition;
4) Boundary Waters and Algoma require longer periods of monitoring to detect a significant reduction in sulphate deposition due to the large percentage of deposition due to background deposition, and,
5) the variability in the monitored data is large and tends to "mask" the size of the magnitude of change required to detect a

significant reduction in sulphate deposition. As a result, large reductions are required to detect any significant reductions.

ACKNOWLEDGEMENTS

The research was sponsored in part by an NSERC Strategic Grant and the Ontario Ministry of the Environment. This paper documents an independent research study. It does not, in any way, represent the views, opinions or positions of any government agency.

REFERENCES

Barrie, L.A., and J.M. Hales, "The Spatial Distribution of Precipitation Acidity and Major Ion Wet Deposition in North America During 1980", Tellus 36B, pp. 333-355, 1984.

Ellenton, G., B. Ley and P.K. Misra, Atmospheric Environment, Vol. 19, pp. 727-737, 1985.

Hirsch, R.M. and E.J. Gilroy, "Detectability of Step Trends in the Rate of Atmospheric Deposition of Sulphate", Water Resources Bulletin, American Water Resources Association, Vol. 21, No. 5, Oct. 1985.

Iman, R.A. and W.J. Conover, "A Modern Approach to Statistics", John Wiley and Sons, 1983.

Kompter, M.G., "Detectability of Step Trends in the Rate of Atmospheric Sulphate Deposition", M.A.Sc.Thesis, Department of Civil Engineering, University of Waterloo, 1987.

Kompter, M.G., and E.A. McBean, "A Seasonal Long-Range Transport Model of Acid Pollutants with Precipitation Variability", submitted to Water, Air, and Soil Pollution, 1988.

Olsen, A.R. and A.L. Slavich, "Acid Precipitation in North America: 1984 Annual Data Summary from Acid Deposition System Data Base". U.S. Environmental Protection Agency, Research Triangle Park, N.C., EPA/600 /4-86/033, 1986.

Ontario Ministry of the Environment, "The Case Against the Rain, A Report on Acidic Precipitation and Ontario Programs For Remedial Action", 1980.

Schiermeier, F.A. and P.K. Misra, "United States - Canada: Memorandum of Intent on Transboundary Air Pollution". Toronto, Atmospheric Sciences and Analysis, Work Group 2, Report No. 2F-M, Oct. 15, 1982.

Shipley, K.B., E.A. McBean, G.J. Farquhar and J.M. Byrne, "Incorporation of Wind Roses in a Statistical Long Range Transport Model". Water, Air, and Soil Pollution, 1987.

Tang, A.J.S., W.H. Chan and M.A. Lusis, "An Analysis of the Effects of the Sudbury Emission Sources on Wet and Dry Deposition in Ontario". OMOE-ARB-124-84-ARSP, 1984.

Unified Deposition Data Base Committee, "A Unified Wet Deposition Data Base for Eastern North America: Data Screening Calculation Procedures, and Results for Sulphates and Nitrates". Report for the Canadian Federal-Provincial Research and Monitoring Co-ordinating Committee, 1980.

Unified Deposition Data Base Committee (1980-1983). "A Unified Wet Deposition Data Base for Eastern North America Addendum with Results for Sulphates and Nitrates". Report for the Canadian Federal-Provincial Research and Monitoring Co-ordinating Committee.

Venkatram, A., B.E. Ley and S.Y. Wong, Atmospheric Environment, Vol. 16, pp. 249-257, 1982.

Table 1 Annual Monitored Data Summary
Between Stations at an Airshed

		1980	1981	1982	1983	1984	Average
BW	$\overline{X}$	8.6	8.9	10.8	9.0	8.0	9.0
	s		2.2	1.0	1.8	1.4	1.0
	CV		0.25	0.09	0.20	0.18	0.11
	n	1	4	6	4	5	20
AL	$\overline{X}$	13.0	14.2	13.9	14.2	11.8	13.4
	s		4.5	4.9	4.0	2.1	1.0
	CV		0.32	0.35	0.28	0.18	0.07
	n	1	2	4	2	3	12
MU	$\overline{X}$	26.5	29.7	25.0	26.6	25.5	26.7
	s	0.8		1.4	3.3	3.1	1.8
	CV	0.03		0.06	0.12	0.12	0.07
	n	2	1	2	4	5	14
QC	$\overline{X}$	26.9	23.7	21.2		24.0	24.0
	x		6.9	0.1			2.3
	CV		0.29	0.00			0.10
	n	1	2	2		1	6
NH	$\overline{X}$	23.7	28.9	20.2	22.4	23.1	23.7
	s	3.2	9.1	0.1	1.2	5.7	3.2
	CV	0.14	0.31	0.00	0.05	0.25	0.14
	n	2	2	2	2	4	12
AD	$\overline{X}$	28.1	30.5	24.1	29.2	26.4	27.7
	s	3.8	6.7	4.0	5.5	7.8	2.5
	CV	0.14	0.22	0.17	0.19	0.30	0.09
	n	4	3	4	5	4	20
WP	$\overline{X}$	35.4	34.9	33.4	31.3	35.2	34.0
	s	4.1	5.1	3.4	4.6	5.2	1.7
	CV	0.12	0.15	0.10	0.15	0.15	0.05
	n	4	3	4	5	4	20

$\overline{X}$ - mean sulphate deposition (kg/ha)
s - standard deviation sulphate deposition (kg/ha)

CV - coefficient of variation ($s/\overline{X}$)
n - number of monitoring stations data for the airshed

Table 2 Changes in Average Annual Acid Deposition, Given Number of Years to Detect Change (n_2)

	$\overline{X}$	s	n_1	n_{2_1}	n_{2_2}	n_{2_3}	n_{2_4}	n_{2_5}	$n_{2_{10}}$	$n_{2_{25}}$	n_{2_∞}
BOUNDARY WATERS (BW)	8.42	1.62	10	3.11	2.28	1.92	1.71	1.57	1.26	1.03	0.84
ALGOMA (AL)	12.80	2.68	6	5.83	4.25	3.59	3.22	2.97	2.44	2.07	1.80
MUSKOKA (MU)	26.26	2.78	8	5.59	4.09	3.45	3.09	2.85	2.30	1.92	1.62
QUEBEC CITY (QC)	24.55	4.26	4	11.21	7.87	6.56	5.85	5.42	4.49	3.91	3.50
NEW HAMPSHIRE (NH)	24.66	5.83	8	11.72	8.57	7.23	6.47	5.97	4.83	4.02	3.39
ADIRONDACKS (AD)	28.13	5.85	11	11.08	8.08	6.79	6.05	5.56	4.42	3.58	2.90
WEST PENNSYLVANIA (WP)	35.18	4.28	11	8.10	5.91	4.97	4.43	4.07	3.23	2.62	2.12

Table 3 Average Changes in Sulphate Deposition at Selected Sensitive Airsheds, Given the Percentage Emission Changes at Sudbury

	% Emissions				
	100%	75%	50%	25%	0%
Boundary Waters	0	0.03	0.06	0.09	0.12
Algoma	0	0.09	0.19	0.28	0.37
Muskoka	0	0.93	1.87	2.80	3.74
Quebec City	0	0.36	0.72	1.08	1.44
New Hampshire	0	0.26	0.52	0.78	1.04
Adirondacks	0	0.38	0.77	1.15	1.54
West Pennsylvania	0	0.25	0.51	0.77	1.02

Table 4 Average Changes in Sulphate Deposition at Selected Sensitive Airsheds, Given the Percentage Emission Changes in Eastern North America

	% Emissions					
	100%	75%	65%	50%	25%	0%
Boundary Waters	0.00	0.8	1.2	1.6	2.5	3.3
Algoma	0.00	1.8	2.6	3.7	5.5	7.4
Muskoka	0.00	5.0	7.0	10.0	15.0	20.0
Quebec City	0.00	4.2	5.8	8.3	12.5	16.7
New Hampshire	0.00	4.1	5.8	8.3	12.4	16.6
Adirondacks	0.00	5.5	7.7	11.0	16.6	22.1
West Pennsylvania	0.00	6.7	9.4	13.4	20.2	26.9

Table 5 The Number of Years of Monitoring Required to Detect a Significant Difference in Acid Deposition Based on Emission Reductions at Sudbury

	Emission Level				
	100%	75%	50%	25%	0%
Boundary Waters	∞	∞	∞	∞	∞
Algoma	∞	∞	∞	∞	∞
Muskoka	∞	∞	>25	<6	<3
Quebec City	∞	∞	∞	∞	∞
New Hampshire	∞	∞	∞	∞	∞
Adirondacks	∞	∞	∞	∞	∞
West Pennsylvania	∞	∞	∞	∞	∞

Table 6 The Number of Years of Monitoring Required to Detect A Significant Difference in Acid Deposition for Eastern North America

	Emission Level					
	100%	75%	65%	50%	25%	0%
	n_2	n_2	n_2	n_2	n_2	n_2
Boundary Waters	∞	∞	<12	<5	<2	<1
Algoma	∞	∞	<8	<3	<2	<1
Muskoka	∞	<2	<1			
Quebec City	∞	<13	<5	<2	<1	
New Hampshire	∞	<20	<6	<3	<1	
Adirondacks	∞	<6	<3	<2	<1	
West Pennsylvania	∞	<2	<1			

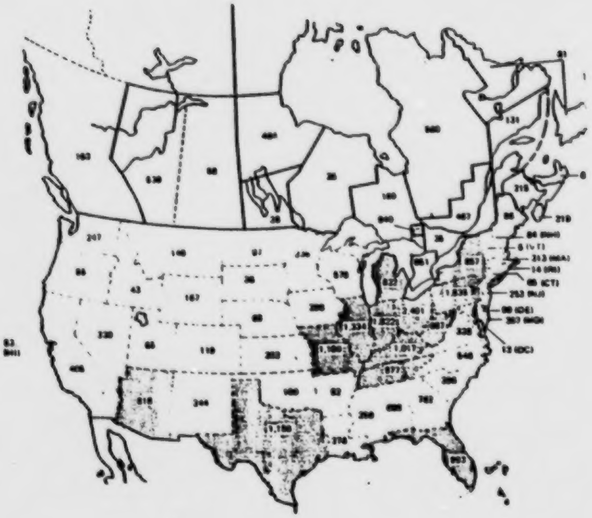

131
215
219
8 (VT)
213 (MA)
14 (RI)
(CT)
252 (NJ)
(DE)
(MD)
13 (DC)
2,401
1,017
207
140
167
43
119
244
762

Figure 1 North American SO_2 Emissions in 10^3 Tonnes (1980) (Barrie and Hales, 1984)

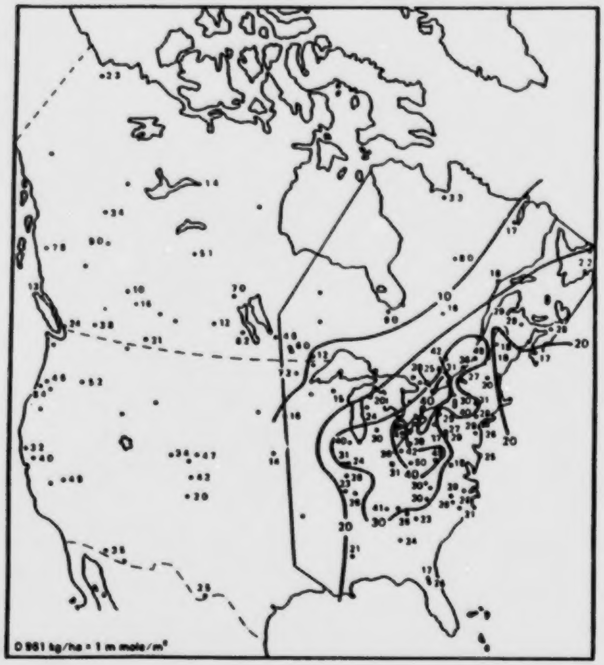
0.961 kg/ha = 1 m mole/m²

Figure 2 Spatial Distribution of Sulphate (SO_4) Deposition in Eastern North America for 1980 (Barrie and Hales, 1984)

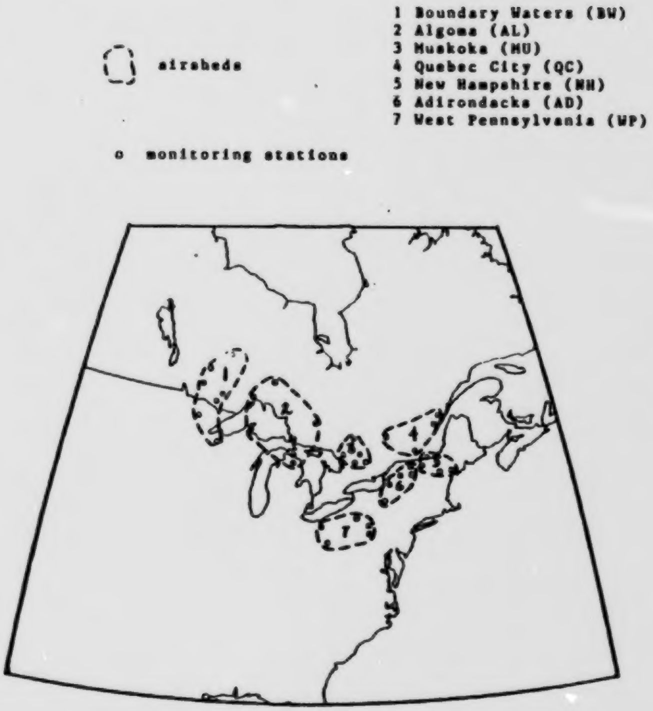
airsheds
o monitoring stations
1 Boundary Waters (BW)
2 Algoma (AL)
3 Muskoka (MU)
4 Quebec City (QC)
5 New Hampshire (NH)
6 Adirondacks (AD)
7 West Pennsylvania (WP)
1
2
3
4
5
6
7

Figure 3 Airshed Locations With Monitoring Stations Within the Airshed Denoted

A14

INCINERATOR AND STEEL PLANT CONTRIBUTIONS TO AIR PARTICULATES AS DETERMINED BY SIZE-SPECIFIC RECEPTOR MODELLING

A. C. Chan, R. E. Jervis and Z-J Kang

Department of Chemical Engineering and Applied Chemistry
and Institute of Environmental Studies
University of Toronto, Toronto, Canada M5S 1A4

Abstract

Photon and thermal neutron activation anlysis were used to analyze airborne particulate matter at various control sites in Ontario to study incinerator and iron and steel works contributions to ambient aerosol. Elemental concentrations along with particle-size distributions were subjected to factor analysis to facilitate the identification of various emission sources at the control sites. Iron and steel works, a major industry in Hamilton and Sault-Ste Marie, contributed 39% and 13% to the airborne particles respectively. Fly ash samples obtained from local incinerators were analyzed to provide local source 'profiles' which could be used in the chemical element balance to achieve a more precise source apportionment calculation. It was observed that there was a discernible amount of Se,Sb,Cd,Zn,Pb in the incinerator ash samples.

Introduction

The abatement of air pollution has become one of the most important environmental issues of the 1980's. Various types of emission sources are found to contain many inorganic elements which are toxic and hazardous to humans (1,2,-5,6,7,8,9,10,11,13). Air pollution researches conducted previously (1,2,6) in our laboratory in the University of Toronto and was supported by the Ontario Ministry of Environment were able to identify various air particulates emission sources and quantify their respective contribution to the total inorganic constituents in the ambient aerosol using receptor modelling.

Receptor modelling involves the measurement of the properties of airborne particulate matter at the receptor site, and the apportionment of them to various emission sources. These properties include particle-size, shape and elemental distribution. However, traditional receptor modelling cannot be applied to every set of aerosol data without flaw. Its weakness in distinguishing collinear sources has posed a great problem to source apportionment studies. Attempts in our laboratory to overcome this difficulty was to utilize size-fractionating sampling using Hi-Vol Sierra 5-stages cascade impactors and include particle-size distribution as an extra variable in source identification and apportionment computations. It was found that the application of size-specific elemental mass balance was able to apportion more closely to reality the contributions of vehicle emissions and lead refining industry ,which had similar 'key marker' elements such as Pb and Zn, to the atmosphere (2,6).

The main objectives of the present study are to further develop and verify receptor modelling approaches capable of resolving mixed dominant sources in urban environments and achieving quantitative source apportionment through extensive field sampling at selected sites in Ontario. With co-operation from the Ontario Ministry of Environment, air filters from Sault-Ste Marie and Hamilton are studied to assess steel plant contributions to ambient particulates in urban airsheds. Also, a more thorough study of the impact of incinerator emissions to the atmosphere is carried out at a site closer to the emission sources than a previously studied site (1,2,6). The present study aids the determination of elemental distributions of iron and steel works and incinerator emissions which acts as a prelude to the development of conclusive receptory source link in air pollution studies, particularly in the more complex airsheds where there are multiple industrial, municipal/domestic sources each making appreciable contribution.

For this research, factor analysis is utilized to facilitate the identification of various ambient emission sources to the receptor site, and chemical element balance is used to quantify their respective contribution to the atmosphere (12).

In order to apply receptor models for source assessment, the analytical methods used have to be able to analyze as many elements as possible small in mass. Activation analysis is ideal because it is sensitive, non-destructive, instrumental and multi-elemental. The use of IPAA and INAA as complementary methods allows the determination of most of the elements in the aerosol and the analysis of some elements by both methods as a form of precision control.

Methods

Air particulate samples as well as fly ash samples were collected in order to study incinerator contributions to air particulate matter. Fly ash samples were collected at three different incinerators located in Toronto: The Commissioners Street Municipal Incinerator, The Main Sewage Treatment Plant in

Leslie Street and Toronto Western Hospital. Preparation of these fly ash samples for analytical purposes involved air-drying, homogenization by agitation, and weighing them into acid pre-washed polyethylene vials. Air particulate samples were collected using a Sierra 5-stages cascade impactors at regular intervals during the period between July and September, 1988 at a site in Comissioners Street. This site was about 300 metres from both the refuse incinerator and the sewage treatment plant. This study attempted to characterize the emissions of both incinerators as well as nearby industries to the ambient aerosol. The sampler was operated at a flow-rate of 40 ft^3/min. for 12 hours periods, and the total volume collected was about 800 m^3. Whatman #41 filter paper coated with 1:10 (v/v) vaseline-hexane solution was employed both as the impactor substrate and the back-up filter because of its low trace element content (3,5). Glass-fibre, a standard hi-vol collection medium, was extremely unsuitable for instrumental neutron activation analysis because of its high sodium and ash content. After the twelve hours collection period, the loaded filter papers were transferred using a zip-lock type plastic bag back to the laboratory, and they were trimmed and packed into clean polyethylene capsules. In order to study steel plant contributions to the airborne particulates, various aerosol samples were collected by the Ontario Ministry of Environment staff in Hamilton and Sault-Ste Marie between Nov,1985 and July,1987 using dichotomous samplers, which separated air particulates into a coarse fraction (2.5um<d<10um) and a fine fraction (d<2.5um), and teflon membrane as the collection medium.

For multi-elemental analysis, the filters and the ash samples were subjected to thermal neutron activation analysis(INAA) at the University of Toronto SLOWPOKE-2 Reactor. These samples were irradiated under flux ranging from 1 to 2.5×10^{11} n/cm^2.s for periods from 5 minutes to 16 hours. Since INAA could not be used to analyze some important toxic elements, such as Pb,Ni, in the ambient air particulates accurately, photon activation analysis(IPAA) was performed on the samples employing the LINAC at NRC in Ottawa.

Irradiated samples were then transferred to clean vials and counted using Ge(Li) spectrometer. Quantitative information was extracted by the comparator method in which an accurately known weight of element of interest was irradiated and counted under the same conditions as the unknown sample. National Bureau of Standards(NBS) reference materials, 1632a,1632b and 1635, were used as the multi-elemental standards.

Results and Discussion

The average concentrations of the elements measured in the air particulates collected at Hamilton and Sault-Ste Marie are given in Table 1a. Sault-Ste Marie and Hamilton are areas with iron and steel works as one of their major industries. Table 1 indicates that the levels of Fe,Mn,Zn,Pb,Sb are elevated in the ambient at these two sites (14).

Table 1a & 1b

(1a)Elemental Concentrations in Airborne Particle Matter (ug/m^3) and (1b) in Ash Samples from Comissioners Street Incinerator (ppm)

Element	S.S. Marie (1a)	Hamilton (1a)	Ash (1b)
Al	0.91	0.64	5.6%
Ag	-----	-----	70
As	0.0019	0.0024	130
Br	0.057	0.040	390
Ca	0.68	1.95	5.68%
Ce	0.0021	0.0054	28
Cd	-----	-----	430
Cl	0.25	0.077	4.22%
Co	0.00041	0.00051	19
Cr	-----	-----	710
Cs	-----	-----	4.0
Cu	0.063	0.018	-----
Eu	-----	-----	0.53
Fe	1.00	2.47	9.0%
Hf	-----	-----	2.7
I	-----	-----	2.7
In	-----	-----	6.2
K	0.049	0.50	5.3%
La	0.00043	0.0038	15
Mn	0.080	0.15	0.11%
Na	0.34	0.34	5.08%
Ni	0.033	0.084	-----
Pb	0.19	0.23	-----
S	1.60	3.36	-----
Sb	0.00030	0.0019	740
Sc	0.00007	0.00007	4.8
Se	0.00076	0.0015	22
Si	1.33	0.77	-----
Sm	-----	-----	2.0
Ti	0.051	0.096	5750
V	0.0021	0.010	46.5
Zn	0.18	0.25	1.7%

In order to identify the possible emission sources contributing to the receptor sites, the data sets of the elemental concentrations measured in the aerosol at the two sites were subjected to factor analysis. The resulting rotated factor patterns are listed in Table 2 and Table 3.

Table 2

Rotated Factor Pattern for the Sault-Ste Marie Aerosol

F1	F2	F3	F4	F5	F6
Mn (0.94)	Al (0.91)	Pb (0.93)	Cl (0.67)	Zn (0.95)	Se (0.83)
Cr (0.93)	Si (0.83)	Br (0.73)	Zr (0.65)	Cu (0.89)	As (0.58)
Fe (0.91)	Sc (0.78)	S (0.61)			
Ca (0.79)	La (0.74)				

Table 3

Rotated Factor Pattern for the Hamilton Aerosol

F1	F2
Fe (0.93)	Br (0.99)
Mn (0.93)	Pb (0.91)
Cr (0.91)	

Six factors are resolved to represent the Sault-Ste Marie aerosol data set, and these factors can be interpreted as six emission sources: iron and steel works, entrained soil, vehicle emissions, refuse incineration, salt and oil/coal combustion. Only two prominent emission sources can be resolved for the Hamilton aerosol which are iron and steel works and vehicle emissions.

In order to quantitatively apportion the airborne particulate matter collected at Sault-Ste Marie and Hamilton among the emission sources, chemical element balances were applied to the aerosol data. Except for iron and steel works, the source 'profiles' used in the chemical element balance were taken from a compilation of literature data (1,6,12,13). Source 'profiles' for iron and steel works were obtained by measuring three source samples from Hamilton (14). The measured elemental concentrations were weighted by $1/s^2$ where s is the analytical precision. The percentage contribution of each emission source to the inorganic aerosol at the two sites studied are presented in Table 4. Iron and steel works, contributing 13% and 39% respectively to the ambient particulates in Sault-Ste Marie and Hamilton, is the most dominant anthropogenic source whereas the impact of the other emission sources are less significant on the inorganic aerosol at the two sites.

Table 4

Chemical Element Balance Source Contributions(%)

Source	Sault-Ste Marie	Hamilton
Soil	71	43
Iron and Steel	13	39
Coal and Oil	5	9
Salt	5	1
Vehicle Emissions	4	3
Refuse Incineration	2	5

Air particulates were collected in a downwind area and multi-elemental analysis performed using INAA and IPAA to evaluate the impact of incinerator emissions in urban environments. This study has been initialized since Mid-July and the results are still under preparation. Ash samples were also obtained from several incinerators, and the concentrations of the elements in the Commissioners Street refuse incinerator ash samples are listed in Table 1b. A discernible amount of certain toxic elements, such as Cd,Sb,Se,Zn and As is found in the ash samples which agrees well with the results from previous studies of incinerators by Greenberg et al. (9,10,11). These elements usually condense on fine particles after emission from the stack.

Conclusions

Dichotomous air samples from Hamilton and Sault-Ste Marie were analyzed by INAA and were subjected to factor analysis and chemical element balance to identify and quantify various emission sources to the inorganic aerosol at the receptor sites. Iron and steel works, contributing 13% and 39% to the ambient particulate matter in Sault-Ste Marie and Hamilton respectively, was the major anthropogenic source at these two sites. Source 'profiles' for incinerators were calculated by measuring ash samples obtained from a local incinerator. An observable amount of Cd,Sb,Se,Zn and As was found in those samples.

Acknowledgements

The authors would like to acknowledge the Ontario Ministry of Environment for financial support in this project. Also, the staff of the LINAC Facility at the National Research Council and the Staff of the University of Toronto SLOWPOKE-2 Reactor Facility are acknowledged for their assistance. Financial support for the SLOWPOKE-2 Reactor Facility is provided by NSERC.

References

1. Pringle,T.G., Jervis,R.E., Proceedings, Technology Transfer Conference No.7 Part 1 Air Quality Research (1986) 196
2. Jervis,R.E., Pringle,T.G., Chan,A.C., Proceedings, Technology Transfer Conference No.8 Part 1 Air Quality Research (1987)
3. Dams,R., Rahn,K.A., Winchester,J.W., Envir. Sci. and Tech., 6 (1972) 441
4. Gordon,G.E., Envir. Sci and Tech. 14 (1980) 792
5. Paciga,J.J., Ph.D. Thesis University of Toronto (1975)
6. Pringle,T.G., Ph.D. Thesis University of Toronto (1988)
7. Kowalczyk,G.S., Choquette,C.E. and Gordon,G.E., Atmos. Envir. 12 (1978) 1143
8. Gladney,E.S., Zoller,W.H., Jones,A.G. and Gordon,G.E., Envir. Sci. and Tech. 8 (1974) 551
9. Greenberg,R.R., Gordon,G.E. and Zoller,W.H., Envir. Sci. and Tech. 12 (1978) 1329
10. Greenberg,R.R., Zoller,W.H. and Gordon,G.E., Envir. Sci. and Tech. 12 (1978) 566
11. Greenberg,R.R., Zoller,W.H. and Gordon,G.E., Envir. Sci. and Tech. 15 (1981) 64
12. Hopke,P.K., Receptor Modelling in Environment Chemistry, Wiley-Interscience, New York (1985)
13. Scheff,P.A., Wadden,R.A. and Allen,R.J., Envir. Sci. and Tech. 18 (1984) 923
14. Kang,Z-J, M.A.Sc Thesis University of Toronto (1988)

A15

A STUDY ON THE SOURCES OF ACID PRECIPITATION IN ONTARIO, CANADA

Y. Zeng and P. K. Hopke
Institute for Environmental Studies and
Department of Civil Engineering
University of Illinois
1005 W. Western Avenue
Urbana, IL 61801

Abstract

Since 1980, the Acid Precipitation in Ontario Study (APIOS) Event Wet/Dry Deposition Network has collected a substantial precipitation chemical data base. Data from the three stations in Dorset, Kingston and London were selected for investigation of the sources of the chemical constituents found in the collected precipitation. Factor analysis was applied to the chemical data sets. Three factors reproduce the concentrations observed in precipitation. These factors represent the acid gas sources (SO_2 and NO_x sources), Ca and Mg sources (soil dust), and Na and Cl sources (marine aerosol). The acid gas sources are responsible for the acidity of the precipitation. To locate these sources in terms of geographic region, air parcel back trajectories corresponding to the precipitation sample time periods are incorporated into factor analysis with the chemical data. This information is in the form of the geographic distribution of back trajectory endpoints. The region in which the trajectory endpoints fall is divided into subregions. New variables are defined as the number of the endpoints in each of the subregions. They reflect the residence time of the air parcels in the subregions. Factor analysis is applied to the combined chemical and endpoint variable data sets. The results show the relationship between the chemical nature of the sources and the geographic regions that the air parcels passed. The potential source contribution function (PSCF) is another approach to locate the sources. PSCF is a conditional probability function calculated for each 1° longitude by 1° latitude cell by dividing the number of trajectory endpoints that correspond to samples with factor scores or pollutant concentrations greater than pre-specified values by the number of total endpoints in the cell. Source areas are indicated by high PSCF values. Both of the approaches suggest that the Ohio River Valley and some areas along east coast are major source regions for the observed precipitation acidity in Ontario.

INTRODUCTION

Acid precipitation is a serious regional environmental problem in eastern North America. In order to understand the origins of this phenomenon and then develop corresponding strategies to decrease the acidity of the precipitation, it is necessary to understand the chemical characteristics of the sources of the acid precipitation and their geographical positions. Although it is known that sulfate and nitrate transformed from SO_2 and NO_x in the atmosphere are major acid species and the distribution of emission rate of SO_2 and NO_x over North America is available, it may not be necessarily true that high SO_2 or NO_x emission rate areas are the dominate contributing source areas to the acidity of precipitation at a specific receptor in North America. Therefore, a study is necessary for a receptor area to offer evidence to show where the sources come from.

The formation and transport of acid precipitation is a complicated process. If a dispersion model is used for source area identification, comprehensive studies are needed that include a survey of emissions over a large scale, collection of meteorological data, field tests to determine the dispersion parameters, and mechanistic studies on the chemical transformation and scavenging of gases and particles by droplets. In addition, the dispersion model can only handle the sources that are known to contribute to acid precipitation, essentially the identified SO_2 and NO_x emission sources. It will not identify the possibilities of other sources.

Receptor models have been used in regional pollution aerosol studies (Rahn and Lowenthal, 1984, 1985; Lowenthal and Rahn, 1988; Lowenthal et al., 1988), especially in the studies of aerosol sulfate. Basically, these studies belong to tracer methods or chemical mass balance type of models in receptor modeling (Hopke, 1985). In principle, receptor models can take the chemical measurements of the precipitation samples collected from monitoring sites (receptors) as the data base, and identify the possible sources in terms of their chemical nature, and even estimate the importance or contribution of these sources. In these studies, regional source profiles have been developed to identify the general area from which the acidic material has come.

However, the normal receptor models can not determine the specific location of sources. To overcome this shortcoming, meteorological information needs to be incorporated into receptor model. Malm et al. (1986) proposed an approach in their study of the sources of particles at the Grand Canyon, Arizona. In their study, an air parcel trajectory model (Bresch et al., 1984) was used. For each sample, the back trajectories ending at the receptor site were calculated to get the track of the each sampled air mass. The region surrounding the receptor site is divided into subregions. A new variable is defined as the number of endpoints (the output from the trajectory model) shown in each of the defined subregion. This variable reflected the residence time of the air parcel in the specific subregion, and was used in factor analysis (Hopke, 1985) with the chemical data. The factor loadings show the relations between the chemical characteristics of the sources and residence time of the air parcels in the sources areas.

In this paper, precipitation chemistry data sets from Ontario, Canada, will be investigated with the emphasis on the chemical characteristics and geographic location of the sources. The approaches described by Malm et al. will be used to study the sources of precipitation constituents in Ontario.

DATA BASE

The Acidic Precipitation in Ontario Study (APIOS) Event Wet/Dry Deposition Network has run since 1980 (Chan et al., 1985). This network consists of 16 stations over lower Ontario (Figure 1). The stations 1 to 13 are aligned along the prevailing wind direction for the southern part of Ontario and these areas have significant levels of precipitation acidity based on historical data. Measurements are made for the collected daily wet deposition samples of sample volume in ml (VOLUME), conductivity at 25°C in μmho/cm (COND25), field pH (FWPH), pH (PH), total acidity in mg $CaCO_3$/l (ACDT), sulfate in mg SO_4^{2-}/l (SSO4UR), nitrate in mg N/l (NNO3UR), calcium in mg Ca^{2+}/l (CAUR), chloride in mg Cl^-/l (CLIDUR), magnesium in mg Mg^+/l (MGUR), potassium in mg K^+/l (KKUR), sodium in mg Na^+/l (NAUR), ammonium in mg N/l (NNHTUR), and total acidity in μg H/l (ACDG).

In this work, three stations are considered: stations number 1011, 3011 and 4011 near London, Dorset and Kingston area, respectively. The investigation has been more concentrated on station 3011, Dorset. These data are available from 1980 to 1986. However, only the data for 1984-86 have been used because they are more complete and have been subjected to better quality control. Since more than half of data are missing for FWPH and ACDG, these two variables have been eliminated from the analysis. ACDT also has a considerable number of missing values. In an initial analysis, it was found that ACDT always contributes an unique factor in factor analysis. Thus, it does not provide useful information in this kind of analysis, and was also excluded from data sets used in this analysis. After eliminating the samples with bad data (such as unreliable data), the number of samples analyzed in this study are 312, 235, and 222 for station 3011, 4011, and 1011, respectively.

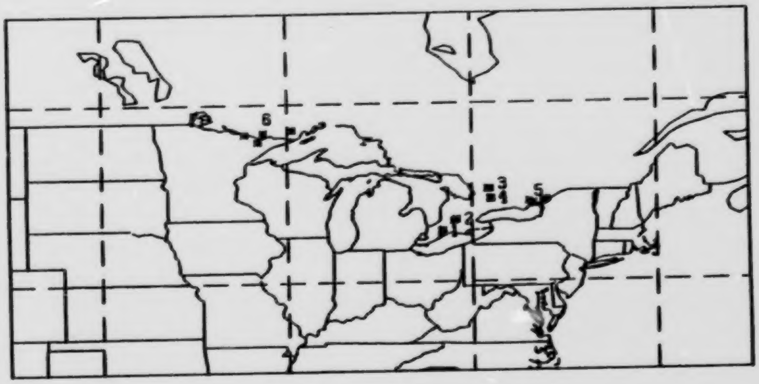

Figure 1. APIOS Event Wet/Dry Deposition Network Station Location Map. 1, stations 1011 and 1021; 2, stations 1031 and 2011; 3, stations 3011 and 3021; 4, stations 3031 and 3041; 5, stations 4011, 4021, 4031, and 4041; 6, stations 6051, 6061, 6071, and 6081. .

Air parcel back trajectories (BT) ending at each station have been calculated by Ontario Ministry of the Environment (OME) (Olson et al., 1978). The BT data are provided in the form of a list of time intervals and coordinates of the trajectory segment endpoints for each trajectory. Trajectories using surface level data are calculated each day at 0:00, 6:00, 12:00, and 18:00 using 3 hour time intervals for 48 hours backward in time. Trajectories at 850 mb level are also available, but they are not suitable for this work because the time interval is 12 hours so that each trajectory segment span over too large a geographical region and the spatial resolution will be lost in the analysis.

DATA ANALYSIS

Table 1 presents average value and standard deviation for each variable of the chemical data set at each station. The pH values for three stations (4.36, 4.28, and 4.35, respectively) are much lower than 5.6 which is the "natural" acidity of rainwater in the form of pH. The correlation coefficient matrix for station 3011 is given in Table 2. Very similar relationships exist for other two stations; it can be seen that the correlation coefficients among COND25, pH, SO_4^{2-}, and NO_3^-, and between Ca^{2+} and Mg^{2+} are very high. The coefficients of the pairs (SO_4^{2-}, NH_4^+), (NO_3^-, NH_4^+), and (Cl^-, Na^+) are also high. To reveal the relations of variables and sources, factor analysis is used.

Factor Analysis

Factor Analysis Applied on the Precipitation Chemical Data Sets

The data sets are reconstructed by multiplying every variable by VOLUME so that the variables are converted from concentrations to total deposited amount (actually, converted to flux). The purpose of this transformation is to eliminate the dilution effect caused by the differences in precipitation volume. At the same time, the variable VOLUME was excluded from further analysis. The number of variables in the final chemical data sets is ten. In addition, pH is transformed to [H] in mMole/l, then to mMole by multiplying VOLUME. R-mode factor analysis (Hopke, 1985) is performed on the chemical data sets for the three sites individually. The factor loadings, communalities, and the explained variance for the three data sets are all listed in Table 3. From Table 3, it can be seen that about 90% of the variance in the system can be accounted for with 3 factors, and the communalities are very high except for K^+ that has a somewhat lower value. Thus, three principal factors (three major sources) are indicated for this system.

Table 1. Average and Standard Deviation of the Variables

Variable		Station 3011		Station 4011		Station 1011	
		Ave.	Std. Dev.	Ave.	Std. Dev.	Ave.	Std. Dev.
VOLUME	(ml)	513.6	564.8	567.6	638.2	632.5	638.6
COND25	(μmho/cm)	30.3	19.5	37.9	24.6	34.8	17.7
pH		4.356	0.307	4.279	0.433	4.352	0.408
SO_4^{2-}	(mg/l)	2.45	2.03	3.07	2.48	3.49	1.96
NO_3^-	(mg N/l)	0.565	0.404	0.712	0.537	0.646	0.392
Ca^{2+}	(mg/l)	0.208	0.238	0.264	0.308	0.525	0.563
Cl^-	(mg/l)	0.148	0.119	0.183	0.166	0.225	0.154
Mg^{2+}	(mg/l)	0.033	0.040	0.035	0.043	0.066	0.071
K^+	(mg/l)	0.033	0.032	0.026	0.028	0.060	0.053
Na^+	(mg/l)	0.051	0.050	0.059	0.065	0.081	0.074
NH_4^+	(mg N/l)	0.297	0.276	0.305	0.276	0.401	0.279

Table 2. Correlation Coefficients Between Variables in Station 3011

	COND25	pH	SO_4^{2-}	NO_3^-	Ca^{2+}	Cl^-	Mg^{2+}	K^+	Na^+	NH_4^+
COND25	1									
pH	.981	1								
SO_4^{2-}	.962	.932	1							
NO_3^-	.913	.879	.825	1						
Ca^{2+}	.628	.541	.700	.660	1					
Cl^-	.797	.750	.733	.811	.608	1				
Mg^{2+}	.625	.534	.699	.637	.940	.605	1			
K^+	.652	.614	.651	.606	.499	.604	.516	1		
Na^+	.524	.466	.490	.538	.482	.759	.503	.559	1	
NH_4^+	.814	.733	.860	.812	.695	.687	.697	.595	.455	1

Table 3. Factor Loadings, Variances, and Communalities (Chemical Data Base)

	Factor 1			Factor 2			Factor 3			Communalities		
Station No.	3011	4011	1011	3011	4011	1011	3011	4011	1011	3011	4011	1011
COND25	.897	.941	.933	.288	.284	.201	.307	.120	.277	.982	.981	.987
pH	.924	.945	.948	.181	.227	.056	.265	.096	.250	.956	.955	.965
SO_4^{2-}	.844	.902	.868	.417	.358	.363	.238	.076	.269	.943	.948	.958
NO_3^-	.799	.811	.842	.343	.327	.372	.345	.284	.278	.875	.845	.925
Ca^{2+}	.325	.334	.247	.892	.848	.888	.243	.041	.115	.960	.832	.862
Cl^-	.572	.530	.585	.284	.439	.244	.670	.578	.715	.857	.809	.913
Mg^{2+}	.308	.211	.244	.892	.926	.840	.268	.070	.275	.963	.908	.841
K^+	.493	.394	.341	.229	.630	.178	.569	.274	.738	.619	.627	.693
Na^+	.179	.091	.139	.231	.055	.157	.920	.965	.916	.932	.942	.883
NH_4^+	.713	.539	.792	.512	.446	.449	.209	.273	.232	.815	.564	.883
Variance	4.32	4.14	4.46	2.45	2.74	2.33	2.13	1.53	2.13			

The results are very similar among these three stations. The analysis for all three sites indicate three factors. Factor 1 always has large loadings on COND25, H^+, SO_4^{2-}, NO_3^-, and medium loadings on NH_4^+ and Cl^-. Nearly 45% of variance in the system can be explained by it. It is the source responsible for the acidity of the precipitation because it relates H^+, SO_4^{2-}, and NO_3^-.

In addition to this acid factor, there are two factors contributing to the precipitation, but not affecting the acidity of the precipitation. These two factors make up about 40-50% of the variance in the system. Factor 2 has large loadings on Ca^{2+} and Mg^{2+}, and medium loading on NH_4^+. A reasonable hypothesis is that Ca^{2+} and Mg^{2+} ions are dissolved into rainwater from suspended soil dust or other Ca^{2+} and Mg^{2+} enriched particles (e.g. limestone) that are washed out by rain droplets. If other elements such as Fe had been measured, more information would be available for this source. Factor 3, with a large loading on Na and a medium loading on Cl, is considered as marine aerosol source.

In summary, the factor analysis on chemical data suggest that there are three kinds of principal sources contributing the precipitation ionic composition: acid sources, Ca and Mg sources, and Na and Cl sources. Special attention should be given to acid sources because they are responsible for the precipitation acidity. The next question is where these sources are located. To investigate location of the sources, the trajectory information is introduced into the analysis.

Factor Analysis Applied on the Data Sets Combined with Chemical and Back Trajectory Data

The trajectory information is in form of the geographic locations of back trajectory endpoints. Fourteen source subregions have been selected within the trajectory covered region (Figure 2). The setting of the subregion boundaries include the consideration of separating potentially interesting source areas, and that a subregion should not be too big, thus losing resolution, or too small so that there are too few endpoints in this subregion. Using these fourteen subregions, fourteen new variables are defined as the number of the endpoints in each subregion for each sample interval.

The factor analysis is applied to the combined data sets with 24 variables (10 chemical variables and 14 BT endpoint variables). Because of the additional spatial variables, additional factors are needed to reproduce the data. Additional factors are included until the chemical data are adequately reproduced. For all cases, factors were formed that have loadings for the chemical

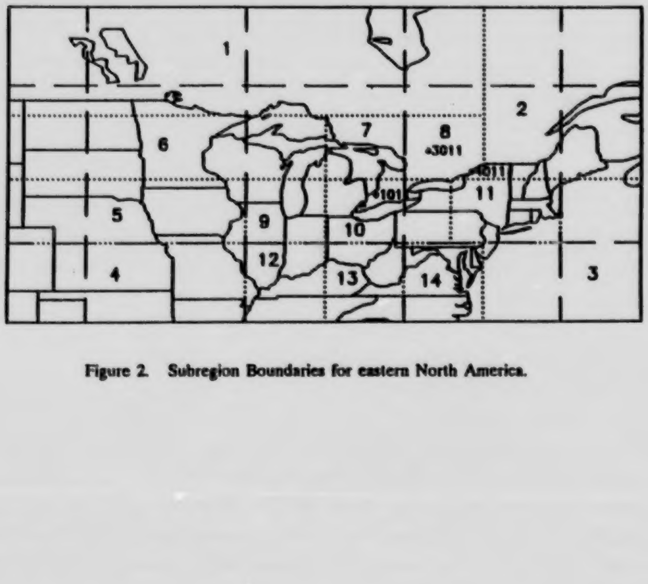
1
2
3
4
5
6
7
8
3011
4011
101
9
10
11
12
13
14

Figure 2. Subregion Boundaries for eastern North America.

variables similar to those given in Table 3. Some factors only have significant loadings for the endpoint variables. These factors only reflect the displacement of air mass from one subregion to another (Malm et al., 1986). Only those factors which have significant loading on the chemical variables are listed in Table 4.

In ideal situation, trajectories only pass through specific pollutant source areas, i.e. the number of endpoints in these areas is large. The air mass will then carry significant amounts of pollutants from these sources to the receptor. The concentration of corresponding pollutants will be high. On the other hand, if trajectories only pass through clean areas rather than source areas, the concentration of the pollutants will be low. Therefore, the number of endpoints in the areas (endpoint variables) and concentrations of corresponding pollutants will covary. In the factor analysis, these endpoint variables and the chemical species (or pollutants) will show high loadings in same factor. However, in actual case, some trajectories pass both source and clean areas. These multiple trajectories for a given precipitation event weakens the covariance so that the factor loadings on the endpoint variables are usually not very high. The loadings in the range of 0.2 to 0.5 are considered to be weak (but significant) to moderate (Malm et al., 1986).

In Table 4, according to the loadings on the chemical variables, factors 1, 2, 3 represent acid sources, Ca and Mg sources and Na and Cl sources, respectively, as in previous section. For the first factor at station 3011, subregions 13 and 10 show loadings of 0.359 and 0.286. They are significant values for endpoint variables. This result indicates that there are acid sources in these subregions, i.e. the Ohio River Valley region. Subregions 12 and 14, with the loadings of 0.194 and 0.144, are considered to be weak source regions. The remaining loadings are very small or negative. Negative loadings mean that either the trajectories passed these subregions and the concentrations of acid species at the receptor are low, or when the concentrations of acid species at the receptor are high, there is little probability that the trajectories passed these subregions. Thus, these subregions are clean or relatively clean regions with respect to acid sources. Similarly, at station 4011, subregions 10 and 13 are major source areas for the acid sources. Subregion 11 may be a source region. All other loadings on endpoint variables are negative or near zero. For station 1011, subregions 12, 13, 10, 14 have relatively large loadings, but they are weaker than at the other stations. These results suggest that the Ohio River Valley region is the major source area of the acid sources in the precipitation of southern Ontario. The effect of this source region is stronger on Dorset, moderate on Kingston and weaker on London, the site closest to the source region.

Table 4. Factor Loadings (Combined Chemical and Endpoint Variable Data Base)

	Factor 1			Factor 2			Factor 3		
Station No.	3011	4011	1011	3011	4011	1011	3011	4011	1011
COND25	.973	.970	.970	.061	.108	.052	.015	.005	.143
pH	.954	.958	.955	-.035	.042	-.081	-.023	.000	.110
SO_4^{2-}	.928	.937	.935	.192	.184	.197	-.012	-.033	.148
NO_3^-	.918	.884	.911	.140	.186	.234	.036	.151	.172
Ca^{2+}	.587	.488	.401	.764	.733	.723	.077	-.006	.134
Cl^-	.822	.697	.702	.129	.328	.138	.341	.433	.624
Mg^{2+}	.582	.398	.417	.763	.825	.742	.083	.029	.261
K^+	.668	.541	.459	.078	.574	.128	.344	.160	.646
Na^+	.541	.233	.284	.168	.086	.119	.658	.859	.861
NH_4^+	.833	.638	.877	.291	.382	.306	-.025	.111	.130
Subregion 1	-.155	-.087	-.149	.029	-.109	.008	-.050	.215	-.028
Subregion 2	-.154	-.177	-.098	.030	.117	.004	-.051	.003	-.070
Subregion 3	-.096	-.045	-.003	.019	-.096	.095	-.004	.286	-.152
Subregion 4	-.027	-.056	-.032	-.016	.003	-.114	.153	-.113	.104
Subregion 5	-.047	-.023	-.083	-.100	-.098	-.195	-.139	.073	-.026
Subregion 6	-.157	-.063	-.152	-.112	-.100	.062	.041	.119	-.023
Subregion 7	-.103	-.077	-.084	.065	.162	-.118	-.069	-.133	-.155
Subregion 8	.010	.001	-.079	-.038	.032	-.244	-.116	-.336	-.084
Subregion 9	-.099	-.065	-.091	.105	.105	.349	-.131	.164	-.183
Subregion 10	.286	.270	.065	.214	.041	.104	-.153	-.183	-.043
Subregion 11	.031	.127	-.079	-.124	-.248	.053	-.025	-.078	.132
Subregion 12	.194	-.096	.194	.042	.117	.364	.031	.010	-.051
Subregion 13	.359	.209	.105	-.010	-.094	-.143	-.254	.237	.153
Subregion 14	.144	.006	.055	-.035	.015	-.322	.489	.091	.099

Factor 2 is Ca and Mg sources. According to the result of station 1011, subregions 9 and 12 seem to be the source areas for these sources. These two subregions also received significant loadings at other two stations. Other loadings around value of 0.1 are on subregions 7 and 10 shown at two stations, also on subregions 2 and 3 shown at one station. These soil sources seem to be wider spreaded than the acid sources, but their regions are more likely to be in Illinois, Indiana and part of Kentucky and Missouri.

The results suggest that the Na and Cl sources are either the Pacific or Atlantic Oceans and the Gulf of Mexico. The largest loadings are on subregions 14 and 4 for station 3011, on subregions 3, 13, 1, 9, and 6 for station 4011, and on subregions 13, 11 and 4 for station 1011. These subregions fall into two group: one is subregions 3, 11, 14, and 13 where the Na and Cl sources, Atlantic or the Gulf marine aerosol, can affect the system; another one is subregions 4, 5, 6, 1, and 9. In most cases in a year, the air motion basically crosses the North American continent from the west coast to the east coast. In this way, the Pacific maritime aerosol can be carried to the eastern part of the country. Since the trajectory data are only calculated for a two-day period, the trajectories do not go further than about 110° longitude so that it makes it appear that the source area is around Iowa, Missouri, Nebraska, and Kansas.

Potential Source Contribution Function (PSCF)

Another approach to investigate the location of the sources of the observed constituents is the Potential Source Contribution Function (Malm et al., 1986). Again the possible source region is subdivided into a grided i by j array. Let N represent the total number of trajectory endpoints during whole study period, T. If n_{ij} endpoints fall into the ijth cell, the probability of this event, A_{ij}, is given by

$$P[A_{ij}] = \frac{n_{ij}}{N} \tag{1}$$

$P[A_{ij}]$ represents the residence time of a randomly selected air parcel on the ijth cell relative to time period T. In same ijth cell, if there are m_{ij} endpoints that correspond to the trajectories that arrived at a receptor site with pollutant concentrations higher (or lower) than some pre-specified value, then the probability of this event, B_{ij}, is

$$P[B_{ij}] = \frac{m_{ij}}{N} \tag{2}$$

$P[B_{ij}]$ refers to the residence time for these contaminated air parcel. The potential source contribution function (PSCF) is then defined as a conditional probability:

$$\mathrm{PSCF} = \frac{P[B_{ij}]}{P[A_{ij}]} = \frac{m_{ij}}{n_{ij}} \tag{3}$$

PSCF is the probability that an air mass with specified pollutant concentrations arrive at a receptor site after having been observed to reside in a specific geographical cell. Cells containing pollutant sources will have high conditional probabilities. Therefore, the conditional probability function, PSCF, will identify those source areas that have a potential to contribute to the high concentrations of contaminants observed at the receptor site (Malm et al., 1986).

PSCF Based on Factor Scores

For each precipitation monitoring station, the PSCF values can be calculated for each 1° longitude by 1° latitude cell for each factor by specifying that the factor score for a given sample event must be greater than 0. This specification means that the contribution of the particular source related to the specified factor for the sample is higher than average since the factor score is standardized to an average value of 0. For any cases in which the factor score is greater than 0 (higher than average), the corresponding trajectories are counted in the m_{ij} total in equation (2). In this way, PSCFs for each factor at each station have been calculated.

In the calculation of the PSCF values, some grid cells will only have 1 endpoint (n_{ij} in equation (3) is 1). If this endpoint happens to correspond to an event trajectory, the PSCFs for these cells will be 1, but the confidence in these PSCFs are very low. In this work, a weight of 0.5 is given to PSCF for the case of $n_{ij} = 1$, a weight of 0.68 for $n_{ij} = 2$, a weight of 0.85 for $n_{ij} = 3$, and weight of 1.0 for $n_{ij} \geq 4$. These weighing values are of arbitrary settings.

The PSCF plots show similar patterns among three stations and only those plots for the Dorsett site (Site No. 3011) are shown in Figures 3-5. The potential contribution probabilities for the acid sources (factor 1) are above 0.6 in a wide area of the midwest and along the east coast. Particularly, the PSCFs are higher than 0.8 along the Ohio River Valley and some areas in the east coast. For stations 3011 and 1011, there are some high density spots in the western part of Missouri. It seems that these spots are shifted westward from St. Louis area (a high NO_x, NH_3, and

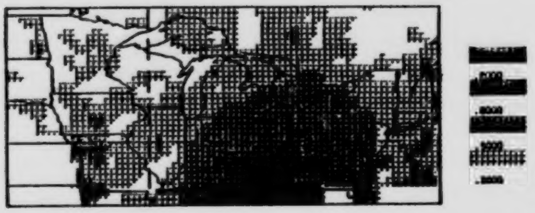

Figure 3. PSCF For Factor 1 at Station 3011.

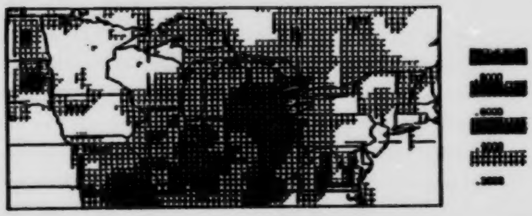

Figure 4. PSCF For Factor 2 at Station 3011.

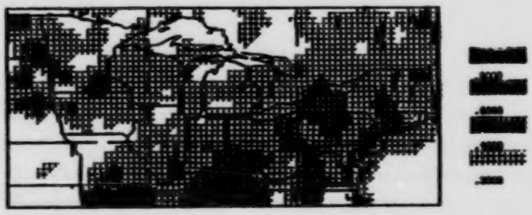

Figure 5. PSCF For Factor 3 at Station 3011.

SO_2 emission area) possibly due to the increasing errors in the trajectories as the distance from the receptor site increases.

The distribution of the dark areas in the PSCF plots (Figure 4) for Ca and Mg sources (factor 2) look more widely spread around the midwest region, but still concentrated a little more on the Ohio River and the Mississippi River Valleys. The distribution for Na and Cl sources (factor 3) are even more dispersed, but seldom in the area north of the stations. These sources are considered to be marine aerosol, that could be carried from the Pacific, the Atlantic, or the Gulf areas as discussed in the previous section.

PSCF Based on Individual Species

PSCF also can be calculated on an individual species basis instead of factor scores. For example, the PSCF for pH (or H) can be calculated in each cell by specifying pH less than the average pH value (instead of factor score greater than 0). These kinds of PSCF plots may provide some more specific information. Figures 6-10 show the PSCF plots for station 3011 for pH, SO_4^{2-}, NO_3^-, Ca^{2+}, and Na^+ with the specified values (average) of 4.36, 2.45 mg/l, 0.565 mg N/l, 0.208 mg/l, and 0.051 mg/l, respectively. The PSCF of pH is similar to the PSCF for factor 1. It reflects that the potential contribution areas of the precipitation acidity are basically the Ohio River Valley, the east coast and St. Louis region. The major contributors to the acidity (pH) are SO_4^{2-} and NO_3^-. From Figures 7 and 8, it can be seen these two acid species come from different areas. SO_4^{2-} comes from the Ohio River Valley. However, more of NO_3^- comes from St. Louis and Chicago areas. The area around Pittsburgh also contributes some of the NO_3^-. These results are consistent with the distribution of emissions of SO_2 and NO_x. Figure 9 shows that Ca^+ comes from the midwest, but the probabilities are not so high. Figure 10 suggests more Na^+ comes from the Pacific. The PSCFs of Mg^+ and Cl^- are similar to that of Ca^+ and Na^+, respectively. Similar results have been obtained for other two stations.

CONCLUSION

The data analysis on the acid precipitation data sets from Ontario shows that there are three principle components contributing to the precipitation chemistry. Based on their chemical nature, these three components can be referred as acid sources, Ca and Mg sources, and Na and Cl sources. They are related to SO_x and NO_x emission, soil dust and marine aerosol, respectively. The acid sources are important and responsible for the acidity of the precipitation. By incorporating

Figure 6. PSCF Based on pH at Station 3011.

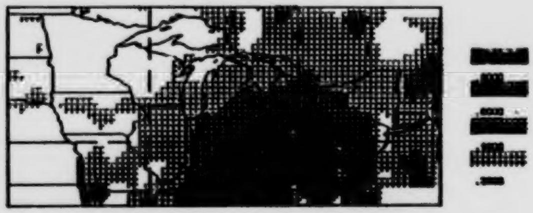

Figure 7. PSCF Based on SO_4^{2-} at Station 3011.

Figure 8. PSCF Based on NO_3^- at Station 3011.

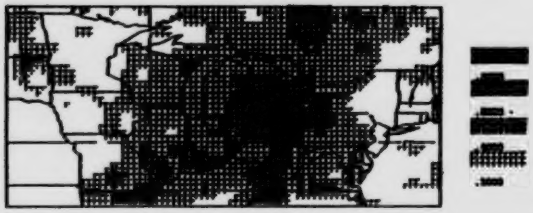

Figure 9. PSCF Based on Ca^{2+} at Station 3011.

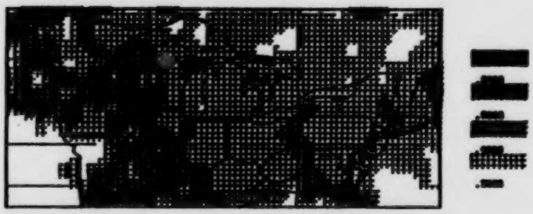

Figure 10. PSCF Based on Na^+ at Station 3011.

the information of air parcel trajectory, the acid sources can be located in the Ohio River Valley and the east coast, the Ca and Mg sources in the midwest, particularly in the converging area of the Ohio and the Mississippi river, and Na and Cl sources from the Pacific, Atlantic, and the Gulf. These results suggest that the Sudbury area is not a source area. The reasons might include the prevailing wind direction (southwest), high stack and relatively short distance from the stack to the monitoring stations.

The approach of incorporating trajectory information into factor analysis in the receptor modeling was originally used in particulate matter study (Malm et al., 1986). It seems more difficult to use this approach in precipitation study since precipitation process involve more chemical and physical process. Particles have a tendency to better maintain their characteristics compared with precipitation. More factors affect the precipitation during the formation and transport within the distance of the trajectory. For instance, if another precipitation event occurs on the way of the trajectory, then most of the material is washed out and the pollutant concentration, e.g. SO_4^{2-} will not be high even though the trajectory has passed a SO_2 emission area. In other cases, there will be several trajectories for same sampling period with some of the trajectories passing through clean areas, but some passing over source areas. However, they all affect the same precipitation event. This mixing of air parcels will interfere with this type of analysis. For this reason, a shorter sampling period may help reduce the interference and increase the precision of such analysis. In addition, if multilayer trajectories are used, the results may be improved.

Acknowledgements

This work was supported by the Ontario Ministry of the Environment under contract No. 697.

REFERENCES

Bresch, J. E., Ashbaugh, L. L., Henmi, T., and Reiter, E. R. (1984), Comparison of a Single-Layer and a Multilayer Transport Model for Residence Time Analysis, 77th Annual Air Pollution Control Assoc. Meeting, San Francisco, California.

Chan, W. H., Orr, D. B., Bardswick, W. S., and Vet, R. J. (1985), Acidic Precipitation in Ontario Study (APIOS); An Overview: The Event Wet/Dry Deposition Network (1st revised edition), Ontario Ministry of the Environment, Report # ARB-142-85-AQM, APIOS-025-85.

Lowenthal, D. H., Wunschel, K. R., and Rahn, K. A. (1988), Tests of Regional Element Tracers of Pollution Aerosols. 1. Distinctness of Regional Signatures, Stability during Transport, and Empirical Validation, Environ. Sci. Technol. 22, 413-420.

Lowenthal, D. H. and Rahn, K. A. (1988), Tests of Regional Element Tracers of Pollution Aerosols. 2. Sensitivity of Signatures and Apportionments to Variations in Operating Parameters, Environ. Sci. Technol. 22, 420-426.

Malm, W. C., Johnson, C. E., and Bresch, J. F. (1986), Application of Principal Component Analysis for Purposes of Identifying Source-Receptor Relationships, in Receptor Methods for Source Apportionment, T.G. Pace, Ed., Publication TR-5, Air Pollution Control Association, Pittsburgh, PA.

Hopke, P. K. (1985), Receptor Modeling in Environmental Chemistry, pp. 155-197. John Wiley & Sons, New York.

Olson, M. P., Oikawa, K. K., and Macafee, A. W. (1978), A Trajectory Model Applied to the Long-Range Transport of Air Pollutants, Report of Atmospheric Environment Service, Downsview, Ontario.

Rahn, K. A. and Lowenthal, D. H. (1984), Elemental Tracers of Distant Regional Pollution Aerosols, Science, 223, 132-139.

Rahn, K. A. and Lowenthal, D. H. (1985), Pollution Aerosol in the Northeast: Northeastern-Midwestern Contribution, Science, 228, 275-284.

A16

ADVANCED TECHNIQUES FOR MOBILE MONITORING OF TRACE ORGANICS IN AIR

G.B. De Brou*, E. Singer, M.A. Sage, R.W. Bell, R.E. Chapman, and D.J. Ogner, Air Resources Branch, Ontario Ministry of the Environment, Toronto, Ontario, M5S 1Z8.

The measurement of trace organic compounds in air poses several challenges to the analytical chemist. Often the compounds of interest are present at trace levels, for short, irregular time periods, in a complex chemical matrix. Since the early 1970's, the Air Resources Branch has recognized the need for state-of-the-art mobile laboratories to gather vital air quality data near the source in the affected community. The original mobile air monitoring units (MAMUs) were equipped to measure only a few classical pollutants , namely: sulphur dioxide, oxides of nitrogen, and carbon monoxide. Owing to the recent advances in analytical instrumentation and an enhanced awareness of volatile organic contaminants, the monitoring capabilities of the MAMUs have been vastly expanded. Today the Ministry operates four MAMUs which provide on-site measurements of a broad range of volatile organic and inorganic compounds. Our latest addition to the MAMU fleet is the mobile TAGA 6000E - a tandem mass spectrometer with real-time, direct air analyses. Supplementing the MAMUs are our lab-based instruments for verification of pollutant identities: an isolation matrix FTIR , triple column GC/MSD, and a dual oven GC.The MAMUs' unique capabilities have proven to be invaluable to the Ministry in a variety of monitoring applications: from tracking plumes of toxic gases in a small community to assisting the Ministry personnel in clean-up operations of chemical spills.

Introduction

The Ministry of Environment (MOE) has been responsible for the protection and assurance of air quality in Ontario since 1968. By the late seventies, the Ministry operated a network of over 125 permanent air monitoring stations throughout Ontario. While this fixed network system serves an adequate surveillance function, it can not respond as efficiently as major environmental problems merit. The Air Resources Branch, which provides specialized services and manages various programs to support the Ministry's mandate, developed a mobile air monitoring system. Today, the Ministry operates four world-class Mobile Air Monitoring Units (MAMUs) throughout Ontario, backed up by a dedicated team of scientists and technicians. These units are completely self-contained mobile air monitoring laboratories that can be dispatched to any area of the Province of Ontario to quickly determine relevant air quality parameters.

Background

The Ministry of Environment started with mobile air monitoring in 1970 on a very modest scale. The first mobile air monitoring unit, a Ford station wagon with a Sign X SO_2 analyzer, was used extensively for the monitoring of SO_2 pollution in the area of Sudbury, prompted by the construction of the INCO superstack. Soon the demand for mobile monitoring went beyond SO_2, to include THC, CO, H_2S, O_3 and Hg. Out of this demand came the second mobile air monitoring unit, a Ford Econoline van. For the first time, power to the scientific instrumentation was supplied either from a shore line or by an onboard generator. The data were recorded by a six-channel line recorder and later manually evaluated in the laboratory - an extremely laborious task, as four weeks were required to interpret one week of data. The first data acquisition system from Hewlett-Packard was a vast improvement, as now all the data could be punched simultaneously onto a single paper tape, and then read at home base into an HP9830 computer.

Around 1975, it became obvious that a larger mobile air monitoring platform was needed to accomplish the tasks required of the unit, as available space in the small Ford Econoline van was by this time substantially limited. A GMC Transmode was eventually chosen as the replacement, and in 1976 the new generation of mobile air monitoring units was born with the introduction of MAMU 1. In 1981 the second MAMU was commissioned to address the increased number of survey requests. MAMUs 1 and 2 have similar capabilities, and, in addition to monitoring common pollutants, they routinely measure up to 133 distinct volatile organic compounds using advanced gas chromatographic techniques.

As the emphasis in mobile air monitoring shifted from the measurement of common inorganic pollutants to the more elusive trace organics, the Ministry examined new technology and, in 1978, acquired a mobile TAGA 3000. Developed in Ontario by SCIEX Inc., the TAGA (Trace Atmospheric Gas Analyzer) is a specialized mass spectrometer with direct air analysis capabilities. This unit later became known as MAMU 3. Finally, in August 1987, the Air Resources Branch added a fourth mobile air monitoring unit to their fleet: MAMU 4. This unit , converted from an Orion bus, contains a significantly improved version of the TAGA 3000 - a tandem mass spectrometer (MS/MS) - TAGA 6000. Both of these units are capable of real time detection and monitoring of a wide range of organic and inorganic compounds. MAMU 4 (TAGA 6000) has the added capability of identifying unknown pollutants in a matter of seconds. MAMUs 3 and 4 are adept at tracking down fugitive emissions and locating the precise source of pollutants.

MAMUs 1 and 2

MAMUs 1 and 2 are housed in GMC Transmode vehicles which are both stylish and practical. The vehicles are characterized by a smooth, low vibration ride due to a self-levelling air bag and torsion bar suspension system. The front wheel drive vehicles provide sufficient flat floor space to accommodate the scientific and monitoring instrumentation. Schematics of MAMU 1 floor plans are shown in Figure 1a.

Each unit is powered by two six-kilowatt generators with electronic frequency controllers. Two independent circuits permit electrical isolation of sensitive scientific instrumentation from the auxiliary equipment. Since each generator can supply power to either circuit, analytical equipment can remain functional in an emergency monitoring situation should a generator fail.

Each MAMU represents a capital expenditure of nearly one million dollars. Thus they are equipped with fire, vandalism, and power loss sensors. A two-way radio system with a unique frequency, plus a cellular phone provides the MAMUs with a communication link with each other and with the Air Resources Branch.

Since the measurement of meteorological data is of paramount importance in air pollution studies , the MAMUs are outfitted with meteorological instruments that continuously record wind speed and direction, temperature, humidity, solar radiation and barometric pressure. Minisondes and automated dual theodolite tracking systems are included in MAMUs 1 and 2. The simultaneous acquisition of meteorological parameters and air quality data is essential for source delineation.

Common Pollutants Instrumentation

MAMUs 1 and 2 are equipped with several discrete analyzers to measure the common, or classical, pollutants on a continuous basis. Instrumentation common to both MAMUs include the following:

-a dual flame ionization analyzer to measure total

hydrocarbons, non-methane hydrocarbons and methane
-a filter correlation spectrometer for monitoring carbon monoxide
-a chemiluminescent, dual channel analyzer to monitor nitrogen monoxide and nitrogen dioxides
-a fluorescent sulfur dioxide analyzer which serves two purposes: the measurement of sulfur dioxide; and the measurement of total reduced sulfur compounds
-an ultraviolet absorption ozone analyzer

In addition to the above analyzers, MAMU 2 contains an ultraviolet spectrometer for the detection of elemental mercury, and a second sulfur dioxide analyzer. Utilizing the SO_2 analyzers, one with a SO_2 scrubber and a high temperature converter system, permits simultaneous measurements of SO_2 and TRS.

The functions of data acquisition, span and zero for all instruments are under computer control (HP 9886). Thus, once the instruments have been calibrated and set in the monitoring mode, air quality data are automatically recorded and reported every 30 seconds. Later the data are transferred to a main frame computer for further data reduction and analysis.

Volatile Organic Compounds (VOCs)

Both MAMUs 1 and 2 utilize identical GC systems developed by the Air Resources Branch laboratory. Volatile organic contaminants are sampled onto a multi-component adsorbent cartridge from a 3 litre air sample. Following thermal desorption, contaminants are focused onto low volume loops cooled to liquid nitrogen temperatures. Then the contaminants are identified using a sophisticated GC (HP 5880) with two high resolution capillary columns of different polarity (DB 1 and DB 5), each coupled to a flame ionization detector. The identification of pollutants is based on a library of retention indices. Pollutants must be confirmed on both columns to be reported as present. The basic components of this system are depicted in Figure 2.

Currently the system is calibrated for 133 hydrocarbons with three to twelve carbon atoms. The following chemical classes are represented: alkanes, alkenes, alkynes, aromatics and chlorinated hydrocarbons. Detection limits are typically in the range of 1 to 5 ug/^{3} for a 3 litre sample. A detailed list of all the pollutants targeted by MAMUs 1 and 2 is presented in Table 1.

MAMU 3 (TAGA 3000) and MAMU 4 (TAGA 6000)

The GCs of MAMUs 1 and 2 can monitor a predetermined number of non-polar hydrocarbons which comprise the retention index library. Owing to the presence of the Napion perma-pure dryers, the GCs are not conducive to the measurement of polar organics which are more reactive, and therefore subject to alteration during sampling and analysis.

On the other hand, the unique TAGA technology of MAMUs 3 and 4 are adept at monitoring ultra-trace levels in complex air matrices. The TAGA is a specialized quadrupole mass spectrometer with an atmospheric pressure, chemical ionization (APCI) ion source that accepts air samples in their original composition. This direct analytical approach circumvents problems associated with conventional trapping methods. The basic features of the TAGA system are shown in Figure 3. Airborne contaminants are sampled directly into the APCI source at high flow rates of five l/sec assuring minimal memory effects. Pollutants are electrically charged via chemical ionization reactions initiated by a corona discharge. Selective detection of chemical classes is accomplished through the addition of the appropriate chemical ionization reagent, for example, benzene is added to the ambient air stream to highlight aromatic species, whereas ammonia selectively ionizes compounds of high proton affinity, such as amines. The ionization of pollutants yields a mixture of pseudo-molecular ions which are subject to mass analysis by low resolution quadrupole mass filters.

The TAGA 3000, being a single quadrupole instrument, yields APCI mass spectra , which ultimately must be interpreted by an experienced TAGA scientist. The resultant pollutant identifications may be tentative, the degree to which depends upon the pollutant, the inherent selectivity of the ionization technique, and sample matrix. The difficulties of contaminant identification are greatly reduced by the superior analytical capabilities of the TAGA 6000.

The TAGA 6000, an APCI/MS/MS system, can rapidly speciate and quantify VOCs on site. The basic operating principle of the TAGA 6000 is sequential mass spectrometry: ions separated by the first quadrupole are fragmented with argon gas in a second quadrupole (RF only), and the fragment ions are analyzed by the third quadrupole. The collisionally activated decomposition (CAD) fragment ion spectra is compared to standard CAD library spectra. Thus the tandem mass spectrometer provides a much greater degree of specificity than the single MS system of the TAGA 3000.

The standard APCI source is particularly sensitive to polar compounds. Compounds previously measured by MAMU 3 include amines, amides, alcohols, sulfides, mercaptans, aldehydes, ketones, phenols, chlorophenols, acids and aromatic hydrocarbons. The real-time limits of detection for the TAGA 3000 range from 0.1 to 10 ug/^{3}, depending on the type of chemicals and the complexity of the sample matrix.

Both the TAGA units are equipped with a ten metre, telescopic tower and meteorological instrumentation to measure local wind speed, wind direction and ambient temperature. All meteorological data are stored by the on-board computer simultaneously with the collection of air quality data. The meteorological data are updated every 30 seconds, allowing the operator to assess the data on site and apply it to the survey strategy.

The MAMU 3 vehicle is also a GMC Transmode. Instrumentation and other equipment in MAMU 3 are powered by two six-kilowatt generators with electronic frequency controllers. An Orion bus was selected as the host vehicle for the TAGA 6000. All the power requirements of the MAMU 4 is supplied by a 17.5 kilowatt generator. For a sketch of the floor plan see Figure 1b.

Survey Strategy

Over the past ten years, more than 120 air monitoring surveys have been conducted by the Monitoring Instrumentation and Development Unit of the Air Resources Branch. During this period, a systematic approach to air monitoring has evolved based on the unique strengths (and limitations) of the MAMUs and the accumulated experience of the MAMU staff.

When planning and executing a survey strategy the following are considered:

- survey objectives
- type and description of environmental problem
- source inventory and production schedules
- monitoring capabilities and resources
- climatology
- local topography and accessibility
- real-time measurements of target compounds
- other neighbouring sources

Basically, the survey strategy is to acquire and analyze representative air samples downwind of the suspected source. To isolate the source, upwind samples are also collected. On occasion, concurrent upwind and downwind air sampling by MAMUs 1 and 2 is performed to key in on a particular source in a heavily industrialized area. Further delineation of the source is possible by correlating meteorological data with the ambient air quality data. A main advantage of using the MAMUs for pollution surveys is their ability to produce monitoring results in the field. The survey scientists can assess the monitoring strategy on site, and if necessary, alter it to achieve the required survey objectives. The duration of an air monitoring survey will depend on the nature of the environmental problem, the survey objectives, and the frequency occurrence of the preferred wind conditions. On average, the total survey period is about two weeks with a typical working day being 12 hours.

Field Applications

The analytical capabilities of the four MAMUs together provide for the detection of a broad range of organic and inorganic pollutants. Practically every chemical class can be monitored with these sophisticated units (see Table 2). Their versatility allows for their application to an assortment of environmental concerns.

Air studies are initiated by the Ministry's six Regional Offices that request assistance in monitoring. The MAMUs have undertaken many monitoring tasks including regulatory monitoring, emergency response to chemical spills, assessing general air quality, identifying specific pollution sources, checking the effectiveness of industrial abatement measures, and odour source characterization.

These units have been used to investigate the emissions from a variety of industrial sources, for example, kraft mills, smelters, oil refineries, landfill sites, incinerators, steel mills, tar plants, generating stations, auto plants, and many types of chemical plants. MAMU 3 has responded to several environmental emergencies, such as the train derailments in Mississauga and Medonte, and most recently, the PCB warehouse fire in St. Basile Le Grand, Quebec.

Cited below are examples of some recent field studies which showcase the analytical capabilities of the MAMUs and the Ministry's on-site approach to the analysis of airborne contaminants.

EXAMPLE 1: Common Pollutants - MAMU 1

During one of the first air quality surveys undertaken by MAMU 1 (1978 Nanticoke), the on-site aspect of mobile monitoring was exemplified. At a downwind distance of 16 kilometres, fumigation of the Nanticoke generating station plume was monitored and the classical NO_x/O_3 sink-source relationship of this SO_2 plume was clearly revealed. Outside the fumigation area the ambient levels of SO_2 and NO_x were below the Ministry Standards; ozone concentrations were above the Standard. As the plume passed overhead, the O_3 concentration decreased from 0.12 ppm to 0.07 ppm, while there was a marked increase in NO_x (0.02 ppm to 0.10 ppm) and SO_2 (0.05 ppm to 0.25 ppm). Today these pollutants are still used to track plumes to their point of impingement. This classical example of common pollutants behaviour is shown in Figure 4.

EXAMPLE 2: VOCs - MAMU 2

With the inclusion of a gas chromatograph (GC) system, the monitoring capabilities of MAMUs 1 and 2 were increased to include 133 volatile organic compounds (VOCs). Subsequently, the emissions could be chemically characterized, allowing source fingerprinting. For example, in 1987 MAMUs 1 and 2 conducted an extensive air quality survey in a highly industrialized area of Southern Ontario.

There was particular interest in three industries: a tar plant, a steel mill, and a foundry. The total VOCs averaged approximately 800 ug/m^3, 600 ug/m^3, and 250 ug/^{3} respectively. In comparison, the VOCs totalled 180 ug/m^3 in the nearby downtown area. The contribution of individual VOCs reveals significant differences in contaminant patterns for the various sources (see Figure 5). For instance, the highest levels of benzene were observed downwind of the tar plant, whereas the foundry was a major contributor of xylenes. Naphthalene was primarily detected in ambient air samples collected in the vicinity of the tar plant. Thus detailed knowledge of several VOCs can serve to fingerprint sources in a high density industrial area.

Example 3: VOCs - MAMU 3

This example demonstrates the importance of recording the meteorological data during the acquisition of contaminant levels. Figure 6 shows the real-time response to dimethyl sulfide (DMS) which was monitored downwind of a pulp and paper mill. A revealing feature in this Figure is that the instantaneous levels of DMS surged between the 6 and 10 minute mark while the wind speed and direction remained relatively constant. Apparently this episode of DMS was due to the purging of the digesters at the mill. The short-term level approached 120 ppb , roughly ten times the time-weighted-average, certainly high enough to cause an obnoxious odour in the immediate vicinity. Note that conventional trapping methods would not have been able to fully characterize this phenomenon for they do not reveal temporal distributions.

Example 4: VOCs - MAMU 3 and MAMU 4

During the spring of 1983, the mobile TAGA 3000 conducted an air monitoring study in response to odour complaints in the vicinity of a rubber chemicals plant. Aniline and benzothiazole were identified from the mass fingerprints. A mobile survey was undertaken where these compounds were measured while the TAGA criss-crossed the streets immediately downwind of the plant. The real-time response to these contaminants is shown in Figure 7. From these data it is apparent that both aniline and benzothiazole originate from the same source, in fact, they were tracked to the same building as clearly indicated by the aniline isopleth map. This data also shows the plume concentrations as a function of distance, or the dispersion characteristics which may be helpful for planning the location of stationary VOC monitoring equipment.

In August 1988, the mobile TAGA 6000 (MAMU 4) returned to this area to test the identification capabilities of MS/MS. The CAD spectra for masses 136 and 94 (see Figure 8) were searched against the library of standard spectra. The two contaminants, aniline and benzothiazole, were the same two identified downwind of this source five years previously using the TAGA 3000.

Once the compounds have been identified it is possible to ascertain the levels of specific contaminants by recording the real-time response to two or more parent/daughter ion pairs. Figure 9 shows the data recorded for ambient levels of aniline using the parent/daughter ion pairs of 94/77 and 94/51. Note the excellent agreement in the concentration profiles.

Laboratory Support

Evolution of GC Technology for VOC Analysis

Between 1979 and 1981, the Air Resources Branch was involved in developing a program to collect, detect and determine polychlorinated biphenyls (PCBs) in ambient air. Samples collected on florisil cartridges were analyzed on a GC with a packed glass column preceded by a rigorous solvent extraction and clean-up procedure. The glass column was 3.6 m X 2 mm ID X 6 mm OD containing 1% Derosil 400 on Anakrom A 90/100 mesh. An EC detector was used for its selective sensitivity towards halogenated compounds.

Although retention times were stable and peak areas were relatively constant, the columns exhibited a highly variable baseline, particularly at higher temperatures. More importantly, the resolution provided by packed columns was inadequate. This was proven when several samples were rerun on capillary GC columns, and large peaks were resolved into several multiple peaks. It was determined that packed columns significantly overestimated the levels of PCBs in ambient air. The new fused silica capillary columns developed by Hewlett-Packard were selected due to their advantages over both packed and glass capillary columns. These advantages include flexibility, inertness, thermal stability, high efficiency and inherent straightness. In the first quarter of 1980 analyses were performed using 0.2 mm ID 25 m column coated with SP2100 on an HP 5840 GC with an ECD detector. Although greatly improved, the co-elution of impurities with the PCB isomers still existed, due to the complexity of the sample matrix.

The next stage in the development involved converting the system to a dual capillary column analyzer. A sample was split and passed through two columns differing in polarity. Co-elution of peaks that occurred on one column were, in many instances, resolved on the other, thus improving the quantitation of PCB isomers by an order of magnitude over single capillary analysis. Two sets of columns were used: SP2100-/Carbowax 20M, and OV-1-/SE54. The initial combination was eventually discarded due to its inadequate temperature limit of 220°C. The columns, a combination of OV-1-/SE-54, were prototypes from Hewlett-Packard with a temperature limit of 350 °C. Further improvements in column stability have been brought about through the development of cross-linking techniques.

The dual column techniques were accelerated using a new and advanced GC: HP 5880A equipped with dual EC detectors. The computer's additional memory afforded more accurate quantitation programmes, based on Kovat's theory of retention indices, in place of the less reproducible retention times.

Measurement of VOCs in a mobile laboratory situation began after the completion of the PCBs work in 1980. Injecting a large gas volume quantitatively into a gas chromatograph has always presented problems, particularly when using capillary columns. In order to prevent a loss of column efficiency, the sample must be introduced to the column as an infinitely narrow band. To achieve this, a pre-focusing step is required to increase the concentration of trace components and reduce sample volume.

Sample concentration was achieved by using an adsorbent cartridge. Two basic extraction techniques, solvent and thermal desorption, were available. Direct thermal desorption of the adsorbent cartridge was selected because of its inherent advantages over solvent desorption: speed (no sample preparation); the entire sample is analyzed; there are no solvent peak interferences; contamination introduced during sample clean-up is eliminated; it can be easily automated for repetitive sampling ; and its simplicity of operation is conducive to field work.

The next step involved introducing the sample to the GC column in a narrow band. With the introduction of capillary columns, the direct desorption of a relatively bulky adsorbent onto the column was not feasible. Desorption gas flows of 5 - 30 ml/min. for 15 minutes were required to completely remove the VOCs from the adsorbent. The gas flow to the capillary column, typically 0.5 - 2 ml/min., would require an extremely long time for complete desorption. A trapping interface was therefore required that allowed removal of analytes under high gas flow, held them in a narrow band and then transferred them to the capillary column under low (carrier) gas flow conditions.

The method selected was cryogenic focusing. The cartridge is desorbed with an inert gas (helium) at 10 - 30 ml/min. through a 0.04" ID nickel capillary, cooled with liquid nitrogen. The sample components are condensed in the small volume of the nickel loop, then heated ballistically to pass the sample onto the capillary column as quickly as possible. The GC column is cooled to -50 °C to maintain the sample in a narrow band. The system, now automated and operated routinely in MAMUs 1 and 2 and the laboratory, can also handle cartridges collected remotely.

Presently, the system contains a water dryer (Napion, permapure), a system based on permeation distillation to remove water from the sample before it enters the nickel capillary.

Unfortunately this system also removes oxygenated and other polar compounds from the sample stream. Therefore, the classes of compounds currently being quantified are restricted to the aliphatic, aromatic, and chlorinated hydrocarbons.

An example of a chromatograph obtained with the present GC system is shown in Figure 10. The analysis of an air sample taken downwind of a tar plant in 1985 indicates the presence of several VOCs with the major components being aromatic hydrocarbons. At the time of this particular survey, naphthalene was not in the retention index library and consequently the large peak at 20.30 minutes was initially unidentified. Since this peak accounted for 22 per cent of the total area, identification of this unknown was imperative. Cartridge samples collected at this site with a portable sampler were later analyzed using a Hewlett-Packard Mass Selective Detector (MSD). The best match chosen by the library searching algorithm was naphthalene. In later surveys of the same source naphthalene levels were quantified (see Figure 2).

Hyphenated Techniques

New hyphenated techniques are currently under development in the laboratory to improve upon the positive identification of volatile organic compounds. A system is now in place that includes three capillary columns, two connected to flame ionization detectors and the third to a mass selective detector (see Figure 2). Mass spectral data are often used to help positively identify sample components. Other hyphenated techniques in the development stage are dual oven (GC/GC) gas chromatography and GC/FTIR. The latter will be used as an identification tool in a similar manner to the mass selective detector.

Multidimensional Gas Chromatography

Techniques using multidimensional gas chromatography are being developed to improve the resolution of compounds in a complex mixture which is typical of airborne contaminants. Even though recent improvements in column technology have produced capillary columns which approach the theoretical limits of efficiency, a single column is usually not able to resolve all the compounds in an airborne sample. Consequently, the use of two different columns connected in parallel or in series, known as multidimensional gas chromatography, is being applied to address this problem. The series approach is being studied, whereby the first column is used for the initial separation and a selected portion of the elutant is transferred, by flow switching, to a second column of different polarity for enhanced separation.

This work is being performed on a Siemens Sichromat 2 gas chromatograph which has two independently controlled ovens, one for each column, allowing the separate temperature programming of the two columns. Presently a microwave desorber unit is being adapted to the Sichromat for the purposes of rapidly vaporizing of organic compounds into the gas chromatograph. A further enhancement of this system will be the addition of a mass selective detector to improve identification of unknown contaminants.

GC/MI/FTIR

The recent marriage of Fourier Transform Infrared (FTIR) spectroscopy and low temperature matrix isolation (MI) is proving to be an exceptional technology to reliably identify environmental contaminants emerging from a gas chromatograph. The Air Resources Branch laboratory has recently procured a Cryolect 4800 or GC/MI/FTIR. This instrument will significantly improve the capabilities of identifying trace VOCs. At present, the Cryolect system is being evaluated using the 133 compounds targeted by the GC systems of MAMUs 1 and 2.

The enhanced sensitivity and specificity of the Cryolect 4800 is due to the isolation of the GC elutants in an argon matrix held at a nominal temperature of 12 K. The gas chromatograph fractions are mixed with argon and rapidly frozen onto a rotating disk. Then the frozen fractions are rotated into the optical path of the FTIR spectrometer where the IR spectra are generated. The fact that each sample molecule is trapped in a solid argon cage leads to very narrow, intense adsorption bands.

Trapping the sample on the cold disk allows for repetitive scanning up to 5000 times , subsequently increasing the signal-to-noise ratio and improving the sensitivity. Most infrared absorbers of medium strength are detectable at the sub nanogram levels.

With the high resolution provided by the MI\FTIR system it is possible to distinguish between compound isomers. Figure 11 shows the infrared spectra of the three isomers of dimethylxylene: ortho-, meta- and para-xylenes. The spectral peculiarities are obvious and are particularly valuable for distinguishing between meta- and para-xylenes, which usually co-elute on high resolution GC systems.

Another positive feature of the GC/MI/FTIR is the spectral deconvolution of partially merged compounds. Known library spectrum of one of the suspected compounds is subtracted from the sample spectrum and the resultant spectra is subjected to library search techniques, leading to the identification of the unknowns. An example of the spectral deconvolution technique is shown in Figure 12. The two co-eluting compounds were hexane and trichloroethene. Hexane started to elute first and an infrared spectrum was taken at 16.74 minutes (see Figure 12ii). At 17.19 minutes a trichloroethene peak co-eluted with hexane yielding a mixture. As clearly seen in Figure 12iii, the infrared spectrum displays features of both hexane and trichloroethene. However, when the hexane spectrum was subtracted from the mixture spectrum, the signature of trichloroethene is clearly evident (see Figure 12i).

Future

The identification, detection and quantitation of trace organic compounds in air is a complicated task, just in the infancy stages of development. An estimated 40,000 chemicals are manufactured worldwide on an industrial scale. Furthermore the number of chemicals produced as byproducts is an unknown factor. It is estimated that the number of compounds present in a sample of clean air in concentrations of low ug/m^3 or less total some 10^4 to 10^6 organic compounds.

The complex chromatogram of Figure 13 is indicative of an air sample containing a high number of volatile organics. Although the total organic loading was approximately 400 ug/m^3, the large number of unresolved peaks limits the effectiveness of the dual column GC technique. This particular chromatogram represents a 30 litre sample recently collected with a three stage cartridge downwind of a waste oil refinery. Of the 178 peaks detected, only 84 were identified. Moreover, the identification of these compounds is tentative because of the lack of baseline resolution and the obvious co-elution of several compounds. A possible solution to this unfortunate phenomenon is to heart cut a portion of the sample with a second column, identify peaks and subject the elutants to more sophisticated techniques such as MS/MS or FTIR.

In addition to the current work, the Air Resources Branch laboratory is studying advanced techniques of sample concentration, separation and detection; namely, the application of GC/GC, GC/MI/FTIR and MS/MS. Eventually, the FTIR will be integrated with a multidimensional gas chromatograph and a MSD producing the optimal analytical system. Simultaneous output from the detectors will be computer correlated to give unequivocal identification of trace VOCs.

Another program in the early stages of development is diffusion sampling. Semipermeable silicone membranes will be used to test their efficacy in separating both polar and nonpolar compounds from water. Eventually this research may lead to a solution to the inherent water problems associated with cryogenic concentration techniques of the current GC system.

Future plans for MAMUs 1 and 2 include the possible installation of a MSD to improve compound identification. There are also plans to integrate a GC with the TAGA 6000 to permit the analysis of adsorbent cartridges. This may enhance the capabilities for rapid analysis of soils and water samples for toxic contaminants. In addition, a program will be undertaken to expand the scope of compounds detectable by the TAGA 6000 by replacing the APCI source with the low-pressure CI. Preliminary studies indicate the low-pressure CI source is more sensitive toward chlorinated and aromatic hydrocarbons.

ACKNOWLEDGEMENTS

The authors are grateful to all members, past and present, of the MID unit for their contributions to the data reported in this work. A special thanks goes out to Mr. Robert Tooley and Ms. Cat Williams for their valuable contributions in the preparation of this document.

Table 1:

CHEMICAL COMPOUND LIST FOR MOBILE AIR MONITORING UNITS #1 AND #2

The Volatile Organic Compounds

ALKANES

ETHANE
PROPANE
2-METHYLPROPANE
BUTANE
2-METHYLBUTANE
PENTANE
2,2-DIMETHYLBUTANE
2,3-DIMETHYLBUTANE
2-METHYLPENTANE
3-METHYLPENTANE
HEXANE
2-METHYLHEXANE
2,3-DIMETHYLPENTANE
3-METHYLHEXANE
2,2,4-TRIMETHYLPENTANE
HEPTANE
2,5-DIMETHYLHEXANE
2-METHYLHEPTANE
4-METHYLHEPTANE
3-METHYLHEPTANE
OCTANE
4-METHYLOCTANE
2-METHYLOCTANE
3-METHYLOCTANE
NONANE
DECANE
UNDECANE
DODECANE

CYCLOALKANES

CYCLOPROPANE
CYCLOPENTANE
METHYLCYCLOPENTANE
CYCLOHEXANE
METHYLCYCLOHEXANE
TRANS12DIMETHYLCYCLOHEXANE
PROPYLCYCLOPENTANE
cis-1,3-DIMETHYLCYCLOHEXANE
ETHYLCYCLOHEXANE
tert-BUTYLCYCLOHEXANE
BUTYLCYCLOHEXANE

ALKENES

PROPADIENE
1-BUTENE
1,3-BUTADIENE
3-METHYL-1-BUTENE
1-PENTENE
2-METHYL-1,3-BUTADIENE
TRANS-2-PENTENE
cis-2-PENTENE
2-METHYL-2-BUTENE
4-METHYL-1-PENTENE
3-METHYL-1-PENTENE
1-HEXENE
TRANS-3-HEXENE
1-HEPTENE
TRANS-3-HEPTENE
1-OCTENE
TRANS-4-OCTENE
2-METHYL-1-HEPTENE
2-OCTENE
1-NONENE
1-DECENE

CYCLOALKENES

CYCLOHEXENE
4-METHYLCYCLOHEXENE

ALKYNES

PROPYNE
1-BUTYNE

AROMATICS

BENZENE
TOLUENE
ETHYLBENZENE
M-XYLENE
P-XYLENE
STYRENE
O-XYLENE
ISOPROPYLBENZENE
PROPYLBENZENE
4-ETHYLTOLUENE
3-ETHYLTOLUENE
1,3,5-TRIMETHYLBENZENE
2-ETHYLTOLUENE
tert-BUTYLBENZENE
1,2,4-TRIMETHYLBENZENE
ISOBUTYLBENZENE
sec-BUTYLBENZENE
1,2,3-TRIMETHYLBENZENE
ISOPROPYL-4-METHYLBENZENE
INDAN
1,3-DIETHYLBENZENE
1,4-DIETHYLBENZENE
BUTYLBENZENE
1,2-DIETHYLBENZENE
T-DECALIN
C-DECALIN
1235-TETRAMETHYLBENZENE
1234-TETRAMETHYLBENZENE
1234-TETRAHYDRONAPHTHALENE
1,4-DIISOPROPYLBENZENE

CHLORINATED AROMATICS

CHLOROBENZENE
2-CHLOROTOLUENE
3-CHLOROTOLUENE
4-CHLOROTOLUENE
1,3-DICHLOROBENZENE
(CHLOROMETHYL) BENZENE
1,2-DICHLOROBENZENE

CHLORINATED ALKANES

CHLOROMETHANE
CHLOROETHANE
DICHLOROMETHANE
2-CHLORO-2-METHYLPROPANE
2-CHLOROBUTANE
TRICHLOROMETHANE
1,2-DICHLOROETHANE
1,1,1-TRICHLOROETHANE
1-CHLOROBUTANE
TETRACHLOROMETHANE
DIBROMOMETHANE
1,2-DICHLOROPROPANE
1-CHLORO-3-METHYLBUTANE
1-CHLOROPENTANE
1,1,2-TRICHLOROETHANE
1,3-DICHLOROPROPANE
1,2-DIBROMOETHANE
1-CHLOROHEXANE
1,4-DICHLOROBUTANE
1,1,2,2-TETRACHLOROETHANE
1,2,3-TRICHLOROPROPANE
1,5-DICHLOROPENTANE
3-(CHLOROMETHYL)HEPTANE

CHLORINATED ALKENES

CHLOROETHENE
3-CHLOROPROPENE
trans-1,2-DICHLOROETHENE
cis-1,2-DICHLOROETHENE
3-CHLORO-2-METHYLPROPENE
2,3-DICHLOROPROPENE
TRICHLOROETHENE
TETRACHLOROETHENE
trans-1,4-DICHLORO-2-BUTENE

The Common Contaminants

TOTAL REDUCED SULPHUR COMPOUNDS
SULPHUR DIOXIDE
CARBON MONOXIDE
TOTAL HYDROCARBONS (THC, TH-M AND CH4)
MERCURY
OZONE
OXIDES OF NITROGEN (NOx, NO2 AND NO)

METEOROLOGICAL :

WIND SPEED & DIRECTION
AMBIENT TEMPERATURE
DEW POINT TEMPERATURE
BAROMETRIC PRESSURE
SOLAR RADIATION
UPPER AIR RAWINSONDE SOUNDINGS

ARB Mobile Air Monitoring Unit (MAMU 1)

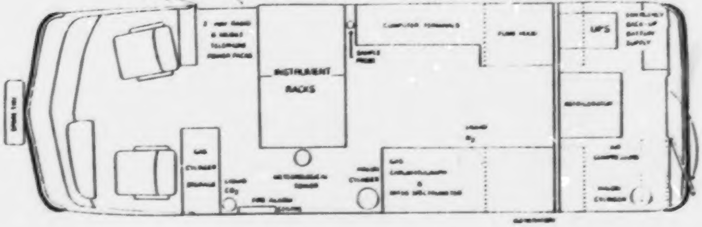
INSTRUMENT RACKS
SAMPLE PROBE
UPS
LIQUID CO_2

ARB Mobile TAGA 6000E (MAMU 4)

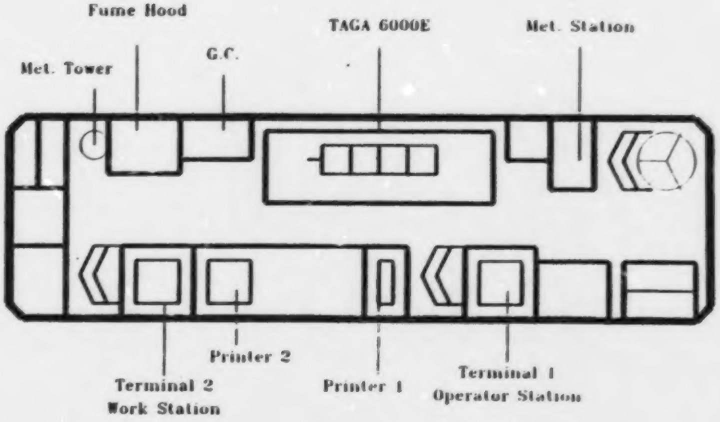
Fume Hood
TAGA 6000E
Met. Station
G.C.
Met. Tower
Printer 2
Terminal 2
Work Station
Printer 1
Terminal 1
Operator Station

Figure 1(a): (top) Floorplan of the MAMU 1.
1(b): (bottom) Floorplan of the MAMU 4.

Table 2:

SUMMARY OF THE MAMU'S ANALYTICAL CAPABILITIES
TYPE OF COMPOUNDS DETECTED AT TRACE LEVELS

MAMUs 1 and 2	MAMUs 3 and 4 (TAGA)
• classical pollutants (e.g. NOx, CO, SO2, TRS, O3, THC, etc.) • C3 to C12 non-polar hydrocarbons including alkanes, alkenes, alkynes, aromatic, and chlorinated hydrocarbons.	• polar compounds including amines, amides, acids, aldehydes, alcohols, ketones, esters, phenols, sulfides, mercaptans, chlorinated aromatics, etc. • inorganic acids, halides

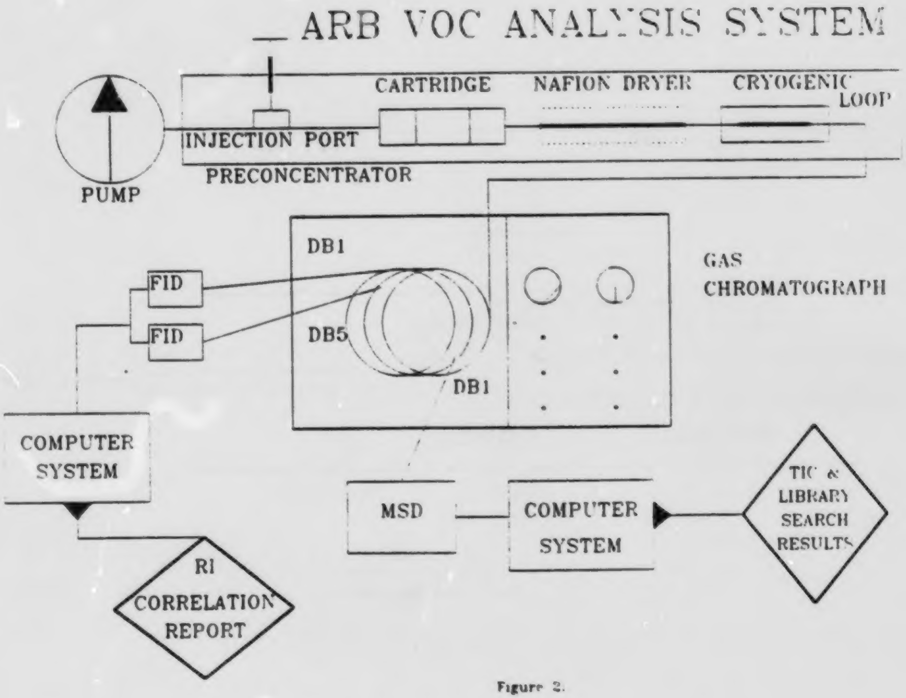
ARB VOC ANALYSIS SYSTEM
PUMP
INJECTION PORT
CARTRIDGE
NAFION DRYER
CRYOGENIC LOOP
PRECONCENTRATOR
DB1
DB5
DB1
GAS CHROMATOGRAPH
FID
FID
COMPUTER SYSTEM
RI CORRELATION REPORT
MSD
COMPUTER SYSTEM
TIC & LIBRARY SEARCH RESULTS

Figure 2.

MOE TAGA 6000E FRONT END AND VACUUM CHAMBER

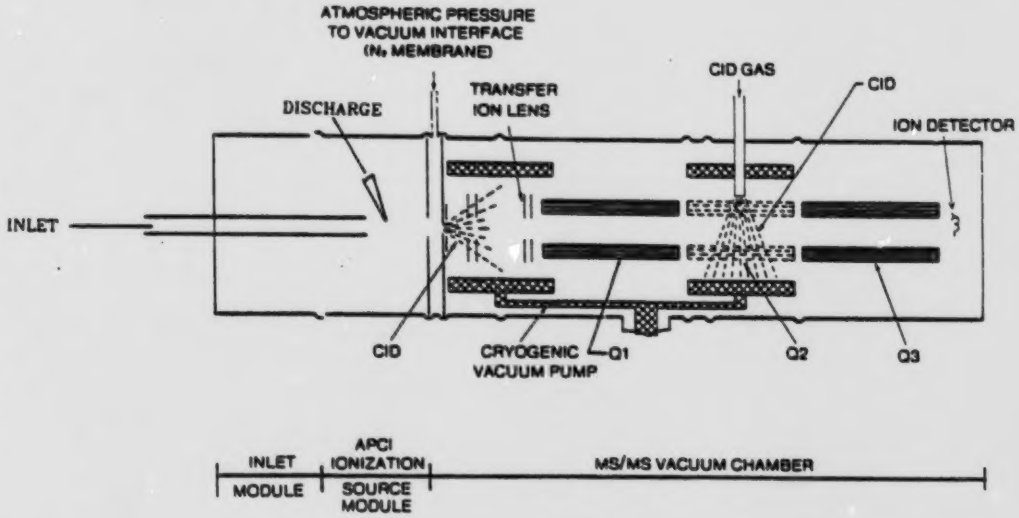
ATMOSPHERIC PRESSURE TO VACUUM INTERFACE (N_2 MEMBRANE)
CID GAS
CID
DISCHARGE
TRANSFER ION LENS
ION DETECTOR
INLET
CID
CRYOGENIC VACUUM PUMP
Q1
Q2
Q3
INLET MODULE
APCI IONIZATION SOURCE MODULE
MS/MS VACUUM CHAMBER

Figure 3:

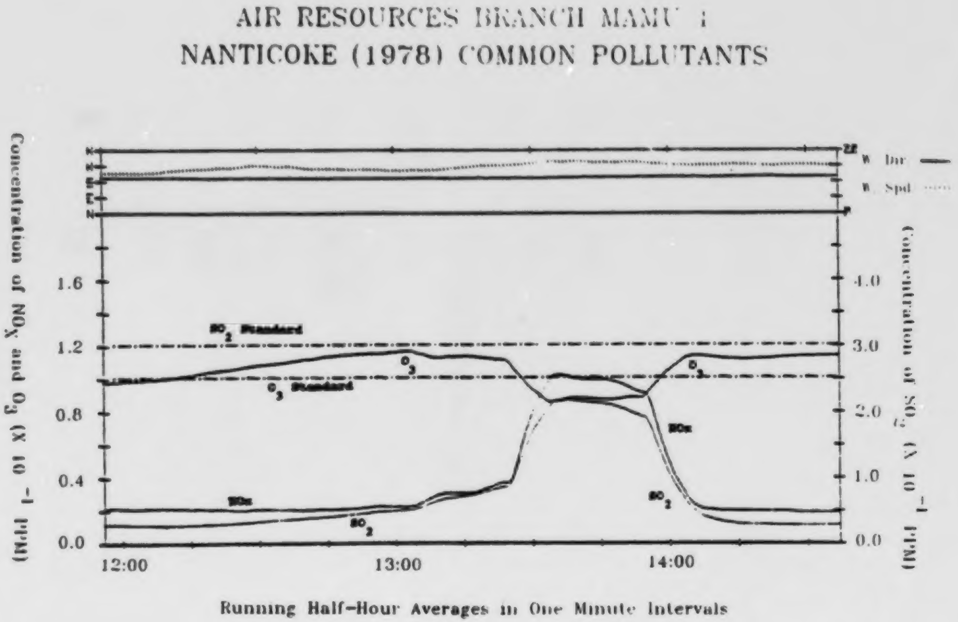
AIR RESOURCES BRANCH MAMU 1
NANTICOKE (1978) COMMON POLLUTANTS

Figure 4: Ambient levels of SO2, O3, and NOx recorded by MAMU 1 in Nanticoke, 1978.

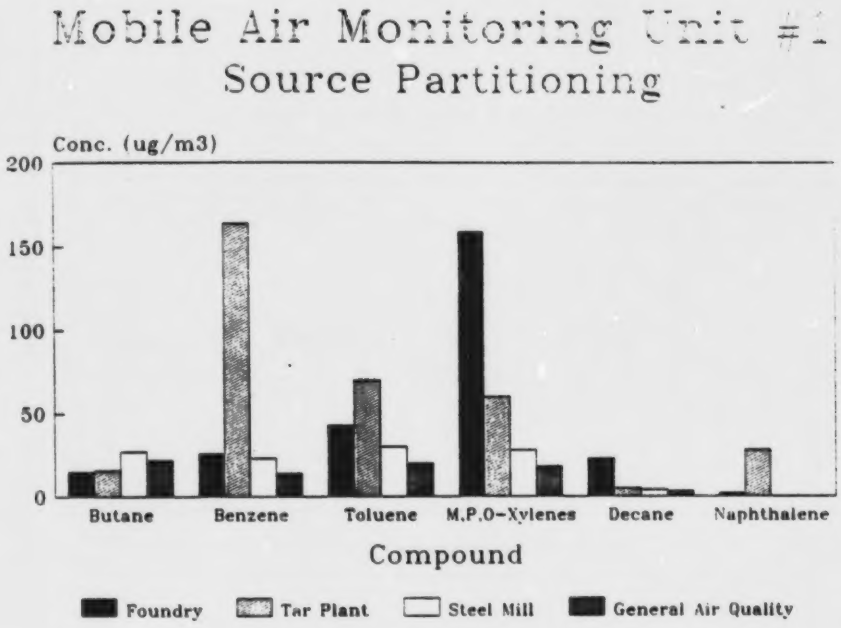

Figure 5: Source partitioning of selected VOCs
MAMUs 1 (and 2) Industrial Complex 1987.

Dimethylsulfide vs. Meteorological Data

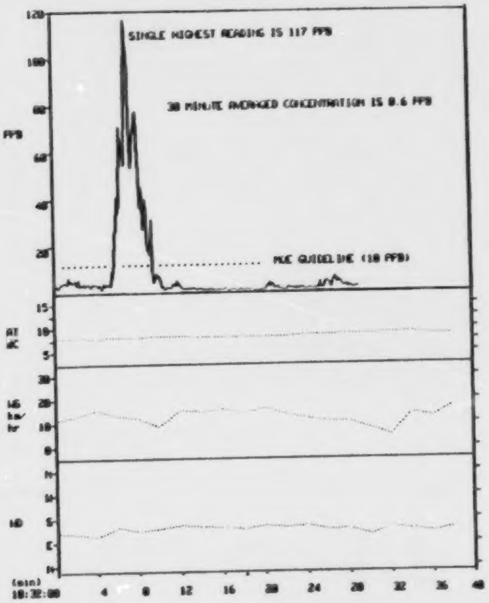

Figure 6 : Real-time monitoring of dimethyl sulfide downwind of a paper mill while simultanously montoring meteorolical data.

Figure 7

ANILINE ISOPLETHS (CHEMICAL PLANT)

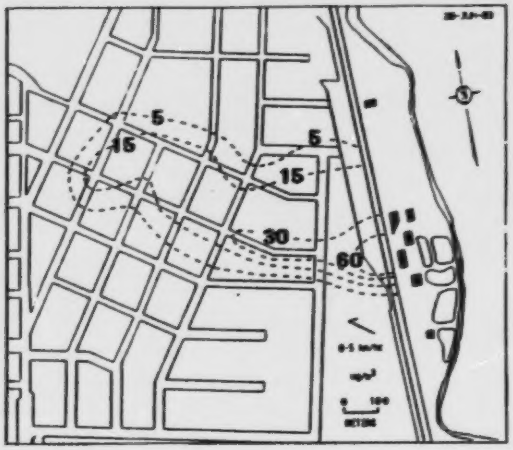
5
15
5
15
30
60
ug/m³
0
100

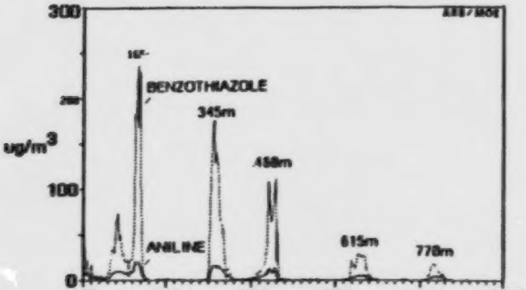

MOE TAGA 6000 Field Test 1, August 1988

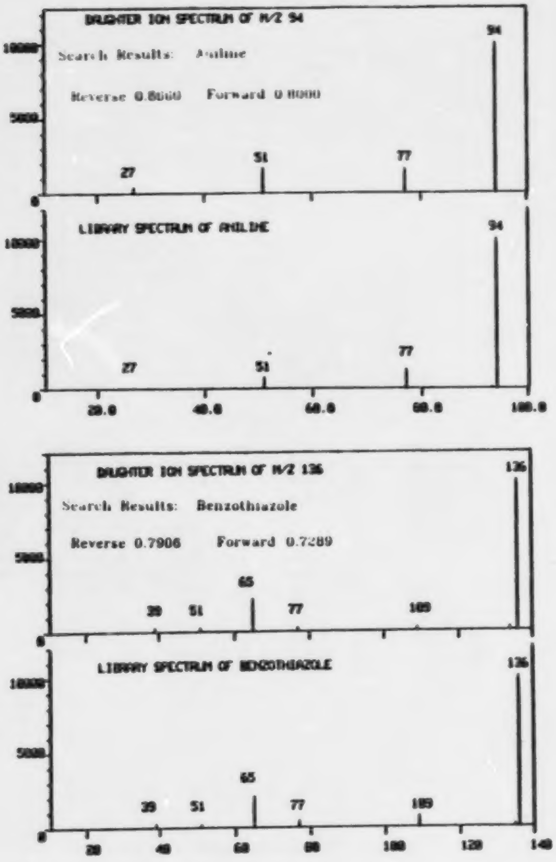

Figure 6: MOE TAGA 6000 search results for CAD spectra parent ions 94 (top) and 136 (bottom). Chemical rubber plant (August 1988).

MOE TAGA 6000 Field Test 1, August 1988

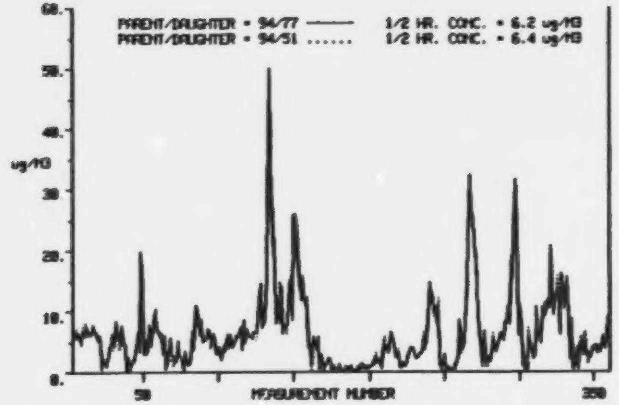

```
L1  52.000    MU -4100.0    ST       10.    M1  77.000    F1  94.000
L2  34.000    IM  650.00    EM      250.    M2  51.000    F2  94.000
L3  37.000    FP  50.000    MM 0.00000      M3 0.00000    F3 0.00000
L4  20.000    GR 0.00000                    M4 0.00000    F4 0.00000
L5 0.00000    TH       11.  PE  5.0000      M5 0.00000    F5 0.00000
L6 0.00000    MT        0.  SC       MRM    M6 0.00000    F6 0.00000
              OP            CT        1.    M7 0.00000    F7 0.00000
              SY      300.  IS      APCI    M8 0.00000    F8 0.00000
RE      120.  DM 0.15000    RO  30.000      Q2  3.5000    MO 0.10000E-02
1R      135.  1D 0.12000    R1  30.000      R2 -12.000
G1 0.00000    G2 0.00000    G3 0.00000
C1  60.950    C2  55.015    C3  1.0000      C4  1.0000
C5 0.00000    C6 0.00000    C7 0.00000      C8 0.00000
11-AUG-88     A1  4929.3    DI  2.0700      CG  22.925
16:11:20      A2  1476.0
```

Figure 9: MOE TAGA 6000 instantaneous measurements of aniline using two daughter ion pairs (94/77 and 94/51).

Note: the excellent agreement in the calculated 1/2-hour averages for the two parent daughter ion pairs.

Figure 10: VOC's Downwind of Tar Plant (MAMU 2 GC/FID)

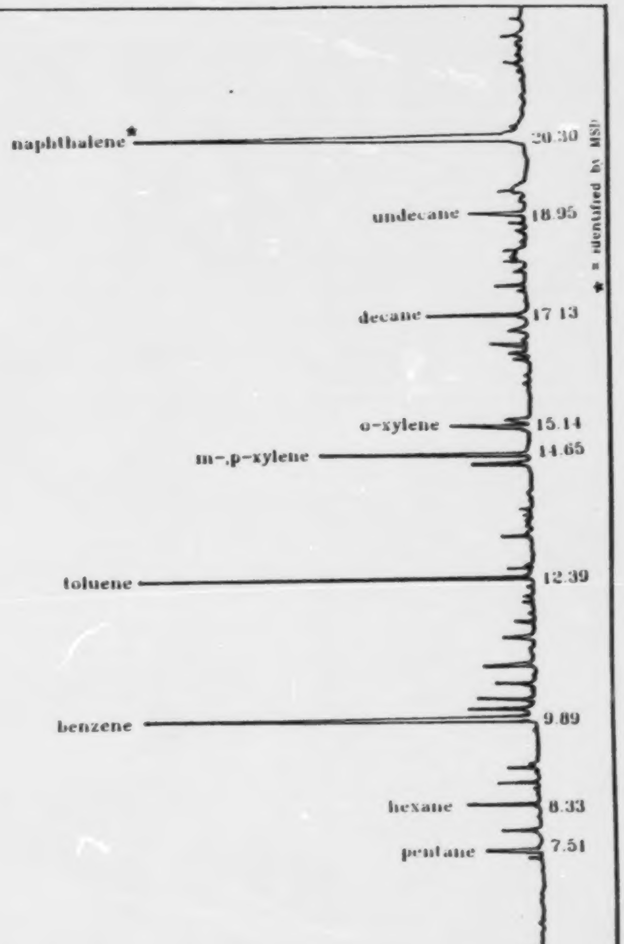

* = identified by MSD

Figure 11: SPECIATION OF DIMETHYL BENZENE ISOMERS BY GC/MI/FTIR

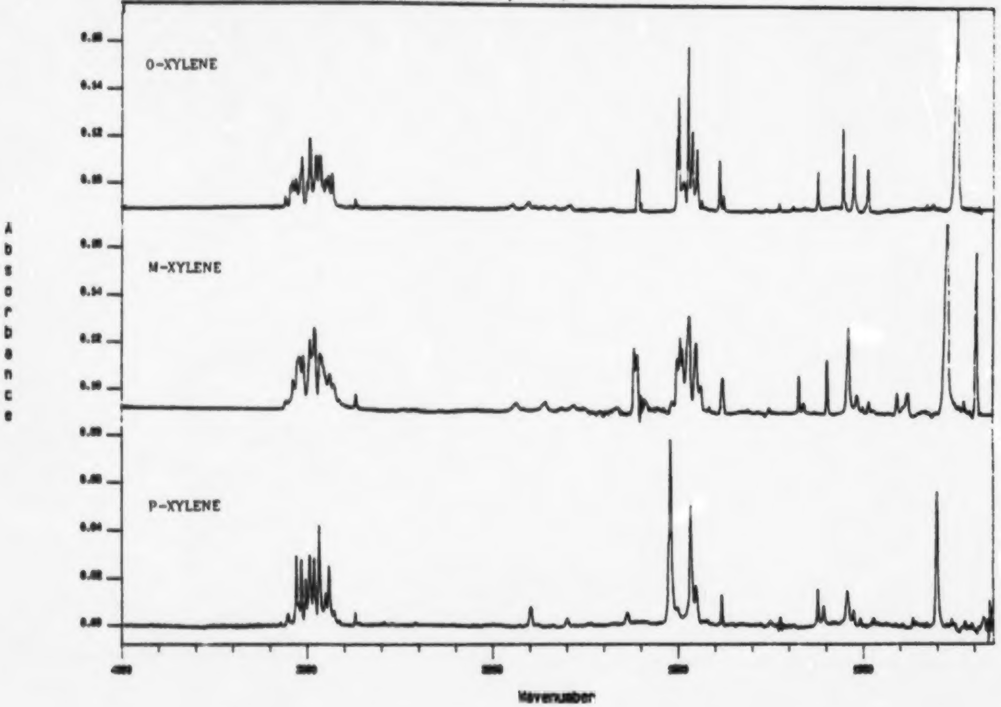

Figure 12: SPECTRAL DECONVOLUTION OF MERGING COMPOUNDS BY GC/MI/FTIR

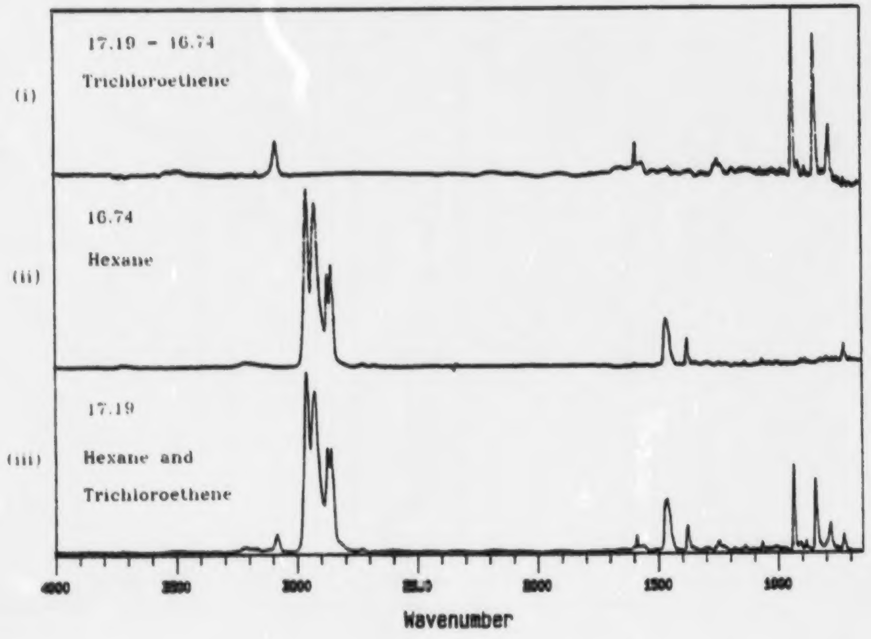

Figure 13:

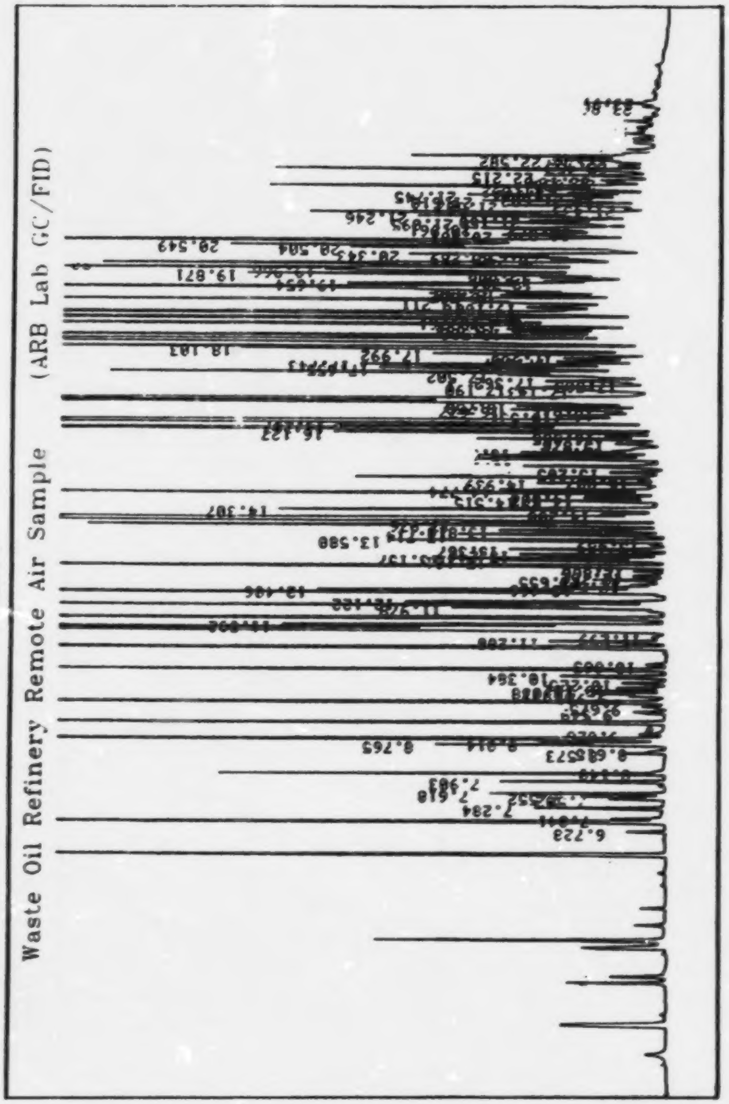
Waste Oil Refinery Remote Air Sample (ARB Lab GC/FID)

A17

ATMOSPHERIC TRACE GAS MEASUREMENTS
USING A
TUNABLE DIODE LASER ABSORPTION SPECTROMETER

D. R. HASTIE and H. I. SCHIFF

Chemistry Department
and
Centre for Atmospheric Chemistry
York University

INTRODUCTION

A knowledge of the detailed oxidation mechanisms operating in the atmosphere is essential if we are ever going to be able to control the atmospheric environment. We currently have a fair understanding of the major processes responsible for turning the reduced gases such as NO, NO_2, CS_2, H_2S, DMS (CH_3SCH_3), CH_4 and higher hydrocarbons into the thermodynamically favoured forms in the atmosphere NO_3, $SO_4^=$ and CO_2.

Oxidation is the dominant chemical process occurring in the atmosphere but very few gases actually react directly with oxygen. Most oxidation is performed by other more reactive oxidants. The oxidation cycle for most gases starts with NO_2 photolysis to yield an oxygen atom which in turn makes ozone.

$$NO_2 + h\nu \dashrightarrow NO + O(^3P)$$

$$O(^3P) + O_2 + M \dashrightarrow O_3 + M$$

These two reactions are the only tropospheric source of ozone. The most likely fate of the ozone is reaction with NO to regenerate the NO_2.

$$NO + O_3 \dashrightarrow NO_2 + O_2$$

The result of these three reactions is to produce a small steady state concentration of ozone, but to prevent high concentrations of ozone from being generated. While ozone can oxidize unsaturated hydrocarbons, it cannot oxidize most other atmospheric species. More reactive radical species are necessary. These come from ozone photolysis which occurs slowly at wavelengths less than 320nm (τ > 400 mins at mid latitudes) to give an excited oxygen atom.

$$O_3 + h\nu \dashrightarrow O(^1D) + O_2$$

This oxygen atom will generally collisionally deactivate to the ground state $O(^3P)$ atom and regenerate the ozone. However it may encounter a water molecule in which case it will react to produce two hydroxyl radicals.

$$O(^1D) + H_2O \longrightarrow 2HO.$$

The hydroxyl radical is believed to be the key to atmospheric oxidation. It is a very strong oxidant capable of reacting with almost all the species known to be emitted into the atmosphere. For example hydroxyl radicals initiate methane oxidation, the major reaction pathways being:

$$\begin{aligned} HO + CH_4 &\longrightarrow CH_3 + H_2O \\ CH_3 + O_2 + M &\longrightarrow CH_3O_2 + M \\ CH_3O_2 + NO &\longrightarrow CH_3O + NO_2 \\ CH_3O + O_2 &\longrightarrow CH_2O + HO_2 \\ HO_2 + NO &\longrightarrow HO + NO_2 \end{aligned}$$

The formaldehyde (CH_2O) produced will react further with HO or will photolyse and be further oxidized to CO and CO_2. This is a simplified mechanism for the simplist hydrocarbon, the full methane mechanism and the mechanisms for higher hydrocarbons are obviously more complex. It does, however, illustrate a number of points. Firstly the HO radical is essential to the oxidation. Secondly NO also gets oxidized to NO_2 in the cycle, this can then photolyse to generate additional ozone. Thirdly the hydroxyl radical is regenerated so that the oxidation is NO catalysed. Thus the production of HO and the balance between HO and HO_2 radicals are determined by the nitrogen oxides and the hydrocarbon.

This interwoven chemical picture continues when we look at the removal of species from the atmosphere. Take for example the removal of NO_2 and hydroxyl radicals. The major loss process for both species, in areas with sufficient nitrogen oxides, is through oxidation of NO_2 to HNO_3

$$HO + NO_2 + M \; -\!\!> HNO_3 + M$$

with subsequent physical deposition.

Thus the nitrogen oxides and hydrocarbons are involved in both the production and loss of oxidants in the atmosphere. The complexities of the chemistry mean that the oxidizing capacity of the atmosphere is highly dependent on local atmospheric composition. The local composition depends on the amount of material being emitted into the atmosphere from local sources, the amount being transported in from other regions, which is a function of the meteorology, as well as the local chemistry.

Due to the complex chemistry and the importance of meteorology the only way to really tell if we understand the atmosphere is to develop computer models of the processes. This involves combining the three disciplines of laboratory kinetic studies, field measurements, and computer modelling. A model will consist of a chemical mechanism of a number of chemical reactions each of which has (hopefully) a measured rate coefficient and product distribution. It will include some air motion consistent with the application under study, which could be anything from none at all to the best meteorology available,and will require some input parameters such as trace gas concentrations, which come from field measurements. This model is then run and made to predict the atmospheric composition at some future time. The model is tested by comparing these predictions against a second set of field measurements, or against a data set that was not used as an input to the model. While a model may, in its simplist case, be a few reactions written on a piece of paper it is clear from the discussion of the chemistry and meteorology above that models quickly become too large to handle in this way and so must be computerized.

Before we can use a model in a predictive mode, i.e. to examine the chemistry in an unstudied or as yet non-existing system, the model must be shown to be capable of giving an accurate picture of the current atmosphere from a knowledge of the basic science.

The Ministry of the Environment, the Atmospheric Environment Service of Environment Canada, the Electric Power Research Institute (EPRI), and Umweltbundesamt (West Germany) are supporting the development of the Acid Deposition and Oxidant Model (ADOM). This is a state-of-the-science Eulerian model designed to study the chemistry of acid rain and oxidant formation over North Eastern North America. It divides the area into 100km square blocks and includes the best available three dimensional meteorology, our best knowledge of sources of gases to the atmosphere, the most complete gas and aqueous phase chemistry possible, and our best measurements of trace gas concentations and has a resolution of approximately 100km. A second similar model, RADM (the Regional Acid Deposition Model) has been developed at the National Center for Atmospheric Research for the U.S. Environmental Protection Agency (EPA). Both models are now available.

Recognising the importance of the predictions of these models it was thought neccessary to evaluate the models to establish their credibility by comparison with observation. Consequently the Eulerian Model Evaluation field study was planned. This aimed to gather sufficient field data to be able to allow a full evaluation of these models.

The first stage of this study was undertaken in the summer of 1988. The Canadian component of this study involved data collection from the MOE-APIOS and AES CAPMoN networks. In addition two sites were designated as intensive or enhanced sites. These were the AES site at Egbert, (near Barrie) and the MOE site at Dorset. The purpose of these sites was to obtain data using enhanced techniques that required operation by specially trained scientific personnel or at a frequency not possible under normal operating conditions.

While the field study was put in place for the model evaluation it became clear that the data obtained, especially that from the enhanced sites, could be used to address a number of additional issues. The Canadian Institute for Research in Atmospheric Chemistry (CIRAC) took the lead in the co ordination of the Canadian Air Chemistry Experiment which aimed to ensure the collection of a complete data-set capable of addressing some specific atmospheric chemistry questions. Potentially the most important idea was that the two enhanced sites (Egbert and Dorset) could be used as sampling points on a "flow reactor" to investigate some sub eulerian scale processes that are critically important for Ontario.

Both the Canadian Air Chemistry Experiment and the Eulerian Model Evaluation field study required the measurement of the concentration of short lifetime species. Two particularly important species are H_2O_2 and CH_2O.

Formaldehyde is an produced in the oxidation of all hydrocarbons, in a similar manner to the methane oxidation above. It is also removed rapidly by reaction making it a relatively short lived intermediate whose concentration depends critically on that of a number of other species. Predictions of its behaviour by models will be very sensitive to the chemistry used and so comparing measured formaldehyde concentrations with model predictions will be a very good test of the model.

Hydrogen peroxide is produced in the atmosphere by the combination of hydroperoxy radicals.

$$HO_2 + HO_2 \rightarrow H_2O_2 + O_2$$

Thus it is highly dependent on the HO_2 concentration which is very dependent on the details of the nitrogen oxide initiated hydrocarbon oxidation occurring at that point. Thus it, like formaldehyde, would be a good test of the model. Forcing the model to predict both species would be an even more stringent test especially if ozone and nitrogen oxide concentrations were measured simultaneously.

In addition to the need for these species for the model evaluation, they are also key species in atmospheric oxidation and other processes in which the Canadian Air Chemistry Study was interested.

We undertook to measure CH_2O and H_2O_2 at the Dorset site.

The measurement of these species is particularly difficult. The combination of their high reactivity and the time resolution constraints on the measurements, precluded the use of grab or integrated sampling techniques. The only instrument capable of measuring both species which is suitable for this study is the Tunable Diode Laser Absorption Spectrometer (TDLAS).

A TDLAS measures the absorption of infrared radiation, emitted by a tunable diode laser, by a single rotational vibrational line in the infrared spectrum of a single species at low pressure. The narrow linewidths of the laser and the absorption feature ensure that only a single species is being measured. By using a frequency modulated laser, suitable demodulation and computerized data aquisition and analysis, absorptances of 5×10^{-6} can be measured. Consequently a TDLAS incorporating a path length of 150 meters can be used to measure the concentrations of most gases at or below the 0.5 ppbv level. As the residence time in the instrument is only a few seconds relatively reactive species such as those already mentioned can be measured.

The only condition on the use of the technique are that it be possible to get the trace gas into a cell at reduced pressure and that the molecule have a resolved rotational fine structure. This is true for both the target molecules.

THE FIELD MISSION

A trailer housing the TDLAS and some other supporting instrumentation was transported to the Dorset site on July 5. The TDLAS system was new and had only been tested at the component level, having never been used for trace gas measurements prior to transportation to Dorset. Table 1 summarizes the data collected by the York group from July 11 to August 31. In addition to the continuous monitors we took 3 grab samples per day for hydrocarbon analyses by a number of other groups and a number of integrated aldehyde samples for analysis by another York group. The supporting measurements NO, NO_x, NO_2, O_3, and the met parameters were given a lower priority than the TDLAS measurements as these parameters were being measured for the Evaluation Study by MOE, using their network instrumentation adjacent to our trailer.

Clearly there is a large amount of data. While the TDLAS gives preliminary data on site, the data requires reanalysis after the field study to fully utilise the sensitivity of the technique. This reanalysis is proceeding.

PRELIMINARY RESULTS

Only a small amount of data has been fully analysed but we can give an example of some potentially interesting data. Figure 1 shows the preliminary formaldehyde, ozone and temperature data for August 5. The most obvious feature is the strong diurnal variation in all three parameters. Note also that ozone exceeds 80 ppbv for a total of 4 hours during the day. The fast rise in ozone from 30 ppbv at 0800 to 60 ppbv 1 hr and the corresponding formaldehyde increase from 2.5 to 5 ppbv appear too fast to be the result of chemistry. Similarly the precipitous decrease in ozone at around 2000 must be due to other than chemical effects. At first glance it appears as if a nighttime inversion was set up on both nights. The air trapped below the inversion is depositing most of the ozone and formaldehyde to the surface, thus lowering the ambient concentration. In the morning the air aloft, which has been isolated from the ground and so still contains the previous days concentrations of ozone and formaldehyde, is brought down as the inversion breaks up thus increasing the surface concentrations.

This data is strongly influenced by this local effect which is on too small a scale for the either the Eulerian Model or the Canadian Air Chemistry Study. Thus care must be taken in presenting the data so as not to attempt to force the models to predict conditions for which they were not designed.

TABLE 1
DATA COVERAGE FROM DORSET FIELD STUDY
(in hours and minutes)

DATE	CH2O	H2O2	NO	NO2	NOx	O3	CO	Radiation	MET
July 11	7								
July 12	14								
July 13	17								
July 14	12	4							
July 15	8	9							
July 16		6							
July 17		6							
July 18	3	2			all day	all day		all day	all day
July 19		10			all day	all day		all day	all day
July 20		11			12:10	17:30		17:30	17:30
July 21					all day	all day		all day	all day
July 22					13:00	all day		all day	all day
July 23					20:40	13:20	04:40	all day	all day
July 24	12	6			21:40	all day	all day	all day	all day
July 25	13	21			22:00	22:00	22:00	19:50	19:50
July 26	18	18			all day	all day	all day	all day	all day
July 27	24	24			15:50	10:50	10:50	10:50	10:50
July 28	23	23			16:10	10:00	10:00	10:00	10:00
July 29	24	24			19:20	22:50	22:50	22:50	22:50
July 30	21	21			13:30	22:20	22:20	22:20	22:20
July 31	23	23			17:50	17:50	17:50	17:50	17:50
August 1	23	23			20:20	23:30	23:30	23:30	23:30
August 2	17	17			13:50	13:40	13:40	13:40	13:40
August 3	13	13		04:30	21:30	22:50	22:50	22:50	22:50
August 4	24	24		all day	all day	21:00	all day	all day	all day
August 5	20	20		22:30	22:30	all day	all day	all day	all day
August 6	24	24		22:30	22:30	all day	23:10	all day	all day
August 7	22	22		22:20	22:20	23:10	23:10	23:10	23:30
August 8	18	19		22:30	22:30	all day	all day	all day	all day
August 9	23	10		22:20	22:30	all day	all day	all day	all day
August 10	24			21:00	21:00	all day	all day	all day	all day
August 11	24			22:50	22:50	all day	all day	20:40	all day
August 12	11			all day	all day	all day	all day		all day
August 13	11	11		all day	all day	all day	all day	12:30	all day
August 14	24	24		19:10	19:10	all day	all day	all day	all day
August 15	12	22		21:40	21:40	all day	all day	all day	all day
August 16	24	24		19:30	20:00		23:15	23:15	23:15
August 17	10	10		22:15	22:15		23:20	all day	all day
August 18	21	21		18:30	18:30		22:40	22:40	22:40
August 19	12	21		18:20	18:20		22:40	22:40	22:40
August 20	24	24		22:30	22:30		22:30	22:30	22:30
August 21	21	21		21:40	21:40		all day	all day	all day
August 22	22	22		all day	all day		all day	all day	all day
August 23	20	18		all day	all day		all day	all day	all day
August 24	19	17		19:40	19:40	11:20	23:20	23:20	23:20
August 25	6	15		19:20	19:20	19:20	19:20	19:20	19:20
August 26	23	23	05:00	all day	all day	all day	all day	all day	all day
August 27	24	24	all day	all day	all day	all day	all day	all day	all day
August 28	21	21	20:00	20:00	20:00	all day	all day	all day	all day
August 29	24	24	23:30	23:30	23:30	23:30	23:30	23:30	23:30
August 30	20	20	23:00	23:00	23:00	all day	all day	all day	all day
August 31	18	24	01:10	01:10	01:10	01:10	01:10	01:10	01:10

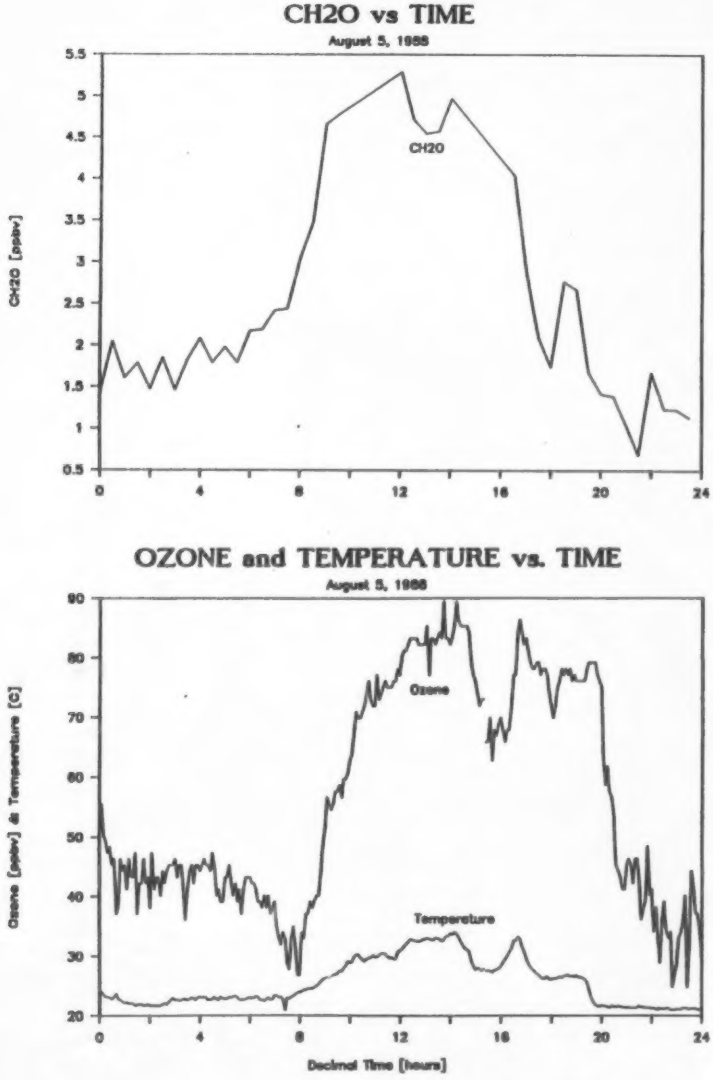
CH2O vs TIME
August 5, 1988
CH2O [ppbv]
5.5
5
4.5
4
3.5
3
2.5
2
1.5
1
0.5
CH2O
0
4
8
12
16
20
24
OZONE and TEMPERATURE vs. TIME
August 5, 1988
Ozone [ppbv] & Temperature [C]
90
80
70
60
50
40
30
20
Ozone
Temperature
0
4
8
12
16
20
24
Decimal Time [hours]

FIGURE I

A19

A STUDY OF HIGH TEMPERATURE PHOTOCHEMICAL KINETICS OF SULPHUR DIOXIDE AND NITROGEN OXIDES FOR A FLUE GAS TREATMENT PROCESS. J.E. Hunt*, P. Fellin, K.A. Brice, D.L. Ernst, D.R. Glendenning, R.B. Caton, C.S. Fung, K. Smith, Concord Scientific Corporation, Toronto, Ontario, M3H 2V2

MANUSCRIPT NOT AVAILABLE

A20

Modelling the Photochemical Decomposition of Chlorinated Phenols by Sunlight

Nigel J. Bunce and Jamie S. Nakai

Guelph-Waterloo Centre for Graduate Work in Chemistry
Department of Chemistry and Biochemistry
University of Guelph
Guelph, Ontario, Canada. N1G 2W1

Abstract

The quantum yields for the photodegradation of a series of chlorophenols have been measured, and used to estimate their rates of solar photodegradation in the atmosphere. These rates have been compared with the calculated rates of attack by atmospheric hydroxyl radicals upon chlorinated phenols. The two processes are rather complementary, with photolysis being fastest for pentachlorophenol, and OH attack being fastest for monochlorinated phenols. As a result, it is predicted that most chlorophenol congeners will have atmospheric half-lives of no more than one week.

Introduction

The chlorinated phenols comprise a group of 19 congeners, consisting of mono-, di-, tri-, and tetrachlorophenols, and pentachlorophenol. All are crystalline solids at room temperature, with the exception of 2-chlorophenol, which is a liquid. They were first synthesized in the 19th century, and interest in them arose mainly because of their antiseptic properties [1,2]. Since the 1930s, chlorophenols have been used as fungicides, herbicides, and insecticides, and as chemical intermediates. Their annual wordwide production (1978) was estimated to be 200,000 tonnes, pentachlorophenol (PCP) representing approximately 90,000 tonnes of the total [1,3].

Most environmental contamination by chlorophenols is a result of the use of PCP as a wood preservative [1,4]. For example, an estimated 1,900 tonnes of PCP was used in Canada in 1976 [5], wood preservation accounting for approximately 95% of the total. PCP and its derivatives can also function as fungicides, bactericides, and insecticides [2,3,6]. Swedish pulp and paper mill plants have employed PCP as a slimicide. However, this use was discontinued in the 1970s because of its toxic effects on aquatic species [7,8].

Environmental residues of PCP not only result from its direct use, but also accumulate through degradation of related chemicals such as hexachlorobenzene and pentachlorobenzene [9,10]. Wood preservation sites and PCP production plants act as point sources of environmental contamination; leaching from treated lumber and breakdown of related chemicals are non-point sources [11].

The use of 2,4-dichlorophenol (2,4-DCP) has been almost exclusively for agricultural products. It is a precursor for the production of the herbicide 2,4-dichlorophenoxyacetic acid (2,4-D) and its derivatives, which have been employed as herbicides and bactericides, and methylated chlorophenols, which are used for moth-proofing, disinfectants, and antiseptics. Likewise, 2,4,5-trichlorophenol has been used mostly in the production of hexachlorophene and the herbicide 2,4,5-T. Point sources of 2,4-DCP are 2,4-DCP and 2,4-D production plants; waste water effluents from 2,4-D manufacturing plants can contain as much as 125μg/L of 2,4-DCP [2]. Non-point sources of environmental contamination by 2,4-DCP include agricultural runoff; 2,4-D and related herbicides degrade back to the parent chlorophenol both microbially and photochemically [12-15].

Another source of environmental contamination by chlorophenols is through the chlorination of drinking water and industrial and municipal waste waters for disinfection. This results in spontaneous halogenation of phenols present in these waters [1,2,16]. This process occurs principally at the 2, 4, and 6 positions affording 2,4-dichlorophenol (45%), trichlorophenols (40-50%), and monochlorophenols (4-10%) [2].

Chlorinated phenols enter into the environment through four main pathways: by direct application, accidental spillage, industrial wastes, and through transformation of other compounds. Once in the environment, they can circulate between air, land, and water.

Although they are normally considered water and soil contaminants, chlorophenols possess moderate volatility. Reported vapour pressures range from 1 mm at 12°C for 2-chlorophenol to 1 mm at 100°C for 2,3,4,6-tetrachlorophenol (Table

I)[16]. These compounds may therefore volatilize, but they never reach their equilibrium vapor pressures since the atmosphere provides a reservoir which is impossible to saturate.

Volatilization is considered an important mechanism for removal of pesticides (and presumably chlorophenols) from soil[6,17]. This notion is consistent with data for other chlorinated aromatics such as PCBs, which are even less volatile than chlorophenols. An estimated 900 tonnes of PCBs circulate through the air above the United States each year[18], the main source being volatilization, principally from landfills[18,19]. Although PCP is one of the least volatile of the chlorophenols, volatilization is an important source of loss from pentachlorophenol-treated materials. For example, 30-80% of PCP from dip- or brush-treated coniferous wood may by lost by volatilization within 12 months[3].

A limited number of measurements of atmospheric PCP loadings have been made. For example, the atmosphere of a rural mountain region in Bolivia was to found contain 0.25-0.93 ng PCP/m^3, whereas an urban area in Belgium was contaminated by 5.7-7.8 ng PCP/m^3[3]. Similar concentrations of PCP were detected in Switzerland; levels ranged between 0.9 - 5.1 ng/m^3[3]. In general, the level of chlorinated phenols in ambient air has not been well monitored.

Relatively little is known regarding volatilization of chloroaromatics from water. For many PCB congeners, volatilization from Lake Superior was found to be a more important loss process than sedimentation[20]. Only the un-ionized form of chlorophenols (Table I) is volatile; evaporation of PCP from surface waters above pH 6 should be quite low[21], but may be significant for other congeners. Disposal of PCP contaminated waste water from wood preservation sites is sometimes handled by allowing the water to evaporate[3], a practice which obviously contributes to PCP air pollution.

Once a chemical enters the atmosphere, wind transport can carry it a long distance before eventual deposition. For example, PCBs have been detected in Antarctic snow, far from any industrial activity[22]. Atmospheric deposition of PCBs has been recognized recently as a major source of contamination into the Great Lakes basin[20,23]. Aerial transport of chlorophenols occurs year-round;

measurable quantities of chlorophenols have been detected in rain in Portland, Ore. [23], and in snow samples in Ontario [5].

The objectives of the present work are to assess the importance of photochemical transformation of chlorinated phenols in the atmosphere under the influence of sunlight. Chlorophenols absorb in the deep ultraviolet, but there is some overlap between their absorption spectra and the spectrum of sunlight in the troposphere. Consequently, their degradation by sunlight is possible in principle. Our approach to the problem is first to measure in the laboratory the quantum yields for decomposition of representative chlorophenols. The quantum yield is the efficiency of the decomposition process once light has been absorbed. By combining the chlorophenol quantum yield and absorption spectrum with the solar intensity, we are able to calculate the rate of decomposition in the troposphere. Finally, we compare the estimated rate of photolysis with the rate of reaction of the chlorophenols with hydroxyl radicals, the other principal reaction channel.

Results and Discussion

Quantum Yields[25]

Quantum yields for vapour phase photodecomposition were measured at 254 nm for a representative series of chlorinated phenols (Table I). Each value is the average of at least five replicates.

Table I. Physical properties and quantum yield data for chlorophenols

Chlorophenol Congener	Temp, °C 1mm pressure	pKa	ϕ
2-Cl	12	8.49	0.45 ± 0.07
3-Cl	44	8.85	0.18 ± 0.05
4-Cl	50	9.18	0.12 ± 0.03
2,4-Cl_2	53	7.68	0.064 ± 0.02
3,4-Cl_2	–	7.39	0.16 ± 0.05
2,4,5-Cl_3	100	7.43	0.097 ± 0.02
Cl_5	–	4.92	0.018 ± 0.007

As in our previous work on chlorinated benzenes and biphenyls, we concluded that the measured quantum yields were independent of size of the reaction flask (Table II), and hence that surface effects were not of major importance [26].

Table II. Photodecomposition of 2-chlorophenol at 254 nm in various round bottom flasks.

Moles of 2-Chlorophenol decomposed x 10^6

Volume	250 ml	500 ml	1000 ml	2000 ml
	0..68	0.52	0.64	0.60
	0..51	0.77	0.64	0.66
	0..60	-	-	-
Ave ± S.D.	0..60 ± 0.12	0.65 ± 0.18	0.64	0.63 ± 0.04

The quantum yields are relatively high and are comparable in magnitude with those of the chlorobenzenes and chlorobiphenyls [27]. They show a trend towards decreasing as the number of chlorine substituents on the aromatic ring increases. This phenomenon may be explained partially by the fact that chlorine is considered a "heavy atom" which increases spin orbital coupling, facilitating intersystem crossing. This is important in that most reported photochemistry of chloroaromatics occurs from the lowest excited triplet state because of the relatively long life of the triplet compared with the corresponding singlet state.

This increase in intersystem crossing rates affects both the rate at which the lowest triplet state is populated, and the rate at which it decays to the ground state. In addition, since a chlorine atom replaces hydrogen on the ring, vibrational energy levels become more closely spaced and as a result, energy dissipation and a return to the ground state are facilitated. A decrease in the quantum yield for photodecomposition with increased chlorine substitution is therefore understandable in terms of the rates of these photophysical processes.

The low-pressure, mercury arc lamp used in these experiments had a maximum output at 254 nm, a wavelength not available in the troposphere. We decided against using a source having an emission at wavelengths more relevant environmentally (i.e. >300 nm) because at these wavelengths the chlorophenols absorb only a very small fraction of the total light output. In our experiments, the amount of light absorbed by the sample is determined by the difference between the lamp output and the photons transmitted through the sample. If the fraction of photons transmitted is very large (i.e., very little light is absorbed), all the precision in measuring the amount of light absorbed is lost. At 254 nm the chlorophenols absorb more strongly so that a larger proportion of the total photon output is absorbed.

We note from Table I that the standard error associated with each quantum yield is quite high (approximately 20%). This is because the experimental protocol requires that a relatively large number of experimental measurements be made to extract even one quantum yield value. These measurements are: the quantity of test compound before and after photolysis, the actinometer blank, and two separate actinometer measurements. Small experimental errors associated with each of these are propagated into a much larger error. Although substantial, the uncertainties are not out-of-line with those associated with other reported quantum yields. For example, in the gas phase photolysis of perfluoroglutaric anhydride $\phi = 0.34 \pm 0.07$ at 254 nm [28] and for 3-chloro-3-methyldiazirine $\phi = 0.87 \pm 0.13$ at 313 nm [29], comparable uncertainties of 21% and 15%, respectively.

Rates of Environmental Vapour Phase Photolysis

The key question to be addressed is, "Does photodegradation occur at a rate which is environmentally significant?" Four relevant points must be considered for an environmental vapour phase photolysis [47].

1. Solar spectrum and intensity in the troposphere
2. Pollutant absorption spectrum
3. Pollutant ambient concentration in the atmosphere
4. Pollutant quantum yield

Atmospherically, most chlorinated aromatics are found only in the troposphere. Their tropospheric half-lives are relatively short, and so they do not rise into the stratosphere. Natural sunlight in the troposphere is composed of radiation with wavelengths greater than approximately 290 nm because the short wavelength, high energy radiation of the solar spectrum is absorbed in the upper atmosphere by molecules such as oxygen and ozone. Data regarding the solar spectrum and intensity in the troposphere are available in the literature [48].

The pollutant absorption spectrum is the second point which must be considered. Most chlorinated aromatics, including the chlorophenols, tend to absorb in the deep UV region where the tropospheric solar spectrum is either very weak or nonexistent. For an environmentally significant photoreaction to occur, the pollutant absorption spectrum must overlap, at least partially, with the tropospheric solar spectrum. If this condition is not satisfied, a photoreaction cannot take place since no light will be absorbed by the compound. Therefore, to determine the rate of environmental photodecomposition of chlorophenols, it is necessary to measure their absorption spectra in the region of the tropospheric solar spectrum. In this work, the pollutant absorption spectrum was obtained experimentally. Although we were interested in vapour phase reactions, measurement of ε for a compound in the vapour phase is a non-trivial task because of the difficulty in calculating vapour phase concentrations. Therefore, ε was calculated in cyclohexane solution as a model for the vapour phase (see example, Table III).

Pollutant ambient concentration in the troposphere is the third point to consider. Since the rate of photoreaction depends on the pollutant concentration, the total amount of pollutant undergoing reaction is also concentration dependent. Ambient pollutant levels may or may not be available in the literature; as we have already noted, the chlorophenols in general have not been well monitored. Nevertheless photochemical half lives can still be calculated as demonstrated below.

The final point to consider is the pollutant quantum yield for photodegradation. The quantum yield (ϕ) is a measure of the photoefficiency of a process. It represents the fraction of all photons absorbed by the reactant which causes a particular photoreaction to occur. The quantum yields for photodegradation are determined experimentally, as already described.

These four points are now combined to determine the rate of direct solar degradation in the vapour phase.

From Beer's Law of light absorption, we derive equation [1]:

$$I_{trans}/I_0 = 1 - I_{abs}/I_0 = 10^{-\varepsilon cl}$$

$$I_{abs}/I_0 = 1 - 10^{-\varepsilon cl} = 1 - e^{-2.303\varepsilon cl} \qquad [1]$$

Here, I_0 is the incident light intensity, I_{abs} and I_{trans} represent the light

Table III. Molar absorptivity of 3-chlorophenol in cyclohexane.

Wave-length	Absorb 1*	$\varepsilon1$ ($cm^{-1}M^{-1}$)	Absorb 2†	$\varepsilon2$ ($cm^{-1}M^{-1}$)	ε_{ave} ($cm^{-1}M^{-1}$)
290	0.030	81	0.726	79	80
291	0.026	71	0.617	67	69
292	0.020	54	0.483	53	54
293	0.016	43	0.391	42	43
294	0.013	35	0.321	35	35
295	0.011	30	0.276	30	30
296	0.011	30	0.240	26	28
297	0.010	27	0.209	23	25
298	0.009	24	0.184	20	22
299	0.008	22	0.162	18	20
300	0.006	16	0.142	15	16
301	0.005	14	0.124	13	14
302	0.005	14	0.106	12	13
303	0.004	11	0.091	10	11
304	0.004	11	0.077	8	10
305	0.003	8	0.066	7	8
306	0.003	8	0.055	6	7
307	0.002	5	0.047	5	5
308	0.002	5	0.040	4	5
309	0.002	5	0.034	4	5
310	0.002	5	0.029	3	4
311	0.001	3	0.026	3	3
312	0.001	3	0.023	2	3
313	0.001	3	0.022	2	3
314	0.001	3	0.020	2	3
315	0.001	3	0.019	2	3
320	0.002	5	0.018	2	4
325	0.002	5	0.020	2	4
330	0.001	3	0.022	2	3
340	0.001	3	0.023	2	3
350	0.001	3	0.021	2	3

* 3.684×10^{-4} M in cyclohexane

† 9.210×10^{-3} M in cyclohexane

intensity absorbed and transmitted, respectively, by a depth l of the atmosphere, while ε and c are the molar absorptivity and concentration of the compound respectively.

For small values of absorbance, the expansion of $e^{-2.303\varepsilon cl}$ can be truncated at the first term.

$$\text{i.e.} \qquad e^{-2.303\varepsilon cl} = 1 - 2.303\varepsilon cl$$

$$I_{abs}/I_o = 2.303\varepsilon cl$$

$$I_{abs} = 2.303\varepsilon clI_o \qquad [2]$$

Equation [2] is valid only at a single wavelength, since both the molar absorptivity and the solar spectrum are highly wavelength dependent. The amount of light absorbed is therefore the total of $I_{abs,\lambda}$ summed over all relevant wavelengths i.e. where both solar intensity and pollutant absorption are significant.

From the definition of the quantum yield, we obtain [3].

$$\begin{array}{c}\text{conc. pollutant reacted}\\ \text{per unit time}\end{array} = \phi \cdot \begin{array}{c}\text{conc. photons absorbed}\\ \text{per unit time}\end{array}$$

$$= \phi \cdot \sum I_{abs,\lambda} \qquad [3]$$

We assume that ϕ is independent of wavelength, since all the photochemistry involves the same absorption band of the chlorophenol compound. When ε in the conventional units of $cm^{-1} \cdot M^{-1}$ is changed to ε' in $dm^{-1} \cdot M^{-1}$ ($= dm^2 \cdot mol^{-1}$), we obtain [4], where the product $\sum \varepsilon'_\lambda \cdot (I_o)_\lambda$ has units of $time^{-1}$ when $(I_o)_\lambda$ has units moles per unit area per unit time, and l = 1 dm.

$$\text{conc.pollutant reacted/time} = 2.303\phi cl \sum \varepsilon'_\lambda \cdot (I_o)_\lambda \qquad [4]$$

If percent decomposition of reactant per unit time is required, then equation [5] may be applied.

$$\text{\% substrate reacted per unit time} = 230.3\phi \sum \varepsilon'_{\lambda} \cdot (I_0)_{\lambda} \qquad [5]$$

Note that in equation [5], pollutant concentration is not required for the calculation. This is useful in cases such as the present where atmospheric ambient concentrations are not available in the literature.

By the use of the foregoing approach we have calculated the percentage of pollutant reacted per hour by environmental solar degradation for a series of chlorophenols. A sample calculation for the case of 3-chlorophenol is given in Table IV.

Table IV. Solar degradation calculation for 3-chlorophenol.

Midday summer solar values, 40°N latitude under clear skies

Wavelength Range (nm)	Intensity Photons/cm^2/s	Molar Absorptivity (l/mol/cm)	I x ε hr^{-1}	Σ(Ixε) hr^{-1}
295-297.5	6.48 x 10^{11}	22	8.52 x 10^{-8}	8.52 x 10^{-8}
297.5-300	2.19 x 10^{12}	20	2.61 x 10^{-7}	3.47 x 10^{-7}
300-302.5	6.57 x 10^{12}	11	4.32 x 10^{-7}	7.79 x 10^{-7}
302.5-305	1.63 x 10^{13}	10	1.64 x 10^{-6}	2.42 x 10^{-6}
305-307.5	2.74 x 10^{13}	5	1.33 x 10^{-6}	3.74 x 10^{-6}
307.5-310	4.44 x 10^{13}	5	1.92 x 10^{-6}	5.67 x 10^{-6}
310-312.5	6.43 x 10^{13}	3	1.50 x 10^{-6}	7.16 x 10^{-6}
312.5-315	8.36 x 10^{13}	3	1.85 x 10^{-6}	9.01 x 10^{-6}
315-317.5	1.03 x 10^{14}	3	2.17 x 10^{-6}	1.11 x 10^{-5}
317.5-320	1.21 x 10^{14}	4	1.82 x 10^{-5}	2.94 x 10^{-5}
320-330	7.62 x 10^{14}	4	2.09 x 10^{-5}	5.03 x 10^{-5}
330-340	8.75 x 10^{14}	3	1.68 x 10^{-5}	6.71 x 10^{-5}
340-350	9.38 x 10^{14}	3	1.79 x 10^{-5}	8.51 x 10^{-5}
350-360	1.00 x 10^{15}			8.51 x 10^{-5}

$\sum(I \times \varepsilon) = 8.51 \times 10^{-5}\ \mathrm{hr}^{-1}$; % Reacted per hour = 3.5 %

From these data, it is also possible, in principle, to calculate the half-life for direct solar degradation. For a first order process, $t_{1/2} = (\ln 2/k)$, where k is the first order rate constant. Therefore, if x is the percentage decomposition per hour, then the half-life is calculated through equation [6].

$$\ln (100 / (100-x)) = k \cdot 1hr$$

$$t_{1/2} = 1hr.\ln 2 / \ln (100/100-x) \qquad [6]$$

The calculated rates of environmental photolysis, together with some calculated photolytic half-lives, are given in Table V.

Table V. Summary of rates for photolytic degradation and hydroxyl radical attack upon chlorophenols.

Chloro-Phenol Congener	ϕ	Photochemical		OH Attack			
		% per h[a]	"$t_{1/2}$"[b]	$k \times 10^{11}$[c]	% per h[d]	"$t_{1/2}$"[e]	rate hν[f] / rate OH
2-Cl	0.45	0.024	4 months	1.3	41	1.7 hours	6×10^{-4}
3-Cl	0.18	3.5	1 day	3.2	99	0.7 hours	4×10^{-2}
4-Cl	0.12	0.022	4 months	1.3	41	1.7 hours	5×10^{-4}
2,4-Cl_2	0.064	0.11	1 month	0.35	11	6 hours	1×10^{-2}
3,4-Cl_2	0.16	6.5	10 hours	0.88	29	2 hours	0.2
2,4,5-Cl_3	0.097	2.3	30 hours	0.25	8	9 hours	0.3
Cl_5	0.018	6.2	11 hours	0.047	1.5	2 days	4

[a] Midday summer solar intensity, 40°N, ref. 30

[b] Assuming continuous noon time sunshine

[c] units cm^3 $molecule^{-1}$ s^{-1}

[d] Using peak noon time OH concentration of 8.7×10^6 OH radicals cm^{-3}, summer 48°N, ref. 40

[e] Assuming constant noon time OH concentration as (c)

[f] Ratio rate of noon time photolysis/rate of noon time OH attackfor pentachlorophenol, but the calculated percentage loss of PCP by environmental photodegradation is almost 260 times greater. This is solely the result of PCP's superior spectral overlap with the solar spectrum.

We note that the chlorophenol congeners with at least one chlorine in a 3-(meta) position are calculated to photolyze the fastest in the atmosphere. This is not because these congeners are intrinsically the most photolabile (highest quantum yields), but rather because there is better overlap between their absorption spectra and the tropospheric solar spectrum. This last factor more than compensates for their lower quantum yields. For example, the quantum yield for photodecomposition of 2-chlorophenol is approximately 25 times larger than that for pentachlorophenol, but the calculated percentage loss of PCP by environmental photodegradation is almost 260 times greater. This is solely the result of PCP's superior overlap with the solar spectrum.

The atmospheric photolytic half-lives are of more practical interest than percent decomposition per hour. They encompass a wide range; two orders of magnitude for the summer solar intensities, and three orders of magnitude for the winter values (not shown). However, these calculated half-lives considerably underestimate the true environmental values for the following reasons. 1) The quantum yields were measured at 254 nm, a wavelength not available tropospherically (tropospheric light has $\lambda > 290$ nm). We have assumed that quantum yields are independent of wavelength, but because short wavelength irradiation is inherently more energetic than long wavelength irradiation (from $E = hc/\lambda$), the measured quantum yields could be greater than those observed in the environment. 2) The solar fluxes used in the solar degradation calculation apply to clear skies at midday, 40° N latitude [19]. The calculated half-lives are strictly valid only under continuous illumination conditions as described. These conditions are subject to extreme fluctuation throughout the course of a day; for example, cloud cover attenuates the photon flux, as could smog in a heavily industrialized area. Averaged over a 24 hour period, and realizing that the shortest wavelengths are attenuated the most as the zenith angle increases away from midday, the actual atmospheric half-lives for photodegradation are much longer than the estimated minima. For example, a calculated half-life of one day may be more realistically estimated at approximately one week, while a calculated half-life of several months translates more realistically to several years.

Hydroxyl Radicals in Tropospheric Chemistry

Photodegradation is not the only loss process available to chlorinated phenols; hydroxyl radical attack is another important degradative mechanism for all chlorinated aromatics. Hydroxyl radical (OH) has been well established as playing a central role in the chemistry of both the natural and polluted troposphere [31,32].

The formation of OH radicals in the troposphere is mainly the result of the following series of reactions.

$O_3 + h\nu\ (\lambda < 320\ nm) \dashrightarrow O_2^* + O^*$

$O^* + H_2O \dashrightarrow 2\ OH$ (Major)

$O^* + R_3CH \dashrightarrow OH + R_3C$ (Minor)

Photolysis of HONO and H_2O_2 are minor sources of OH.

$HONO + h\nu\ (\lambda < 400nm) \dashrightarrow OH + NO$

$H_2O_2 + h\nu\ (\lambda < 360\ nm) \dashrightarrow 2OH$

Another important atmospheric source of OH is reaction of hydroperoxyl radicals (HO_2) with NO.

$HO_2 + NO \dashrightarrow OH + NO_2$

Rate constants for the reaction of OH with a number of compounds of atmospheric interest have been measured in the laboratory [32-36]. These biomolecular rate constants (k) may be used to calculate the atmospheric half-life of an organic compound with respect to OH reaction if the atmospheric OH concentration is known, i.e.,

$$t_{1/2} = \ln 2 / (k \cdot [OH])$$

where $(k \cdot [OH])$ is a pseudo first order rate constant.

These calculated half-lives strictly apply only instantaneously because the rate constant, k, is temperature dependent; temperature fluctuates diurnally and decreases with increasing altitude in the troposphere [36-37]. Also, the OH concentration varies diurnally, seasonally, altitudinally, and geographically [33]. A frequently-quoted estimate of the annually averaged 24 hour tropospheric OH radical concentration is ~$5\text{x}10^5$ molecules·cm^{-3} in the northern hemisphere [38].

Experimental observations of diurnal variations in the OH concentration have revealed a definite trend to a peak around midday, followed by a decrease towards evening [39,40]. These two studies indicate that the concentration of hydroxyl radical in the troposphere parallels the diurnal fluctuation in solar intensity. This is reasonable since photolysis of ozone by sunlight is a major pathway for the atmospheric formation of OH. In the most recent measurements (taken in the Black Forest, Germany, 48°N latitude in June), the observed OH concentrations varied from 2×10^6 molecules·cm^{-3} in the morning or evening hours, up to peak values of approximately 8×10^6 molecules·cm^{-3} around midday [40].

In the present work rate constants for the reaction of OH with chlorophenols were estimated according to the method of Zetzsch [41], who has demonstrated that the room temperature rate constants for addition of OH to substituted aromatics correlate well with the sum of the electrophilic substituent constants σ^+ [42]. Equation [7] [43] is a slightly refined version of the original expression developed by Zetzsch.

$$\log k\ (\mathrm{cm^3 \cdot molecule^{-1} \cdot sec^{-1}}) = -11.64 - 1.31 \cdot \Sigma\, \sigma^{+} \qquad [7]$$

According to this estimation procedure[41], a) steric hindrance is neglected, and the electrophilic substituent constant for the ortho position is defined as equal to that for the para position; b) $\Sigma\, \sigma^{+}$ for any position on the aromatic ring is the sum of σ^{+} for all substituents connected to the ring; c) the rate constant is calculated for the position yielding the most negative value of $\Sigma\, \sigma^{+}$ for addition of OH to the ring (preferably a free position); d) if all positions on the ring are occupied, the ipso position is treated as a meta position.

Since the rate constants for the addition of OH to the aromatic ring of chlorinated phenols were not available in the literature, they were calculated according to equation [7] (Table V). The calculated values of k are comparable in magnitude with those previously reported for the chlorobiphenyls, but are generally larger than those of the chlorobenzenes [13]. In all cases, the rate constants are strongly dependent upon the number of chlorine substituents on the ring and less so upon their location. This is reasonable in that chlorine is electron withdrawing and decreases reactivity towards electrophilic reactants such as OH. Although many common radicals react with aromatics by abstraction of a "side group" hydrogen (e.g. $CH_3\cdot$ abstracts the phenolic hydrogen from phenol), the hydroxyl radical reacts by addition reaction to the aromatic ring of phenols [43]. The electrophilic hydroxyl radical adds to the ring, which is somewhat electron-rich even when substituted by chlorine, rather than abstracting hydrogen from the electronegative oxygen atom of the phenolic OH. The larger rate constants for addition of OH to a chlorinated phenol compared with a comparably chlorinated benzene are the result of activation of the aromatic ring by the phenolic hydroxy group, leading to faster attack by the electrophilic OH radical.

The results in Table V were obtained on the basis of Platt's [40] peak noon time OH concentrations. Like the photochemical data presented in the same table, they underestimate the true half lives; for example, if the "averaged" [28] OH concentration of 5×10^5 radicals cm^{-3} is used, these half lives range from about 1 week for the lower chlorophenols to 1 month for pentachlorophenol.

Photodegradation vs Hydroxyl Radical Attack

In this final section we attempt to compare the rates of photolysis and of OH attack upon the chlorophenols. In order to make the fairest comparison, we used in Table V solar intensities (40°N) and OH radical concentrations (48°N) appropriate for high noon in the summer. (We reiterate that the true environmental half-lives will be much greater than those given in Table V. Nevertheless, the **ratios** of the rates should fluctuate less than the rates themselves as the season and the time of day change, because the OH radical concentration is principally governed by the solar intensity [40]). From Table V we conclude that photolysis and OH radical attack are complementary processes, those chlorophenols that are least susceptible to photolysis being the most reactive towards OH. As a result, we predict that all the lower chlorophenols will react in the atmosphere principally with OH radicals, while for the most heavily chlorinated congeners photolysis will become more important and, for pentachlorophenol, the dominant reaction channel.

Our perspective of the present results is seen by comparing the three potential fates of any compound after it enters the atmosphere, namely deposition, chemical/photochemical transformation, or transport. The extent of transport is determined by the residence time of the substance in the atmosphere. For the PCB's this has been estimated to be on the order of one week [18]. Although the chlorophenols are generally more volatile, their residence times are likely to be no longer than those of the PCBs for three reasons. First, chlorophenols are more polar than PCBs and consequently, their adhesion to particles is better, aiding dry deposition. Second, chlorophenols are more water soluble, enhancing their washout in precipitation. Third, many chlorophenols have realistic half-lives in the atmosphere for chemical and photochemical change of approximately one week; as such, substantial alteration of these pollutants prior to their transport or deposition may be predicted. Therefore, in contrast to the PCBs, which have been detected in the Antarctic [28], we do not anticipate that the chlorinated phenols will travel great distances through the atmosphere to very remote locations.

On the basis of some very preliminary product studies [44] we predict that both photolysis and OH radical attack will have the effect of adding a second oxygenated substituent on to the aromatic ring, with or without the expulsion of a chlorine substituent. The result is to increase both photolability (absorption spectrum red shifted) and the rate of OH attack (second activating substituent). The atmospheric reaction products of chlorophenols are therefore more reactive in the atmosphere than their chlorophenol parents, and are unlikely to build up to detectable concentrations.

Finally we outline the studies which are planned and in progress for the remainder of this project. We are trying to obtain more detailed information about the relative importance of solar photodegradation and hydroxyl radical attack. Two approaches are being tried.

1. We are attempting to calculate solar intensities as a function of he time of day in order to determine whether the hydroxyl radical concentration can be estimated from the solar intensity. This is not unreasonable, given that solar photolysis is the principal source of the hydroxyl radical, as shown above. We plan to model the Black Forest data[40] to ascertain whether there exists a linear relationship between

the experimental concentration of OH and the calculated solar intensity. If so, then the latter calculation could be used as an estimator of the OH radical concentration. This would be of value, because so few actual measurements of [OH] in the troposphere currently exist. Since chlorophenols and ozone are photochemically active in the same spectral region, we might expect that the rates of hydroxyl radical attack and solar photolysis might change in parallel.

2. We are trying to develop a kinetic model of the behaviour of the most important reactions involving the OH radical in its interactions with organic pollutants in the troposphere. We hope that it may be possible to select the most important reactions so that the size of the calculation can be restricted to something that can be executed on a microcomputer. Full models, by contrast, require a supercomputer. The relationship of this part of the project to (1) above is that so few actual measurements of [OH] and its diurnal and seasonal variation exist that any ability to model the chemistry of this most important atmospheric constituent will greatly assist in understanding the chemistry of organic pollutants in the troposphere.

Details on our progress with these latter parts of the project and, we hope, preliminary results will be available be the time of the presentation.

References

1. U.G. Ahlborg and T.M. Thunberg, "Chlorinated phenols: occurrence, toxicity, metabolism, and environmental impact", CRC Crit. Rev. Toxicol. 7, 1 (1980)
2. J.H. Exon, "A review of chlorinated phenols", Vet. Hum. Toxicol. 26, 508 (1984)
3. World Health Organization, "Environmental Health Criteria 71: Pentachlorophenol", United Nations Environment Programme, International Labour Organization and World Health Organization (1984)
4. A. Bevenue and H. Beckman, "Pentachlorophenol: a discussion of its properties and its occurrences as a residue in human and animal tissue", Residue Rev. 19, 83 (1967)
5. P.A. Jones, "Chlorophenols and their impurities in the Canadian environment", Environment Canada Report EPS 3-EC-81-2 (1981)
6. I. Rosen, R.A. DiSanza and A. Hirsch, "New derivatives of phentachlorophenol and their fungistatic activities", J. Org. Chem. 23, 149 (1958)

7. A. Stark, "Analysis of pentachlorophenol residues in soil, water, and fish", J. Agric. Food Chem. 17, 871 (1969)
8. L. Rudling, "Determination of pentachlorophenol in organic tissues and water", Water Res. 4, 533 (1970)
9. R. Engst, R.M. Macholz and M. Kujawa, "The metabolism of hexachlorobenzene (HCB) in rats", Bull. Environ. Contam. Toxicol. 16, 248 (1976)
10. J. Kohli, D. Jones and S. Safe, "The metabolism of higher chlorinated benzene isomers", Can. J. Chem. 54, 203 (1976)
11. S.M. Somani, R.G. Teece and D.J. Schaeffer, "Identification of carcinogens and promotors in industrial discharges into and in the Illinois River", J. Toxicol. Environ. Hlth. 6, 315 (1980)
12. M. Alexander and M. Aleem, "Effect of chemical structure on microbial decomposition of aromatic herbicides", J. Agric. Food Chem. 9, 44 (1961)
13. D.G. Crosby and H.O. Tutass, "Photodecomposition of 2,4-dichlorophenoxyacetic acid", J. Agric. Food Chem. 14, 596 (1966)
14. R.G. Zepp, N.L. Wolfe, J.A. Gordon and G.L. Baughman, "Dynamics of 2,4-D esters in surface waters", Environ. Sci. Technol. 9, 1144 (1975)
15. K.R. Krijgsheld and A. van der Gen, "Assessment of the impact of the emission of certain organochlorine compounds on the aquatic environment - part I: monochlorophenols and 2,4,-dichlorophenols", Chemosphere 15, 825 (1986)
16. Chemical Rubber Co., R.C. Weast (ed.), "CRC Handoook of Chemistry and Physics, 56th edition", CRC Press, Cleveland, Ohio (1976)
17. W.F. Spencer, W.J. Farmer and M.M. Cliath, "Pesticide volatilization", Pest. Rev. 49, 1 (1973)
18. T.J. Murphy, W. Formanski, B. Brownawell and L.A. Meyer, "Polychlorinated biphenyl emissions to the atmosphere in the Great Lakes region", Environ. Sci. Technol. 19, 942 (1985)
19. R.G. Lewis, B.E. Martin, S.L. Sgontz and J.E. Howes, "Measurement of fugative atmospheric emissions of polychlorinated biphenyls from hazardous waste landfills", Environ. Sci. Technol. 19, 986 (1985)
20. D.L. Swakhamer, B.D. McVeety and R.A. Hites, "Deposition and evaporation of polychlorinated congeners to and from Siskiwit Lake, Isle Royal, Lake Superior", Environ. Sci. Technol. 22, 664 (1988)
21. National Research Council of Canada, "Chlorinated Phenols: Criteria for Environmental Quality", NRCC Report No. 18578 (1982)
22. R.W. Risebrough, W. Walker, T.T. Schmidt, B.W. de Lappe and C.W. Connors, "Transfer of chlorinated biphenyls to Antarctica", Nature 264, 738 (1976)
23. C. Leuenberger, M.P. Ligocki and J.F. Pankow, "Trace organic compounds in rain for identities, concentrations and scavenging mechanisms for phenols in urban air and rain", Environ. Sci. Technol. 19, 1053 (1985)
24. J.G. Calvert, and J.N. Pitts, Jr., "Photochemistry", John Wiley and Sons, New York (1966)
25. N.J. Bunce, "On the determination of quantum yields of reaction in solution", J. Photochem. 15, 1 (1981)
26. N.J Bunce, J. Langshaw and J.S. Nakai, "Gas phase photochemistry in round bottomed flasks", J. Photochem., in press (1988)
27. N.J. Bunce, J.P. Landers, J. Langshaw and J.S. Nakai, "An assessment of the importance of direct solar degradation of some simple chlorinated benzenes and biphenyls in the vapour phase", Environ. Sci. Technol., submitted for publication (1988)
28. G.A. Arguello, E.R. de Staricco and E.H. de Starrico, "Quantum yield and total pressure effect in perfluoroglutaric anhydride photolysis in the gas phase", J. Photochem. 30, 1 (1985)
29. J.M. Figura and A. Tobar, "Photodecomposition quantum yields of 3-chloro-3-methyldiazirine in the gas phase", J. Photochem. 10, 473 (1979)

30. R.G. Zepp and D.M. Cline, "Rates of direct photolysis in aquatic environment", Environ. Sci. Technol. 11, 359 (1977)

31. R. Atkinson, K.R. Darnall, A.C. Lloyd, A.M. Winer and J.N. Pitts, "Kinetics and mechanisms of the reactions of the hydroxyl radical with organic compounds in the gas phase", Adv. Photochem. 11, 375-488 (1979)

32. R. Atkinson, "Kinetics and mechanisms of the gas-phase reactions of the hydroxyl radical with organic compounds under atmospheric conditions", Chem. Rev. 86, 69 (1986)

33. D.D. Davis, S. Fischer and R. Schiff, "Flash photolysis - resonance fluorescence kinetics study: temperature dependence of the reactions $OH + CO \rightarrow CO_2 + H$ and $OH + CH_4 \rightarrow H_2O + CH_3$", J. Chem. Phys. 61, 2213 (1974)

34. H. Niki, P.D. Maker, C.M. Savage and L.P. Breitenbach, "Mechanism for hydroxyl radical initiated oxidation of olefin-nitric oxide mixtures in parts per million concentrations", J. Phys. Chem. 82, 132 (1978)

35. K.-M. Jeong and F. Kaufman, "Kinetics of the reaction of hydroxyl radical with methane and with nine Cl- and F- substituted methanes. 1. Experimental results, comparisons and applications", J. Phys. Chem. 86, 1808 (1982)

36. R. Atkinson and S.M. Aschmann, "Rate constants for the gas-phase reaction of hydroxyl radicals with biphenyl and the monochlorobiphenyls at 295 ± 1 K", Environ. Sci. Technol., 19, 462 (1985)

37. B.J. Finlayson-Pitts and J.N. Pitts Jr., "Atmospheric Chemistry: Fundamentals and Experimental Techniques", John Wiley and Sons, Inc., Toronto, Ont. (1986)

38. P.J. Crutzen, in "Atmospheric Chemistry: The global distribution of hydroxyl", pp. 313-328, D.G. Goldberg (ed.) Ann Arbor Press, Ann Arbor, M.I. (1982)

39. C.C. Wang, L.I. Davis Jr., C.H. Wu, S. Japar, H. Niki and B. Weinstock, "Hydroxyl radical concentrations measured in ambient air", Science 189, 797 (1975)

40. U. Platt, M. Rateike, W. Junkermann, J. Rudolph and D.H. Ehhalt, "New tropospheric OH measurements", J. Geophys. Res. 93, 5159 (1988)

41. C. Zetzsch, "Predicting the rate of OH-addition to aromatics using σ^+-electrophilic substituent constants for mono- and polysubstituted benzene", 15th Informal Conference on Photochemistry, Abstract No. A-11, Stanford CA, June 27-July 1, 1982

42. H.C. Brown and Y. Okamoto, "Electrophilic substituent constants", J. Am. Chem. Soc. 80, 4979 (1958)

43. K.U. Ingold, in "Free Radicals, Vol. 1", Kochi, J.K. ed.; John Wiley and Sons, Toronto (1973)

44. J.S. Nakai, M.Sc. Thesis, "The Vapour Phase Photolysis of Chlorinated Phenols: An Atmospheric Assessment" (1988)

SESSION A

AIR QUALITY RESEARCH

Poster Presentations

AP1

STOCHASTIC MODELLING OF DISPERSION FROM SINGLE ELEVATED SOURCES. E. Robertson and P.J. Barry, Atomic Energy of Canada Limited, Chalk River Nuclear Laboratories, Chalk River, Ontario, K0J 1J0

Short range (e.g. distances <50 km) atmospheric dispersion models have traditionally been used for two main purposes: a) to predict real time concentrations during accidental releases of noxious gases, and b) to predict long-term average concentrations for the purpose of controlling pollution levels from single sources during routine operations.

For several decades Gaussian Plume dispersion models together with published default dispersion parameters have been used for both purposes. However, during the last decade an increasing number of studies have shown that the reliability of such models and parameter values is poor when used to estimate pollutant concentrations for averaging periods of 1 hour or less.

These studies have been restricted to comparison of predicted to observed short-term concentrations in real time, but, by implication it is often implicitly assumed the model will be unreliable on the longer term as well. We have been conducting studies around an isolated stack that continuously released a short-lived radioactive noble gas, Argon-41, at a steady rate. This work has confirmed that on a one-to-one basis in real time the Gaussian plume model is a poor predictor for shorter averaging times with discrepancies by a factor of 10 or more occurring 80% of the time. However as the averaging time increases the reliability increases also and when the averaging time exceeded a month the predictions were acceptable. Annual predicted averages agreed with those observed within a factor of 2. It was also found that the cumulative frequency distributions of predicted hourly averaged concentrations agreed reasonably well with the observed distributions. Thus while the model gave relatively poor predictions of individual hourly average concentrations in real time it nevertheless yielded a reasonably correct ensemble of concentrations.

Thus it follows that, for prediction of long-term average concentrations, or the frequency distribution of concentrations, the model need not necessarily be driven by real time meteorological data, but rather by data synthesized from their frequency distributions, which are available in climatological summaries. The latter method is easier and thus less costly.

A stochastic dispersion model based on these ideas was therefore developed using the following methodology. The code performs Monte-Carlo simulations with variable input meteorological data fed to a standard Gaussian plume dispersion equation. The needed meteorological variables are wind speed and direction and a measure of the atmospheric stability. The climatological summary should provide the frequencies of wind directions on as fine an angular degree interval as possible; however, in the case of data derived from routine synoptic stations sectors of 22.5° intervals will have to be accepted. The cumulative frequencies are calculated going from 0° to 359° in whatever sector intervals are available. The resulting curve is fitted to a polynomial equation of the type

$$D = a + bF + cF^2 + dF^3 \cdots$$

where D is the wind direction, F the cumulative frequency derived from the data, and a, b, c -- etc. constants. Most computing systems support routines for the evaluation of the constants in a polynomial of any reasonable degree. The polynomial equation is written into the code. To select a wind direction for each "trial", a random number from 0 to 1 is generated, substituted for F into the above equation and D calculated. The complexity of the shape of the wind direction frequency curve determines the order of the polynomial that will give a reasonable approximation to the one observed. For the Chalk River site, where the wind is strongly channelled into two relatively narrow angular bands, a 9th order was required.

A similar procedure is followed to obtain values for wind speed and stability. Stability can be obtained using synoptic station data and the "STAR" program from which the occurrence frequencies of classes A to F can be obtained. Stability obtained this way is a discrete variable so that particular class is selected from the random number within ranges. For example suppose classes A, B and C occur with frequencies 2%, 10% and 15% respectively. Then Class A is selected whenever the random number lies between 0 and 0.02, class B when it lies between 0.02 and 0.12 and so on. Since wind speed and stability, as defined by the STAR program, are directly related, 6 wind speed distribution frequencies are used.

Once the class has been selected, values for the horizontal and vertical dispersion parameters can be calculated for the receptor distance from the equations provided by Briggs (1974) or Hosker (1974). These values together with a stack emission rate for the hours are used to solve the bivariate Gaussian plume equation and obtain a concentration for each receptor. The process is repeated as many times as necessary to obtain a smooth frequency of occurrences of concentrations or a stable estimate of the long term mean.

If the stack emission rate is independent of weather conditions it too may be selected randomly from a frequency distribution of values.

This model is to be applied to other sites to test its usefulness generally. As a first step it is to be applied to the smelter stack at Sudbury and the predictions derived from it compared with concentrations of SO_2 measured at several locations in the surrounding district.

If the model is found to be widely valid, it provides a relatively simple and straightforward way of calculating the stochastic characteristics for a climatology of air pollution events.

Predicting the long term mean is a useful product but knowing the frequencies of occurrences of different pollution levels about the mean enables regulators to also control the frequency of occurrence of toxic or nuisance levels. Alternatively if air pollution levels are regulated by applying meteorological control over sources, both regulators and regulated need to know the frequency and hence the potential costs of production cutbacks associated with any given strategy for pollution abatement.

References

Briggs, G.A., 1974, "Diffusion estimates for small emissions", Environmental Research Laboratories Air Resources, Atmosphere, Turbulence and Diffusion Laboratory, Annual Report 1973 USAFC Report ATDL-106, National Oceanic and Atmospheric Administration.

Hosker, R.P. Jr., 1974, "Estimates of dry deposition and plume depletion over forests and grasslands", in Proc. of IAEA Symposium, "Physical behaviour of radioactive contaminants in the atmosphere", Vienna, November 1973, IAEA, Vienna.

AP2

FEASIBILITY STUDY FOR ASSESSING AND MODELLING MICROCLIMATIC CONDITIONS ON THE FONTHILL KAME

by

Dr. Tony B. Shaw, Brock University
Dr. Terry Gillespie, University of Guelph
Dr. Bhartendu Srivastava, Environment Canada
Dr. Peter Taylor, Environment Canada
Dr. Hans Teunissen, Environment Canada
Dr. René Verreault, University of Quebec

The Fonthill Kame, located in the Town of Pelham, is the most important tender fruit area above the Niagara Escarpment. The combination of a favourable climate and well-drained sandy loam soils permits the successful cultivation of tender fruits along with other fruit crops. The steep slopes of the Kame, projecting above the surrounding flat plain, facilitate the drainage of cold air under radiation frost conditions. The mixing of cold surface air with warmer air above moderates the temperature near the ground and thus helps to reduce the risk of freeze damage. Moreover, the high elevation results in a lower mean temperature which helps to delay blossoming until the danger of spring frost is past. The distinct microclimate of the Fonthill Kame together with its well-drained soils make this area unique for the production of tender fruits. However, the Kame also contains the most important land-based deposits of commercial sand and gravel in the Niagara Region. These deposits, which occur in areas of primary and secondary significance as defined by the Ministry of Natural Resources, also coincide with lands identified for tender fruit production by the Ministry of Agriculture and Food. Consequently, there may be conflicts in the way these resources are utilized in this rather small area.

Since the microclimate of the Fonthill Kame is to a large extent related to its topography, it is argued by some that structural changes to the topography of the Kame will modify this microclimate. The chief concern is that cold-air drainage on which the production of tender fruits depends could be altered significantly on those slopes which may support aggregate extraction. A modified climate could impact adversely on tender fruit crops on the Kame itself with possible consequences for areas contiguous to the Kame. This study presents essential background information on the Fonthill Kame and recommends ways in which the unique microclimate of this area can be better understood so as to assess the impacts of the multiple and competing land uses found here.

The chief concern is with the disruption on cold-air drainage and the resultant effects on the temperature of the slopes and nearby off-site areas. Accordingly, the principal objectives of this study are:1) to determine whether methodologies exist for assessing changes to the Fonthill Kame's microclimate stemming from topographic modifications and 2) to evaluate the predictive capabilities of these methodologies for assessing the impact on the microclimate of future proposals for extraction on the Kame. The study also poses a series of related questions considered to be crucial to the problem of microclimate modification that ought to be addressed in future studies of the Fonthill Kame.

We suggest two criteria for assessing modification to the Fonthill Kame's microclimate: any topographic change, particularly slope changes, which will result in (a) a decrease of nocturnal minimum temperature by 1°C below threshold values as specified for tender fruit crops and (b) a reduction in wind speed below 1m/sec under radiation inversion conditions. We review and recommend three methodologies. Two are empirical field study methods (surface-based and aircraft-based) and the third is a conceptual, numerical modelling approach. The choice of these approaches rests on two important considerations: the need to obtain a detailed accurate assessment of the existing microclimate of the Kame and the ability to predict the impact of future topographic changes on the microclimate, particularly its temperature.

We recommend that all three approaches should be fully integrated and that future impact studies be undertaken over a two year period to allow the creation of a reliable data base.

AP3

CRITICAL EVALUATION OF ATMOSPHERIC POLLUTANT PARAMETERIZATION FROM SATELLITE IMAGERY

N. T. O'Neill*, A. Royer, L. Hubert, **CARTEL**, Université de Sherbrooke, Sherbrooke, Qué.,

J. R. Miller, J. Freemantle, **CRESS**, York University, Downsview, Ont.,

G. Austin, A. Davis, McGill University, Montréal, Qué.

In spite of overwhelming advantages in spatial samping density and spatial coverage the remote sensing of atmospheric constituents represents a monitoring methodology which is often more qualitative than quantitative. The sensitivity of existing techniques for the inversion of satellite imagery data is not well understood in terms of discriminating constituent types and threshold levels of detection. The objective of the present study was to simulate the atmospherically scattered signal received by a satellite sensor and hence to evaluate the sensitivity of this signal to atmospheric aerosols in general and to atmospheric pollutants in particular. In the long term this type of research is geared towards the development of an operational satellite monitoring system within the context of the long range transport of atmospheric pollutants (LRTAP) programs.

The simulations were performed as a function of environmental, geometrical and operational parameter constraints. The environmental modelling included the effects of urban and rural type aerosols where the absolute and relative concentration of water soluble (sulphate) particles was allowed to vary and where particle growth and refractive index effects of relative humidity variations was incorporated. Combined aerosol modes which included fine particle (sulphate based) coarse particle (silicate based) and absorptive aerosols (carbon based) were incorporated as external (independent) aerosol mixtures. Some tests were performed in terms of internal aerosol mixtures in order to evaluate the effect of the mixture assumption on the results of the sensitivity study.

The variability of the simulated signals indicate that information on the vertically integrated contribution of submicron scattering and absorbing aerosols can be usefully extracted. Inasmuch as the dominant optical variations occur in the lower troposphere this extracted information can be correlated with ground level concentrations. Furthermore, investigations into the dependence of the satellite signal on variations in optical mixing ratios with altitude indicated a degree of insensitivity which significantly simplifies the radiative transfer calculations and the inversion methodology.

The optical effects of ground level sulphates (predominantly in the form $(NH_4)_2SO_4$) are strongly influenced by the ambient relative humidity. This is less an effect of a change in refractive index than an increase in particle size according to the mechanisms of droplet growth. Such induced variations in optical activity result in a ground level sulphate scattering power which may vary by a factor of 4 or 5 across the naturally occurring range of relative humidity. The implications of this variation in terms of satellite remote sensing is that one must be aware of the average atmospheric water vapour parameters in order to obtain quantitative inversions for ground level sulphate concentration. As well the relative weakness of the signal in dry atmospheric conditions represents a degradation factor in terms of sulphate sensitivity.

The specificity of coarse (spectral) band remote sensing for sulphate detection is more a function of the dominance of fine particle (water soluble) aerosols in terms of optical effects and in turn the predominance of the sulphate fraction in the water soluble component. At ground level the optical contribution due to sulphates is typically the largest particularily in conditions of high relative humidity and total extinction. Accordingly, even in the absence of information relating to the contribution of other components one can extract an estimate of wet sulphate number density to within a factor of 2 or 3. The extraction of dry sulphate number density can then be performed given relative humidity information.

An improvement of this figure can only be obtained by (1) effectively calibrating the satellite data with ground based concentration measurements or (2) by employing multispectral and temporal data to extract information on other contributions to the satellite signal. The atmospherically averaged aerosol size distribution, in addition to the integrated aerosol content, can be extracted if three or more absorption free wavelengths in the spectral region from 0.4 to 2.5 microns are available. Inversions for water vapour and NO_2 content can be performed if measurements are made at two or more wavelengths straddling absorption peaks in the near IR and near UV respectively.

The operational parameter constraints were keyed to the specifications of selected remote sensing satellites which are either operational or will be by at least 1995. These included the NOAA and GOES meteorological satellite series, the Landsat and SPOT resource monitoring satellites, the oceanographic satellite SEAWIFS, and the high spectral resolution imaging spectrometers (MODIS and HIRIS) which will be incorporated into the space station package. The meteorological satellites offer a relatively high rate of image repetition over the same area but are constrained to one or two coarse spectral bands and a large spatial resolution. The current SPOT and Landsat satellites acquire high spatial resolution images (order of tens of meters) at comparatively high spectral resolution but with a repetition cycle (order of weeks) which is not suited to the time scale of regional transport studies. The next generation of resource satellites SPOT-4 and SEAWIFS offer both a spectral resolution and a repetition rate (2 days) which more closely approximates the requirements for passive atmospheric remote sensing. Within the near future the HIRIS and MODIS sensors possibly coupled with vertical structure data from the laser sounder (LASA) represent the realisation of a sensor package for which one of the major design constraints was the remote sensing of atmospheric constituents.

A comparison of radiative transfer models indicated that the analytical 5S model developed by D. Tanré and co-workers represented the most optimal comprimise of speed and accuracy in terms of applying a pixel by pixel inversion algorithm to large satellite images. Comparison with a multiple scattering, multiple layer model demonstrated however that, for certain geometrical conditions, inversion errors of the order of .1 in aerosol optical depth could result. This necessitated certain model refinements which were related to the manner in which aerosol and molecular scattering were coupled.

The study also showed that special algorithms were required to overcome difficulties associated with inversion singularities over surfaces whose reflectances were such that the effects of surface transmission and atmospheric scattering were counterbalanced. The extraction of atmospherically scattered signals from the total signal received by the satellite sensor implies some apriori knowledge of the ground surface reflectance in the satellite image. To a certain degree this requirement can be circumvented by restricting measurements to water bodies and by utilizing bands in the near IR spectral region. However to fully exploit the potential of the satellite data requires a calibration program involving the establishment of reflectance calibration sites and the temporal analysis of repetitive satellite images.

The simulation analysis was sufficiently promising to warrant a program of simultaneous ground based, airborne and satellite measurements as a subsequent phase to the present work. This program should include as well the acquisition and analysis of high spectral resolution airborne data to address the specificity problem.

AP4

A 3-D MESOSCALE WIND FIELD MODEL
AND
ITS APPLICATION FOR EMERGENCY PLANNING AT NUCLEAR PLANTS IN ONTARIO

H. Sahota, P. K. Misra, R. Bloxam and D. Rhee
Atmospheric Modelling Unit
Air Quality and Meteorlogy Section
Air Resources Branch
Ontario Ministry of Environment
Toronto, Ontario

INTRODUCTION :

The Ontario Ministry of Environment in co-operation with the Ministry of Solicitor General and Ontario Hydro, has developed an emergency response program for the release of radio-nuclides in the event of an accident at any of the nuclear plants in Ontario.

Two important pieces of information, required for this program, are, the wind field (i.e. wind speeds and directions downwind of the plants) and the ground level concentration level fields. Generally measurements of winds are sparse and hence either extrapolation from a single measurement point or meteorological forecasts are needed to generate the wind fields. This introduces a degree of subjectivity to the determination of the direction in which the radio-nuclides propagate downwind after their release.

It would be desirable to develop an objective scheme to simulate the wind fields in the vicinity of the nuclear power plants. We propose a three dimensional wind field model for this purpose. The model is briefly described in the next section. Several criteria were used in the development of the model. These are described below:

a) The model has to include sufficient physics to account for the complex flow patterns which are expected near a lakeshore. It is noted that all of Ontario's nuclear power plants are located on the lake shore.

b) The model has to be computationally feasible to run in a short time to enable usto effectively respond in an emergency situation.

The above criteria are very often in conflict with each other. The model described in this paper attempts to fulfill these criteria in an optimum manner.

MODEL DESCRIPTION :

The model is time dependent and is governed by the basic Navier Stokes equation. Atmosphere is assumed to be in a hydrostatic equilibrium i.e. vertical accelrations are neglected. Topography is included by defining a vertical coordinate which includes the local terrain height. Eddy exchange coefficients for momentum and heat are parameterized in the model(for a detailed description of the model see Maddukuri 1983).

The model has ten irregularly spaced vertical levels. Spacing is closer near the ground where higher resolution is required and is larger elsewhere.

Figure 1 shows the model domain and Figure 2 the topography, as it is implemented for the Pickering Nuclear Generating Station. The model grid size is 5 km and covers an area 145 km x 145 km.

The model uses a preprocessor to compute the initial conditions that vary both horizontally and vertically. The preprocessor uses gridded (327 km) data (isobaric heights and temperatures) provided by Canadian Meterological Centre (CMC) of Atmospheric Environment Services. Using orthognal polynomials the preprocessor interpolates this data down to 5 km grid points. CMC balance winds or geostrophic winds are used as initial winds in the model.

Surface temperature which is the driving force for mesoscale circuilations is derived from observed screen temperature, cloud cover and using empirical relationships developed by van Ulden and Holstag (1985).

The preprocessor program writes all the initial data onto appropriate files which are subsequently read by the main program. A time step of six minutes is used in the program.

MODEL OUTPUTS (AN EXAMPLE):

The model coumputes various parameters such as isobaric heights, temperature, horizontal and vertical components of the wind, potential temperature etc. Data can be averaged over any desired time interval. Usually hourly averages are reported unless specified. Vertical averaging for wind speed is used to reduce noise in the data. Typically the model is used to forecast winds for six to twenty four period.

Figure 3. shows the surface map for great lakes area on June 24, 1988. Southern Ontario under the influence of a high pressure system had clear skies and temeperatures were in the uppper twenties. Figure 4. shows the initial conditions as computed at 8.00 AM local time. As the surface temperature increases due to soalr insolation a lake breeze is set up. Figure 5. shows the model output at 15.00 PM. The shift in wind direction and magnitude is quite evident.

The mesoscale model is also being verified with the data from a field study being conducted by Atomic Energy Board of Canada, Environment Canada, Ministry of Solicitor General and Ministry of Environment. One such comparison is presented in Figure 6. The agreement between observed and predicted wind speed and direction is quite good.

CONCLUSIONS :

The model is capable of generating good mesoscale wind forecasts. Model verification with field data is currently underway. Initial results show a good agreement between observed and predicted windfileds. Additional tests are currently underway. After evaluation is completed, the model will be implemented on microcomputer for use in emergency planning by Ministry of Solicitor General.

FUTURE PLANS :

After the model has been verified with the field data, it will be implemented on a COMPAQ 386 microcomputer. Software will be developed to interface directly with OME's MDAS (Meterological Data Acquisition System) so that meterological data can be transferred directly without manual entry. This total pacakage will be then be able to make mesoscale windfiled forecasts on a routine basis and the data then could be used for emergency planning.

REFERENCES :

Maddukuri, C. S. and P. R. Slawson (1983): A three dimensional wind field model for the planetary boundary layer, Parts I and II; ARB Report No. 107-84-AQM, Ontario Ministry of Environment.

van Ulden, A.P. and A.A.M. Holtslag (1985) :Estimation of atmospheric boundary layer parametrs for diffusion applications; Journal of Climate and Applied Meteorlogy, 24 p 1196-1207.

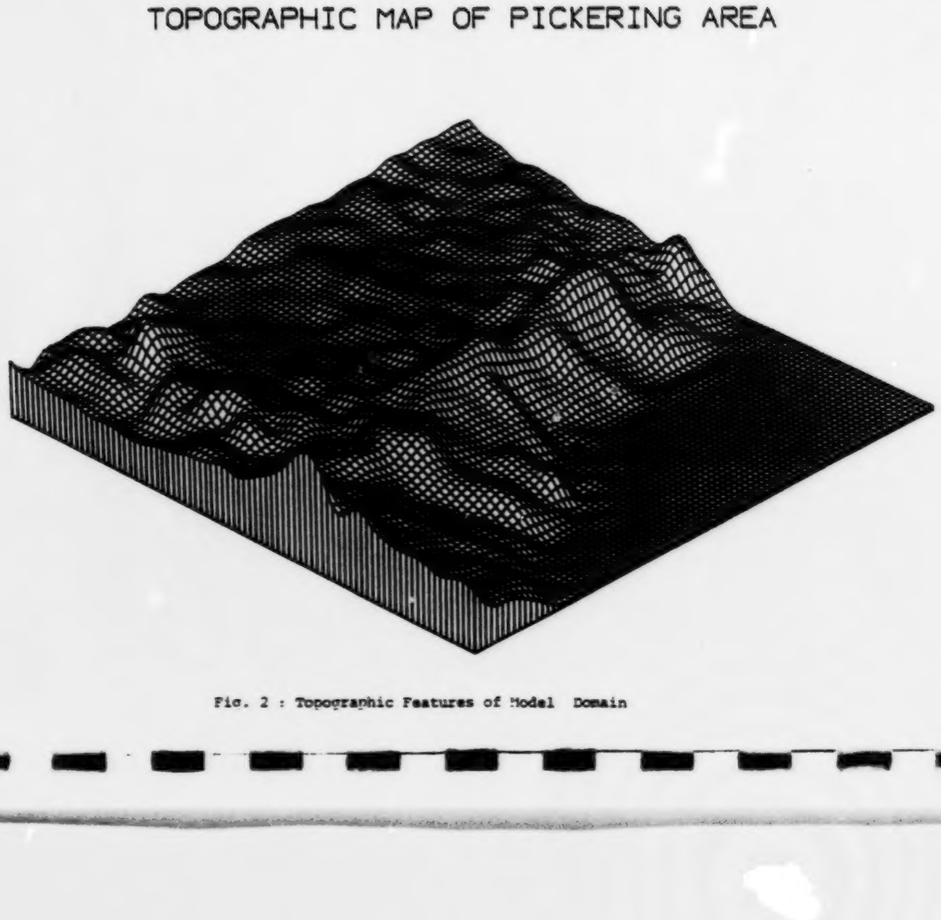
TOPOGRAPHIC MAP OF PICKERING AREA

Fig. 2 : Topographic Features of Model Domain

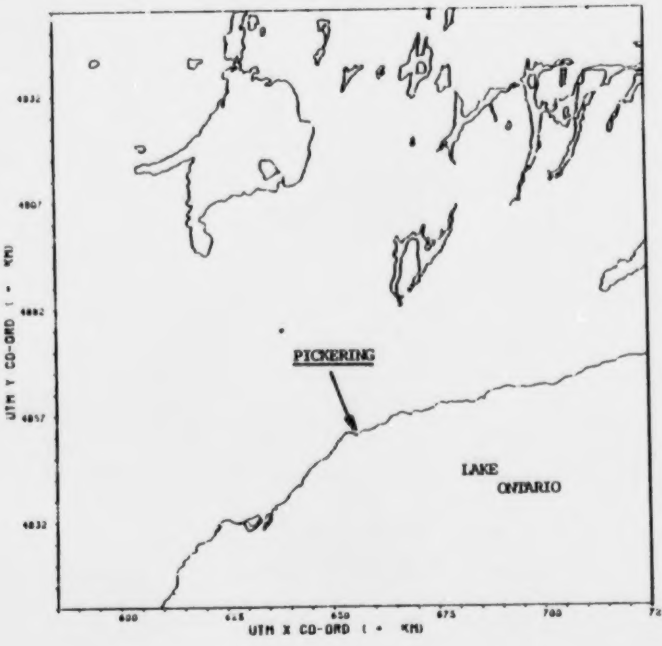
4932
4907
4882
4857
4832
UTM Y CO-ORD (* KM)
600
625
650
675
700
725
UTM X CO-ORD (* KM)
PICKERING
LAKE
ONTARIO

Fig. 1 : Mesoscale Wind Field Model Domain

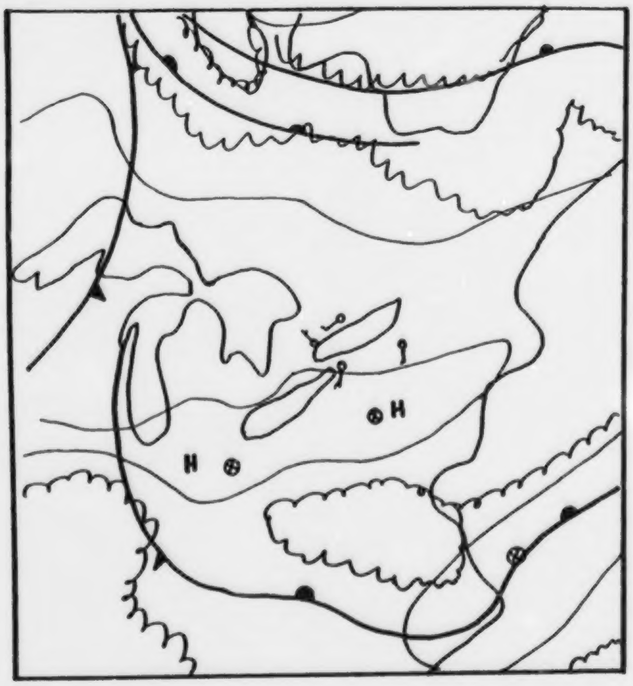

Fig. 3

SURFACE MAP

JUN 24, 1988 TIME: 0700

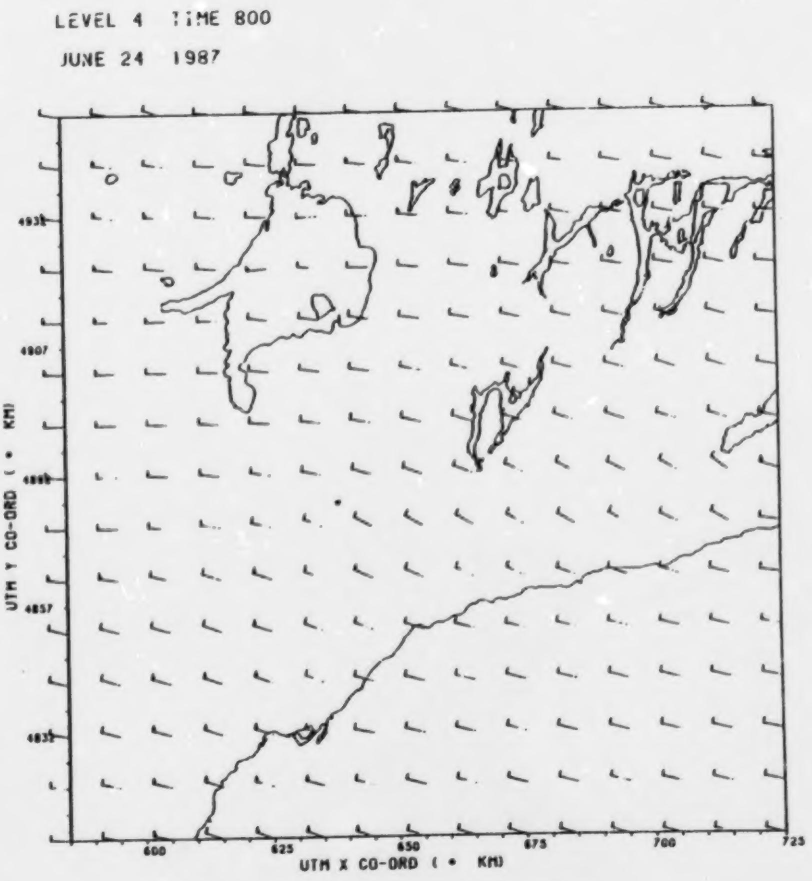
LEVEL 4 TIME 800
JUNE 24 1987
4932
4907
4882
4857
4832
UTM Y CO-ORD (• KM)
600
625
650
675
700
725
UTM X CO-ORD (• KM)

Fig. 4 : Initial Winds at Level Four (10 m)

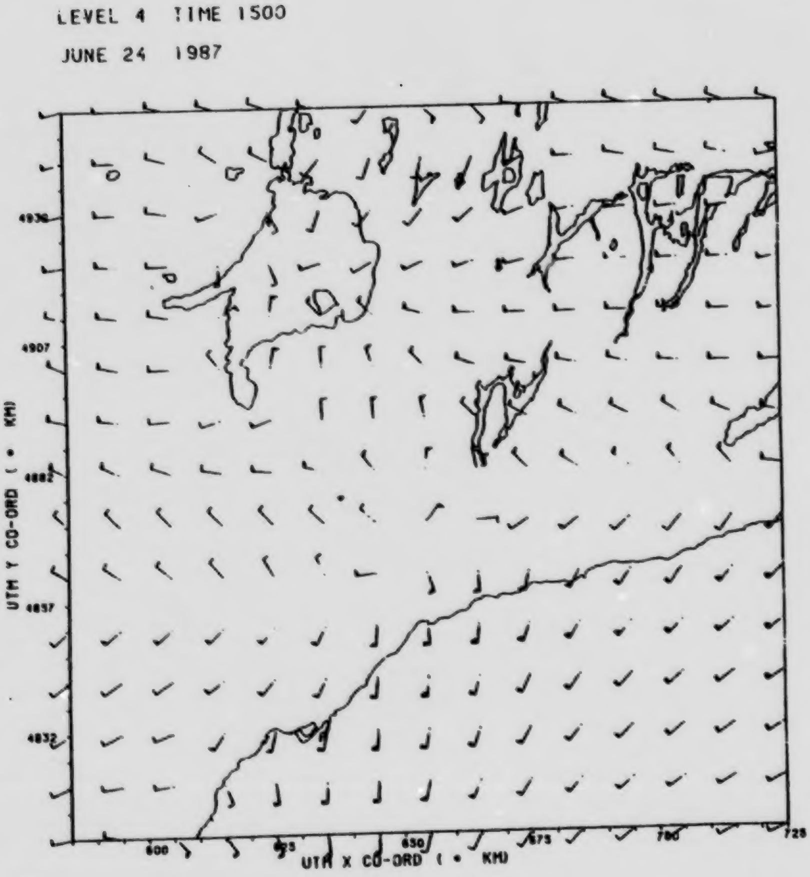
LEVEL 4 TIME 1500
JUNE 24 1987
4932
4907
4882
4857
4832
UTM Y CO-ORD (• KM)
600
625
650
675
700
725
UTM X CO-ORD (• KM)

Fig. 5 : Model Predicted Winds at Level Four (10 m)

MARCH 17. 1988

1500 LOCAL TIME

STATION	W/S	DIR	W/S	DIR
	(OBSERVED)		(MODEL)	
PICKERING	3.08	296	3.05	315
CHERRYWOOD	3.86	317	4.05	320
TORONTO AIR	4.5	300	3.76	306
TORONTO ISL	N/A		3.37	306

Fig. 6 : Comparison Between Observed and Predicted Winds

AP5

POLLUTANT TRANSPORT AND ACID RAIN FORMATION IN A FIELD OF CONVECTIVE CLOUDS: RESULTS FROM A MESOSCALE MODEL SIMULATION

Michal Niewiadomski
Department of Physics, University of Toronto
Toronto, Ontario, M5S 1A7

1 INTRODUCTION

Transport, scavenging and chemical transformations of sulphur and nitrogen pollutants in a field of convective clouds are studied in this paper by means of a three-dimensional mesoscale model, with horizontal resolution of 10 km and parameterized subgrid effects. Attention is focused on the average effects of cumulus convection, as well as the relative importance of different microphysical and chemical processes.

The paper is an outcome of the author's stay at the GKSS Forschungszentrum Geesthacht GmbH in Geesthacht, West Germany and the collaboration with its staff on the development of a mesoscale model of transport and transformations of atmospheric pollutants.

The University of Toronto and Ontario Hydro cloud chemistry model (Iribarne and Melo, 1988) has been coupled for this study with the developed at GKSS cloud microphysics module (Levkov et al., 1987) and a parameterization scheme for the subgrid effects of cumulus convection (Levkov et al., 1986a). These models are driven by a relatively simple dynamical model, which will be replaced in future with a sophistcated mesoscale model GESIMA being developed at GKSS. The model is briefly described below. More detailed description is given by Niewiadomski et al. (1989). Detailed formulas can be found in appropriate reports referenced in section 2.

2 THE MODEL

2.1 Dynamics

The dynamical module is based on the model of Beniston (1981). Detailed formulas can be found in papers of Levkov et al. (1986a,b). The model solves the hydrostatically approximated prognostic equations for momentum, potential temperature, specific humidity, hydrometeor mixing ratios, and chemical variables. The turbulent transport is parameterized through first-order closure; surface fluxes are computed according to Businger et al. (1971). Source terms due to microphysical and chemical processes as well as due to the subgrid effects of cumulus clouds are provided by the described below microphysical, chemical and cloud modules.

2.2 Cloud microphysics

The model follows the 'bulk microphysics' approach. The liquid water is divided into rain and cloud water fractions. Cloud ice and snow are combined in one variable, which will be refered to as 'snow'. The following microphysical processes are included: condensation, evaporation and freezing of cloud water, autoconversion of cloud water to rain, sublimational growth of snow, accretion of cloud droplets by rain and snow particles, freezing and evaporation of rain and melting of snow. Transfers of pollutants between cloud water, rain and snow due to microphysical processes are computed in the chemical module. Detailed formulas can be found in Levkov et al. (1987). Various aspects of this model are also discussed by Levkov et al. (1988).

2.3 Chemistry

The chemical module, computing the source terms for chemical variables due to chemical and microphysical processes is a slightly modified version of the model of Iribarne and Melo (1988). Its basic ideas are described by Iribarne and Cho (1988). The rates of the microphysical transfer processes are provided by the microphysical module.

The following chemical processes are included in the model:

a. Oxidation of SO_2 in cloud and rain water by H_2O_2 dissolved from the air.

b. Oxidation of SO_2 in cloud and rain water by O_3 dissolved from the air.

c. Oxidation of NO_2 by OH in gaseous phase with subsequent dissolution in cloud water of the HNO_3 formed.

d. Oxidation of NO by OH in gaseous phase with subsequent dissolution in cloud water of the HNO_2 formed.

Note, that while the H_2O_2 concentration in both, cloud and rain water is a separate prognostic variable, the air concentrations of ozone and OH, as well as CO_2, are assumed constant. No chemical reactions take place in the ice phase, the snow is however a medium of vertical transport of pollutants and of their transfer between cloud water and rain.

2.4 Cumulus parameterization

Parameterization of the subgrid effects of cumulus convection is based on the ideas of Augstein and Wendel (1981). The scheme, which uses a simple, one-dimensional, entraining cumulus model to obtain the cloud parameters is briefly described below. For details see Levkov et al. (1986a).

The scheme is applied in each column of the model, where the large scale vertical velocity (computed by the dynamical module) exceeds a prescribed value at the lifting condensation level. If that criterion is fulfilled, the in-cloud parameters (temperature, momentum, hydrometeor mixing ratios, and chemical variables) are computed with the 1-D cloud model, using the microphysical parameterization described above, and the entrainment coefficient given by an exponentially increasing function of the altitude above the cloud base (LCL). The model is started at the cloud base with vertical velocity equal to the Deardorff's convective velocity scale. The computed vertical velocity is at each level reduced by a constant factor accounting for the partial coverage of the grid cell by clouds.

For each prognostic variable of the model, effects of convection are then assumed at each level as proportional to the in-cloud vertical velocity, entrainment function and the difference between the values of the considered variable in and outside the cloud (i.e. between the values provided by the dynamical module and the 1-D cloud model).

3. THE EXPERIMENT

The model was run with time steps of 20 s in a domain of 200 x 200 x 10 km with horizontal resolution of 10 km and vertical grid step 50 m for the lowest layer and 500 m for all other ones. Three runs of the model, with two pollution scenarios, imposed on two meteorological cases with different characteristics of microphysical processes, were performed. Their results are discussed in section 4. The input data for these cases are described below. The model was run for two hours of real time, simulating therefore rather early stages of the cloud development. For each run this time was however significant precipitation reaching the ground.

The meteorological conditions used in the runs 1 and 3 represent moderate latitude maritime convection, and are derived from the 13 Oct. 1981 case of the North Sea KonTur experiment. The data for the run 2 come from the 2 Sept. 1974 case of GATE and is characteristic for the intertropical convergence zone.

The behaviour of the dynamical and microphysical parts of the model for these two cases is discussed by Levkov et al. (1986a, 1986b). The rainfall rate, as well as the cloud water and snow mixing ratio at the

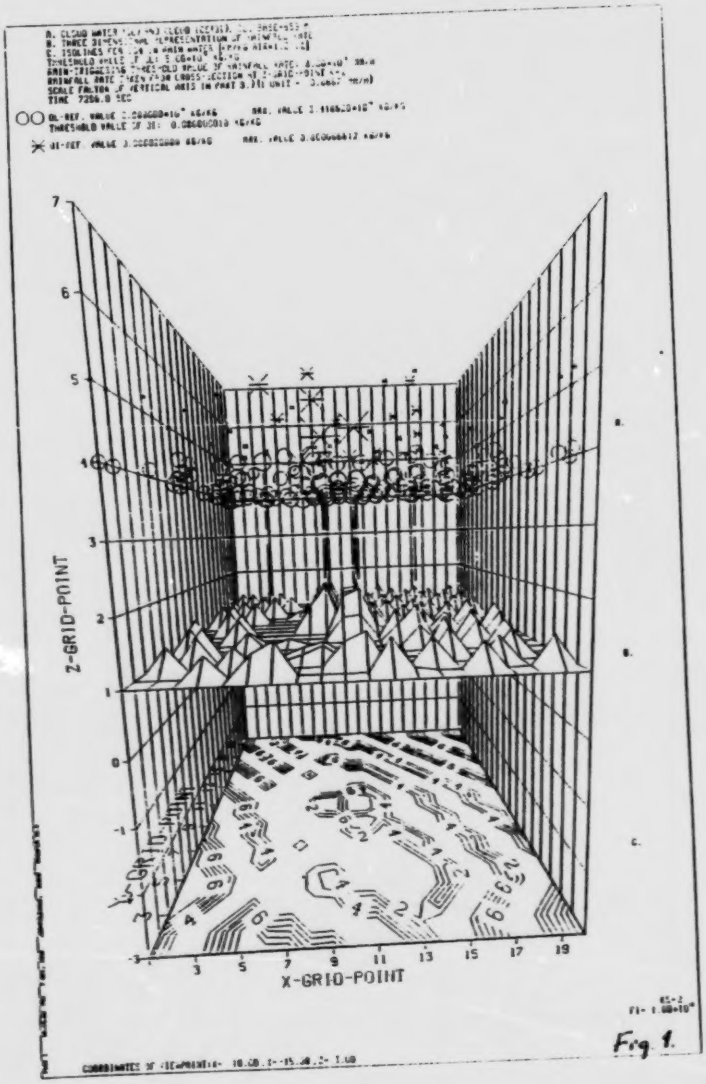
TIME 7200.0 SEC
7
6
5
4
3
2
1
0
-1
-3
Z-GRID-POINT
Y-GRID
1
3
5
7
9
11
13
15
17
19
X-GRID-POINT
A.
B.
C.

Fig. 1.

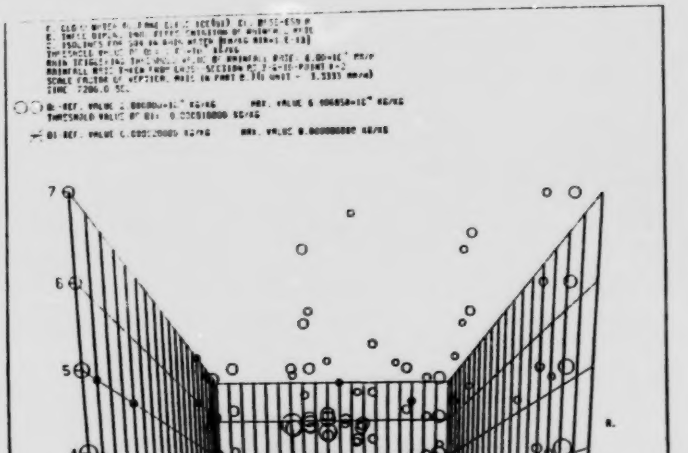
TIME 7206.0 SEC.
THRESHOLD VALUE OF QI: 0.000010000 KG/KG
7
6
5
4
2
1
0
-1
-3
Z-GRID-POINT
3
5
7
9
11
13
15
17
19
X-GRID-POINT
A.
B.
C.
6
3

Fig. 2.

end of simulations, are presented at Fig 1 (run 1) and Fig 2 (run 2), along with isolines of rainwater sulphate content close to the ground. The tropical case (run 2) produces much more cloud water and eventually more rain, but the rain develops slower and by the end of the second hour of simulation its concentration is in some grid cells higher, but the total content in the domain lower than in the Kon'Tur case (runs 1 and 3).

The two arbitrarily assumed pollution cases represent summer (runs 1 and 2) and winter (run 3) conditions of moderate pollution. For each chemical variable of the model a uniform concentration was assumed in the lowest levels of the model (up to 1500 m) and another, uniform concentration above that level. These initial profiles are presented in Table 1. The main difference between these cases is the much lower concentration of H_2O_2 for the winter case.

TABLE 1

Initial concentrations, a. below 1500 m, b. above 1500 m

		run 1&2 (a)	run 1&2 (b)	run 3 (a)	run 3 (b)
SO_2	(ppb)	15	0.10	15	0.10
NO	(ppb)	1	0.02	5	0.02
NO_2	(ppb)	4	0.08	25	0.08
n_A	(10^{-11} kg eq/ kg air)	3	3	3	3
$SO_4 =$	(10^{-9} kmole/ kg air)	2	0.2	2	0.2
H_2O_2	(ppb)	1	2	0.1	0.2
O_3	(ppb)	100	70	30	30
OH	(10^{-14} atm)	5	5	0.5	0.5

4 RESULTS

Elements of the sulphate budget are presented in Table 2. The values given in that table are, the integrated over the whole domain and two hours of simulation, source terms for the sulphate variables, computed in the chemical module. The difference between the source and sink terms is the contribution of in cloud and below-cloud processes to the total content of sulphate in the domain of the model. No snow melting took place in any case.

As can be seen, the hydrogen peroxide is the main oxidant. Even in the run 3, with low H_2O_2 content, more SO_2 is oxidized by H_2O_2 then by ozone. The below cloud scavenging was of secondary importance, especially in summer cases. Comparison of the results of the runs 1 and 3, with the same microphysics (i.e. nucleation scavenging) but different oxidant content, shows that in the summer case the oxidation accounts for roughly 50% of the deposited sulphate, the remaining part coming from the nucleation and below cloud scavenging of aerosol. The effects of oxidation were, even for run 3, significantly higher then those obtained by Niewiadomski (1989) for a field of Cu clouds, with a model with resolution of 1 km and H_2O_2 reaction removed. This difference results, at least partly, from the lower coverage by clouds in that model.

During the two hours of simulation the oxidation consumed about 2% (run 1), 7% (run 2), and 0.4% (run 3) of the SO_2 available in the domain. The consumption of H_2O_2 was 4%, 14%, and 4% respectively.

The oxidation of NO and NO_2 accounted for about 50% of nA (acidity parameter) produced in the model in run 1, 25% in run 2 and 79% in run 3. However only a fraction of the nA produced in gas phase by NOx oxidation can actually enter the cloud water and affect the acidity of rain. Rain deposited 116 kg equiv of nitrate in run 1, 76 in run 2 and 93 in run 3.

5 CONCLUSIONS

The chemical, microphysical and cumulus parameterization modules coupled for this study proved to be an effective tool for studying the mesoscale effects of cumulus clouds. After further improvements the modules will be incorporated in a more sophisticated dynamical model.

H_2O_2 was the main oxidant in cases studied, with sulphate production strongly dependent on the ammount of H_2O_2 available. Sulphate production was depended also on the ammount of liquid water in the domain. NOx oxidation was of secondary importance in this study.

The average vertical profiles of SO_2 in air and cloud water are given Fig.3 for run 1 in 30 min intervals. The upward transport of SO_2 is clearly seen. The profiles resemble those obtained by Niewiadomski (1966) for a passive pollutant with a resolution of 1 km.

TABLE 2.

The sulphate budget, kg equivalents

			run 1	run 2	run 3
Produced by SO_2 oxidation:					
in cloud water,	by	H_2O_2	1510	5100	147
in cloud water,	by	O_3	50	20	117
in rain,	by	H_2O_2	7.9	0.9	2.6
in rain,	by	O_3	0.2	0.5	0.9
cloud to rain transfer			598	851	237
cloud to snow transfer			23	0	8.5
below cloud scavenging			144	44	129
wet deposition			578	220	280

6. ACKNOWLEDGEMENT

The valuable discussions with Dr. Lubomir Levkov and his help in adapting for this study the dynamical and microphysical modules, as well as the help of Mr. Manuel Resch in preparing the plots for this paper are greatly appreciated.

7. REFERENCES

Augstein, E. and W. Wendel, 1981: Modelling of the time-dependent atmospheric tradewind boundary layer. Contr. Atmos. Phys., 53, 509-538.

Beniston, M., 1984: A numerical study of atmospheric mesoscale cellular convection. Dyn. Atmos. Ocean, 8,223-242.

Businger, J.A., J.C. Wyngaard, Y. Izumi, and E.F. Bradley, 1971: Flux-profile relationships in the atmospheric surface layer. J. Atmos. Sci., 28, 181-189.

Iribarne, J.V. and H.-R. Cho, 1988: Models of cloud chemistry. Tellus, in press.

Iribarne, J.V. and O.T. Melo, 1988: The role of clouds in the long-range transport of atmospheric pollutants and acid rain formation in Canada. Vol 3: Cloud chemistry. Canadian Electrical Associacion,

CEA No. 403 G 348

Levkov, L., D. Eppel and H. Grassl, 1986a. On the simulation of convective structures. GKSS/86/E/35

Levkov, L., D. Eppel and H. Grassl, 1986b. Simulation of convection over the ocean in the region of the intertropical convergence zone. GKSS 86/E/55

Levkov, L., D. Eppel and H. Grassl, 1987. Parameterization of phase changes of water in a mesoscale model. GKSS 87/E/44

Niewiadomski, M., 1986. A passive pollutant in a three dimensional field of convective clouds: numerical simulations. Atmospheric Environment, 20, 139-145.

Niewiadomski, M., 1989. Sulphur dioxide and sulphate in a three dimensional field of convective clouds: numerical simulations. Atmospheric Environment, in press.

Niewiadomski, M., L. Levkov, D. Jacob, and D. Eppel, 1989. Three-dimensional numerical simulations of pollutant transport and acid rain formation in a mesoscale field of convective clouds. To appear in preprints of the Symposium on the Role of Clouds in Atmospheric Chemistry and Global Climate, Anaheim, California, Jan. 23 - Feb. 3, 1989.

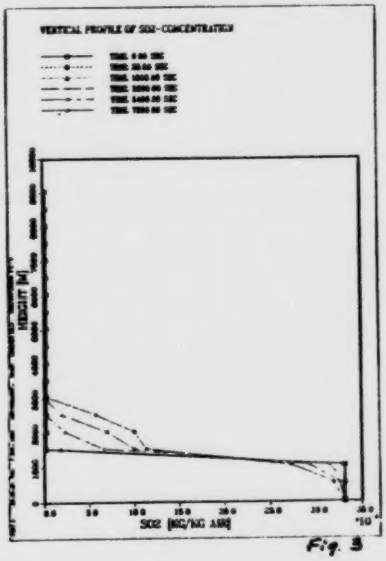

Fig. 3

AP6

DOSE RESPONSE FOR SELECTED ENVIRONMENTAL AIR POLLUTANTS:

A STUDY ON RUNNERS

R.B. Urch, F. Silverman, P. Corey,
and
R.J. Shephard

The Gage Research Institute, Departments of Medicine
and Preventive Medicine and Biostatistics, and School of
Physical and Health Education, University of Toronto

Ontario Ministry of the Environment
Project #219RR

INTRODUCTION

There has been a recent increase in the number of joggers and people competing in races and "fun runs" in urban areas, specifically Toronto. This may pose a health risk to the joggers, due to pollutant exposure. Although the pollutant levels in Toronto are relatively low, the "jogger" or "runner" is breathing at a high ventilation rate and thus is exposed to a much greater dose of pollutant than when at rest. Also, the jogger may experience "pockets" or high areas of pollution, such as alongside congested traffic arteries. Finally, exposure to most compounds is exacerbated by the fact that a high demand for oxygen may result in mouth breathing, by-passing the normal filtration mechanism of the nose. The consequences of this pollutant exposure may result in an impairment of cardiorespiratory function and a decrease in performance. Problems although exist in the measurement of personal pollutant exposure, specifically in joggers, who may traverse a large area. Any uni-site and/or remote (e.g. central station) method of measuring the pollutant exposure may not be representative of the personal exposure level (1). A multi-site method of measuring pollutant levels would better approximate the personal exposure level. The best method would be a personal monitor, carried by the subject, or in close proximity to the subject. An important feature of the current research is the measurement of the runner's personal exposure, using bicycles, carrying monitors sampling pollution concentrations along the running route, over the course of training runs.

METHODS

Subjects are selected from the Longboat Roadrunners Club which carries out weekly training runs covering distances of 10 km and 17 km over an area in downtown Toronto and along the Lakeshore corridor during rush hour. Pulmonary function (forced vital capacity (FVC), forced expiratory volume in one second (FEV_1), peak expiratory flow rate, inspiratory capacity and forced expiratory flow at 50% and 75% of forced vital capacity), and an oxygen rebreathing estimate of carboxyhaemoglobin concentration (COHb%) are measured before and after training runs; individual performance, subject evaluations, respiratory symptomatology and other health/illness information are also obtained.

Pollution measurements are obtained from existing Ministry of the Environment (MOE) air pollution monitoring network data at a central Toronto site (Breadalbane, central MOE). This data is supplemented by portable multipollutant samplers: sulphur dioxide (SO_2), nitrogen dioxide (NO_2) and respirable suspended particulate matter (RSPM). The portable samplers, designed and developed at the Gage Research Institute, use a glass and teflon impinger system with appropriate absorbing solutions for NO_2 and SO_2, described previously (2). Respirable particulates (less than 10 microns) are collected using a standard cyclone and filter assembly. Gage samplers are placed at the central MOE station (stationary samplers), and are carried on bicycles following the runners (mobile personal samplers). There are two bicycles, one follows the 10 km group of runners while the other follows the 17 km group of runners: both bicycles carry continuous electrochemical carbon monoxide (CO) monitors (Industrial Scientific Devices, model CO-260), readings being taken at specific sites along the route: the 17 km bicycle also carries a temperature/humidity sampler (Jenway, model 5500), readings being taken at four points along the route.

PRELIMINARY RESULTS

Using only NO_2, SO_2, CO and RSPM with FVC, FEV_1, eye irritation, sore/dry throat and COHb%, no relationship between estimates of exposure and 1) pulmonary function or 2) symptoms have been uncovered in a preliminary analysis. The estimates of exposure can be improved by taking into account the run distance and calculating a pollutant dose for each runner.

Pollutant dose can be estimated using the product of pollutant concentration, run time and the average respiratory minute ventilation over the run. Although ventilation cannot be measured directly on the run, an estimate can be made using heart rate as a surrogate. Each runner has a treadmill test performed in the laboratory to establish the relationship between heart rate and ventilation, over the range achieved during individual training runs. Highly significant correlations have been obtained using this protocol. During the training runs, each runner measures his/her heart rate by palpation. This heart rate is then used to estimate ventilation during the training run from each individual's experimental regression equation (ventilation versus heart rate) developed in the laboratory. This provides a more refined estimate of personal exposure than pollutant concentration alone.

ACKNOWLEDGEMENTS

The support of the Ontario Ministry of the Environment is greatly appreciated (through both its grant program and the assistance and cooperation of its staff). We also acknowledge the excellent cooperation of the Longboat Roadrunners Club and the time and effort spent by the staff of The Gage Research Institute.

REFERENCES

1. Silverman, F., Corey, P., Mintz, S, Olver, P., Hosein, R. A study of effects of ambient urban air pollution using personal samplers; a preliminary report. Environment International 8:311-316, 1982.
2. Mintz, S., Hosein, H.R., Batten, B., Silverman, F. A personal sampler for three respiratory irritants. JAPCA 32:1068, 1982.

AP7

CLASSICAL PAH FORM A MINOR PORTION OF MUTAGENS DETECTED IN HAMILTON AIR PARTICULATES.

B.E. McCarry[1], D.W. Bryant[2] and D.R. McCalla[2]. Departments of Chemistry[1] and Biochemistry[2], McMaster University, Hamilton, Ontario L8H 3Z5. MOE Project No. 386G

INTRODUCTION

The objective of this research programme is to examine the potential health hazard presented by PAH and PAH derivatives adsorbed to respirable urban particulate. To achieve this goal, we are using a celss sensitive chemical fractionation procedure and an analysis of the fractions by a combination of chromatographic methods and mutagenicity assays. This approach focuses attention on the genotoxic activity of each fraction then on the compounds within that fraction that are responsible for that genotoxic activity.

Chemical analyses of organic material associated with air particulates have produced a bewilderingly complex picture of the composition of urban air. The chemical analysis of organic extracts of total suspended respirable particulate has been extensively reported (Butler *et al.*, 1987; Hoff and Chan, 1987; Yamauchi and Handa, 1987; Daisey *et al.*, 1986; Greenberg *et al.*, 1985). By comparison, suprisingly few of the chemicals identified have been examined using short term tests (STTs). It must be pointed out that not all chemicals which are known to be carcinogenic are detected by all or indeed any of the STTs. Indeed, the analysis of organic extracts of urban air particulate employing STTs have met with limited success (Butler *et al.*, 1987; Pyysalo *et al.*, 1987; Wolff *et al.*, 1986). Application of biological assays for genotoxic activity to total extractable material is generally crude and uninformative. While these biological techniques can be extremely sensitive with individual compounds, their behavior with complex mixtures does not match analytical chemical methodologies.

MATERIALS AND METHODS

Air particulates were collected on 8 x 10 inch galss fiber filters using a hi-vol air sampler (General Metal Works L-2000 H) with flow controller set at 40 ft^3/min (1630 m^3/24h) Samplers were located on the roof of an OME station located near the centre of downtown Hamilton. Particulate samples were acquired over a period between April 4, and May 31, 1988. This period was characterized by frequent atmospheric inversions. Filters were weighed and stored at -80°C until extraction. Filters (22) from eleven days with loadings ranging from 200 to 360 milligrams per 24h (total: 5.528 g) were pooled and extracted with dichloromethane (DCM) and methanol (MEOH) in a soxhlet apparatus for 16h. The organic extract was fractionated according to the scheme presented in Figure 1. Pooled DCM and MeOH extract was applied to a neutral alumina column. Sequential elution with solvents of increasing strength yielded the following fractions: 60 mL hexane [A1], 50 mL benzene [A2], 70 mL cloroform with 1% methanol [A3], 50 mL methanol [A4], 50 mL 4:1 methanol/water [A5], and 50 mL water [A6]. Fractions [A2] and [A3] as well as [A4] and [A5] were pooled to yield [A23] and [A45]. Aliphatics which were a major contaminant of [A23] were removed by a chromatographic step elution from Sephadex LH20. Additional details of chromatography are given in the figure legends.

The Salmonella typhimurium/microsome assays for mutagenic activity with or without Araclor 1254 induced rat liver S9 (4%) were performed as described by Maron and Ames (1983).

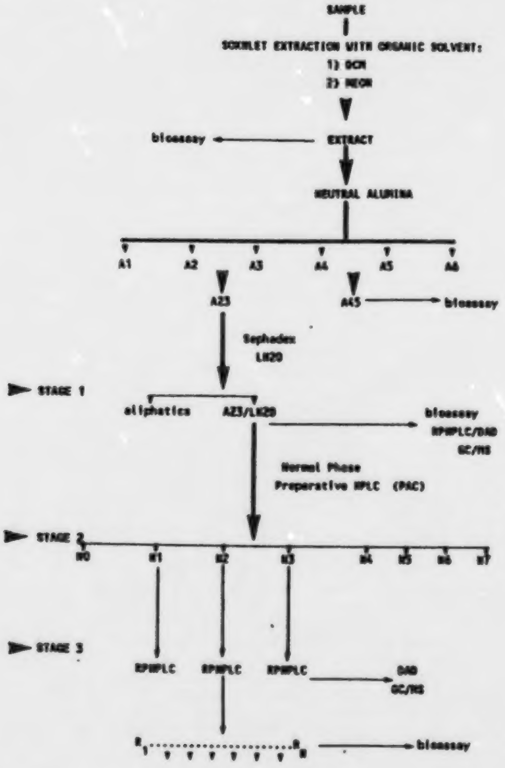
SAMPLE
SOXHLET EXTRACTION WITH ORGANIC SOLVENT:
1) DCM
2) MEOH
bioassay
EXTRACT
NEUTRAL ALUMINA
A1
A2
A3
A4
A5
A6
A23
A45
bioassay
Sephadex
LH20
STAGE 1
aliphatics
A23/LH20
bioassay
RPHPLC/DAD
GC/MS
Normal Phase
Preparative HPLC (PAC)
STAGE 2
N0
N1
N2
N3
N4
N5
N6
N7
STAGE 3
RPHPLC
RPHPLC
RPHPLC
DAD
GC/MS
R1
RN
bioassay

FIGURE 1 The scheme used for fractionation of organic extracts of urban air particulates.

RESULTS

Table 1 shows the mutagenic activity found in the crude alumina fractions from the pooled May filters. Activity, expressed as revertants per m^3 air, was determined from dose response curves. Detectable mutagens were divided between the two pooled eluant fractions A23 and A45. No mutagenic activity was lost after the passage of A23 through Sephadex LH20 (a step used to remove non-mutagenic aliphatics). Direct acting mutagens (-S9) were about equally divided between these two fractions (A23LH20: 51.1%; A45: 46.3%), while activity requiring the addition of rat liver microsomal activation (+S9) was largely found in fractions eluted with less polar solvent (A23LH20: 78.6%; A45: 21%). These results clearly indicate that while much of the mutagenic activity is associated with classical PAH (A23LH20), we have found a significant quantity of material which may be characterized as polar PAH derivatives.

TABLE 1 Mutagenic Activity of Neutral Alumina Fractions: Slope of Linear Regression of Dose Response Curves

FRACTION	Revertants per m^3 Air			
	TA98-S9	TA98+S9	TA100-S9	TA100+S9
A1	0.15	0.13	ND[a]	ND
A23LH20	5.31	26.00	2.2	27.66
A45	4.81	6.95	1.65	5.11
A6	0.12	ND	ND	ND

[a] ND: Activity not detected (background)

The A23LH20 pooled material was further divided into eight fractions (N0..N7) by normal phase chromatography as shown in Figure 2. The selection of cut points for N fractions was based both on the distribution of mutagenic activity and on chemical class. N1 = PAH, polyaromatic furans and polycyclic sulphur compounds; N2 = nitro-PAH and oxy-PAH; N3 = dinitro-PAH and polyaromatic quinones; N4 to N6 = polyaromatic ketones and polyaromatic quinones; N7 = polyaromatic nitrogen compounds (McCalla et al. 1988). Figure 2C shows the distribution of mutagens in these fractions. Column eluant was pooled for each fraction and assayed for mutagens. N1, N2 and N7 all showed a greater mutagenic response with microsomal activation while the remainder were about equally divided between direct and indirect activity. Comparing the proportion of the total mutagenic activity found across the chromatogram, N3 with 54% of the direct acting (-S9) and 41% of the indirect acting (+S9) mutagens had the majority of detected activity. This was followed by N2 (11% [-] & 13% [+]), N6 (12% & 9%), N4 (14% & 6%), N7 (3% & 10%), N5 (5% & 3%) and N1 (0% & 13%). No significant mutagens were found in N0.

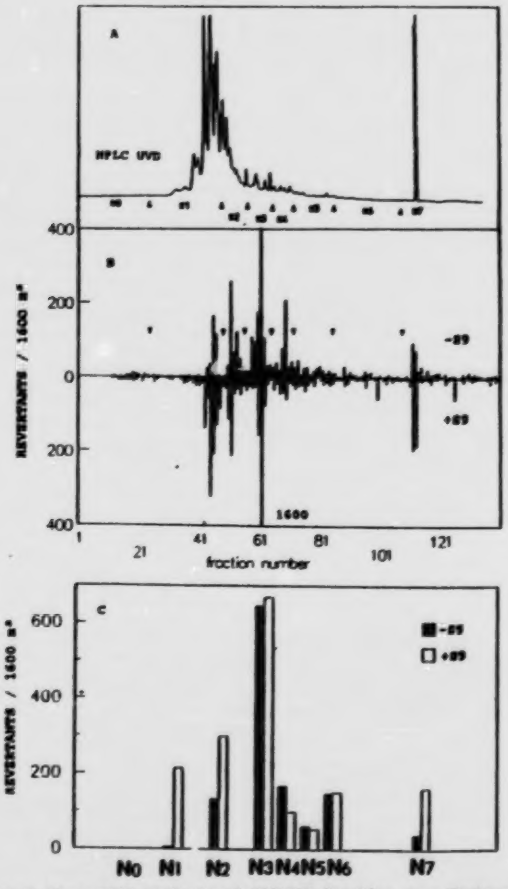

FIGURE 2 Normal phase HPLC analysis of A23LH20 fraction on a Whatman M9-PAC column. Gradient: hexane to 100% CH_2Cl_2 over 30 min; hold 100% CH_2Cl_2 to 50 min, then 0-100% ETOH to 55 min. Panel A: UV detection (250nm-400nm). Panel B: The eluant from HPLC analysis was collected in 0.5 min fractions. Solvent was evaporated and the residue taken up in DMSO for mutagenic assay in *S.typhimurium* TA98. Each fraction was assayed with (+S9) and without (-S9) microsomal activation. Panel C: Eluant from HPLC analysis was collected in 8 fractions numbered N0..N7 as indicated by the arrows in A. Solvents were evaporated and a portion of each residue analyzed for mutagens in TA98 as indicated on the figure.

Reverse phase chromatography of the H2 fraction of A23LH20 is shown in Figure 3. Here, the mutagens were divided between those with both direct and indirect activity and the more polar mutagens which only expressed genotoxicity with microsomal activation. It is also noteworthy that the less polar mutagens would not be detected if uv absorbance (250-400nm) were the criterion for selection. This also implies that while some of the compounds of the H2 class were not abundant, they possessed significant genotoxic potential.

Additional data including mutachromatograms of fraction H3 of A23LH20, and A45 from May '88 will be presented at the conference. We will also present preliminary data on particulates collected during the summer.

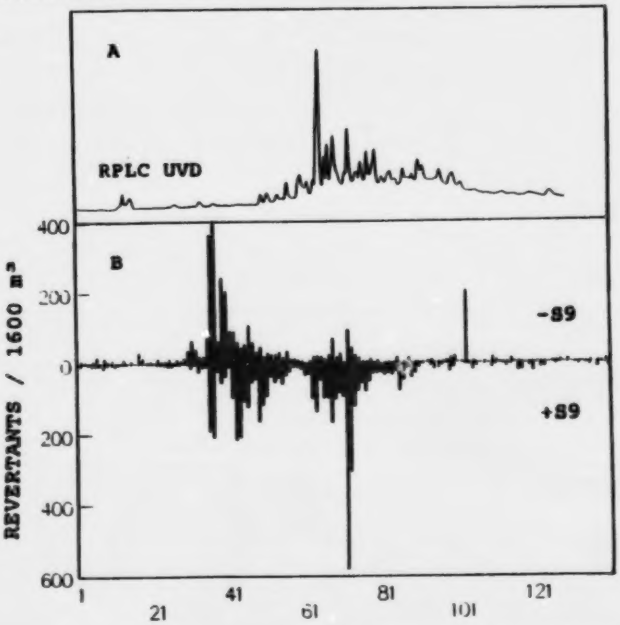

FIGURE 3 Reverse phace HPLC analysis of Fraction H2 on two 25 cm x 0.46 cm Vydac 201TP columns linked in tandem. Gradient: 60% acetonitrile (ACN)/water to 100% ACN over 30 min and hold at 100% ACN. Panel A: UV detection. Panel B: The eluant from RPHPLC analysis was collected in 0.5 min fractions and analyzed for mutagenicity as in Figure 2B.

BIBLIOGRAPHY

Butler, J.P., Kneip, T.J. and Daisey, J.M. (1987) An investigation of interurban variations in the chemical composition and mutagenic activity of airborne particulate organic matter using an integrated chemical class/bioassay system. Atmospheric Environment 21, 883-892.

Daisey, J.M., Cheney, J.L. and Lioy, P.J. (1986) Profiles of organic particulate emissions from air pollution sources: status and needs for receptor source apportionment modeling. JAPCA 36, 17-33.

Greenberg, A., Darack, F., Harkov, R. Lioy, P. and Daisey, J. (1985) Polycyclic aromatic hydrocarbons in new Jersey: A comparison of winter and summer concentrations over a two-year period. Atmospheric Environment 19, 1325-1339.

Hoff, R.M. and Chan, K. (1987) Measurement of polycyclic aromatic hydrocarbons in the air along the Niagara River. Environ. Sci. Technol. 21, 556-561.

Maron, D.M. and Ames B.N. (1983) Revised methods for the *Salmonella* mutagenicity test. Mutation Research 113, 173-215.

McCalla, D.R., Quilliam, M.A., Kaiser-Farrell, C., Tashiro, C., Hoo, K., Gibson, K.S., Lockington, M.J., Kerr, A.A., and Sheldrake, C. (1988) Integrated approach to the detection and identification of steel foundry mutagens. In *Carcinogenic and Mutagenic Responses to Aromatic Amines and Nitroarenes*, C.M King, L.J. Romano and D. Schuetzle, eds. Elsevier, NY. 47-63.

Pyysalo, H., Tuominen, J., Wickstrom, K., Skytta, E., Tikkanen, L., Salomaa, S., Sorsa, M., Nurmela, T., Mattila, T. and Pohjola, V. (1987) Polycyclic organic material (POM) in urban air. Fractionation, chemical analysis and genotoxicity of particulate and vapour phases in an industrial town in Finland. Atmospheric Environment 21, 1167-1180.

Wolff, G.T., Siak, J., Chan, T.L. and Korsog, P.E. (1986) Multivariate statistical analyses of air quality data and bacterial mutagenicity data from ambient aerosols. Atmospheric Environment 20, 2231-2241.

Yamauchi, T. and Handa, T. (1987) Characterization of aza heterocyclic hydrocarbons in urban atmospheric particulate matter. Environ. Sci. Technol. 21, 1177-1181.

AP8

Mutagenicity Studies and Risk Estimation of Complex Mixtures of Organic Airborne Contaminants

A.S Raj and D.M. Logan

Department of Biology
York University
North York, Ont. M3J 1P3

Typical human exposure to atmospheric pollutants rarely involves only a single chemical. Rather, most natural atmospheres contain complex mixtures of such potentially dangerous chemicals as polycyclic aromatic hydrocarbons (PAHs), nitro pyrenes and halogenated hydrocarbons. Although the risk associated with individual chemicals can be assessed, the risk due to mixtures is much more difficult to anticipate since the components may interact in several different and unpredictable ways. Our general approach to this problem has been to measure the mutagenicity of both individual chemicals and defined mixtures of the same chemicals. From these data we hope to identify basic principles of chemical interaction, as they relate to human risk, in natural atmospheres.

The research reported here involves two groups of chemicals (i) Benzo(a)pyrene (BaP), 7,12-Dimethyl benz(a)anthracene (DMBA) and 1 Nitro pyrene and (ii) Benzo(b)fluoranthene, Dibenz(a,h) anthracene and 1,1,1,-Trichloroethane. All have been tested alone and in combinations in two short term bioassays; the Ames Salmonella assay and the in vivo murine bone marrow micronucleus assay.

The data obtained suggest some basic principles concerning complex atmospheric mixtures and indicate where further testing is required.

Materials and Methods

a) *Chemicals*: BaP, DMBA, 1-Nitropyrene, Dibenz(a,h)anthracene, Benzo(b)fluoranthene, and 1,1,1-Trichloroethane were obtained from Aldrich Chemical Company.

b) *Bacterial Strains*: Histidine auxotrophs of *Salmonella typhimurium* strains TA 98 (frame shift mutant), and TA 100 (substitution deletion strain) were obtained from Professor B. Ames.

c) *Mice*: $B6C3F_1$ male mice, were purchased from Harlan Sprague Dawley Inc. The mice were used at 8-9 weeks of age.

d) *Ames' Salmonella assay*: The procedure described by Maron and Ames (1983) was followed. The "Plate incorporation test" was used for mutagenicity testing. All the mutagens were tested with and without S9. Mutagenicity, in units of revertants/µg, was calculated from the initial linear portion of the dose (µg/plate) response curve.

If the solvent control value was within normal range, a test chemical or mixture that produced a positive dose response over three concentrations, with the highest increase equal to at least twice the solvent control value for TA 98 and TA 100, was considered mutagenic.

e) *In vivo bone marrow micronucleus assay*: This assay measures chromosomal breakage in bone marrow cells. The assay procedure used was that of Heddle and Salamone (1981) which is a modification of the original procedure of Schmid (1973, 1975).

Results

a) Ames Assay

(i) Group I tested individually.

BaP, DMBA, 1-Nitropyrene are mutagenic to strains TA 98 and TA 100. However, BaP and DMBA are mutagenic only with S9 metabolic activation, whereas 1-Nitropyrene is mutagenic even in the absence of S9 metabolic activation.

(ii) Group II tested individually.

Neither Benzo(b)fluoranthene nor Dibenz(a,h)anthracene is mutagenic to strain TA 98 in the presence or absence of activation.

(iii) Group I tested in combinations.

Pairwise combinations of Group I and all three tested together produce more complicated responses which are shown in Table I. Tests of Group II in combinations have not yet been completed.

b) Micronucleus Assay

All chemicals were tested over dose ranges from approximately 10 mgm/kg to several hundred mgm/kg. (The actual doses depended on the previously measured LD$_{50}$). All samples were collected and assayed 48 hr after injection. The data obtained are shown in Table 2. In Group I BaP and DMBA were mutagenic and 1 Nitropyrene weakly mutagenic. BaP and DMBA combined show less than additive. In Group II Benzo(b)- fluoranthene and Dibenz(a,h)anthracene are mutagenic while 1,1,1-Trichloroethane is not. All combinations of Group II show less than additive effects.

TABLE 1.

Ames assays of potential atmospheric pollutants

Chemical(s) tested		S9	Mutagenicity with TA 98	TA 100	Remarks
GROUP I					
A.	BaP	(-	-	-	
		(+	+	+	
B.	DMBA	(-	-	-	
		(+	+	+	
C.	1-Nitropyrene	-	+	+	Direct acting mutagen
	(A + B)	+	+	+	(1)
	(A + C)	-	+	+	(2)
	(B + C)	-	+	+	(3)
	(A + B + C)	-	+	+	(4)
GROUP II					
D.	Benzo(b)fluoranthene	(-	-	NT	
		(+	-	NT	
E.	Dibenz(a,h)anthracene	(-	-	NT	
		(+	-	NT	
F.	1,1,1-Trichloroethane		NT	NT	

NT = not tested

(1) Less than additive with TA 98. Synergistic with TA 100.
(2) Synergistic with both tester strains.
(3) Synergistic with both tester strains.
(4) Less than additive with both tester strains.

TABLE 2.

Micronucleus assay of potential atmospheric pollutants

Chemical(s) Tested	Mutagenicity
GROUP I	
A. BaP	Positive
B. DMBA	Positive
C. 1-Nitropyrene	Very weakly mutagenic
(A + B)	Less than additive
(B + C)	NT
(A + C)	NT
(A + B + C)	NT
GROUP II	
D. Benzo(b)fluoranthene	Positive
E. Dibenz(a,h)anthracene	Positive
F. 1,1,1-trichlorethane	Negative
(D + E)	Less than additive
(D + F)	Less than additive
(E + F)	Less than additive
(D + E + F)	Less than additive

NT = not tested

Discussion

The preliminary data presented here demonstrate many of the difficulties encountered when one is trying to assess the biological risk of complex atmospheric mixtures. Such problems include; mutagenicity in one test system but not another (Benzo(b)fluoranthene and Dibenz(a,h)anthracene), synergism with one tester strain in the Ames assay and inhibition with another, the requirement for activation in one test system but not another, etc. Although much of the data is preliminary, when it is considered in conjunction with other testing of PAHs in our laboratory (Raj et al. 1988) some initial observations appear. For example, (1) Pairwise assays rarely give additive responses in the test systems we have used. (2) Pairwise combinations of a promutagen and a direct acting mutagen usually produce a synergistic response in the Ames Assay. Such a response is achieved even in the absence of S9 although it is even higher in the presence of S9. (3) Most synergistic responses are in the range of 1.5 to 3.0 X the additive responses. (4) The micronucleus assay rarely exhibits an additive or synergistic response.

Clearly it is premature to suggest broad principles of pollutant interaction, however the results of our experiments encourage us that such principles exist and await only further research to reveal them.

References.

Heddle, J.A. and Salamone, M.F. (1981). The micronucleus assay: In vivo. In: Short-term tests for carcinogenicity, Eds, H. Stich and R.H.C. San, Springer-Verlag, New York, pp. 243-249.

Maron, D. and Ames. (1983). Revised methods for the Salmonella mutagenicity test. Mutation Res., 113:173-215.

Raj, A.S., Wilson, A.A. and Logan, D.M. (1988). The mutagenic activity of complex mixtures of PAHs derived from ambient air particulate matter. Env. Mol. Mutagenesis (submitted for publication.

Schmid, W. (1973) Chemical testing on in vivo somatic mammalian cells. Agents and Actions, 312:77-85.

Schmid, W. (1975). The micronucleus test. Mutation Res., 31:9-15.

AP9

Extended Abstract

IN SITU MONITORING OF THE ENVIRONMENT FOR GENOTOXICITY LEVELS USING RODENTS

M. Petras*, M. Vrzoc, S. Meddins, K. Hill and T. Sands
Department of Biological Sciences, University of Windsor, Windsor, Ontario

Contamination of the environment with a plethora of man-made genotoxic agents has led to the need for a MONITORING SYSTEM which would provide an EARLY WARNING for CHANGES in ENVIRONMENTAL GENOTOXICITY since these agents attack the DNA of organisms inducing MUTATIONS and/or CARCINOMAS. The former result in long term, multigeneration effects, whereas the latter involve damage that can be seen within a single generation. Both have a significant impact on individuals and society. Towards this end two procedures have been examined: the SISTER CHROMATID EXCHANGE (SCE) TEST on bone marrow tissue and the MICRONUCLEUS (MN) ASSAY on peripheral erythrocytes. Both assays are sensitive to a broad range of genotoxicants and both have been modified so that adequate sized samples can be examined within a reasonable time period. Attempts have been made to improve the sensitivity of both, and both have been applied in the determination of genotoxicity to a number of different situations.

The organism selected at the outset for both procedures was the house mouse (*Mus domesticus*). Subsequently deermice (*Peromyscus maniculatus*) and meadow voles (*Microtus pennsylvanicus*) were also used. House mice were selected because they are ubiquitous, associated with human habitats, easily maintained in the laboratory, readily obtained in large numbers, and easily housed in corn-filled enclosures. Furthermore, inbred strains are available for controlled and genetic studies, and mice have activation and detoxification enzymes similar to those of man. Deermice and voles were used because they too were abundant in the study region and because their natural habitats are grassy areas such as those associated with landfill sites.

The wild mice used in this study were collected at various sites throughout southwestern Ontario. Laboratory mice were also placed in either 75 litre galvanized containers or 20 litre plastic enclosures. These containers, if half filled with dried corn, would provide sufficient food and moisture to keep a group of five mice alive for six to eight weeks.

For the SCE analysis, chromosomes were prepared by implanting paraffin coated tablets subcutaneously in anesthetized mice. Twenty-four hours later colchicine was injected intraperitoneally and then three hours later the mice were sacrificed. Bone marrow cells were flushed out with hypotonic solution and fixed in glacial acetic acid-methanol. The cell suspension was then applied to slides dropwise. After aging for 24 hours, the slides were incubated in a fluorescent stain (Hoechst 33258), exposed to fluorescent lights for about 26 hours and stained with Giemsa. This resulted in one sister chromatid being stained darker than its counterpart. Any exchanges between sister chromatids are easily recognized.

The MICRONUCLEUS ASSAY PROCEDURE ON PERIPHERAL ERYTHROCYTES is not as complicated. Mice were bled into heparinized capillary tubes. A drop of blood was then place on a slide and spread. After drying, the slides were fixed in absolute methanol and stained with the fluorescent dye, ACRIDINE ORANGE (after Tice, personal communication). Slides were scored for micronuclei (MN) in newly formed erythrocytes (POLYCHROMATIC ERYTHROCYTES or PCEs) and in older erythrocytes (NORMOCHROMATIC ERYTHROCYTES or NCEs) which range from 2 to 30 days in age. The MN-PCEs are indicators of recent exposure to mutagens whereas the MN-NCEs give information on chronic exposure. Finally, the ratio of PCEs to the total number of erythrocytes was determined. This is a measure of erythrocyte production.

Before either of these assays could be used in monitoring the environment the effects of a number of factors on SCE and MN levels had to be determined.

The first of these was SEX of the mice being typed. A thorough study was done on the relationship between SCE levels and sex in the 1985 samples of wild mice. In each sample females gave higher SCE values than males. The overall values in 1985 were 6.65±2.05 SCE/cell in females and 5.37±1.00 in males. The difference was significant at the 0.001 level. In general, females gave 1.2 times as many SCEs as males. This SCE difference between the sexes has held in all samples examined since 1985 and also in inbred strains. Furthermore, on treatment with a mutagen such as cyclophosphamide (CP), females gave higher SCE values than males. As a result, in comparisons of SCE levels, data from the two sexes are treated separately. The two sexes, however, did not show significantly different MN levels in peripheral erythrocytes.

Next the effect of AGE on both SCE and MN levels was considered. Mice collected from natural populations obviously vary in age. Reports that age did have an effect on SCE levels in different strains of mice (Reimer and Singh, Mech. Aging Dev. 9:303) and in human fibroblasts (Schneider and Gilman, Hum. Genet. 46:57), led to the examination of laboratory-born descendents of wild mice of different ages. No correlation between baseline SCE levels and age was observed. The mice varied in age from 2 to 12 months. Similarly, the age of the mice did not appear to affect the SCE level induced by a 50 mg/kg CP treatment. In trying to determine the effect of age on MN levels, recently caught wild mice were taken and divided into three age groups, juveniles, young adults and mature adults. The three age groups gave similar MN-PCE values. In a second study both inbred and wild mice were examined at 2, 12 and 24 months. All three age groups gave MN-PCE counts that did not differ significantly from 2.00/1000 PCEs before treatment and from 25.00/1000 PCEs after treatment with 50 mg/kg CP. So for subsequent studies mice of different age groups were pooled for both SCE and MN studies.

Since, unlike inbred strains, wild mice are highly heterogeneous another concern was the effect that GENETIC HETEROGENEITY had on both SCE and MN values. The fact that SCE induction is at least partly under genetic control has been well-established (Reimer and Singh, Genet. 105:169; see also King, Banbury Report 16:377). To test this hypothesis the induction of SCEs in the offspring of 20 wild mice was compared with that of inbred strains. The wild mice appear to be more susceptible to CP than members of inbred strains. For instance, on treatment with 4.5 mg/kg CP, 10.00 and 12.61 SCE/cell were observed in wild and inbred C3H mice, respectively. The variances in the two groups were not statistically different (Bartlet's Test of Homogeneity). Similarly, genetic heterogeneity had no effect on the variability of MN induction by CP. As a result, in both assays the genetic heterogeneity of wild mice was ignored.

The MONITORING OF NATURAL POPULATIONS OF MUS DOMESTICUS has now been carried out over a five year period. These mice were collected from corn cribs as they were being emptied. Two patterns are seen in the SCE RESULTS. There is a TEMPORAL PATTERN that is seen in most years. The SCE levels are highest during and just after the SPRAYING SEASON. This is a period beginning about the middle of May and extending to the end of June. The second pattern is a GEOGRAPHIC CLINE. In most seasons mice coming from samples in the western part of distribution (near Windsor/Detroit) show higher SCE values than those from the eastern sector.

The MN assay showed no seasonal or geographic patterns. These results were taken to indicate that the MN assay is less sensitive than the SCE assay in monitoring ambient levels of genotoxicity.

In attempting to develop an approach that would make the monitoring of open areas independent of farming practices, inbred mice were housed in CORN-FILLED 75 LITRE METAL CONTAINERS which were placed in five strategically located spots in the study area. The SCE values gave temporal and geographic patterns similar to those seen in the wild mice. Again the MN levels showed no distinct patterns.

Mice were also placed in CORN-FILLED 20 LITRE PLASTIC PAILS lined with hardware cloth. These containers with their mice were placed at a number of sites including: a plastics-molding plant, a diesel-repair shop, a chrome-plating plant, an apple orchard during the spraying season, and a tobacco-curing barn. The SCE counts in the mice housed in the plastic-molding plant and diesel garage showed modest, but statistically significant (0.05 level), increases over the controls. In the former a heat transfer oil, when injected into mice, gave a significant increase of SCEs. Although mice placed in the chrome-plating plant showed no increase in SCE values, they did show a doubling of SCE values when exposed to chromic acid in the laboratory. The MN assay did not show any significant increases in MN-PCEs in any of these cases.

Even though in a number of cases significant increases in SCE levels were observed, these were generally relatively subtle. As a result attempts have been made to enhance the sensitivity of the SCE assay. Towards this end, a series of experiments were begun involving MUTATION PROMOTORS. These included arsenic, caffeine and cyclamic acid. Alone none of these increased SCE counts significantly over baseline levels. Cyclamic acid and arsenic appeared to inhibit rather than enhance CP induction of SCEs and caffeine appeared to have no effect. Caffeine, however, did increase slightly SCE induction by mitomycin C. The other two had no effect. The effect of several MUTAGEN INHIBITORS on baseline SCE values and CP induction of SCE was also examined. The inhibitors selenium and ascorbic acid had no effect on baseline values after a 16 day exposure. There was, however a decrease in CP-induced SCE levels. This decrease was significant at the 1% level.

Attempts to increase the usefulness of the MN assay involved changing species since the peripheral blood MN assay in the house mouse did not detect genotoxicity at levels encountered under natural conditions. This was prompted by the fact that there were two species of rodents frequently encountered in the study area. These were *Peromyscus maniculatus*, the deermouse and *Microtus pennsylvanicus*, the meadow vole. Assays of peripheral blood for MN-PCEs and MN-NCEs showed values of 2.0/1000 cells and 0.0/1000 cells, respectively in newly caught *Peromyscus* and 0.0/1000 cells for both in newly caught *Microtus*. Exposure of both species to 50 mg/kg CP resulted in increases in MN-PCEs. In *Peromyscus* the peak, 11.64/1000 cells, was reached 40 hr after exposure. In *Microtus* the peak which was considerably less, 2.10/1000 cells was attained after only 24 hr. No increases were observed in MN-NCEs but this is not surprising because of the longevity of the NCEs. Similar results were obtained with 2 mg/kg mitomycin C treatments.

Multiple injections of CP resulted in a substantial increase of MN-PCEs in both *Peromyscus* and *Microtus*. In *Peromyscus* the peak reached with a series of 50 mg/kg injections was 24.90 MN-PCEs/1000 PCEs. In *Microtus* the value was 6.42. The MN-NCE levels were low, less than 1.6 MN-NCEs/1000 NCEs in both species. The low MN-NCE values suggested that as in the rat and man, the spleen was removing MN cells preferentially and so the same experiment was attempted with splenectomized rodents. In splenectomized *Peromyscus* the MN-PCE peak reached was 126.76/1000 PCEs on treatment with a series of 50 mg/kg CP injections. The MN-NCE peak was 45.11/1000 NCEs. In *Microtus*, the peaks were 20.72/1000 PCEs and 5.67/1000 NCEs,respectively. Splenectomy appears to enhance the usefulness of both *Peromyscus* and *Microtus* in the monitoring of genotoxicity.

In testing the suitability of the above approaches for monitoring genotoxicity in the environment one of the situations required should involve an accidental spill or crisis condition. No suitable situations of this nature were encountered so, such a crisis situation was simulated by having 'benzene spills' under controlled conditions. The amount of benzene 'spilt' and the length of exposure were varied. These experiments showed: that the SCE assay in *Mus* will detect short term exposures to low levels of mutagens; that the MN assay in *Mus* is less sensitive detecting only much higher levels of exposure; that the MN assay in intact *Peromyscus* will also detect only significant exposures; and that the MN assay in intact *Microtus* is of no value. The MN assays on peripheral blood erythrocytes of splenectomized *Peromyscus* and *Microtus* have considerable potential. This is especially true in *Peromyscus* where the response to mutagens such as CP or benezene appears enhanced by splenectomy.

In SUMMARY, the SISTER CHROMATID EXCHANGE ASSAY appears more sensitive than the MICRONUCLEUS ASSAY IN PERIPHERAL ERYTHROCYTES in the house mouse, *Mus domesticus*. SCE studies on wild mice have shown temporal and geographic patterns. No such patterns were observed with the MN ASSAY. Attempts to enhance the sensitivity of both techniques in the house mouse were not very successful. Preliminary studies on two other species of rodents, *Peromyscus* and *Microtus* suggest that, if the animals are splenectomized, the MN ASSAY may have the sensitivity required.

[This study has been supported in part by a grant from the Ontario Ministry of the Environment.]

AP10

METHOD DEVELOPMENT FOR THE MONITORING AND ANALYSIS OF ODOROUS ORGANICS IN AMBIENT AIR

C.C. Chan*, L. Vainer and J.W. Martin, Mann Testing Laboratories Ltd., Mississauga, Ontario L4Z 1P1.

A. Szakolcai and B. Foster, Air Resources Branch, Ministry of the Environment.

In recent years, a large number of air pollution complaints have involved odorous organic emissions. These malodorants are usually discharged into the air from a variety of municipal, industrial and agricultural activities. Nuisance caused by these activities can be attributed to four compound classes: aldehydes and ketones, amines, low molecular weight fatty acids and sulfur-containing compounds. These compounds are generally present in ambient air at very low concentrations, but due to their low odour thresholds, they are readily detected by the olfactory system.

Unfortunately, the ultra low determination of these odorous organics has been hampered by the lack of reliable sampling systems and sensitive instrumentation for analysis. In addition, many offensive odor compounds are highly reactive and their ambient concentrations are usually too low for determination by direct analysis.

This paper describes the progress of an in-depth development project to establish reliable sampling and analysis methods for these odorous organics at the parts per trillion levels. The sampling and analytical procedures will be developed separately while keeping the complete sampling system in mind. Several methods are examined in this work which include: adsorption on a solid sorbent followed by thermal or solvent elution; collection on absorber with suitable reagent and analysis by gas or liquid chromatography; use of impregnated sorbents for collection and in-situ derivatization; collection by canister followed by concentration and analysis. Our overall strategy is to develop simple methods that give prompt results with good accuracy and precision.

To date, our efforts have been concentrated on the development of reliable sampling and detection of aliphatic amines. These compounds are of environmental concern due to their irritating and sensitizing characteristics, as well as their potential photochemical conversion to carcinogenic N-nitrosamines. Aside from environmental concerns, amines are foul smelling and depict a fishy-like ammoniacal odour. Aliphatic amines are extensively used in many industries and are commonly found in the production of herbicides, insecticides, surfactants pharmaceuticals, dyes, textiles, rubber processing, photodevelopers, explosives and rocket fuels. They are also commonly found in close proximity to rendering and petroleum reprocessing plants. Threshold limit values for most amines are relatively high (up to 10 ppm/8 hrs.) while odour thresholds are extremely low, with some going as low, or below existing method detection limits. Target compounds were selected on the basis of their relative odour strengths, volatility and potential frequency of occurrence.

Several analytical techniques have been evaluated for the detection of aliphatic amines in ambient air, each one with its own biases and drawbacks. When we used gas chromatography, we were able the detect pure underivatized amines, where detection limits with a nitrogen-phosphorous specific detector are above average. The main drawbacks in a GC approach are in the separation; peak tailing, ghost peaks and column decomposition are common problems associated with such types of packed-column techniques. These problems increase with the basicity of the compound and decrease with heavier compounds. Low molecular weight primary amines are therefore most susceptible while heavier, tertiary amines will chromatograph well.

In this project, we have developed and evaluated a method for the concentration, derivatization and detection of these compounds in ambient air. The derivatization procedure utilizes 7-chloro-4-nitro-2,1,3-benzoxadiazole (NBD-Cl) as the derivative and is necessary to produce a fluorescent derivative which can subsequently be detected at very low levels by a sensitive fluorescence detector. The resulting derivative brought the method detection limits for several amines down to 40 ppt. The fluorescence detector was coupled, in series to a UV/Diode Array Detector. The latter detector was not as sensitive as the fluorescence detector, but gave confirmation UV spectra for the derivatives at higher levels. After derivatization, the sample is stable for 1 to 2 weeks, if kept in a cool, dry place. The derivatization method provides sufficient sensitivity and specificity, resulting in very few interferences. The major drawback to the above technique lies in the derivatization step. For the reaction to occur, the amine in question must be primary or secondary. This eliminates the possibility of analyzing trimethylamine with this method. To overcome this problem, an alternate technique in addition to the LC method was evaluated. An Adsorption-Thermal Desorption/ Gas Chromatography/ Mass Spectroscopy (ATD/GC/MS) method was used, where three layer sorbent cartridges trapped all organics and were subsequently desorbed, concentrated, and passed through the GC/MS. Though an in-depth evaluation was not carried out, the compound chromatographed well, producing well matching spectra at low concentrations. Coupling ATD/GC/MS with the liquid chromatography method will also give an insight into any interferences, and compounds which are not on the target list.

Several sampling adsorbents were evaluated for trapping and eluting aliphatic amines. After several preliminary experiments, Sep-PAK C_{18} cartridges were found to have maximum breakthrough volumes and no memory effects. They were the easiest to use, were purchased pre-packed, and were easily regenerated.

Method evaluation gave reproducible, reliable results with an RSD of less than 15% at low levels. Recoveries ranged from 80%-100% while an extensive storage stability study indicated that a charged Sep-PAK can be stored for up to 4 weeks prior to sampling. Spiked Sep-PAKS were stored in a cool, dry place; amine levels were stable for up to two weeks.

In conclusion, the above technique provides a sensitive, easy and reliable method for the determination of short chain aliphatic amines in ambient air. This method will also be easily adaptable to a universal monitoring system for the analysis of all four, odorous compound classes.

AP11

CHEMICAL SENSORS FROM FLUOROMETRIC TRANSDUCTION OF SELECTIVE PERTURBATIONS OF DOMAIN STRUCTURES WITHIN LIPID MULTILAYERS

U.J. KRULL, J. BRENNAN, R.S. BROWN, G. MCGIBBON, K. STEWART

Chemical Sensors Group, Department of Chemistry, Erindale Campus, University of Toronto, 3359 Mississauga Road North, Mississauga, Ontario, Canada L5L 1C6

INTRODUCTION

A form of artificial chemoreception suitable for development of sensitive chemical sensors can be derived from physical perturbation of a stabilized lipid membrane by "receptor" molecules that participate in selective binding processes [1,2]. The perturbation can be physical and/or electrostatic, and may be used to transduce the chemical signal of analyte concentration into corresponding electrochemical or optical signals. A fluorescent optical sensing strategy provides many advantages with respect to the electrochemical system, the paramount being the availability of simultaneous multidimensional analysis using the parameters of wavelength, intensity, polarization and lifetime which can be derived directly from a fluorescently-tagged "receptor", or a fluorescent lipid membrane [3]. Concurrent analysis of this large quantity of data may uniquely define selective binding events while also quantitatively detecting interference effects and providing self-calibration by means of signal ratioing.

One important aspect of the electrochemical sensing system is the sensitivity derived from an intrinsic amplification process. A single selective binding event between a "receptor" and one target molecule can result in an increase of transmembrane conduction involving thousands of ions. An analog in the optical experiment would necessitate that hundreds or thousands of fluorescent molecules should be influenced by a single selective binding event. This can be achieved by means of modulation of the phase structure of the lipid membrane by the binding event.

Recent work with fluorescence microscopy of lipid monolayers at the air-water interface has shown that membranes of both homogeneous and heterogeneous lipid composition often are formed from a number of phases in co-existence [4,5]. Fluorescently tagged lipid molecules can be used as probes of phase structure by the partitioning of such species into the least structurally ordered areas. The resulting microscopic fluorescent image may show areas of brightness and darkness on the order of 10-200 um diameters as a function of the relative concentration of the fluorescent species available for imaging. It has been shown that these domains within lipid monolayers are sensitive to surface pressure, electrostatic potential and edge active species [6,7]. This provides significant opportunities for domain or phase structure alteration by manipulation of these latter properties using selective chemical reactions. Analysis of lipid membranes in different phases has shown that large differences in the multidimensional parameters associated with fluorescence can be observed, thereby demonstrating an optical method to achieve an intrinsic amplification of selective binding events [3].

Previous work reported during this project indicated that lipid multilayers could be prepared by repetitive casting of monolayers from an air–water interface to various supports, and that these multilayers could be prepared with sufficient thickness and transparency to operate as waveguides [8]. The present work extends investigations to determine the structure of such waveguides, and whether sufficient molecular mobility exists within multilayers stabilized on solid supports to permit phase transitions to occur.

EXPERIMENTAL

Stearic acid multilayers were prepared on commercial silicon wafers (orientation N(100); 3" diameter, Arrel Co., St. Charles, MO) for waveguiding studies. A custom designed trough using a Wilhelmy plate transducer and a pneumatic film lift was used for monolayer depositions [9,10]. Characterization of multilayer thickness and structural regularity was done by ellipsometry (Auto EL, Rudolph Research, Flanders, NJ). Fluorescence demonstrating multilayer waveguiding was obtained by irradiation of the wafers by means of a shielded fibre–optic cable at various angles with at 488 nm from an argon–ion laser (Coherent Innova 70) [8]. Fluorescence for investigation of the effects of stimulant gases was induced by broad illumination of the lipid multilayer with an approximate incident angle of 60°. The detection system consisted of a Heath monochromator (Schlumberger, Toronto, ON) and a Hamamatsu R928 photomultiplier tube (Hamamatsu Inc., Bridgewater, NJ) operated at 1 KV with a Zeiss Unit P power supply (Carl Zeiss, FRG). A cut–off filter blocking wavelengths shorter than 495 nm was placed between the sample and monochromator entrance slit (slit width 600 µm).

Scanning electron microscopy (Hitachi Model S570) of a number of cleaved and whole samples was done after samples were prepared by coating the surface with gold. Fluorescence microscopy of monolayers on an air–water interface of a Langmuir-Blodgett thin film balance (Lauda Model 1974, Sybron-Brinkman Instruments, Toronto, ON) and multilayers on silicon wafers was done. The laser source was the continuous Argon laser at 488 nm and 10 mW power. A Zeiss inverted fluorescence microscope (Model IM, Carl Zeiss, FRG) was mounted on a stand so that the objective was situated directly above the monolayer under study. The microscope had two perpendicular optical axes which met at a dichroic mirror assembly. The laser beam entered along one axis and was reflected down to the monolayer by the dichroic mirror. The fluorescence emitted from the monolayer was then separated from backscattered laser radiation at the dichroic mirror. A low light level Dage model NTI SIT video camera (Dage Ltd., Michigan City, IN) was used to generate a video image of the fluorescent sample. The camera was linked with the Oculus image processing package (Coreco Inc., Toronto, ON) which digitized the image (480 x 512 pixels) for storage and processing. The microscope, film balance, laser and camera were mounted on a gas damped vibration isolation table, (Melles Griot, Rochester, NY).

RESULTS AND DISCUSSION

Details of the physical processes of multilayer deposition have been previously described [8]. Attention to the reproducibility of monolayer casting, and control of contamination from the environment (eg. dust), provided for optimized multilayer assemblies, which were stable for extended periods in air and during water washes, as determined by ellipsometric refractive index and thickness measurements. Monolayers containing 2% NBD–PE that were deposited on a thick stearic acid multilayer base were not as structurally stable. The small quantity of fluorescent probe sufficiently altered the monolayers to allow them to be removed from the stearic acid base by rinsing with water. This indicates either an increased water solubility of the monolayer constituents, or more likely a reduction of the electrostatic forces associated with formal charge and hydrogen bonding which stabilized adhesion to the substrate. The reduction of stability in water was not reflected in the optical properties of multilayers stored in air, and these membrane systems remained stable indefinitely.

Scanning electron microscopy confirmed the ellipsometric results which had indicated that multilayers were smooth, regular and of thickness of approximately 4 nm per monolayer deposition. The total surface area which was irregular in terms of localized depressions or rough islands was less than 10%, and could be attributed to dust or KCl crystals in most cases. Even though this amount of imperfection in the final surface monolayer was relatively small, it is significant when integrated by the > 200 monolayers which compose the multilayer assembly. A cross-sectional view through a multilayer on silicon shows the presence of many structural irregularities with some spanning many monolayers. These imperfections increase the attenuation of optical power per unit distance by scattering radiation due to localized refractive index variations in lipid multilayer waveguiding experiments. The light scattering process likely served to enhance the intensity of radiation available for excitation of fluorescence in the surface layers of the short waveguides, and would result in a steep gradient of fluorescence intensity observed over greater lengths of waveguide.

Stearic acid monolayers containing 2% NBD–PE were prepared as monolayers at the air-water interface of the Lauda film balance, and were studied by fluorescence microscopy to evaluate phase/domain structure evolution at various surface compression pressures. The pressure-area isotherm indicated the presence of a number of inflection points that have been previously ascribed to phase transitions between the low surface pressure "gas", liquid, liquid-crystal and high pressure gel (crystalline) phases. Corresponding fluorescence images showed no discernable structure of the "gas" phase, but mixed phases in co-existence were observed at all pressures greater than 12 $mN \cdot m^{-1}$ until the collapse pressure. Slow compression and expansion of monolayers indicates that the evolution of mixed phases is dynamic and reversible. Surface pressure, surface potential and the presence of proteins modifies the extent of development of domains and therefore the relative fluorescent signals available during the analytical experiment. A further exciting discovery is that at the transition between surface pressure regimes related to development of new domains (eg. from liquid to liquid crystalline), an enormous transient fluorescence intensity increase may be observed. This is likely due to quantum yield enhancement and fluoxophore concentration quenching reduction as the monolayer enters an overcompressed non-equilibrium state before nucleation and kinetic processes can accommodate formation of the new domains. This intensity enhancement observed during phase "switching" processes may provide a high degree of intrinsic amplification of a selective binding process, if the latter can induce physical or electrostatic membrane perturbations which lead to phase transitions.

The structure of stearic acid monolayers labelled with NBD–PE could be observed by fluorescence microscopy in-situ after deposition by the rapid casting technique onto silicon wafers. The fast casting process, which is necessary for multilayer formation, alters the original domain distribution of the monolayer established on the trough. A "streaking" effect is observed where the striations are aligned with the direction of monolayer casting, and indicate that directional pressure effects lead to oriented domains that can be stabilized for extended periods by deposition onto the stearic acid multilayer. This would imply that relaxation effects and lipid mobility are greatly reduced once deposition to a substrate has been achieved, even when the substrate is a loose association of stearic acid molecules. The limitations imposed by reduction of molecular mobility could compromise the kinetics of formation of new domains upon membrane perturbation by selective and non-selective processes.

Spectrofluorometric analysis of the emission profile and intensity of the NBD-PE probe in stearic acid multilayers when exposed to various stimulant gases indicate that placement in a vacuum provides insignificant effects, but non-selective interactions with gases such as ethanol, hexanes and chloroform all provide fluorescent intensity increases with little alteration of the emission profile. These different gases have previously been shown to cause non-specific expansion of monolayer and bilayer lipid membranes that were not surface-stabilized [11,12]. The fluorescent intensity increase observed for the deposited multilayers is consistent with an average increase in membrane fluidity, where the fluorescent probe could partition into a larger fluid phase component that would provide for a relative reduction of fluorophore concentration resulting in decreased self-quenching [13]. The selective interaction of the fluorescence quenching agent dimethyl aniline with NBD provided an anticipated reduction of fluorescent intensity, and demonstrated the correct operation of the fluorescent probe. A feature of multilayer fluorescence response to stimulant gases that was crucial to further analytical development was reversibility of response. Tests in which the multilayer was placed in the vacuum chambre and repeatedly exposed to stimulant gas and vacuum indicated complete reversibility of the analytical signal within seconds of any change in the environmental content of the stimulant gas. Similar experiments have shown that such functional response can be obtained many months after the initial fabrication of the multilayer assembly. This work is now being extended to systems of greater molecular mobility such as fluorescent phospholipid monolayers on stearic acid multilayers and the modulation of the microscopic phase transitions by selective "receptors" such as acetylcholine receptor.

ACKNOWLEDGEMENTS

We are grateful to the Ontario Ministry of the Environment for financial support of this work, and to the Natural Sciences and Engineering Research Council of Canada, Imperial Oil Canada and the Canadian Defense Research Establishment for further provision of equipment and facilities used during this project.

REFERENCES

1. U.J. Krull and M. Thompson, IEEE-Electron Devices, 32, 1180 (1985).
2. M. Thompson, V.N. Dorn, U.J. Krull, J.S. Tauskela, E.T. Vandenberg and M.E. Wong, Anal. Chim. Acta, 180, 251 (1986).
3. U.J. Krull, R.S. Brown, R.F. DeBono and B.D. Hougham, Talanta, 35, 129 (1988).
4. R.M. Weis, H.M. McConnell, Nature (London), 310, 47 (1984).
5. V.M. Heckl, Ph.D. Thesis, Technical University of Munich, 1988.
6. H.M. McConnell annd V.T. Moy, J. Phys. Chem., 92, 4521 (1988).
7. R.M. Weis and H.M. McConnell, J. Phys. Chem., 89, 4453 (1985).
8. U.J. Krull, R.S. Brown and K. Stewart, Proceedings of the 1987 Technology Transfer Conference, Ontario Ministry of the Environment, Toronto
9. U.J. Krull, M. Thompson and M.E. Wong, Analyst, 110, 1299 (1985).
10. R.S. Brown and U.J. Krull, Analyst, 112, 1165 (1987).
11. J. Reyes and R. Latorre, Biophys. J., 28, 259 (1979).
12. N.R. Clement and J.M. Gould, Biochemistry, 20, 1539 (1981).
13. J.R. Wiener, R. Pal, Y. Barenholz and R.R. Wagner, Biochemistry, 24, 7651 (1985).

AP12

ATMOSPHERIC MEASUREMENTS OF NATURAL HYDROCARBONS USING GAS CHROMATOGRAPHY/MASS SPECTROMETRY

H. Niki and B. B. Khouw
Chemistry Department
and
Centre for Atmospheric Chemistry
York University

SUMMARY

Recent field and modelling studies in the US and Europe have demonstrated that the biogenic non-methane hydrocarbons such as isoprene and the mono-terpenes can have a significant impact on atmospheric formation of various oxidants and acidic compounds in forested rural areas. At present, no comparable data exist on these natural hydrocarbons in a Canadian setting. To obtain an annual data set for a number of key volatile organic compounds (VOC) mainly of natural origin, a 3-year project has been initiated starting from the development and validation of analytical methods. High resolution gas chromatography -mass spectrometry in combination with various sample collection and preconcentration methods is in common use for analysis of these natural VOC. A critical performance evaluation of the two most widely employed sample-handling methods, i.e. (1) cryogenic collection - preconcentration and (2) adsorptive sampling - thermal desorption, is underway as a prerequisite for field measurements. During the summer of 1988, samples collected at the Ministry's site at Dorset and other forested areas have been examined using the cryogenic preconcentration - GC method. Also, to enhance the quality and speed of data acquisition, a fully automated preconcentration - injection system is being developed as a reference sample handling device.

Introduction

Large quantities of non-methane hydrocarbons (NMHCs) are emitted into the atmosphere from vegetation. A recent emission inventory in Ontario indicates that the ratio of natural to anthropogenic NMHCs exceeds a factor of 20.[1,2] The natural NMHCs such as isoprene and mono-terpenes can play an important role in the atmospheric transforamtion of NO_x and SO_2, and in the formation of various oxidants, e.g. ozone, hydrogen peroxide, peroxyacetyl nitrate (PAN) and oxygenated organic compounds which contribute to regional-scale air pollution.[3,4] However, the ambient concentrations of natural NMHCs are presently unknown in a Canadian setting. High resolution GC/MS in combination with various sampling methods is widely employed for atmospheric measurements of NMHCs. However, there is a lack of well-established analytical protocols for these labile organic compounds at sub-ppb mixing ratio ($\leq 10^{10}$ molecule cm^{-3}). Thus, the initial phase of this project is devoted to a critical evaluation and improvement of sample-handling methods for GC/MS analysis.

Experimental

Figure 1 illustrates a schematic of sample handling system for GC/MS analysis. A sample preconcentration system consisting of a "cryogenic" absorption/thermal desorption-injection unit and vacuum gas-handling system constructed of stainless steel throughout have been assembled in-house. Details of the design and operation of this system are described elsewhere.[6] Also, a commercial "sorbent" thermal adsorption/desorption unit has been interfaced to the "cryogenic" system to conduct a direct comparison of the two preconcentration systems.

Results and Discussion

During the summer of 1988, air samples collected in stainless steel flasks at the Ministry's site at Dorset and other forested areas have been examined using the cryogenic preconcentration - GC analysis for C_2 and C_3-C_{10} hydrocarbons. Typically, 500 cm^3 of the air samples were sufficient for analysis of the natural NMHCs, e.g. ethylene, isoprene and terpenes, with a detection limit of <0.1 ppb volume mixing ratio. Possible deterioration of samples during storage was not apparent for light HCs up to a week after collection. Further tests on the sample integrity and preconcentration efficiency as well as performance optimization of the GC/MS system are in progress. Also, to enhance data acquisition speed and reproducibility, a fully automated cryogenic preconcentration system is being assembled.

Acknowledgements

We wish to thank the Air Resources Branch of the Ontario Ministry of the Environment, the Atmospheric Environment Service (AES) of Environment Canada, and the Natural Sciences and Engineering Research Council for financial assistance. We are grateful to Dr. E. Singer of the Ministry and Dr. J. Bottenheim of AES for their advice and encouragement. Technical contributions by the member of our research group (R. Dash, B. Kieser, G. Kiesel, E. Konor, J. Lai, H. Malle, B. Taylor, L. Toth and G. Yarwood) are much appreciated.

References

1. Lusis, M.A. (1986) "Oxidant Control Strategy for Ontario: First Status Report", Ontario Ministry of the Environment internal report.
2. Kurtz, J. (Feb. 1987) "A Review of the Ontario Ozone Problem", Conference Proc. of North American Oxidant Symp. p.363.
3. Trainer, M., E.J. Williams, D.D. Parrish, M.P. Buhr, E.J. Allwine, H.H. Westberg, F.C. Fehsenfeld, (1987) "Models and Observations in the Impact of Natural Hydrocarbons on Rural Ozone", Nature, 329, 705-707.
5. Chameides, W.L., R.W. Lindsay, J. Richardson, and C.S. Kaing, (1988) "The Role of Biogenic Hydrocarbons in Urban Photochemical Smog: Atlanta as a Case Study", Science, 241, 1473-1475.
6. Kieser, B. (1988) "Development of a System for Sample Handling and Preconcentration in the Analysis of Ambient Air Samples for Trace Organic Compounds', Thesis, York University.

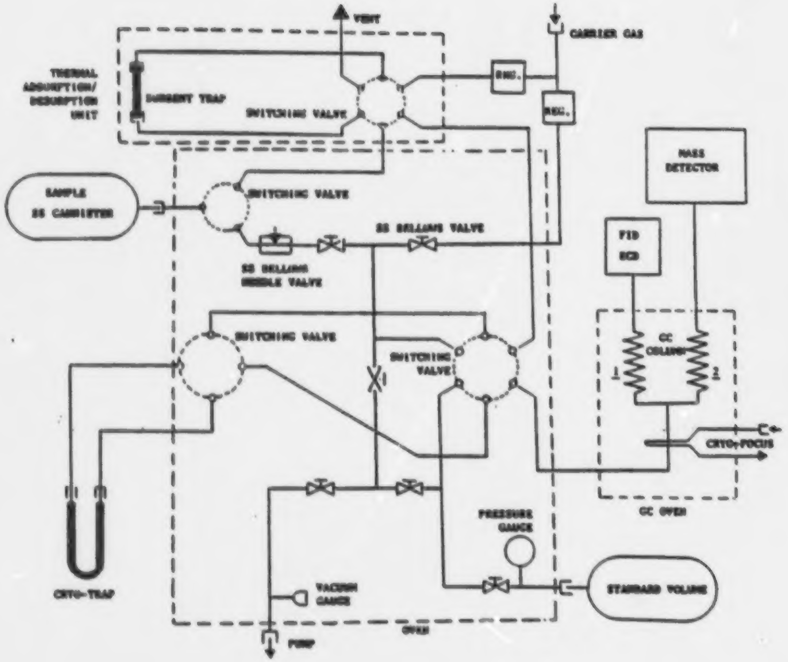
VENT
CARRIER GAS
THERMAL ADSORPTION/ DESORPTION UNIT
SORBENT TRAP
SWITCHING VALVE
REG.
REG.
SAMPLE SS CANISTER
SWITCHING VALVE
SS BELLOWS VALVE
SS BELLOWS NEEDLE VALVE
MASS DETECTOR
FID ECD
SWITCHING VALVE
SWITCHING VALVE
GC COLUMN
1
2
CRYO-FOCUS
GC OVEN
PRESSURE GAUGE
CRYO-TRAP
VACUUM GAUGE
STANDARD VOLUME
PUMP
OVEN

Fig.1: Schematic of Sample Preconcentration System for GC/MS Analysis

AP13

UTILIZATION OF ESTABLISHED AIR POLLUTION MONITORING NETWORKS IN ONTARIO FOLLOWING NUCLEAR INCIDENTS

J.A. Slade and G. Laszlo
Atomic Energy of Canada Limited
Chalk River Nuclear Laboratories
Chalk River, Ontario, K0J 1J0

1. INTRODUCTION

This preliminary study, for the Ontario Ministry of the Environment's Air Resources Branch, was performed by Atomic Energy of Canada Limited's Radiation and Industrial Safety Branch at the Chalk River Nuclear Laboratories. The study was funded by the Ministry's Research Grants Program. The objective of the study was to investigate the potential of using charcoal-loaded filter paper in conventional high volume (HiVol) sampling networks for monitoring of radioactive iodine fission products following nuclear incidents. The emphasis was to evaluate various commercially available sampling media, under controlled laboratory conditions, for radioiodine retention.

Four suppliers of charcoal-loaded filter paper potentially suitable for radioiodine monitoring were identified. From these suppliers eight media types were chosen for evaluation. Samples of these media types were tested for CH_3I and I_2 retention in an environmental chamber under controlled conditions. The parameters varied in the study were: adsorbate concentration (0.1 and 0.01 mg/m^3 for both CH_3I and I_2); challenge gas face velocity (35,50, and 60 cm/s); and relative humidity (40%,75%, and 95%). Temperature for most of the study was set at 25°C, although some low temperature testing (0°C) was performed on one media type. Altogether 279 measurements of CH_3I and I_2 retention were performed on the various media samples.

2. BACKGROUND

Significant benefits can be obtained by monitoring airborne radionuclides within existing air pollution monitoring networks following nuclear incidents. This study investigates the potential of using charcoal-loaded filter paper to monitor radiobiologically significant iodine fission products, with currently installed equipment used for routine monitoring of air pollutants.

Environmental monitoring is a key element in identifying the extent and consequences of releases of radioactive materials to the atmosphere during and immediately following nuclear incidents. Close attention must be paid to the need for the immediate monitoring of the airborne pathway. The potential rapid dispersion of radionuclides in the air after a nuclear incident, and the possibility of direct inhalation of these materials, gives priority to this pathway [1]. As a consequence, nuclear utilities include substantial provisions for deploying both personnel and equipment to monitor airborne radioactivity in their emergency plans. In regions remote from the scene of an accident, where government agencies assume the responsibility of monitoring, logistical problems may be encountered in deploying monitoring equipment. Similar problems can be encountered with monitoring plumes of a transborder origin. Many difficulties could be overcome if existing air pollution sampling networks, utilizing HiVol sampling equipment, could be simply and effectively adapted to collect airborne radionuclides.

For particulate radioactive contaminants, particulate filters already used in HiVol sampling networks are an effective sampling media. However, this media has no ability to trap gaseous radioiodines. Experience in the nuclear industry, and following the accidents at Three Mile Island and Chernobyl, demonstrate radioiodines are predominantly in the gaseous state. Experience has shown that molecular iodine (I_2) is the predominant species particularly in the initial release; however, organic iodides (mainly assumed to be CH_3I) can also form a significant fraction. As they are probably the most radiobiologically significant fission products, an effective monitoring program following a nuclear incident must have the ability to collect radioiodines, the most notable of which is ^{131}I. Several approaches are available to accomplish this. One method would be to deploy expensive portable high volume samplers using special deep-bed charcoal canisters. Another would be to design and manufacture deep-bed charcoal canisters which could be installed on the HiVol sampler. A third method, which requires no additional equipment purchase or modification, is the use of charcoal-loaded filter paper. Although having a lower collection efficiency for radioiodines, particularly organic iodides (methyl iodide), charcoal-loaded filter papers would be the easiest to deploy at a much lower cost.

3. CHARCOAL LOADED FILTER MEDIA SELECTION

Following an extensive literature and product search four suppliers of suitable charcoal-loaded filter paper were identified. From these suppliers eight media types were tested for radioiodine collection efficiency (retention). The suppliers and media types are shown in Table 1. The factors considered in selecting potential media included: the carbon loading of the media (g/m^2); the physical stability and durability of the charcoal/fibre matrix; and the addition of chemicals (KI, triethylenediamine) which enhance the collection of organic iodides. Table 2 shows the properties and specifications of the selected media.

Table 1. Charcoal-Loaded Filter Paper Suppliers

Supplier	Address	Media
Dexter Materials Division	Burlington, Ontario	Grade X3954
"	"	Grade 4703
F&J Specialty Products	Miami Springs, Flor.	CI 47
Whatman Paper Division	Clifton, New Jersey	Grade 72
Extraction Systems Inc.	Norwood, Mass.	Hyperm 16-2
"	"	Hyperm 7-5
"	"	Hyperm 12-5
"	"	Hyperm 13-2

Table 2. Charcoal-Loaded Filter Paper Specifications

Media	Carbon Loading (g/m^2)	Thickness (mm)	Chemical Impregnant
Grade X3954	106	0.84	None
Grade 4703	80	0.82	None
CI 47	n/a***	0.78	None
Grade 72	100	0.80	None
Hyperm 16-2*	540	3.5	TEDA**
Hyperm 7-5	240	1.2	TEDA
Hyperm 12-5	410	1.8	TEDA
Hyperm 13-2	440	2.5	TEDA

* The first number in the numerical coding for the Hyperm media represents the carbon loading in oz/yd^2, the second number represents the pressure drop in mm of water.

** TEDA - triethylenediamine at 5% of charcoal weight.

*** n/a - not available

4. EXPERIMENTAL DESIGN

Representative samples (approximately 50 mm diameter discs) of the charcoal-loaded filter media were tested for both molecular iodine (I_2) and methyl iodide (CH_3I) retention under controlled laboratory conditions. The filter media samples were sealed into P.V.C. envelopes with welded edges, in the center of which were cut 25 mm diameter holes to allow free passage of air through the center of the filters. The media samples were then clamped into test assemblies fabricated from standard 1" I.D. conical glass pipe. The P.V.C. envelopes provided a seal between the glass joints of the test assembly and the filter media, thus eliminating any inleakage of air. The test assemblies were equipped with a deep bed of high efficiency nuclear-grade charcoal downstream of the test media to trap all the iodine gas which passes the filter media.

The charcoal-loaded filter media and back-up charcoal were equilibrated with air at the test face velocity, relative humidity, and temperature for 30 minutes. The media was then challenged with an ^{131}I traced iodine (CH_3I or I_2) and humid air mixture (feed period) for 120 minutes. Following the feed period the charcoal-loaded filter media was purged with the humid air (elution period) for 30 minutes. The ^{131}I retained in both the charcoal-loaded filter media and back-up charcoal was determined using a specially calibrated NaI gamma spectrometry system. The percent retention of the charcoal-loaded filter paper was determined as follows:

$$R(\%) = C_F/(C_F+C_D)\cdot 100$$

Where

C_F = the ^{131}I count rate in counts per second
corrected for detector efficiency on the filter media
C_D = the ^{131}I count rate in counts per second
corrected for detector efficiency on the deep-bed back-up charcoal.

The standard deviation of the retention of each test was computed. The error was also computed at the 95 % confidence interval. The standard deviations were determined through an error propagation analysis of the standard deviations of all the components used to calculate retention. The most significant components were the efficiencies of the detector system at the various counting geometries, and the individual observed count rates. The error propagation analysis followed that outlined in A.S.T.M. Standard D3803-79 [2].

5. RESULTS

Preliminary tests with CH_3I revealed that media types employing non-chemically impregnated charcoal (four of eight) were not suitable for this application. These media exhibited CH_3I retentions of less than 0.2%. The majority of the experimental work was, therefore, concentrated on media using triethylenediamine (TEDA) impregnated activated charcoal. TEDA greatly enhances the charcoal's ability to retain CH_3I, particularly in high humidity conditions, by chemical reaction with CH_3I to produce a quaternary ammonium salt which is strongly bonded to the charcoal. The manufacturer of this media is Extraction Systems Inc of Norwood, Mass., USA. Four media types from Extraction Systems were evaluated. After examining preliminary test results and the physical properties of the four media types the best candidate for this application, Hyperm 12-5, was chosen for detailed evaluation.

For clarity of presentation the media types evaluated were assigned codes, namely: Dexter Grade X3954 (DA), Dexter Grade 4703 (DB), F&J CI 47 (FJ), Whatman Grade 72 (W), Extraction Systems Hyperm 16-2 (EA), Hyperm 7-5 (EB), Hyperm 12-5 (EC), and Hyperm 13-2 (ED).

The mean retentions of CH_3I (averaged over all test conditions) by all media types is shown in Figure 1. An expansion of the CH_3I retention characteristics of the FJ, DA, DB, and W media is shown in Figure 2. The mean retentions of I_2 (averaged over all test conditions) by all media types is shown in Figure 3. The error bars shown indicate the errors calculated at the 95, 90, and 75% confidence intervals.

Figure 1. Error Bars of Efficiency by Media Types (CH_3I cases only)

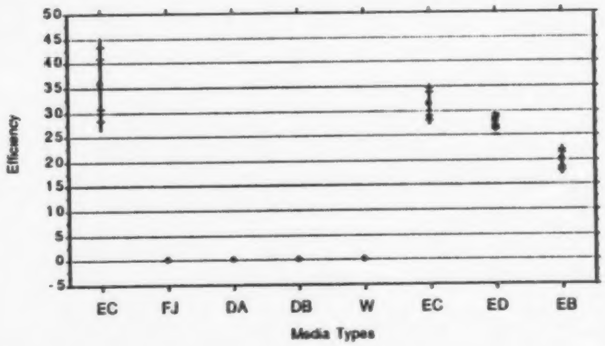

Figure 2. Error Bars of Efficiency by Media Types FJ, DA, DB, W
(CH_3I cases only)

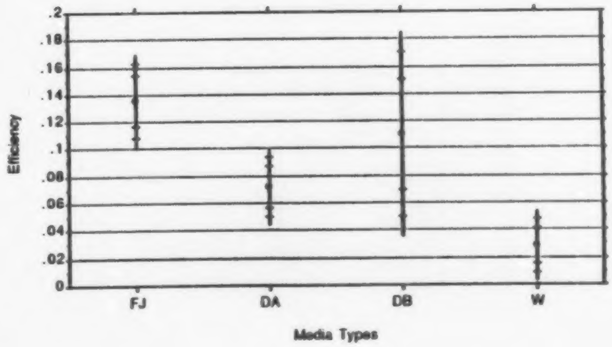

Figure 3. Error Bars of Efficiency by Media Types
(I_2 cases only)

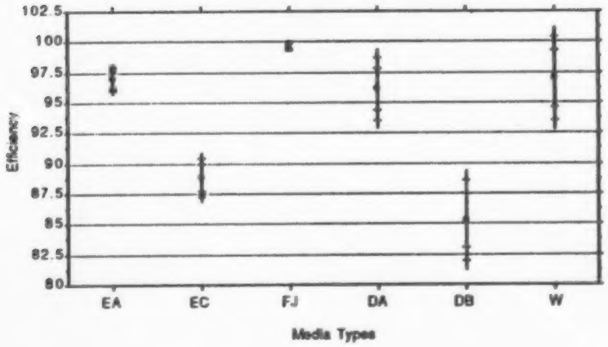

As mentioned above the Hyperm 12-5 (EC) media was evaluated in the most detail. The CH_3I and I_2 retention characteristics of the EC media at all test conditions are shown in Figure 4 and Figure 5 respectively. The code for the averages shown is given in Table 3 below.

Table 3. Profile Curves Codes

Code	Factor@Level
1	overall average
2	velocity = 35 cm/s
3	velocity = 50 cm/s
4	velocity = 60 cm/s
5	rel.hum. = low (27.5%-40%)
6	rel.hum. = medium (75%)
7	rel.hum. = high (90%-95%)
8	concentr. = low (.01 mg/m^3)
9	concentr. = high (.1 mg/m^3)

Figure 4. Profile Curves for Medium EC for 25°C and 0°C (CH_3I cases only)

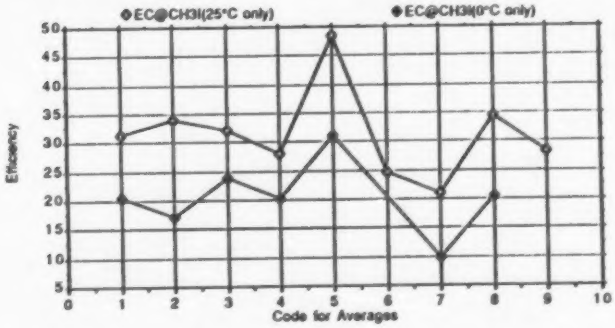

Figure 5. Profile Curve for Medium EC (I_2 cases only)

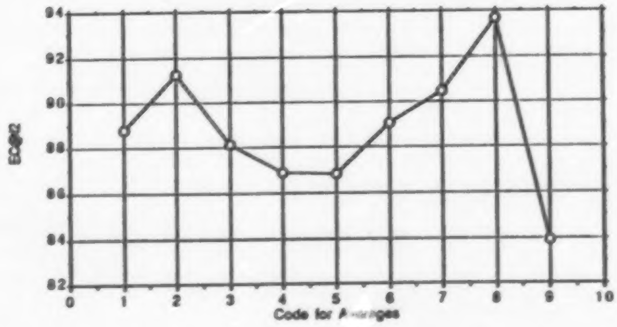

6. CONCLUSIONS AND RECOMMENDATIONS

A literature and product search was undertaken to locate and identify suitable charcoal-loaded filter paper for environmental monitoring of radioiodines. As a result of this search four manufacturers of this media were contacted. From these four manufacturers eight different media type samples were obtained for evaluation under controlled laboratory conditions. Altogether 279 measurements of radioiodine retention (CH_3I and I_2) were made on these media types. Preliminary tests with CH_3I eliminated most of the media types as candidates for radioiodine sampling. Certain physical properties (excessive charcoal loss) precluded others for this application.

From the results of this study the following conclusions and recommendations are made:

1. A suitable charcoal-loaded filter paper for environmental radioiodine monitoring must employ TEDA impregnated activated charcoal to trap and retain organic iodides (CH_3I). Non-impregnated charcoal filter papers were found to retain less than 0.2% CH_3I.

2. A charcoal-loaded filter paper employing TEDA impregnated activated charcoal and exhibiting good physical properties (low charcoal loss) was identified as a potential candidate for environmental radioiodine monitoring. The media, Hyperm 12-5, is manufactured by Extraction Systems Inc of Norwood, Mass., USA. The mean CH_3I and I_2 retentions, over all test conditions, for this media was 31.38% and 88.80% respectively.

3. It was found that all the main factors studied (namely; adsorbate concentration, face velocity, and relative humidity) have a significant negative effect on the retention of CH_3I by Hyperm 12-5. The synergistic effect of all three main factors was also found to be highly significant. The retention of CH_3I by Hyperm 12-5 was also found to be significantly lower at low temperatures (0°C).

4. It was found that for I_2 retention by Hyperm 12-5 only face velocity and adsorbate concentration had significant negative effects. The effect of relative humidity on the retention of I_2 was found to be only marginally significant at best. The synergistic effect of adsorbate concentration and relative humidity was found to be significant.

5. As face velocity was found to have a significant negative effect on both CH_3I and I_2 retention by Hyperm 12-5, and as this parameter is the only one under the operators control, it is recommended that for this application the HiVol flowrate be set at the low end (35-40 ft^3/min).

6. If a reasonably semi-quantitative method is required it is recommended that CH_3I retentions for Hyperm 12-5 be determined at additional low temperatures (perhaps -20, -10, and 10°C) and relative humidities (perhaps 20, 40, 75, and 95%). These tests should be conducted at a single low face velocity (30-35 cm/s) and a single adsorbate concentration.

7. It is recommended that the retention capacity of Hyperm 12-5 for radioxenon and radiokrypton be experimentally determined.

8. It is recommended that the Hyperm 12-5/HiVol sampling method not be used as a highly quantitative method for radioiodine monitoring because of the media's strong dependance on environmental factors such as temperature and relative humidity, and because of the relatively low collection efficiency for CH_3I. This method is suitable, however, as a semi-quantitative procedure to provide additional data to back-up more accurate methods and to confirm the presence or absence of radioiodines in a particular region.

9. It is recommended that full scale radioiodine tests be performed on actual HiVol air samplers. It was hoped that this type of testing could be performed in this study, however, there was not sufficient funds or time available to secure a proper facility large enough to accommodate a HiVol air sampler.

REFERENCES

1. Schleien, B., "Preparedness and Response in Radiation Accidents", U.S. Department of Health and Human Services, Food and Drug Administration, August 1983.

2. ASTM Standard D3803, "Standard Test Methods for Radioiodine Testing of Nuclear-Grade Gas-Phase Adsorbents", 1979.

AP14

A Re-Examination of Ontario's 24 Hour Ambient Air Quality Criterion for Hydrogen Fluoride

The Ontario Government's Ambient Air Quality Criteria for gaseous hydrogen fluoride of 0.86 $\mu g/m^3$ for 24 hours was established in 1974. The criteria is based on the most sensitive receptor in the environment to gaseous hydrogen fluoride which was determined to be vegetation. The level was set using results from the literature available at the time (Adams et al., 1956). In recent years there has been pressure from concerned industries to raise the 24 hour criteria to a higher value similar to that used in the United States. As there has been no new literature relating to short term exposures since the criteria was set in 1974 a standards development project was established at the Ministry of Environment, Phytotoxicolgy Section, Controlled Environment Laboratory to look into the validity of the current 24 hour criteria.

Three species, Manitoba maple (*Acer negundo*), apricot (*Prunus armeniaca* L.), and gladioli (*Gladiolus* sp. var. Snow Princess), where looked at in 1985. The 1985 work was repeated in 1986 using the same three species. The major difference between the 1985 and 1986 work was that older plants were used in the 1986 experiments in order to determine what affect plant age, stage of development and vigor had on their sensitivity to fluoride. In 1987 two varieties of tulip (*Tulipa gesneriana* L. var. Blue Parrot and Preludium) which are used as biological indicators of hydrogen fluoride in the Netherlands (Posthumus, 1976) were also tested.

All of the species studied accumulated fluoride in leaf tissue in a linear manner with increased fluoride dose. Only with gladioli and the Blue Parrot variety of tulip was fluoride content in the leaf tissue related to the amount of injury. The percentage of leaf tissue injured increased with increased fluoride dose in all four species but was highly variable in the apricot and Manitoba maple. Genetic variability appears to be a major factor in plant sensitivity to fluoride. Ranking of the species with respect to fluoride sensitivity placed tulip, gladioli, apricot, and Manitoba maple in that order from most sensitive to least sensitive. The stage of plant development and rate of growth were determined to be significant factors affecting fluoride sensitivity.

Although fluoride injury was observed at concentrations near or below the Ontario Government's 24 hour Ambient Air Quality Criteria of 0.86 ug/m^3 gaseous hydrogen fluoride, this level appears satisfactory for the protection of vegetation. Unlike other standards set by the Environmental Air Standards Setting Committee there is no apparent safety margin implicit in this proposed standard. The very slight injury observed at the lowest doses and the probability that plants growing in outdoor (natural) environments would not respond as sensitively is considered to create a safety margin.

This research will be submitted to an appropriate journal for publication. The published document will form the basis for the new formal standard document.

References

1. Adams, D.F., Shaw, C.G. and Yerkes, Jr. W.D. (1956). Relationship of injury indexes and fumigation fluoride levels. Phytopathology 46: 587-591
2. Pothumus, A.C. (1976). The use of higher plants as indicators for air pollution in the Netherlands. Proceedings of the Kuopio Meeting on Plant Damages Caused by Air Pollution. Kuopio. Lauri Kärenlampi ed. p. 115-120

AP15

Agronomic Evaluation of Ozone Insensitive White Bean Varieties

T. E. Michaels
Department of Crop Science
University of Guelph

White bean (*Phaseolus vulgaris* L.) is among the most ozone-sensitive crops in southwestern Ontario (Ormrod et al. 1980; Linzon et al. 1984). Using ethylene diurea (EDU) as a protectant, Hofstra et al. (1978) estimated yield reductions of 32 and 36% due to ambient ozone exposure at two Ontario locations. Heritable differences in ozone sensitivity have been found among common bean cultivars (Hucl and Beversdorf 1982a,b), suggesting that development of ozone-insensitive cultivars would be one means of reducing the effect of ozone on the white bean crop.

Forty white bean breeding lines were developed from crosses between the ozone-insensitive common bean cultivars French Horticultural Bean and Gold Crop and ozone-sensitive white bean cultivars Seafarer, Ex Rico 23 and Kentwood (Hucl and Beversdorf 1982a). F_2 plants were selected visually after controlled fumigation in growth chambers for ozone insensitivity, and plants with the appropriate maturity, architecture and seed type were selected in the F_5 and F6 generation (Michaels 1988). The cultivar Midnight was included in several crosses as a source of desirable upright plant architecture. Thirty-five of these breeding lines and their parents were used in the development of a digital image analysis method for selecting ozone-insensitive white beans (Michaels 1988). Approximately 65% of the breeding lines were classified as ozone-insensitive based on visual and digital image analysis methods, as would be anticipated for germplasm subject to selection for ozone insensitivity in earlier generations.

To have lasting impact in the white bean industry, a new ozone insensitive white bean cultivar must have seed yield, maturity, disease resistance and cooking quality at least equivalent to currently available cultivars. The Ontario Field Bean Committee coordinates an annual set of White Bean Variety Trials for the purpose of testing agronomic performance of potential new cultivars. This information is used to support candidate cultivars for federal registration. We lacked the preliminary agronomic information required to determine which of these ozone-insensitive white bean lines should be entered into this trial. The objective of this study was to obtain this information by evaluating the agronomic performance and ozone sensitivity of these forty white bean breeding lines under field conditions.

Materials and Methods

Forty breeding lines and eight check varieties described previously (Michaels 1988) were planted at Woodstock, Ontario in 1987 in a randomized complete block design with three replications. Plots were 1 row, 6m long with 0.6m between rows. Seeding density was approximately 225000 plants/ha. Plots were subjectively evaluated during the first week of August for ozone sensitivity on a 1=insensitive to 5=very sensitive scale. Seed yield, days to maturity, 100 seed weight and harvestability were also determined. The latter is a subjective evaluation of the potential harvest losses under direct combine harvest with 1=no losses and 5=severe losses. Seed yield was adjusted to the industry standard of 18% moisture. Seven of the best breeding lines were subsequently entered into advanced yield trials at Elora and Woodstock in 1988.

Results and Discussion

The late maturing check cultivars Midnight, Steuben Yellow Eye and Fleetwood had the lowest ozone injury (Table 1). Low injury of these cultivars in field conditions may be associated with their late maturity and avoidance of the ozone exposure during a particularly sensitive growth stage such as flowering and early pod filling. In contrast, Gold Crop and French Horticultural Bean, which were used as donors of ozone insensitivity, appeared sensitive in this field trial. Eighteen breeding lines showed low levels of sensitivity with scores of 2.7 or lower.

Two of the breeding lines, W02885 and W04885, were significantly higher yielding than the highest yielding white bean check cultivar, Ex Rico 23. Both of these lines were at least 4 days later maturing, however. Since cultivars that are later maturing than Ex Rico 23 are generally undesirable, these lines may be of only limited importance. Twenty-seven lines were not significantly different from Ex Rico 23 in yield. From this group, several lines with favorable combinations of ozone sensitivity, maturity, yield and seed size were be identified. Line W02785, for instance, had an ozone injury score of 2.7, yielded numerically greater than Ex Rico 23 with the same number of days to maturity. This line also had high levels of ozone-insensitivity in a controlled fumigation study (Michaels 1988).

Seven of these breeding lines (W01985, W02185, W02285, W02585, W02785, W02885 and W04885) were entered in advanced yield trials in 1988 at Woodstock and Elora. Preliminary data from the Elora site indicated that all of the lines were late maturing and exhibited potentially undesirably high levels of vining. Lines W02585, W02785 and W04885 again showed desirable levels of ozone-insensitivity. Yield data from these sites are not yet available. A breeding line will be chosen from among this group for entry into the 1989 White Bean Variety Trials based on the final data from the two trials in 1988.

References

Hofstra, G., D. A. Littlejohns and R. T. Wukasch. 1978. The efficacy of the antioxidant ethylene diurea (EDU) compared to carboxin and benomyl in reducing yield losses from ozone in navy bean. Plant Dis Rep. 62:350-352.

Hucl, P. and W. D. Beversdorf. 1982a. The response of selected *Phaseolus vulgaris* L. cultivars to ozone under controlled fumigation and ambient field levels. Can. J. Plant Sci. 62:561-569.

Hucl, P. and W. D. Beversdorf. 1982b. The inheritance of ozone insensitivity in selected *Phaseolus vulgaris* L. populations. Can. J. Plant Sci. 62:861-865.

Linzon, S. N. , R G Pearson, J. A Donnan and F. N. Durham. 1984. Ozone effects on crops in Ontario and related monetary values. Ontario Ministry of the Environment ARB-13-84-Phyto.

Michaels, T. E. 1988. A digital image analysis method for selecting ozone-insensitive white beans. Can. J. Plant Sci. 68:627-632.

Ormrod, D. P., J. T. A. Procter, G. Hofstra and M. L. Phillips. 1980. Air pollution effects on agricultural crops in Ontario: A review. Can. J. Plant Sci. 60:1023-1030.

Table 1 Agronomic performance of ozone-insensitive breeding lines and check cultivars, Woodstock 1987.

Entry	Ozone Injury†	100 seed wt.	Maturity	Harvestability‡	Yield
		g	days		kg/ha
SEAFORTH	4.3	19.6	88	5.0	2455
EX RICO 23	3.0	22.1	104	4.7	3002
KENTWOOD	3.3	24.2	96	4.0	2466
MIDNIGHT	1.7	20.3	107	3.7	4227
GOLD CROP	4.0	32.8	97	4.0	1247
FRENCH HORT.	4.0	51.1	93	3.7	1982
FLEETWOOD	1.0	20.3	108	5.0	2866
STEUBEN Y.E.	1.3	50.3	105	5.0	2231
W80-4 W00285	2.3	20.3	107	5.0	2919
W80-4 W00385	2.3	23.9	107	4.3	3142
W80-4 W00485	2.7	20.4	107	4.7	2905
W80-4 W00685	3.3	20.3	106	4.3	3010
W80-5 W00785	3.3	20.1	107	4.7	2253
W80-5 W00885	3.0	20.3	105	4.3	2410
W80-5 W01185	3.3	20.7	103	4.3	2943
W80-6 W01585	2.7	21.2	105	5.0	3095
W80-6 W01685	3.7	21.6	107	4.7	3147
W80-6 W01785	2.7	20.5	106	4.3	3212
W80-20 W01885	3.3	17.9	105	5.0	2894
W80-20 W01985	3.0	18.3	108	4.3	3176
W80-20 W02085	2.7	17.8	100	4.7	2951
W80-20 W02185	3.0	18.8	107	5.0	3577
W80-20 W02285	2.7	18.7	107	5.0	3189
W80-20 W02485	3.3	19.5	105	5.0	3241
W80-20 W02585	2.7	18.1	106	4.3	3529
W80-20 W02685	3.7	18.0	98	5.0	2954
W80-20 W02785	2.7	19.2	104	5.0	3345
W80-20 W02885	2.3	18.0	108	4.0	3666
W81-4 W02985	4.0	27.7	96	4.0	1505
W81-4 W03085	2.7	19.1	104	5.0	2085
W81-4 W03185	4.0	19.7	101	4.7	1701
W81-12 W03685	3.0	25.6	108	4.0	2745
W81-12 W04485	2.3	27.0	106	4.3	2080
W81-12 W04685	3.7	24.6	97	4.0	2506
W81-12 W04785	3.3	24.9	91	5.0	2789
W81-12 W04885	2.3	22.0	109	4.7	3618
W81-12 W04985	3.0	23.7	96	4.3	2704
W81-12 W05285	3.7	24.4	98	3.7	2253
W81-12 W05485	2.0	25.6	103	4.7	2258
W81-17 W05585	3.0	24.1	96	4.7	2373
W81-17 W05685	2.7	26.3	96	4.0	2530
W81-25 W06385	4.0	22.6	88	3.3	2494
W81-25 W06685	4.7	22.2	88	4.0	2454
W81-25 W06985	4.0	22.1	87	3.3	2476
W81-41 W07585	2.7	20.9	105	4.3	1217
W81-41 W07885	1.7	22.4	103	5.0	1291
W81-41 W08185	2.3	26.1	105	4.7	1667
W81-54 W08385	2.0	24.8	106	4.0	2395
LSD 0.05					591

† 1 = insensitive, 5 = very insensitive

‡ 1 = no harvest losses expected 5 = severe harvest losses expected

AP16

EFFICACY OF FILM-FORMING CHEMICALS FOR PROTECTING ROADSIDE TREES AGAINST SALT SPRAY

by

CALVIN CHONG
Ministry of Agriculture and Food
Horticultural Research Institute of Ontario
Vineland Station, Ontario L0R 2E0

Application of salt to major Ontario highways during the winter is a common practice. Studies have established that salt spray is phytotoxic to vegetation. Eighteen different film-forming chemicals were tested during a three-year period and five were identified as having the potential to reduce salt injury to fruit trees and other roadside vegetation.

The objectives of the present investigations were to obtain additional data from further field trials on the above five chemicals and also test four new formulations for their effectiveness in preventing salt injury to peach trees.

In November 1987, selected branches of 20 eight-year-old trees of 'Garnet Beauty' peach (*Prunus persica*) located in two rows along the southern side of the Queen Elizabeth Highway (QEW) in Grimsby were treated as follows: untreated (control), covered with burlap, or sprayed with Folicote (diluted 1:10 v/v, Aquatrols Corp.), RD 1725 (1:5, International Waxes Ltd.), RD 1726 (1:3, International Waxes Ltd.), Siliconate 51T (1:50, May and Baker) and Joncryl 1938 (1:5, Johnson and Son Ltd.). Each chemical was applied by means of a 20-L backpack sprayer. Triton XR surfactant was used at a rate of 2.5 ml/L of spray mixture. Overspray onto adjacent branches was prevented by covering them with a large polyethylene sheet. Twigs were evaluated in spring of 1988 for Na^+ and Cl^- content and amount of injury.

Twigs of 'Garnet Beauty' peach trees in the row closer to the highway had consistently more twig dieback and greater contents of Na^+ and Cl^- than those further from the highway. Untreated twigs accumulated the greatest quantities of Cl^- (358 ppm) and exhibited the greatest twig dieback (13.6 cm to first flower bud). In contrast, burlapped twigs accumulated only 58 ppm Cl^- and were the least damaged (5.3 cm dieback). All spray-treated twigs accumulated less Cl^- (248-290 ppm) than untreated twigs and exhibited intermediate injury. Twigs sprayed with RD 1726 and Joncryl 1938 had the least dieback (8.7 and 7.4 cm, respectively). Na^+ accumulated least in burlapped twigs (16 ppm), highest in Siliconate-treated twigs (71 ppm), and intermediate amounts (59-62 ppm) in all other treatments, including the control.

When similarly applied to six woody coniferous (black pine, red pine, white pine) and deciduous (lilac, black willow, silver maple) species, the above five spray treatments were ineffective and/or twig samples were insufficient and too variable to obtain meaningful results, except for red pine. All five chemicals resulted in small reductions in injury to twigs of red pine. Except for the Siliconate 51T treatment, all spray-treated red pine twigs contained less Na^+ and Cl^- than unsprayed twigs.

In another investigation, whole 'Madison' peach trees were similarly sprayed with Folicote (1:10), RD 1725 (1:5) and the following four new emulsion-based formulations from International Waxes: RD 2033 (1:3), RD 2034 (1:3), RD 2035 (1:3) and RD 2036 (1:5). Unsprayed trees served as a control. Half of each tree was sprayed at monthly intervals during the winter with a 2% rock salt solution. Twigs were collected from both non-salted and salted sides of each tree at various intervals throughout the winter.

The Na^+ and Cl^- content in twigs of 'Madison' peach increased progressively during the winter, peaking or plateauing in late March, and was persistently higher in salted than in non-salted twigs. Unlike Na^+, significantly less Cl^- (124 ppm overall mean) was present throughout the winter in RD 2033-treated than in control twigs (142 ppm). Also the percentage of dead flower buds was lowest in RD 2033-treated twigs. All other spray treatments were ineffective in reducing Na^+ and(or) Cl^- accumulation or twig injury. In fact, RD 2034-treated twigs accumulated more Na^+ and Cl^- than control twigs. The percentage of dead vegetative buds was not significantly influenced by any of the spray treatments.

The present study confirms that film-forming chemicals reduce build-up of salt in twigs of some roadside trees and provide some protection against salt spray injury. However, because of mild temperatures in recent winters and variability in the results, large-scale or commercial use of these sprays cannot be recommended without further testing.

This is a joint cooperative study by the Ontario Ministries of Agriculture and Food, Transportation, and Environment, and the University of Guelph.

AP17

AN EVALUATION OF THE PROBLEMS OF PARTICULATE EMISSIONS FROM THE WOOD PRODUCTS INDUSTRY

Michael F. Lepage and Anton E. Davies
Rowan Williams Davies and Irwin Inc.
650 Woodlawn Road West, Guelph, Ontario, N1K 1B8

EXTENDED ABSTRACT

Introduction

An evaluation of problems of particulate emission in the wood products industry was conducted on behalf of the Ontario Ministry of the Environment. The objectives of the evaluation were as follows:

(a) to identify the problems and sources of particulate emission in the wood products industry;

(b) to determine how the industry and other regulatory agencies treat these problems;

(c) to provide conclusions and recommendations concerning the resolution of the problems;

(d) to provide a basis for good approval as well as management and operations guidelines for wood storage sites and other sources of fugitive wood particulate emissions;

(e) to provide a basis for improved monitoring of wood particulate to assist in the regulatory process;

(f) to recommend further research that might help to resolve the problems.

Methodology

The objectives were achieved using literature surveys, telephone interviews and field trips. The literature surveys were conducted by means of the CAN/OLE and DIALOG literature data base enquiry systems and the RWDI in-house technical library. Sixty articles pertaining to health effects, monitoring, regulation and control of wood dust were reviewed.

Through the telephone interviews, seventeen North American government agencies, thirteen wood products facilities, three special interest groups and eleve dust control manufacturers or consultants were contacted. Two field trips were conducted. The first trip was to Hearst, Ontario where four wood products sites were visited. The second trip was to Oregon, U.S.A., where four pulp mills, fo particleboard facilities and several sawmills were visited.

Findings

The findings of the evaluation included the following items.

(i) The health effects and other problems associated with wood dust emissions were reviewed. Wood dust has been identified in th literature as a cause of nasal and lung cancers, asthma and oth respiratory diseases, and inflammation of the skin, eyes and nas passage. Higher than normal incidence of these ailments have been observed among woodworkers. The incidence among residents livin near wood products facilities has not been investigate Nevertheless, these residents are known to be exposed to wood du and it is often considered a significant nuissance.

(ii) The principal sources of wood dust emissions were identified. Wo

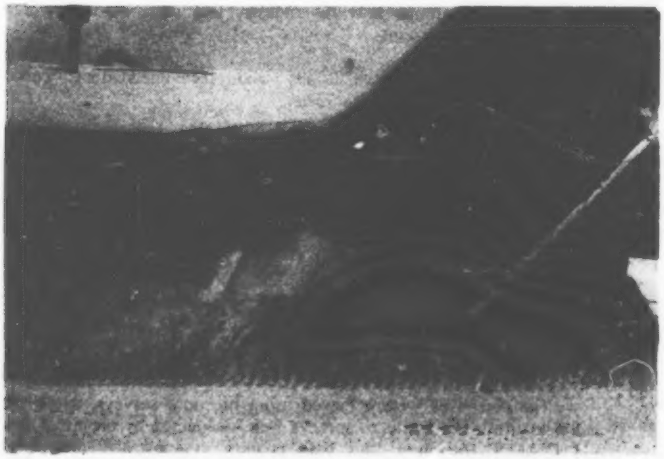

Figure 1 Wood dust emissions at an outdoor truck dump

dust is an inevitable by-product of the manufacture of wood products. The greatest potential for emissions often occurs at particleboard and hardboard plants, where the raw material used in production (wood shavings and trimmings) has a high dust content and is usually stored in abundance. The principal causes of dust emissions are: continuous dropping of material at stackers, blowpipes and other transfer points; batch dropping by front-end loaders and truck dumping (Figure 1); wind erosion of outdoor stockpiles; exhaust emissions from pneumatic material transfer systems and air handling equipment (e.g. cyclones); vehicle activity on dusty surfaces.

(iii) Existing dust control technologies used in the wood products industry were reviewed. Examples of stockpile windbreaks and enclosures (Figure 2), chutes on blowpipes, ventilated truck dump enclosures

Figure 2 Enclosed wood shavings pile (right) and ventilated truck dump enclosure (centre)

and water mist systems were presented.

(iv) Particulate monitoring, approvals and permitting practices among various government agencies were reviewed.

(v) Improved particulate monitoring techniques were reviewed. These included methods of correlating particulate measurements with wind and other meteorological data, as well as improved designs for dustfall collectors.

Recommendations

The recommendations of the evaluation may be summarized as follows:

1. The approval process in Ontario should include requirements for regular reporting of dust control equipment maintenance and compliance with emission standards for fugitive particulate sources (such as blowpipes, stackers, wind erosion of stockpiles, truck loading and unloading and vehicle traffic).

2. There are several fundamental dust control practices that should be implemented at all facilities, in order to help meet both ambient air quality and emission standards. These include indoor storage of sander dust and dry sawdust, enclosure of stackers and blowpipes at outdoor storage piles, use of enclosures or windbreaks at truck dumps and cleaning of roadways. Additional controls should implemented as determined from dispersion modelling studies. These additional controls might consist of strategically located porous windbreaks, streamlined stockpile designs, strategic stockpile management and reduction of operations during windy conditions.

3. Particulate monitoring data should be correlated with wind data to identify the primary particulate emission sources in a multisource region.

4. Further research is recommended to develop better fugitive source emission factors for the wood products industry and to develop a dustfall collector with better collection efficiency.

AP18

RELATIONSHIP OF SUGAR MAPLE DECLINE AND CORRESPONDING CHEMICAL CHANGES IN XYLEM SAP CARBOHYDRATES MICRONUTRIENTS AND TRACE ELEMENTS

S.N. Pathak, T.C. Hutchinson and D.N. Roy
Faculty of Forestry, 203 college Street, University of Toronto, Toronto, Ontario

INTRODUCTION

Irrespective of the aetiology of the maple decline syndrome, loss of vigor, biomass production and decrease in sap production have been equated with decline. Although these symptoms are physical indications of maple decline, the biochemical responses may well occur long before their manifestation. Various cell types of the conducting xylem of sugar maple trees function in the circulation, storage, metabolism, mobilization and assimilation of organic substances (Kozlowski 1971). Xylem sap also contains appreciable quantities of carbohydrates in the soluble form along with various nutrients (Wilson 1970). These chemicals could, therefore, be studied to see if these are different in healthy and declining trees. We had earlier proposed that at the present stage of our knowledge of sugar maple decline, a useful approach might be to study the chemical changes occurring in sap in trees ranging from healthy to seriously in decline. The long-term objective being that if we could index the chemical change in sap matrix of declining maple trees, relationships could then be correlated with a physical assessment criterion, Decline Index (DI), recently formulated by Ontario Ministry of the Environment (MOE) and is currently being used in many related studies. It might be possible to index these trees chemically much earlier than the onset of the physical decline, thereby facilitating the "early warning" syndrome of maple decline. The focus of this research, therefore lies in chemical analyses of sap matrix. This pioneering approach has not yet been pursued by any other research group involved in sugar maple decline research.

METHODOLOGY

1. EXPERIMENTAL DESIGN

The sampling unit of this study is an individual (healthy/declining) tree of any of the five sites selected in a NE to SW directional gradient of southern Ontario. Ten sugar maple trees, differeing in physical health (as determined by DI) and site characteristics (mainly pedological and stand) are selected each from five sites varying in their overall decline status. These sites (namely, A061, A062, A045, A073 and A020) were mapped out in 1986 as part of the Hardwood Decline Survey conducted by MOE. One of these sites has been demarcated as a "base-line site" (site A020), which will provide a stastically acceptable pattern of variability in levels of sap chemicals. Fifty trees at various stages of decline have been marked for study at this site. This site will further provide data to study the extent of intra-site variability in these trees. All sites selected have been unmanaged for at least past 17 years, contain at least 50% sugar maple trees, and are situated on the Crown Land, basically undisturbed by any man-made disturbances.

Xylem sap at breast heights (1.3 meters) of selected trees have been collected at both early and late sap flow seasons in March and April months of 1988, respectively. Stem tissue will be collected in early Fall along with the soil from the rooting zone of each tree. At the time of stem and soil collection, the decline status will be assessed with the physical parameters set forth by MOE. Trees are selected so that the healthy trees have

DI of <10.00 and declining trees are branded DI of >18-20. The major response variables selected for this study include Total sugars, major carbohydrates like Sucrose, Glucose, Fructose, Galactose, Raffinose, Stachyose, Arabinose and Mannose and major inorganic elements, for example, macronutrients (Na, K, P, Ca, S, and Mg), micronutrients (B, Cu, Fe, Mn, Zn) and other elements (Al, Co, Cd, N, Pb, Si, Cr, As, Se, Sb, V, Mo, Ni, and Ba)

2. SAP COLLECTION

For sap collection, aseptic conditions were used to avoid metal contamination which might interfere with the trace elemental analyses. A custom designed polyethylene plastic suction apparatus was designed for the extraction of xylem sap in maple trees in the field by MOE and used for the extraction of sap samples in these sites. A two inch size of hole was drilled by an automatic drill attached onto a chain saw at the south side of the breast height of the trees. A maximum pressure of 120 psi, applied by hand-held lysimeter pump, was enough to yield sufficient amount of sap (30-100) from each tree in 5-20 minutes. In 1988, a total of 180 sap samples were collected (90 early sap season samples and 90 late season samples from 90 trees). The total volume of collected samples varied between 25-100 mL. Each extracted sap sample was aliquoted and distributed equally in 4 sterile plastic vials (30 mL. capacity). The samples were kept cold in the field and frozen at -15^{0}C as soon as possible. The frozen samples were thawed and diluted with deionized water (10-1000 X) prior to analyses.

3. ANALYTICAL PROCEDURES

A. Analyses of Carbohydrates and their derivatives

Simple sugars and di- and oligo-saccharides are being analysed by High Pressure Liquid Ion Exchange Chromatography (HPLIC), a new technique marketed recently by Dionex Corporation (Sunnyvale, California), as BioLC Series 4000i. This is a new chromatographic analysis method utilizing anion exchange separation of carbohydrates with pulsed amperometric detection. Compared to older chromatographic methods with refractive index and ultraviolet detection, anion exchange with pulsed amperometric detection provides specificity, selectivity, sensitivity and reliability. In our laboratory the chromatograph has been interfaced with a Shimadzu CR5A integrator (Shimadzu Corp., Japan). Ultrapure carbohydrate standards (Pfanstiehl Lab. Inc., Illinois, USA) with a detection limit as low as 30 ppb for monosaccharides and 100 ppb for polysaccharides can be separated as anions with a concentration elution gradient program of sodium hydroxide. Retention times and selectivity of the analytes were controlled by varying eluent strength. The separated carbohydrates were detected electrochemically by oxidation of a gold electrode. This potent method of direct separation of carbohydrates offers a timely option to replace other cumbersome and unreliable analytical methods (e.g. HPLC utilizing RI and low UV-detection and GC after derivitization of samples) of carbohydrate analyses. These latter methods were tried earlier to establish the ideal conditions for sap samples with limited success. On the other hand, we have found the Ion Exchange Chromatography to be sensitive (30-100 ppb), linear (upto 600 ppm concentration), reproducible (peak heights vary less than 1% after multiple injections of single sample) and in control of retention at both isocratic and gradient elutions of a sample.

After standardizing the system for representative sugars, detailed carbohydrate analyses of sap samples are now in progress and some of the results will be presented in the

Conference. Samples are being analysed in a calibration analytical run of an elution gradient method in combination with a post-column addition of the higher molarity of the eluent used for the carbohydrate standards and sap samples. A computer program to calculate the concentrations of known sugars based on the absolute normalization method has been developed and is now being used to analyse the field sap samples. At present we have completed a preliminary chromatographic analyses of six known sugars (Arabinose, galactose, glucose, fructose, xylose and Sucrose) in 100 sap samples. Other samples are currently being analysed. These data indicate differences in the nature and amount of sugars in trees based on their decline characteristics. We will be characterising the observed "unknown" peaks in certain sap samples once the preliminary analyses of all the samples is completed. Later on silyl derivatives of sugars will be used for detection and quantitation of sugar derivatives by Gas Chromatography. Sugars of unknown structures will be analysed by HPLC-Mass Spectroscopy. Additional use of ^{13}C NMR might be required for complex sugars. Separation of minor components for optional study, that is, phenols, peptides, aminonitrogens, proteins, organic acids, amino acids (AA's) etc., will be followed by the amino acid analysis using the AA analyser. An attempt will be made to analyse AA's in the GC with a special N-P detector.

B. Physico-chemical Analyses

Some other physico-chemical properties of carbohydrates e.g. pH measurements, refractive indices and optical rotations, have been utilised for gross estimation of sugar content and its changes in sap samples. Data for all these variables have been collected and are in the process of being analysed. These variables will provide a secondary support for the final carbohydrate determination.

C. Trace Elemental Analyses

Flash freeze-dried sap samples (12-25 microgram/ml.) in 6% nitric acid matrix have been analysed for macronutrients (Na, K, P, Ca, S, and Mg), some micronutrients (B, Cu, Fe, Mn, Zn) and other elements e.g. Al, Co, Cd, N, Pb, Si, Cr, As, Se, Sb, V, Mo, Ni, and Ba, by Induced Coupled Argon Plasma Spectroscopy (ICAP). Sodium and Potassium analyses of freeze-dried sap samples were analysed by Atomic absorption Spectroscopy. A preliminary analysis of the 24 elements shows that there is a trend of increasing amounts of Al, and Mn and decreasing amounts of Ca, Mg, P, and Fe, when sap of healthy trees was compared with that of declining trees. Details of these results will be presented during the meeting.

4. DATA ANALYSIS

At present the analytical data are being input in IBM microcomputer programs (Mainly Reflex, Lotus, Dbase III plus and SAS-PC). Once completed, the stored data will be retrieved for computational purposes. Prior to analyses, data in either %age or ppm units will be tested for normality (by univariate statistics), homoscadaticity (by t-tests) and independence of observations (by scatter plots). Appropriate transformations (e.g. log, square root, logistic transfer etc.) will be applied to data to satisfy these assumptions for detailed data analyses to follow. Differences in tree-health parameters (healthy versus declining) and chemical components will be analysed by either a conventional one-way analysis of variance, in conjunction with t-tests (used as a means separation test), or a student t-test (Snedecor and Cochrane 1982). Correlating response variables will be detected by correlation matrices. If response variables do not correlate, analyses of variance with individual chemical concentrations will be done, otherwise correlating variables will be grouped to do multivariate analyses of variance (MANOVA) in a factorial design. General linear models (GLM) will be used for unequal cells. Various regression models (e.g. linear, curvilinear etc.) will be tested to look for trends of changes in sap chemistry in predictor variables i.e. sites and the healthy versus declining trees. Significant differences among chemicals or sites will be examined by Duncan's multiple range test. IBM 4381 Mainframe computer will be used for complex statistical procedures (for example GLM) using SAS under VM/CMS operating system. Basic and Fortran compilers will be used to further modify or reprogram the SAS procedures.

REFERENCESS

Kozlowski, T.T. 1971. Growth and development of trees, Vol. 1. Academic Press, N.Y., London, 519 pp.

Snedecor, G.W., and W.G. Cochran. 1982. Statistical Methods. The Iowa State University Press, Ames, Iowa (USA). 507 pp.

Wilson, B.S. 1970. The growing tree. Univ. of Massachusetts Press. Library of Congress catalogue # 70-123535.

AP19

IDENTIFICATION OF LONG RANGE AEROSOL SOURCES AT THE DORSET ENVIRONMENTAL STATION. John Drake*, Abdul Kabir and Stephen Vermette, Department of Geography, McMaster University, Hamilton, Ontario L8S 4K1

EXTENDED ABSTRACT NOT AVAILABLE

INDICES LISTED FOR REFERENCE

Abstract

SESSION B: WATER QUALITY RESEARCH

Oral Presentations

B1 **Aquatic Biology in the New Regulatory Framework** K. Day, National Water Reseach Institute, Burlington, Ontario.

B2 **Hypothesis Testing in Aquatic Toxicology: QSAR Relationships and Simple Kinetic Modelling** L. S. McCarty*, University of Waterloo, Waterloo, Ontario, G. W. Ozburn and A. D. Smith, Lakehead University, Thunder Bay, Ontario.

B3 **Variations in the Response of Fish Population Characteristics to Environmental Changes** K. R. Munkittrick* and D. G. Dixon, Department of Biology, Universityof Waterloo, Waterloo, Ontario.

B4 **An Examination of Chronic Toxicity of Thiocyanate to Freshwater Fish for the Development of a Water Quality Criterion** D. G. Dixon, R. P. Lanno* and S. D. Kevan, University of Waterloo, Waterloo, Ontario.

B5 **Potential Role of Polycyclic Aromatic Hydrocarbons in the Development of Liver Tumors in Fish from Polluted Sites of Lake Ontario** G. M. Kirby, I. R. Smith, C. Thorn, H. W. Ferguson and M. A. Hayes*, Univeristy of Guelph, Guelph Ontario.

B6 **Plant Bioassays for the Detection of Environmental Mutagens in an Aquatic Environment** W. F. Grant, Department of Biology, York University, Downsview, Ontario.

B7 **Effects of Temperature and Field Procedures on PCB Bioaccumulation in Elliptio Complanata** A. Melkic* and Y. Rollin, Intergrated Explorations, Guelph, Ontario.

Abstract

SESSION B: WATER QUALITY RESEARCH

Oral Presentations

B8 Biomonitoring: Chemical Dependent Quantitative Relationships for the Body Burdens of Organic Chemicals in Aquatic Biomonitors F. Gobas*, R. Russell and G. Haffner, Great Lakes Institute, Univerisity of Windsor, Windsor, Ontario.

B9 Biomonitoring Protocols for Adult Aquatic Insects: Seasonal Availability, Sample Size and Sensitivity Z.E. Kovats and J.J.H. Ciborowski*, Dept. of Biological Sciences, University of Windsor, Windsor, Ontario.

B10 An Ecosystem Approach to the Monitoring of PCB's in Pristine Ontario Lakes C.D. Metcalfe* and C.R. Macdonald, Trent University, Peterborough, Ontario.

B11 Metal Contamination of Wetland Foodchains in the Bay of Quinte, Ontario A. Crowder*, W. Dushenko and J. Greig, Dept. of Biology, Queen's University, Kingston, Ontario.

B12 An Overview of Aquatic Environmental Research in Quebec M. Slivitsky, INRS-EAU, Ste. Foy, Quebec.

B13 Development of an Improved System for the Application of Powdered Activated Carbon in Water Treatment Plants H. Donison*, A. Benedek and J.J. Bancsi, Zenon Environmental Inc., Burlington, Ontario.

B14 Municipal Utilization of Water Demand Management Strategies in Ontario Municipalities R.D. Kreutzwiser* and R.B. Feagan, Dept. of Geography, University of Guelph, Ontario.

Abstract

SESSION B: WATER QUALITY RESEARCH

Oral Presentations

B15 **A Preliminary Study to Determine the Feasibility of Medium Pressure Mercury Lamps for Disinfecting Low Quality Wastewaters** G. E. Whitby and G. Sakamoto, Trojan Technologies Inc., London, Ontario, and G. Palamateer*, Envioronment Ontario.

B16 **Characterization of the Fecal Indicator Bacterial Flora of Sanitary Sewage with Application to Identifying the Presence of Sanitary Waste in Storm Sewers** P. L. Seyfried*, T. Bleier, Y. Xu and R. Harmandayan, University of Toronto, Toronto, Ontario.

B17 **Landsat-5 TM Spectral Responses for Lakes Across Northeastern Ontario** J. R. Pitblado, Geography Department, Laurentian University, Sudbury, Ontario.

B18 **Relationship of Mercury Levels in Sportfish with Lake Sediment and Water Quality Variables** C. D. Wren, B. A. R. Environmental, Quelph, Ontario.

B19 **Trend Analysis Procedures for Water Quality Time Series** A. I. McLeod*, and K. W. Hipel, McLeod-Hipel Associates Ltd., London, Ontario and B. Bodo, Environment Ontario.

B20 **Use of a Bromobenzoate for Cross-Adaptation of Anaerobic Bacteria in Lake Ontario Sediments for Biodegradation of Chlorinated Aromatics** M. Urbanek*, T. Strycek, R. C. Wyndham and M. Goldner, University of Toronto, Toronto, Ontario.

Abstract

SESSION B: WATER QUALITY RESEARCH

Poster Presentations

BP1 The Effects of Agricultural Drainage on Sediment and Water Quality Loadings W.E. Watt, Department of Civil Engineering, Queen's University, Kingston, Ontario.

BP2 WATQUAS 2.0: An Expert System for the Water Quality Assessment of Ontario Rivers W.C. Allison and T.E. Unny, Department of Civil Engineering, University of Waterloo, Waterloo, Ontario, and L. Logan, Environment Ontario.

BP3 Geochemical Characterization, Size Fractionation and Bioavailability of Trace Metal Particulate Associations in the Don River L. Warren and A.P. Zimmerman, Department of Zoology, University of Toronto, Toronto, Ontario.

BP4 The Investigation, Evaluation and Recommendation of Biomonitoring Organisms for Procedures Development for Environmental Monitoring C.A. Jefferson, Curry-Jefferson Environmental Services, Port Perry, Ontario.

BP5 The Ontario Inland Lakes Program and Management of Blue-Green Algae: Three Whole Lake Treatments in 1988 H. Vandermeulen and K.H. Nicholls, Water Resources Branch, Environment Ontario.

BP6 Characterization of the Grazing Fauna Within Five Softwater Lakes With Respect to Accumulations of Metaphytic Filamentous Algae P.M Stokes, E.T. Howell and R.L. France, Institute for Environmental Studies, University of Toronto, Toronto, Ontario.

Abstract

SESSION B: WATER QUALITY RESEARCH

Poster Presentations

BP7 **Sedimentary Chrysophycean Cyst Assemblages as Paleoindicators in Acid Sensitive Lakes** M. Rybak and I. Rybak, ARECO Canada Inc., Ottawa, Ontario, and K. Nicholls, Environment Ontario.

BP8 **Factors Regulating Contaminant Levels In Forage Fish Species** C. E. Herbert and G. D. Haffner, Great Lakes Institute, University of Windsor, Windsor, Ontario.

BP9 **The Isotopic Composition of Upland Forest Soil Sulphate** D. R. Van Stempvoort and P. Fritz, Department of Earth Science, University of Waterloo, Waterloo, Ontario.

BP10 **Recent Trends and Historical Changes in Water Quality of Lake Muskoka** M. Rybak and I. Rybak, ARECO Canada Inc., Ottawa, Ontario, and K. Nicholls, Environment Ontario.

BP11 **In-Situ Determination of Fecal Indicator Bacterial Survival in Agriculturally-Impacted Watersheds** M. J. Walters, Lake Simcoe Region Conservation Authority, Newmarket, Ontario.

BP12 **Development of an Acute and Chronic Sediment Bioassay Protocol Using Larval Mayflies and Juvenile Fathead Minnows** G. Krantzberg and R. Pope, University of Toronto, Toronto, Ontario.

BP13 **Three Hour Pulse Exposure of Potassium Thiocyanate to Rainbow Trout Eggs Before and After Water Hardening** S. Kevan And G. Dixon, University of Waterloo, Waterloo, Ontario.

Abstract

SESSION C: LIQUID AND SOLID WASTE RESEARCH

Oral Presentations

C1 **An Overview of Hydrogeological Aspects of Waste Disposal: Research Results and Implications** J. Cherry, Waterloo Centre for Groundwater Research, University of Waterloo, Waterloo, Ontario.

C2 **Immiscible Liquids and Vapours in Soil: Recent Experiments on Transport and Control** G. Farquhar*, R. Bensen, D. Graham, E. McBean and B. Stickney, Dept. of Civil Eng., University of Waterloo, Waterloo, Ontario.

C3 **Effects of Increasing Amounts of Non-polar Organic Liquids in Domestic Waste Leachate on the Hydraulic Conductivity of Clay Liners in Southern Ontario** F. Fernandez* and R.M. Quigley, University of Western Ontario, London, Ontario.

C4 **Technology Review: Biological Treatment of Hazardous Landfill Leachates** J. Fein*, and P. Yu, Diversified Research Laboratories Ltd., Toronto, Ontario.

C5 **Phase Partitioning Kinetics at Industrial Waste Land Treatment Sites** D. Hockley and W.J. Snodgrass*, Beak Consultants, Toronto, Ontario.

C6 **Preliminary Assessment of a Microfiltration/Reverse Osmosis Process for the Treatment of Landfill Leachate** T.A. Krug* and S. McDougall, Zenon Environmental Inc., Burlington, Ontario.

C7 **Anaerobic Treatment of Landfill Leachate** G.P. Vicevic*, B.J. Forrestal and A. Stevenson, Ontario Research Foundation, Clarkson, Ontario.

Abstract

SESSION C: LIQUID AND SOLID WASTE RESEARCH

Oral Presentations

C8 **The Origin and Distribution of Methane in the Alliston Sand Aquifer** R. Aravena*, J. Barker, M. Bliss and L. Wassenaar, Department of Earth Sciences, University of Waterloo, Waterloo, Ontario.

C9 **The Carbon and Sulfur Cycle in Shallow Unconfined Aquifer Systems** L. I. Wassenaar*, R. Aravena, R. W. Gillham, J. Barker and P. Fritz, Department of Earth Sciences, University of Waterloo, Waterloo, Ontario.

C10 **Determination of Organic and Inorganic Contaminants in the Welland River** I. D. Brindle*, A. W. Chu and X-f Li, Chemistry Department, Brock University, St. Catharines, Ontario.

C11 **Research and Development of Permanent On-site Solutions for Contamination of Groundwater at Waste Disposal and Industrial Sites in Canada** R. J. Rush, CANVIRO Consultants, Kitchener, Ontario.

C12 **The Role of Groundwater in Human Society** R. N. Farvolden, Waterloo Centre for Groundwater Research, University of Waterloo, Waterloo, Ontario.

C13 **Dispersion of the Stouffville Landfill Plume** I. Proulx* and R. N. Farvolden, Waterloo Centre for Groundwater Research, University of Waterloo, Ontario.

C14 **Comparison of an Experimental Municipal Refuse Column Study with Landfill Field Test Cells** S. Pirani and D. W. Kirk*, Dept. of Chemical Engineering, University of Toronto, Toronto, Ontario.

Abstract

SESSION C: LIQUID AND SOLID WASTE RESEARCH

Oral Presentations

C15 **An Alternative to Incineration of Biomedical Waste: Hammermill/Chemical Decontamination** J. Manuel, Waste Management Branch, Environment Ontario.

C16 **Erosion of Landfill Covers** J. Cuthill*, Department of Land Resource Science, University of Guelph, Guelph, Ontario, and K. McKague, Ecologistics Ltd., Waterloo, Ontario.

C17 **Development of Backfill and Construction Application Guidelines for Ontario** M. Kelleher* and B. Whiffin, CANVIRO Consultants, Mississauga, Ontario.

C18 **Panel Discussion: Stemming the Rising Tide of Waste**
Moderator: D. Mackay, University of Toronto

Abstract

SESSION C: LIQUID AND SOLID WASTE RESEARCH

Poster Presentations

CP1 **Retractable Composite Absorbents for Environmental Clean-up** B. Gillies, E. Stubley, I. Treurnicht and L. Read, EcoPlastics Ltd. Willowdale, Ontario and O. Meresz, Laboratory Services Branch, Environment Ontario.

CP2 **Treatment and Disposal of Hauled Sewage Under ', 'Part VII, Environmental Protection Act** J.L. Smith, Oliver, Mangione, McCalla & Associates Limited, Nepean, Ontario.

CP3 **Factors Affecting the Concentration of Metal Ions in Municipal Refuse Leachate** G. Kosta, S. Pirani and D. Kirk, Department of Chemical Engineering and Applied Chemistry, University of Toronto, Toronto, Ontario.

CP4 **Slow Rate Infiltration Land Treatment and Recirculation of Landfill Leachate in Ontario** R.A. McBride, A.M. Gordon, P.H. Groenevelt, T.J. Gillespie and L.J. Evans, Departments of Land Resource Science and Environmental Biology, University of Guelph, Guelph, Ontario.

CP5 **Establishing Vegetation on Erosion-prone Landfill Slopes in Ontario, Year Two** T.W. Hilditch and C.P. Hughes, Gartner-Lee Ltd., Markham, Ontario.

CP6 **Evaluating Groundwater Velocity in a Low-Permeability Fractured Shale** K.S. Novakowski and J.A. Cherry, Centre for Groundwater Research, University of Waterloo, Waterloo, Ontario.

Abstract

SESSION C: LIQUID AND SOLID WASTE RESEARCH

Poster Presentations

CP7 **The Design and Evaluation of In-Situ Biorestoration Methods for the Treatment of Sludges and Soils at Waste Disposal Sites** K. L. Berry-Spark and J. F. Parker, Centre for Groundwater Research, University of Waterloo, Waterloo, Ontario.

CP8 **Enhanced Biodegradation of Aromatic and Chlorinated Aliphatic Compounds in a Leachate-Impacted Aquifer** -D. W. Acton, M. Shaw, J. F. Barker, C. I. Mayfield and J. A. Cherry, Univeristy of Waterloo, Waterloo, Ontario.

CP9 **Waste Management Planning for Pharmaceutical Industry** R. Staris and R. Makhija, Trent University, Peterborough, Ontario.

Abstract

SESSION D: ANALYTICAL METHODS

Oral Presentations

D1 **Analytical Chemistry in a Regulatory Environment** R. Kagel, Dow Chemicals, Midland, Michigan, U.S.A.

D2 **Adaptation of Water Preconcentration Techniques Developed for PCDD Analysis to Other Target Organic Pollutants.** E. Dowdall*, B.R. Hollebone, L. Brownlee and C. Shewchuk, Carleton University, Ottawa, Ontario.

D3 **The Purpose and Significance of Ultratrace Analysis of Dibenzo-p-Dioxins: The Concept of Risk** L. Brownlee* and B.R. Hollebone, Chemistry Department, Carleton University, Ottawa, Ontario.

D4 **Procedures for the Analysis of 2,3,7,8-Substituted PCDD & PCDF Isomers and Other Target Compounds in Environmental Samples** F.W. Karasek*, T.S. Thompson and K.P. Naikwadi, University of Waterloo, Waterloo, Ontario.

D5 **The Closed-Loop Stripping Technique, Applied to Potable Water to Solve Taste and Odour Problems** J.P. Palmentier*, D. Robinson and V. Taguchi, Laboratory Services Branch, Environment Ontario.

D6 **Solid Supported Processes in Environmental Analysis** J.M. Rosenfeld, Department of Pathology, McMaster University, Hamilton, Ontario.

D7 **Synthesis and Use of Liquid Crystalline Polysiloxane Substrate in Capillary Column GC-MS for Isomer Specific Separation of Toxic Isomers of PCDD and PCDF** K.P. Naikwadi* and F.W. Karasek, University of Waterloo, Waterloo, Ontario.

Abstract

SESSION D: ANALAYTICAL METHODS

Oral Presentations

D8 Development of Mobile Infrared Spectroscopy for On-site Speciation of Organic Wastes P. Yang* and J. Osborne, Laboratory Services Branch, Environment Ontario.

D9 Mobile Laboratory: On the Development and Real World Application Aspects D. Toner*, B. Dalton, D. Morse, K. Hom, P. Yang and J. Osborne, Laboratory Services Branch, Environment Ontario.

D10 Regiospecific Synthesis of All Isomeric Nitrofluorenones and Nitrofluorenes by Transition Metal Catalyzed Cross Coupling Reactions V. Snieckus*, T. Iihama, J.-m Fu and M. Bourguignon, University of Waterloo, Waterloo, Ontario.

D11 Preparation of Heterocyclic Polynuclear Aromatic Compounds as Analytical Standards E. Lee-Ruff*, B.E. George, F.J. Ablenas and Y.S. Chung, Department of Chemistry, York University, Downsview, Ontario.

D12 Application of ICP Spectrometry in Health and Environment: A Case Study of Soil Ingested by Children R. Barnes, University of Massachusetts, Amherst, Massachusetts, U.S.A.

D13 Direct Sample Insertion into an Inductively Coupled Plasma for Atomic Emission and Mass Spectrometry L. Blain* and E.D. Salin, Department of Chemistry, McGill University, Montreal, Quebec.

Abstract

SESSION D: ANALYTICAL METHODS

Oral Presentations

D14 **Analysis of Germanium and Tin by Hydride Generation D.C. Plasma Atomic Emission Spectrometry: Application to Determinations of Germanium and Tin in Air Filters** I.D. Brindle*, B. Buchanan and X-c. Le, Brock University, St. Catharines, Ontario.

D15 **Use of the Hot Slurry Technique for Solid Sample Introduction for ICP-AES** L. Gervais* and E.D. Salin, Department of Chemistry, McGill University, Montreal, Quebec.

D16 **Advanced Technology for Destruction of Waterborne Organic Pollutants** H. Al-Ekabi* and M. Robertson, Nulite, A Division of Nutech Energy System Inc., London, Ontario.

D17 **Development of ACexpert 2: Implementation of an Expert System for Automated Metal Analysis by Atomic Absorption Spectroscopy** M.J. Stillman*, T.A. Cox and W.R. Browett, University of Western Ontario, London, Ontario.

D18 **Adaptation of Water Preconcentration Techniques of Trace Metal Detection** K.L. Singfield*, B.R. Hollebone, L.J. Brownlee, Dept. of Chemistry, Carleton University, Ottawa, Ontario, and P. Vijan, Environment Ontario.

D19 **Comparison of Various Leachate Extraction Procedures for the Characterization of Inorganics in Wastes** J.R. Kramer*, P. Brassard, J. Gleed and P.V. Collins, Department of Geology, McMaster University, Hamilton, Ontario.

Abstract

SESSION D: ANALYTICAL METHODS

Oral Presentations

D20 2,4-Dichlorophenoxylacetic Acid (2,4-D) Determination in Water, Urine and Soil Extracts by Enzyme Immunoassay (EIA) and Radioimmunoassay (RIA)
J.C. Hall* and K. Krieg, Dept. of Environmental Biology, University of Guelph, Guelph, Ontario.

Abstract

SESSION D: ANALAYTICAL METHODS

Poster Presentations

DP1 **Derivatization of Acidic Organic Compounds Using Phase Transfer Catalysis** V. Y. Taguchi and O. W. Berg, Laboratory Services Branch, EnvironmentOntario.

DP2 **New Chemical Ionization Reagents Directed Toward Mass Spectrometric Analysis of Trace Organics** T. B. McMahon, K. Froese and C. E. Allison, Department of Chemistry and Guelph-Waterloo Centre for Graduate Work in Chemistry, University of ', 'Waterloo, Waterloo, Ontario.

DP3 **An Interrupted Segemented Flow Stream Microwave', 'Solid Sample Decomposition for ICP-AES** E. D. Salin And B. Liu, Department of Chemistry, McGill University, Montreal, Quebec.

DP4 **Solid Phase Extraction of PAH's From Drinking Water and Analysis of Chlorophenols and Phenoxy-acid Herbicides in Water** W. G. Craig and C. D. Hall, Paracel Laboratories Ltd., Nepean, Ontario.

DP5 **Automated Water Preconcentration Sampler for Dioxin Detection at the Parts Per Quadrillion Level** C. Shewchuk, B. Hollebone, L. Brownlee and E. Dowdall, Carleton University, Ottawa, Ontario, and R. Hunsinger, M. Uza, H. Tosine and S. Suter, Environment Ontario.

DP6 **Automated HPLC Method for Low Level Polynuclear', 'Aromatic Hydrocarbon (PAH) Analysis of Drinking Water** P. W. Crozier and C. D. Hall, Laboratory Services Branch, EnvironmentOntario.

Abstract

SESSION D: ANALYTICAL METHODS

Poster Presentations

DP7 **Supercritical Fluid Extraction of Trace Organics From Solid Matrices** P. Kruus and R.C. Burk, Department of Chemistry, Carleton University, Ottawa, Ontario and G. Crawford, Laboratory Services Branch, Environment Ontario.

DP8 **Automated Sample Introduction and Pre-treatment', 'with Flow Injection ICP-ES** J.F. Hopper, F. Mo and D.W. Boomer, Laboratory Services Branch, Environment Ontario.

DP9 **Applications of Flow Injection Technology to ICP-MS** M.J. Powell, J.F. Hopper and D.W. Boomer, Laboratory Services Branch, Environment Ontario.

DP10 **Investigation of the In-Situ Acetylation Process and its Applicability to the Analysis of a Wide Range of Phenolic Compounds in Water** R. Lega, O. Meresz and M. Savu, Laboratory Services Branch, Environment Ontario.

DP11 **Robustness of the Student's T-test with Censored Environmental Quality Data** E.E. Creese, Creese Environmental Consulting, Waterloo, Ontario.

DP12 **Automation of Solid Supported Reactions by Robotics** J.M. Rosenfeld and E. Pevolinas, McMaster University, Hamilton, Ontario.

Abstract

SESSION E: ENVIRONMENTAL ECONOMICS

Oral Presentations

E1 **Understanding Environmental-Economic Integration** P.A. Victor, VHB Research Ltd., Toronto, Ontario.

E2 **Economic Valuation Disparities and Environmental Policies** J.L. Knetsch, Economics Department, Simon Fraser University, Burnaby, British Columbia.

E3 **The Physco-social Impacts of Exposure to Environmental Contaminants in Ontario: A Feasibility Study** S.M. Taylor*, J. Frank, M. Haight, D. Streiner, S. Walter and N. White, McMaster University, Hamilton, Ontario.

E4 **Economic Assessments of MISA Regulations for Direct Industrial Dischargers in Ontario** O.E. Salamon* and J.A. Donnan, Policy and Planning Branch, Environment Ontario.

E5 **The Extra Strength Sewer Surcharge to Regulate Industrial Sanitary Waste Discharges** M. Fortin*, Ecologistics, Waterloo, Ontario, G. Zudovs, CANVIRO, and J. Donnan and G. Zegarac, Environment Ontario.

E6 **A Study of the Economic Factors Relating to the Implementation of Resource Recycling or Zero-Discharge Technologies for Heavy Metal Generating Industries in Canada** B. Fleet*, J. Kassirer, T. Burrell, T. Sanger, C. Small and B. Cardoza, University of Toronto, Toronto, Ontario.

E7 **Determinants of Participation in Solid Waste Source-Separation Programs in High-Rise Apartment Buildings** V.W. Maclaren, Department of Geography, University of Toronto, Toronto, Ontario.

SESSION E: ENVIRONMENTAL ECONOMICS

Poster Presentations

EP1 The New Economics of Sustainable Development R. Z. Rivers, Water Planning and Management Branch, Canada Centre For Inland Waters, Environment Canada, Burlington, Ontario.

EP2 The Environmental Effects of Forestry Operations in Ontario: How Much Do We Know? J. A. Dunster, Federation of Ontario Naturalists, Toronto, Ontario.